JUL 22

Journal of Research

of the

National Bureau of Standards

UNIVERSITY OF MICHIGAN
JUL 18 1957
PHYSICS LIBRARY

JULY 1957

VOLUME 59 NUMBER 1

VOLUME
NUMBER

JOURNAL OF RESEARCH
of the
NATIONAL BUREAU OF STANDARDS

THE NATIONAL BUREAU OF STANDARDS

The functions of the National Bureau of Standards are set forth in the Act of Congress, March 3, [illegible] in Public Law 619, 1950. These include the development and maintenance of national standards of measurement and the provision of means and methods for making measurements consistent with these standards; the determination of physical constants and properties of materials; the development of methods and instruments for testing materials, devices, and structures; advisory services to Government Agencies on scientific and technical problems; invention and development of devices to serve special needs of the Government; and the development of standard practices, codes, and specifications. The work includes basic and applied research, development, engineering, instrumentation, testing, evaluation, calibration services, and various consultation and information services. A major portion of the Bureau's work is performed for other Government Agencies, particularly the Department of Defense and the Atomic Energy Commission. The scope of activities is suggested by the listing of divisions and sections on the inside of the back cover.

Publications

The results of the Bureau's work take the form of either actual equipment and devices or published papers and reports. These papers appear either in the Bureau's own series of publications or in the journals of professional and scientific societies. The Bureau itself publishes three monthly periodicals, available from the Government Printing Office: The Journal of Research, which presents complete papers reporting technical investigations; the Technical News Bulletin, which presents preliminary reports on work in progress; and Basic Radio Propagation Predictions, which contains information for determining the best frequencies to use for radio communications throughout the world. There are also five series of nonperiodical publications: The Applied Mathematics Series, Circulars, Handbooks, Building Materials and Structures Reports, and Miscellaneous Publications.

Information on the Bureau's publications can be found in NBS Circular 460, Publications of the National Bureau of Standards ($1.25) and its Supplement ($0.75), available from the Superintendent of Documents, Government Printing Office, Washington 25, D. C.

Order all publications from the Superintendent of Documents
U. S. Government Printing Office, Washington 25, D. C.

Use of funds for printing this publication approved by the Director of the Bureau of the Budget (May 3, 1960).

Journal of Research of the National Bureau of Standards Vol. 59, No. 1, July 1957 Research Paper 2768

Thermal Length Changes of Some Refractory Castables

S. J. Schneider and L. E. Mong

Physics Library
QC
1
.456

The changes in length exhibited by a variety of refractory castables during complete heating and cooling cycles were determined. The tests consisted of determinations on castable specimens that had been heat treated at either 110°, 1,050°, or 1,300° C. A detailed description of the apparatus is given, especially that of the dilatometer assemblies. These assemblies incorporated differential transformers to give a record of length changes as they occurred. The data suggested that the same general length-change characteristics were exhibited by castables that had received the same curing and heat treatment. Length-change curves of all three groups illustrated silica inversions. Curves of the 110° C group indicated contractions associated with cement reactions, namely, the loss of water of hydration and the conversion of amorphous alumina to γ alumina.

1. Introduction

Invaluable aid can be gained by using thermal-expansion and contraction curves as guides in defining what allotropic changes occur, in determining at what temperatures reversible and irreversible volume changes take place; and by indicating the tendency of materials to spall [1].[1] This is especially true of refractories, the life and serviceability of which are directly affected by these thermal characteristics. This report endeavors to supply some of the needed information on one particular family of refractories, "the refractory castable." To provide a comprehensive study of this type of refractory, the investigation included length change determinations on commercial brands, as well as laboratory-prepared castables.

2. Specimens

2.1. Composition

Fourteen commercial brands and six laboratory-prepared groups of castables were used for tests conducted in this investigation. The commercial brands, selected to provide materials having a wide range of refractoriness, were obtained from a number of different manufacturers. Laboratory-prepared castables contained either 10, 20, or 30 percent of domestic high-alumina cement as the bonding material. These percentages of cement, in addition to appropriate amounts of aggregate, either calcined Kentucky flint clay or crushed high-heat-duty firebrick, constituted the experimental laboratory mixes. The more important properties of the aggregates, the cement, and the commercial castables used in this investigation were given by Heindl and Post in previous reports [2, 3].

2.2. Preparation

Prismatic 2- by 2- by 10-in. bars were prepared from the laboratory mixes and the commercial brands as outlined in Heindl's first report [2]. Four test specimens, approximately 1- by 1- by 7¼-in., were cut from each 2- by 2- by 10-in. bar. In order to insure proper dilatation values, the ends of each specimen were ground plane and perpendicular to the long axis. Irregular or rough ends could cause displacement or misalinement of the specimen, which in turn would result in erroneous expansion values. To facilitate grinding, a moderate coat of shellac was applied to the ends of all friable specimens.

3. Apparatus

3.1. Assembly

The apparatus used in this investigation is essentially automatic, needing little supervision once started. For the purpose of description, it can be divided into three separate units, each having its own distinct operation. They are (1) dilatometer, (2) furnace, and (3) instruments for temperature measurement and control. Figure 1 illustrates the assembled apparatus used for the determination of thermal length changes.

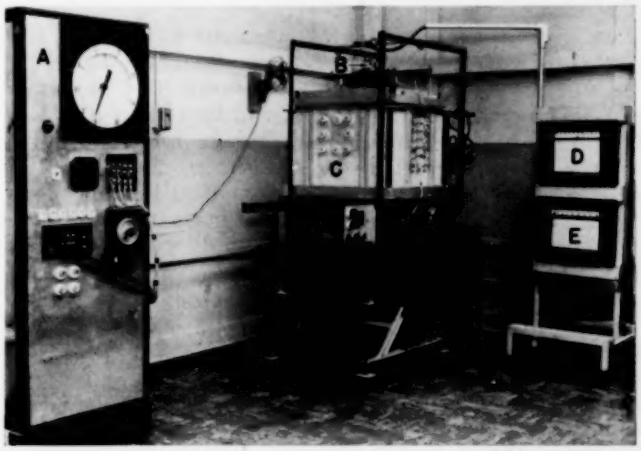

FIGURE 1. *Assembled apparatus used for determining thermal length changes.*

(A) Program controller; (B) dilatometer assemblies; (C) furnace; (D) differential length change recorder; (E) temperature recorder.

[1] Figures in brackets indicate the literature references at the end of this paper.

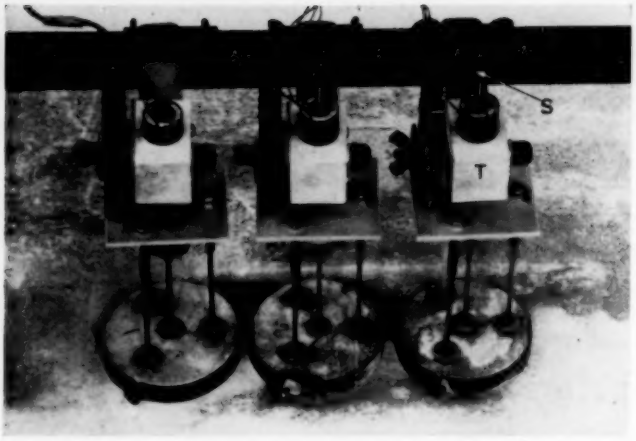

FIGURE 2. *Upper portion of dilatometer assemblies.*

(S) Spring that restrains upper portion of dilatometer assembly from horizontal but not from vertical movement; (T) differential transformer and mounting. The three outer sapphire rods support the mounting. The center rod connects armature to top of specimen.

3.2. The Dilatometer

Figures 2 and 3 show the assembly of parts for the dilatometer. Except for the use of a differential transformer in place of a dial indicator, the entire assembly is similar to that described by Geller and Yavorsky [4]. The transformer is preferable for this application because of its automatic recording features. Also, its internal frictional forces and its force exerted on the specimen are only a fraction of those produced by the dial indicator. Kelly and Harris [5] have reported expansion equipment that also utilizes differential transformers in a similar manner.

The theory and operation of the differential transformer are described in detail in various bulletins and manuals [6, 7]. In essence, the transformer consists of a primary coil, a secondary coil, and a permeable armature. The armature is attached directly to a sapphire rod, which in turn rests on top of the specimen. As the specimen expands or contracts, the armature correspondingly moves axially in the coils, thus generating a signal proportionate to the differential length change between the specimen and the sapphire rods. This signal, when amplified and balanced, is recorded on the strip chart of the differential length-change recorder (fig. 1 (D)). The percentage of thermal expansion or contraction was calculated from these data and corresponding temperature measurements. The sensitivity of the differential length-change measurements was considered to be 0.0005 in., and the accuracy was estimated to be ± 0.0005 in.

3.3. The Furnace

The furnace, a box-like structure composed of insulating firebrick suitable for use at 3,000° F, encased in a Transite and steel framework, (fig. 1 (C)) contained a chamber of 6½ in. wide, 13 in. long and 13½ in. deep. In order to obtain uniform temperatures, the furnace utilized 16 silicon-carbide heating rods, 14 horizontal and 2 vertical, systematically spaced in the chamber. A variable transformer capable of supplying 50 amp at 270 v to the heating rods enabled the furnace to attain temperatures up to 1,500° C. A total of three dilatometer assemblies, each holding one specimen, can be heated simultaneously in this furnace. Figure 3 incidates the relative position of one specimen and dilatometer assembly in this furnace.

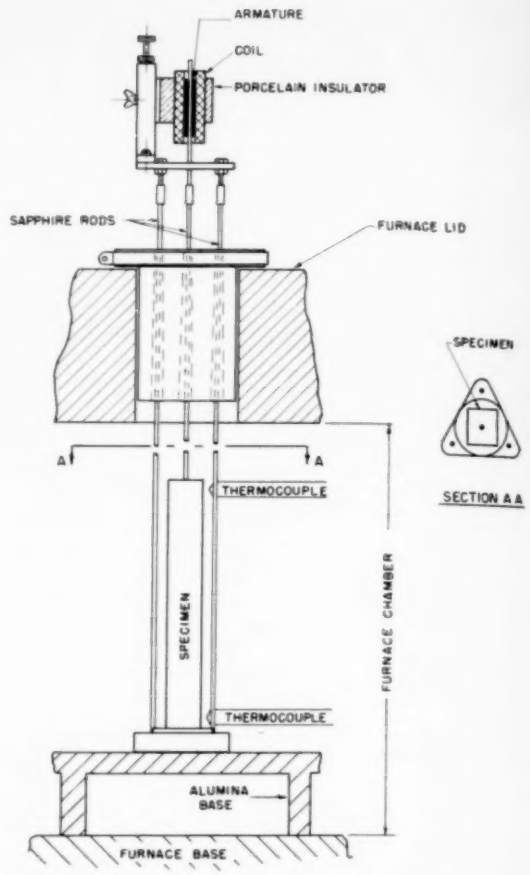

FIGURE 3. *Schematic diagram of a dilatometer assembly and related parts.*

One of the three sapphire rod supports is not shown in the vertical section.

3.4. Temperature Measurement and Control

A circle-chart-recording potentiometer with a cam-type program attachment, (fig. 1 (A)) regulated furnace temperatures. Temperatures near the specimens were recorded on a six-point strip-chart recorder by means of six noble-metal thermocouples. The sensitivity and accuracy of the temperature measurement were estimated at 3 deg and ± 5 deg C, respectively. The relative positions of the thermocouples and specimen are indicated in figure 3. A few additional temperature readings obtained by means of thermocouples placed near the midpoint

of the specimens indicated that the vertical temperature gradient was approximately linear. The vertical gradient ranged between 5 deg and 15 deg C over a 7-in. span.

4. Experimental Procedure

All specimens were first cured for 24 hr at 21° C and 95-percent relative humidity, then air-dried for at least 3 months and finally heat treated at either 110°, 1,050°, or 1,300° C.[2] Specimens initially subjected to the latter two heat treatments were fired in a gas furnace at a rate of 37.5 deg C/hr with a 5-hr soaking period at the top temperatures. The furnace and specimens were cooled naturally to room temperature. For the 1,050° and 1,300° C heat treatments, the specimens were set in muffles.

Prior to the actual expansion determination, each specimen was dried overnight at 110° C, cooled, and then measured for length. Immediately following the length measurements, the specimens, specimen holders, differential transformers, and related parts were positioned in the furnace as shown in figure 3 and figure 1(B). The furnace temperature was raised by using a control cam that called for a 100-deg C rise per hour, with a 15-min holding period at each 100-deg C interval and at 250° and 550° C. After a 15-min holding period, the temperature existing in the specimen approached but did not attain the temperature indicated by the thermocouples. This error affected the results to approximately the same extent as the error in measuring length changes. When the strip chart of the recorder (fig. 1(D)) indicated a differential length change of at least 0.0005-in./min the furnace was shut off and allowed to cool to room temperature. The temperature at which this rate of differential length change occurred was called the "deformation temperature." Temperatures and differential changes in length were recorded, (figs. 1(D) and (E)) during both heating and cooling. One specimen, or more, from each heat treatment was tested in this manner.

The same procedure was followed in obtaining necessary calculation and calibration data. The following equation was used throughout this investigation for the calculation of thermal length changes at any given temperature:

$$S=\frac{100R}{L}+A,$$

where

S=percentage length change,
R=differential length change in inches, as indicated by recorder (fig. 1(D)),
L=specimen length in inches at room temperature following 110° C heat treatment,
A=percentage expansion for sapphire taken from figure 4.

[2] Percentage permanent linear-change values due to similar heat treatments determined on other specimens were reported previously by Heindl and Post [3].

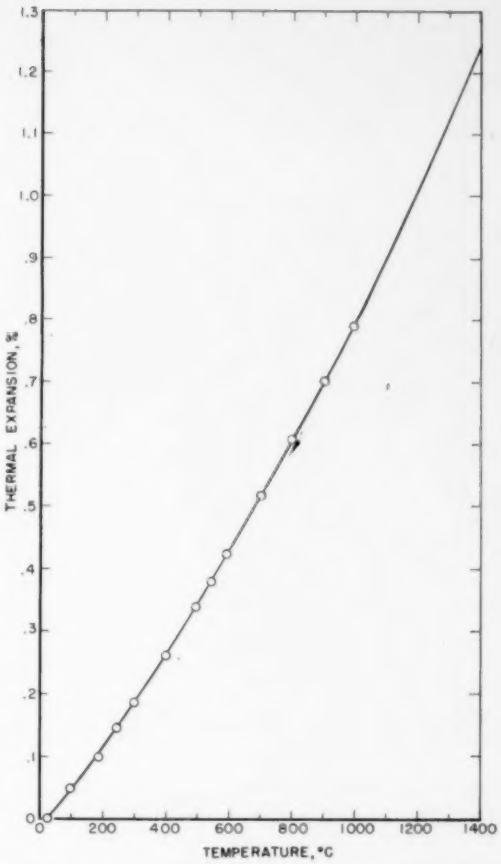

FIGURE 4. *Thermal-expansion curve for one-eighth-inch-diameter sapphire rod measured along an axis 62°30′ ± 1°30′ from C-axis.*

Figure 4 was obtained from expansion tests conducted with the dilatometer, using a fused-silica specimen as a reference material. Expansion values above 1,000° C were extrapolated. The difference between these results and those obtained by others [4] did not exceed 0.0002 in./in. This discrepancy could be attributed to differences in rod orientation.

5. Results

Thermal length changes of neat high-alumina cement, commercial brands[3] of castables, and laboratory-prepared castables are illustrated graphically in figures 5 through 12. All curves show the changes exhibited during complete heating and cooling cycles.

Repeated tests made on either fused-silica or polycrystalline alumina specimens proved the reproducibility of data. The difference in results obtained on these specimens from test to test was within experimental error. Figure 6 indicates the

[3] The length-change curves of only 5 of the 14 commercial brands tested are reported in this paper. The five brands were considered typical of the entire lot.

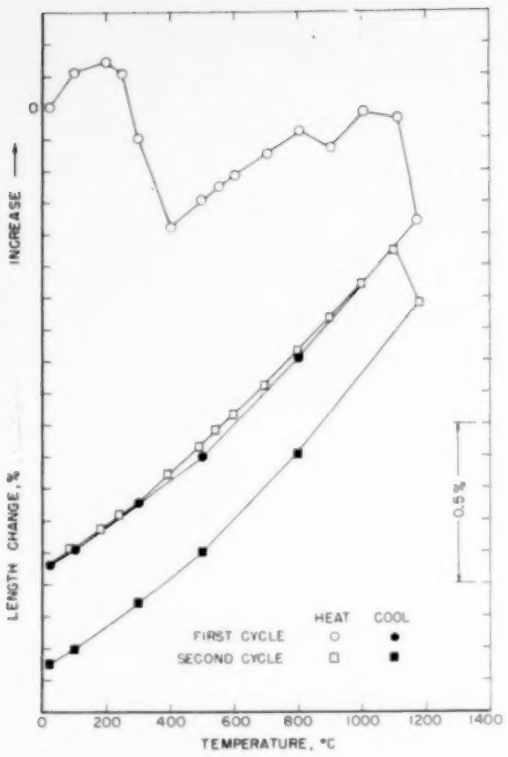

FIGURE 5. *Thermal length changes of neat high-alumina cement after being cured for 28 days in a "fog room" and heat treated at 110° C.*

Length-change values were determined by W. L. Pendergast and S. F. Holley, National Bureau of Standards.

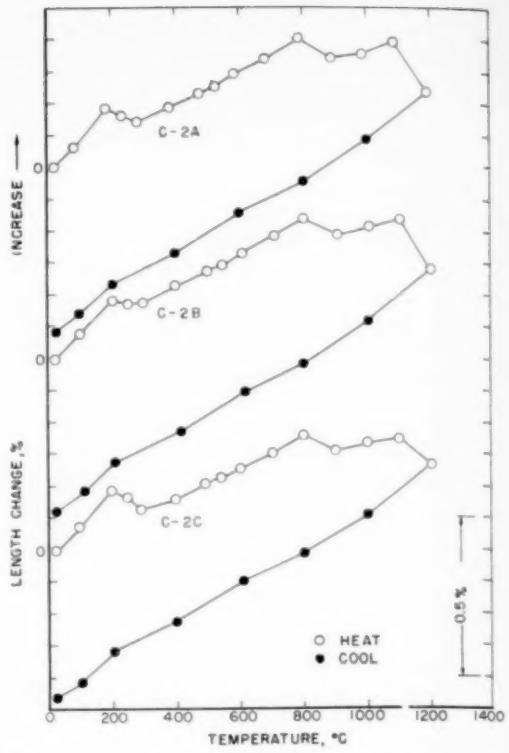

FIGURE 6. *Thermal length changes of a commercial castable heat treated at 110° C.*

Curves C-2A, C-2B, and C-2C represent three specimens cut from one bar, which was cast as a unit.

reproducibility of results obtained on three specimens of ostensibly the same castable material. Small, but significant differences in the length change curves of these specimens are apparent.

6. Discussion of Results

6.1. Neat Cement

The thermal length-change characteristics of a neat high-alumina cement would influence the expansion or contraction properties of any castable, heat treated at 110° C, in which the cement is a constituent. Examination of the curve showing length changes of neat high-alumina cement during the first heating (fig. 5) reveals two features that appear as characteristics of both neat cement and castables. They are (1) rapid contraction occurring between 200° and 400° C, and (2) a lesser contraction between 800° and 900° C.

Due to the complex nature of high-alumina cement, there is no general agreement as to its exact constitution. Wells found that anhydrous high-alumina cement contained $CaO{\cdot}Al_2O_3$ and $3CaO{\cdot}5Al_2O_3$ as its major constituents, and $2CaO{\cdot}SiO_2$ and iron compounds as its minor constituents [8]. Petrographic examination of the cement used in this investigation revealed that it was composed essentially of monocalcium aluminate, tetracalcium aluminoferrite, and glass (uncrystallized material) [2]. It is assumed that the cement, when hydrated, cured, and air-dried, contains varieties of hydrated alumina and hydrated calcium aluminates, possibly gibbsite ($Al_2O_3{\cdot}3H_2O$) or hydrated amorphous alumina, together with one or more hexagonal calcium aluminate hydrates and perhaps tricalcium aluminate hexahydrate ($3CaO{\cdot}Al_2O_3{\cdot}6H_2O$) [8]. These compounds have also been found by Wells et al., in their study of the CaO-Al_2O_3-H_2O system [9].

On the basis of these assumptions, explanation can be offered for the rapid contractions that occur between 200° and 400° C and between 800° and 900° C. It is logical to assume that the first contraction (200° to 400° C) is caused by the loss of water of hydration. This is substantiated by differential thermal analysis and by water-loss curves obtained in different investigations [3, 10]. Gibbsite, by losing its water of hydration, converts to the amorphous form of alumina, provided it is intimately mixed with the other hydrated cement constituents [11, 12]. It is noteworthy that studies by Peppler and Wells [13] indicated that boehmite ($Al_2O_3{\cdot}H_2O$) may be intermediately formed before the amorphous variety. Definite conclusions applicable to this particular investigation cannot be made because their work was performed above atmospheric pressure.

Gibbsite, when heated alone to temperatures as low as 600° C, apparently is converted to γ alumina. Insley suggested that a greater "activation energy"

and a higher "threshold temperature" are required for this conversion when the amorphous alumina molecules are separated by rigid silica molecules, as they are in dehydrated kaolin [11]. The effect of the silica on the amorphous alumina conversion is evidently repladed by the effect of intimately mixed dehydrated calcium aluminates on the conversion of amorphous alumina in high-alumina cement. Differential thermal-analysis curves of dehydrated kaolin [11] and dehydrated high-alumina cement [3] show that the γ-alumina conversion is retarded until approximately 900° C. Comparison of these differential thermal-analysis curves with the length-change curve of high-alumina cement (figure 5) seem to offer evidence that the contraction occurring between 800° and 900° C is caused by the conversion of amorphous alumina to γ alumina. X-ray patterns taken on samples of neat high-alumina cement that had been heated to either 700° or 900° C, and then air-quenched, showed no perceptible γ alumina. However, petrographic examination [4] of the 900° C sample did indicate material was present with an index of refraction similar to that of γ alumina. It could not be identified positively. The 700° C sample, when analyzed petrographically, contained no identifiable γ alumina.

6.2. Aggregate

The aggregate that is used in combination with cement to form refractory castables may vary in type and proportion, dependent on the desired end product. Calcined fire clays, blast-furnace slag, chrome ore, and varieties of crushed firebrick have all been used as the aggregate. Perhaps the aggregate most commonly employed in castables is crushed firebrick. Expansion curves of various firebricks and fire clays are reproduced in numerous articles and books [1, 14, 15]. The outstanding feature of the curves given in these references for the aggregates used in this investigation is the indication that silica is present as a major constituent. Thus, it can be expected that the changes in slope associated with silica inversions might also be present in the length-change curves of the castables.

6.3. Castables, Heat Treated at 110° C

Because a refractory castable is a heterogeneous mixture of a hydraulic high-alumina cement and a heat-resistant aggregate, its thermal-expansion and contraction properties are, except where reactions between the two occur, a composite of the properties of the two separate ingredients. The curves of the laboratory-prepared castables that had been heat treated at 110° C (fig. 8) show the effects of varying percentages of cement.

Although no castable duplicated another in its length-change properties, a definite trend or pattern for each heat treatment is evident at temperatures below 1,100° C. Common characteristics illustrating this general trend, for the 110° C heat-treatment group, are shown by figures 6, 7, and 8. By correlation of data, it is evident which length-change phenomena of castables can be attributed to the cement and which to the aggregate. The 200° to 300° C and the 800° to 900° C contractions, prevalent throughout these typical curves, are caused by cement reactions, namely, the loss of water of hydration and the conversion of amorphous alumina to the γ variety, respectively. Similarly, below 1,100° C, the aggregate is responsible for other noticeable features of the length-change curves, such as the changes in slope occurring in the room temperature to 200° C range. These changes appear to be due to inversions of tridymite and/or cristobalite. Published articles [1, 16] on the expansion properties of silica corroborate this conclusion.

Above 1,100° C, deviation from the general trend is apparent. When rapid contraction occurs, as shown in figures 7 (C–11) and 8 (C, D), normal sintering is taking place. Examination of photomicrographs showed that those castables heated by Heindl [3] at 1,350° C contained very porous material between the aggregate particles. This would indicate that a denser phase, such as a variety of glass, had been formed. The reasons for rapid contraction and subsequent expansion, as illustrated by figures 7 (C–13) and 8 (E), are debatable. A possible explanation is presented by petrographic analysis, which showed that a recrystallization process had occurred at the higher temperatures. These crystals were too small for positive identification [3]. Entrapped gas could possibly cause sudden expansion, or "bloating", at the higher temperatures. However, the common characteristics associated with "bloating" were not apparent.

Reaction between the cement and the aggregate definitely occurred above 1,100° C. This was clearly shown by photomicrographs and petrographic analyses [3]. Although there was no noticeable reaction in the castables heated at 1,050° C, there was considerable evidence of it in those heated at 1,350° C. Amorphous and glassy material, as well as the aforementioned crystals, were present in abundance.

The refractoriness of the castables depended upon the percentages of cement, as indicated by figure 8. Apparently the greater the cement percentage, the less refractory the castable. Table 1 better illustrates this point.

TABLE 1. *Comparison of "deformation temperatures" with the composition of the laboratory-prepared castables of figure 8*

Castable	Heat treatment	Aggregate	Cement	Deformation temperature [a]
	°C		%	°C
A	110	Firebrick	30	−1,265
B	110	do	20	+1,280
C	110	do	10	−1,320
D	110	Flint clay	30	−1,260
E	110	do	20	+1,310
F	110	do	10	−1,345

[a] "Deformation temperature" is here defined as the temperature at which the specimen expanded or contracted at the rate of 0.0005 in./min. (−) indicates contraction, (+) indicates expansion.

[4] The X-ray pattern of the 900° C sample was furnished by A. Posner, Research Associate, American Dental Association at National Bureau of Standards. The other X-ray pattern and all petrographic analyses were furnished by A. Van Valkenburg and G. Ugrinic, Mineral Products Division, National Bureau of Standards.

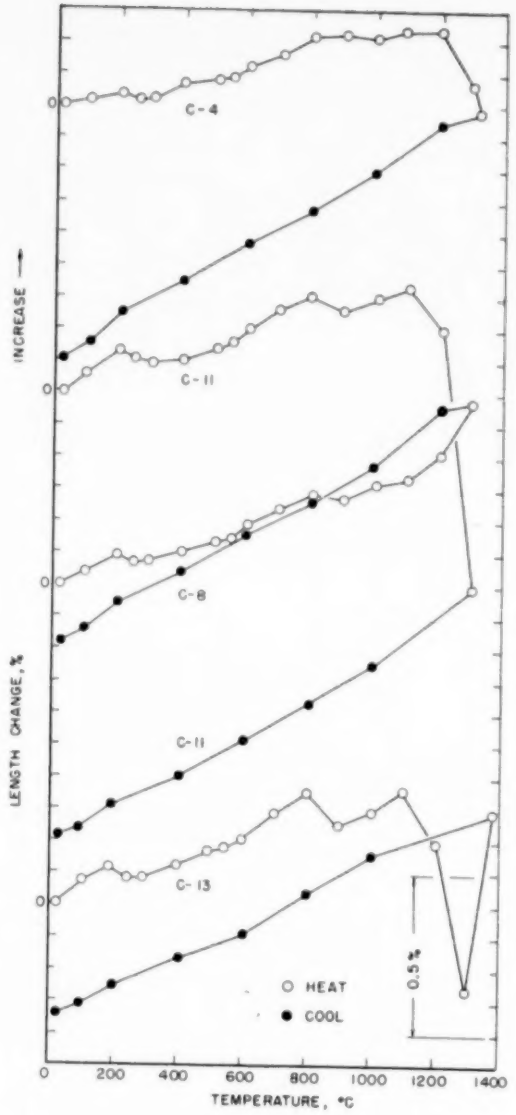

FIGURE 7. *Thermal length changes of four commercial castables heat treated at 110° C.*

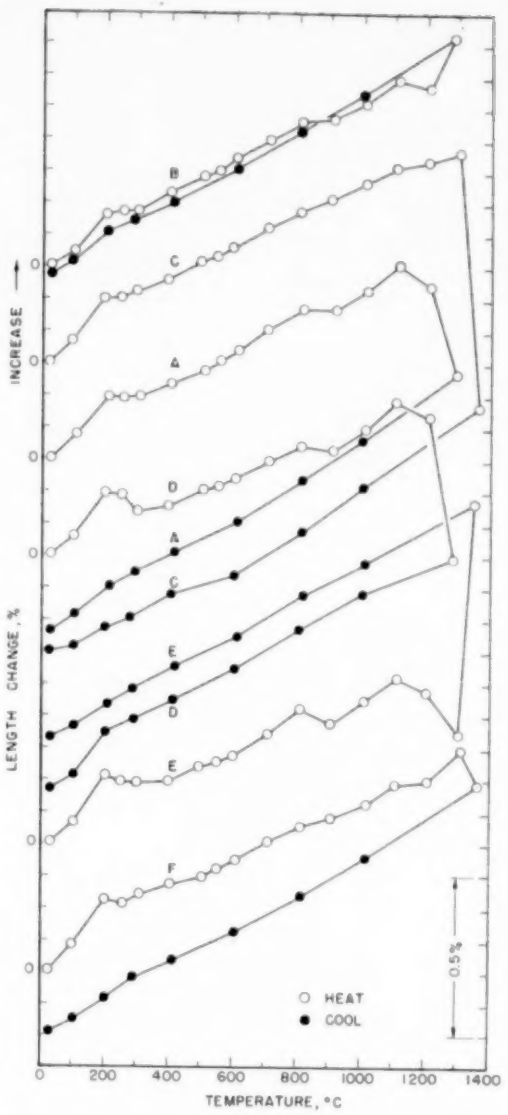

FIGURE 8. *Thermal length changes of laboratory-prepared castables heat treated at 110° C.*

Castables A, B, and C contained crushed firebrick aggregate and 30, 20, and 10 percent of high-alumina cement, respectively. D, E, and F contained calcined flint-clay aggregate and 30, 20, and 10 percent of high-alumina cement respectively.

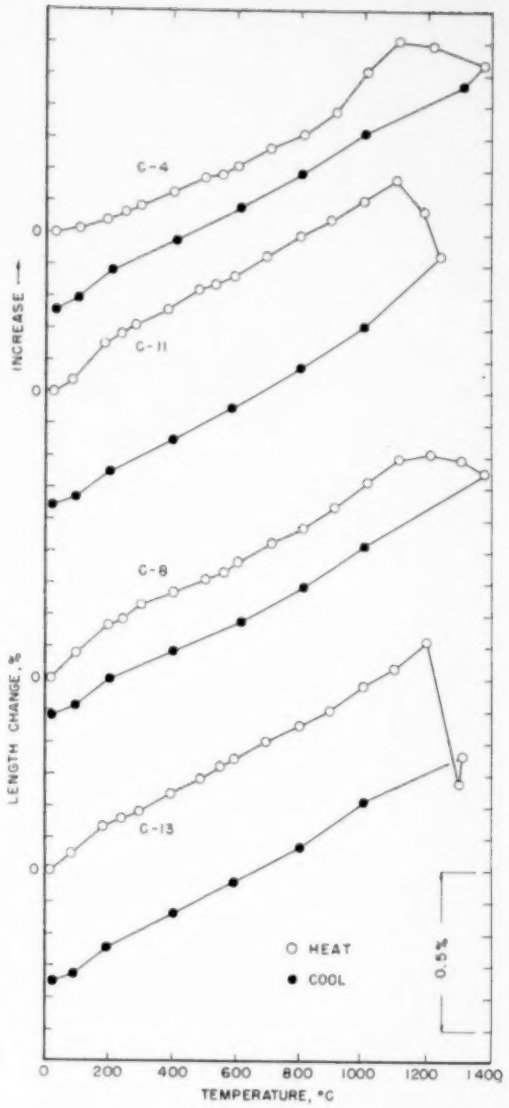

FIGURE 9. *Thermal length changes of four commercia castablesl heat treated at 1,050° C.*

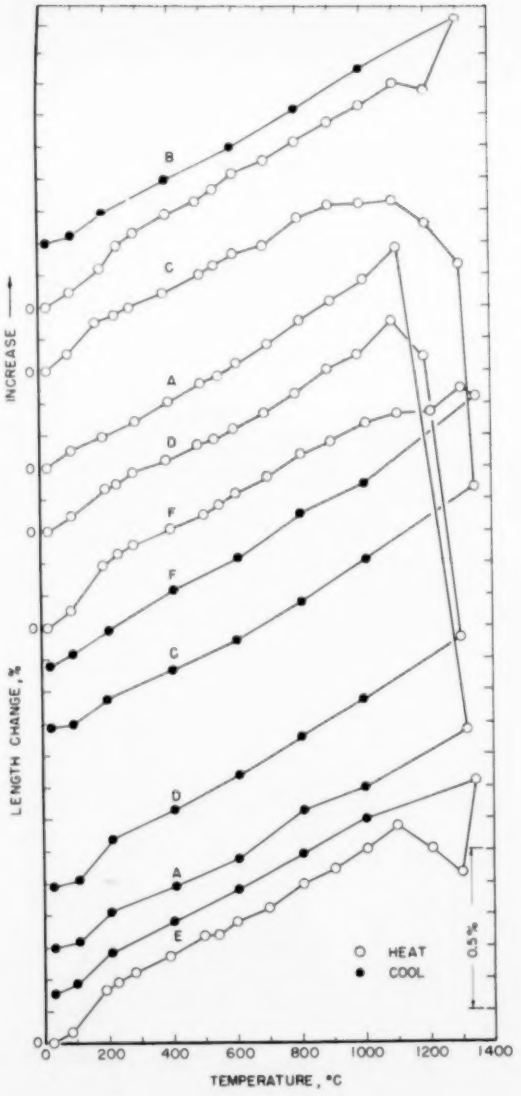

FIGURE 10. *Thermal length changes of laboratory-prepared castables heat treated at 1,050° C.*

Castables A, B, and C contained crushed firebrick aggregate and 30, 20, and 10 percent of high-alumina cement respectively. D, E, and F contained calcined flint-clay aggregate and 30, 20, and 10 percent of high-alumina cement respectively.

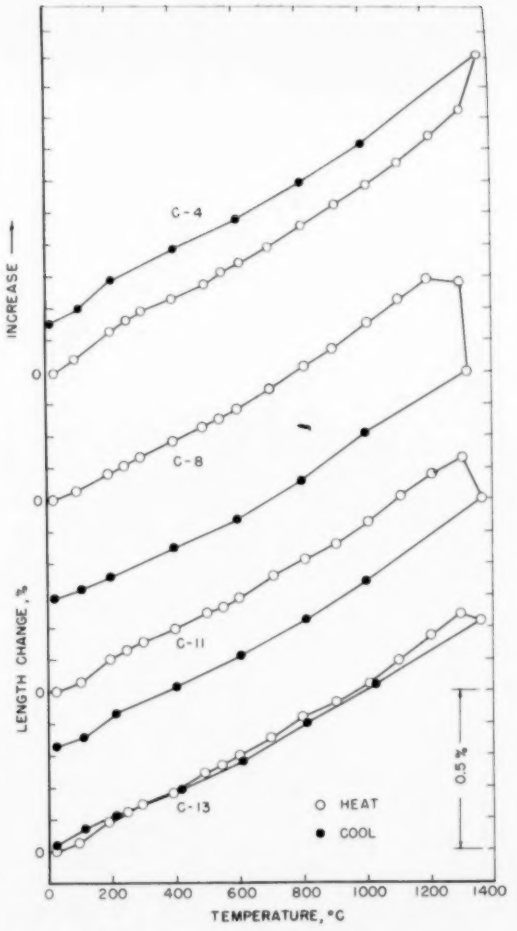

FIGURE 11. *Thermal length changes of four commercial castables heat treated at 1,300° C.*

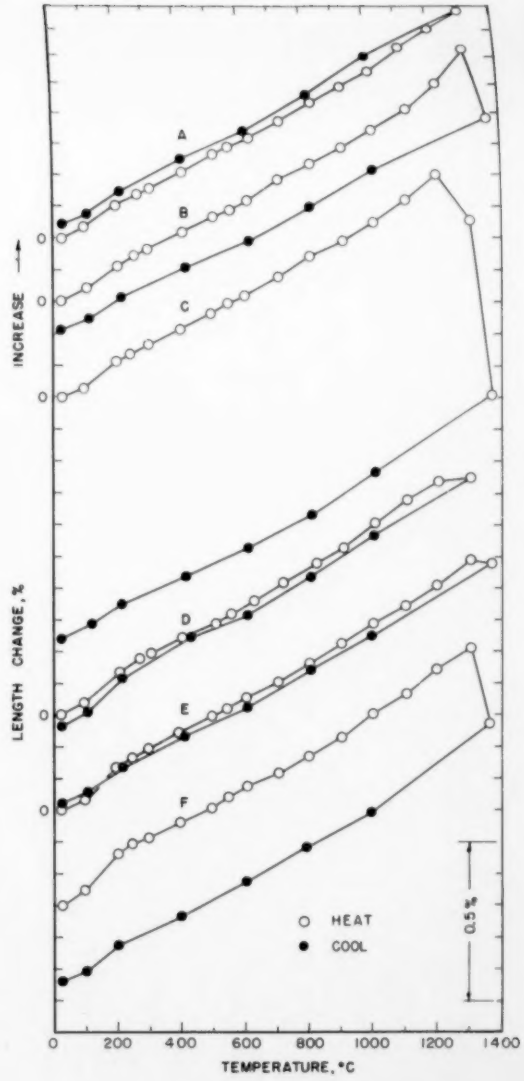

FIGURE 12. *Thermal length changes of laboratory-prepared castables heat treated at 1,300° C.*

Castables A, B, and C contained crushed firebrick aggregate and 30, 20, and 10 percent of high-alumina cement, respectively. D, E, and F contained calcined flint-clay aggregate and 30, 20, and 10 percent of high-alumina cement, respectively.

6.4. Castables, Heat Treated at 1,050° or 1,300° C

The length-change curves of those castables heat treated at 1,050° C (figs. 9, 10) or 1,300° C (figs. 11, 12) indicate that a general trend or pattern is again apparent at temperatures below 1,100° C. Length-change characteristics common to most of the curves, best illustrated by figures 9(C–11) and 12(F), are the changes in slope that occur between room temperature and 200° C. These changes again indicate the presence of a combination of tridymite and cristobolite. Examination of typical 1,050° or 1,300° C length-change curves show that the contractions between 200° and 300° C and between 800° and 900° C (figs. 7 and 8), have been eliminated by heating at elevated temperatures. Because these contractions were permanent and nonreversible, they obviously would not appear after the specimens had experienced either a 1,050° or a 1,300° C heat treatment. Above 1,100° C, castables previously heat treated at 1,300° C reacted somewhat differently from those heat treated at 110° or 1,050° C. Castables heat treated at the latter temperatures (figs. 7, 8, 9, 10) exhibited the same general characteristics above 1,100° C. Those heat treated at 1,300° C (figs. 11, 12) either expanded or contracted, but never did both.

7. Summary

The thermal length-change properties of commercial brands of refractory castables and laboratory-prepared castables were determined by using dilatometer assemblies that incorporated differential transformers as their sensing or indicating device. The effect of heat treatment was shown by length-change determinations on castables initially heat treated at 110°, 1,050°, or 1,300° C. The data are presented graphically. For comparative purposes, the curve for neat high-alumina cement is included.

Examination of the data indicates that the same general length-change characteristics were exhibited by castables that had received the same curing and heat treatment.

Below 1,100° C, the thermal length-change properties of those castables heat treated at 110° C were influenced by the original properties of their constituents, high-alumina cement and heat-resistant aggregate. Length-change curves of this castable group distinctly indicate length changes associated with reactions of the cement, especially the loss of water of hydration and the conversion of amorphous alumina to γ alumina, and silica inversions of the aggregate.

Typical curves of both the 1,050° and 1,300° C groups indicated possible silica inversions. However, the length changes related to cement reactions were absent from these curves. As evidenced by curves of all three groups, sintering of the castables began only at temperatures above 1,100° C.

8. References

[1] F. H. Norton, Refractories, p. 482 (McGraw-Hill Book Co., Inc., New York, N. Y., 1949).

[2] R. A. Heindl and Z. A. Post, Refractory castables: Preparation and some properties, J. Amer. Cer. Soc. [7] **33,** 230 (1950).

[3] R. A. Heindl and Z. A. Post, Refractory castables: II, some properties and effects of heat-treatments, J. Amer. Cer. Soc. [5] **37,** 206 (1954).

[4] R. F. Geller and P. J. Yavorsky, Effects of some oxide additions on the thermal length changes of zirconia, J. Research NBS **35,** 87 (1945) RP1662.

[5] H. J. Kelly and H. M. Harris, An automatically recording thermal-expansion apparatus, J. Amer. Cer. Soc. [10] **39,** 344 (1956).

[6] Automatic Temperature Control Co., Inc., Phila., Pa., Bul. R–30.

[7] Automatic Temperature Control Co., Inc., Phila., Pa., Instruction manuals.

[8] L. S. Wells, Reaction of water on calcium aluminates, BS J. Research **1,** 951 (1928) RP34.

[9] L. S. Wells, W. F. Clarke and H. F. McMurdie, Study of the system $CaO–Al_2O_3–H_2O$ at temperatures of 21° and 90° C, J. Research NBS **30,** 367 (1943) RP1539.

[10] M. L. Longchambon, Les Bétons Refractaires, Mémoires, Société des Ingénieurs Civils de France, Cent-Huitiéme Année, Fascicule II, Mars-Avril (1955).

[11] H. Insley and R. H. Ewell, Thermal behavior of the kaolin minerals, J. Research NBS **14,** 615 (1935) RP792.

[12] R. Roy, D. M. Roy and E. E. Francis, New data on thermal decomposition of kaolinite and halloysite, J. Am. Ceram. Soc. [6] **38,** 198 (1955).

[13] R. B. Peppler and L. S. Wells, The system of lime, alumina, and water from 50° to 250° C, J. Research NBS **52,** 75 (1954) RP2476.

[14] R. A. Heindl, The thermal expansion of refractories to 1,800° C, BS J. Research **10,** 715 (1933), RP562.

[15] R. A. Heindl and W. L. Pendergast, Fire clays; Some fundamental properties at several temperatures, BS J. Research **5,** 213 (1930) RP194.

[16] R. P. Hall and H. Insley, Phase diagrams for ceramists, J. Am. Ceram. Soc., pt. II, fig. 25 (1947).

Washington, April 5, 1956.

Journal of Research of the National Bureau of Standards Vol. 59, No. 1, July 1957 Research Paper 2769

Precise Intercomparison of Acids by Differential Potentiometric Titration with Hydrogen Electrodes*

Roger G. Bates and Edward Wichers

The purity of two preparations of benzoic acid, three of oxalic acid, and three of potassium hydrogen phthalate has been compared by a precise determination of the equivalence of each substance with the same solid reference base, sodium carbonate, the only requirements for which were that its composition be uniform and remain constant throughout the series of measurements. The inflection point in each titration was determined by a differential potentiometric method utilizing two hydrogen electrodes. The procedure, which gives a degree of precision greater than has previously been reported for acidimetric determinations, is described in detail. When about 0.06 equivalent of acid was used in each titration, the reproducibility attainable was better than 0.002 percent. The failure of the inflection point and the equivalence point to coincide exactly has been considered in evaluating the reliability of the procedure.

The purity of one of the samples of benzoic acid, as determined independently from accurate measurements of the freezing point, was 99.997 mole percent. Single crystals of benzoic acid grown from a melt of this material were selected as a reference acid and were regarded to have a purity of 100.000 percent. In terms of this reference, a preparation of potassium hydrogen phthalate consisting of optically perfect crystals was found to have a purity of 100.000 percent. The method is adaptable to a variety of acids and bases and, hence, provides an additional criterion of purity for these substances.

1. Introduction

In order to increase the accuracy attainable in the titration of acids and bases, it is desirable to have precise methods for evaluating the purity of the several substances that are commonly employed as acidimetric and alkalimetric standards. The composition of such standard substances can often be assessed most conveniently and directly by an acid-base titration, and the internal consistency of a series of acidic or basic standards can only be satisfactorily demonstrated when these procedures are developed to a high degree of precision.

The ordinary simple titration of an acidic substance with a solution of a strong alkali is beset by several well-recognized hazards. Among these are contamination of the solution with atmospheric carbon dioxide; drainage and calibration errors, where volumetric techniques are employed; a change in the titer of a standard solution of alkali; and the disparity between the change point of a chemical indicator and the true equivalence point of the acid-base reaction. Although the accuracy of each titration may, nonetheless, approach 1 part in 10,000, errors are often compounded by the necessity of combining the results of 2 or 3 separate operations to obtain the desired assay value.

The differential electrometric titration developed by MacInnes and Cowperthwaite [*1,2*][1] represents the most significant advance in the technique of acid-base titrations that has been reported up to the present time. In their procedure, an accurately weighed quantity of a solution of sodium hydroxide sufficient to neutralize about 99.7 percent of the acid was allowed to react with the solid sample of the acidic substance. The resulting solution was washed into the differential titration vessel and the exact inflection point established by addition of a dilute solution of alkali. The results showed that the method is capable of greater accuracy than is ordinarily attained in acidimetric titrations, even when these are performed with great care.

In the present work, the purity of solid acidic substances has been compared by determining the equivalence of each with a solid reference base, sodium carbonate, the only requirements for which were that its composition be uniform and remain constant throughout the series of measurements. The final adjustment to the inflection point was made, as in the earlier work, by adding a dilute solution of sodium hydroxide. Eight preparations of three acidic substances of unusual analytical interest were selected. These were samples of benzoic acid, oxalic acid, and potassium hydrogen phthalate. The establishment of the inflection point by differential means was studied and certain refinements introduced.

2. Experimental Procedures

2.1. Materials

The anhydrous sodium carbonate used in all of the work was a finely granular product, offered by the manufacturer as a "Primary Standard". When the preparations for a series of titrations were being made, an amount of the carbonate sufficient for the series was placed in covered platinum dishes and heated in a muffle furnace at 350° to 400° C for 3 to 4 hr, with occasional stirring. It was essential that the carbonate be homogeneous. Hence, before the salt had cooled to room temperature, it was mixed thoroughly by tumbling on glazed paper and was then bottled and stored in a desiccator.

*Presented before the XVth International Congress of Pure and Applied Chemistry, Lisbon, September 1956.

[1] Italicized figures in brackets indicate the literature references at the end of this paper.

423777—57——2

Two preparations of benzoic acid, three of oxalic acid, and three of potassium hydrogen phthalate were intercompared, these were designated 1 B, 2 B, 1 Ox, 2 Ox, 3 Ox, 1 P, 2 P, and 3 P. The preparation and purity-evaluation of these substances are described in the following paragraphs.

1 B. Benzoic acid, coarsely granular, from a lot prepared as a reference material for specific-heat calorimetry. The method of purification of this substance, by fractional freezing, and the subsequent treatment to remove water and gases trapped in the crystalline material were the same as those used in preparing the acid for use in thermometric standards issued by the National Bureau of Standards. These procedures are described in two earlier publications [*3,4*]. In fact, the final treatment of the acid and one of the assays for purity were conducted in thermometric cells of the kind described in the second of these publications [*4*]. The purified acid was transferred from the cells by melting and pouring into platinum dishes, which were stored over phosphorus pentoxide until the acid was frozen, to prevent absorption of moisture by the somewhat hygroscopic liquid acid. The purity of the acid, as estimated from its observed freezing temperature in the thermometric cells, was 99.997 mole percent. The acid was congealed in the platinum dishes and then crushed in an agate mortar and sieved through bronze sieves. The portion used was that passing through a No. 10 sieve (U. S. Standard Sieve Series) and retained on a No. 50 sieve. Benzoic acid in this form is not appreciably hygroscopic in the range of humidities experienced in Washington.

The evaluation of purity referred to above was made by comparing the freezing temperature with that of another lot that had been subjected to more exhaustive purification and whose triple-point temperature was the highest ever observed for benzoic acid at the Bureau. Such a comparison is less sensitive and, in general, less accurate than an evaluation based on observation of the changes of temperature as the substance progressively freezes or melts. Calorimetric observation of the melting curve, that is, measurement of the heat capacity of a substance in the temperature range just below its final melting or initial freezing temperature, is commonly regarded as being the most sensitive and the most reliable means of determining the content of liquid-soluble, solid-insoluble impurities in a substance. This procedure was applied to a portion of the granular product prepared in the manner described. A quantity sufficient to fill a platinum calorimeter vessel [*5*] was transferred to a glass ampoule, whose neck was sealed to the calorimeter vessel. After evacuation of the assembled apparatus, the benzoic acid was melted and allowed to flow by gravity into the platinum vessel, which was then separated from the glass ampoule by flame-sealing.

By the calorimetric procedure, the benzoic acid was found to have a purity of 99.999 mole percent. On the basis of extensive experience with benzoic acid, it is believed that the acid used did not contain impurities of the solid-solution, or mixed-crystal, type in sufficient amount to invalidate the purity estimates of 99.997 and 99.999 mole percent as representing the actual approach to ideal purity that was attained with this substance.

2 B. Benzoic acid, prepared by further purification of the material represented by 1 B. For this preparation the starting material (1 B) was transferred by sublimation to a glass vessel designed for growing single crystals of low-melting substances from their own liquids.[2] The capacity of this vessel was about 500 ml. After the acid was melted, the vessel was slowly lowered, by a clockwork, through a bath composed of two immiscible liquids. The lower layer was maintained at about 100° C and the upper layer at 150° C. There was a sharp discontinuity of temperature at the boundary. As the conical tip of the container passed through this boundary, one, or at most a very few, crystal nuclei were formed, from which growth continued as the vessel was progressively lowered through the temperature boundary. By this procedure, impurities tended to be rejected into the remaining liquid and were thus concentrated in the portion of the sample that was the last to freeze.

In this instance, crystal growth was allowed to proceed at the rate of 0.4 mm/hr. The total time of freezing was about 3 weeks. When the operation was completed, the vessel was inverted in the bath and heat applied in such a way as to remelt the small portion that was the last to freeze. This liquid was allowed to flow into a bulb in the stem. After the bulb was sealed off, the vessel was restored to its normal position, the remaining solid was remelted, and the entire operation repeated. The final solid consisted of a large single crystal associated with another portion in which twinning occurred. The vessel was cut open and the single-crystal portion separated from the remainder. The portion of this that was the last to freeze was cut off and the rest transferred to an envelope of platinum foil which was then sealed by gold-soldering so as to exclude further contact with air. The solid acid was crushed to a powder by compressing the foil envelope in a vise.

This preparation of benzoic acid was considered to have ideal purity, subject to the assumption, based on collateral experience, that it did not contain significant impurities present in solid solution. For the purposes of comparison with other acidic substances by titration, it is regarded in this paper as having the exact composition $C_6H_5CO_2H$.

1 Ox. Anhydrous oxalic acid, finely crystalline, prepared by dehydration of a recrystallized hydrated acid. Dehydration was accomplished by heating at 60° C in a vacuum desiccator under a pressure of 1 mm of mercury. After 7 days, the dehydrated material was ground in a mortar and the powdered acid returned to the desiccator for 7 days at 60° C. The product was transferred to weighing bottles and weighed in an atmosphere of 15- to 25-percent relative humidity. The purpose of this and the other oxalic

[2] The apparatus and procedure will be described in a forthcoming publication.

acid preparations was to find whether a substance closely approaching the exact composition $H_2C_2O_4$ could be obatined.

2 Ox. Anhydrous oxalic acid identical with 1 Ox, except that after transfer to weighing bottles, and before weighing, the acid was again placed in a vacuum desiccator at 60° C for 18 hr. The vacuum was broken with dry air and the bottles capped immediately.

3 Ox. Anhydrous oxalic acid prepared by dehydrating at 60° C a product of reagent quality, contained in a flask sealed to a receiving tube, under constant evacuation with a mercury-diffusion pump. After heating at 60° C for 28 hr, the dehydrated acid was warmed to 100° C, whereupon it slowly sublimed into the receiving tube during a period of 48 hr. After transfer to the weighing bottles, but before the weighings were made, the acid was dried again in vacuum at 60° C for 18 hr.

1 P. Potassium hydrogen phthalate. The product used was that issued by the National Bureau of Standards as Standard Sample 84d, a standard for acidimetry. This is a granular material containing numerous very small inclusions of the solution from which the substance was crystallized. The water in these inclusions can be removed virtually completely by crushing the crystals to a rather fine powder and drying at about 100° C. A sufficient amount of the granular standard was crushed and dried in the manner described and stored in a desiccator. This substance is not appreciably hygroscopic in the range of humidities experienced in Washington.

2 P. Potassium hydrogen phthalate. This preparation consisted of portions selected from large single crystals of the substance. These crystals were grown, by the falling-temperature method, in a filtered solution of material identical with 1 P. The growing time was about 45 days, and each of the final crystals weighed between 10 and 25 g. The purpose was to eliminate those impurities, including water, that are known or presumed to be present as entrapped mother liquor in the granular material and, by greatly increasing the ratio of volume to surface, to minimize impurities of the type that may be adsorbed on the surface of the granular crystalline product. These are two important sources of impurities in crystalline substances. The recrystallization could not be expected to change materially the content of impurities present in solid solution. From the relatively high purity of the granular material, as determined by the conventional acidimetric assay, this category of possible impurities was thought not to be important.

The large orthorhombic single crystals were not completely free of imperfections. To eliminate impurities that might be associated with these imperfections, the best of the crystals were broken up into flakes about 1.5 mm thick by systematic cleavages parallel to the [001] faces and the individual pieces painstakingly inspected, selected, and further trimmed, under the microscope, to yield sufficient amounts of small pieces free from discontinuities or inclusions for the intended acidimetric evaluation.

3 P. Potassium hydrogen phthalate. This preparation was identical with 2 P, except for the further refinement that the trimming of the flakes obtained by cleavage along the [001] faces was accomplished by systematic separation parallel to the weak [100] cleavage plane. The selected small pieces of this preparation, therefore, were bounded entirely by the [001] and [100] cleavage planes and the natural [011] faces. This obviated the ragged surfaces resulting from the unsystematic trimming of the primary cleavage flakes of preparation 2 P.

The selected pieces, all of which were inspected with a polarizing microscope at 100 magnifications, were handled exclusively with fire-polished glass implements. To lift and transfer them, gentle suction was applied through a glass tube of small diameter. The inspection and collection of a 10-g sample of this crystalline material required about 2 days.

2.2. Hydrogen Electrodes

The bases for the hydrogen electrodes were pieces of platinum foil about 1 cm square. For titrations of benzoic and oxalic acids, the foils were coated with platinum black by electrolysis for about 1½ min at a current of 300 ma in a 3-percent solution of chloroplatinic acid to which lead acetate trihydrate had been added in the amount of 80 mg/100 ml of plating solution.

It is well known that the platinum-hydrogen electrode is unstable in solutions of potassium hydrogen phthalate.[3] Electrodes coated with palladium nevertheless behave well in phthalate solutions [7]. Hence, the platinum foils were coated with palladium black instead of platinum black for use in solutions of potassium hydrogen phthalate. The plating solution contained about 1 percent of palladium and the same concentration of lead acetate as the platinum solution. The current density and time of plating were the same as for platinizing. A piece of palladium strip served as an anode.

The electrodes were freshly prepared for each titration and were stored in distilled water for 1 to 2 hr before use. At the completion of a titration, they were cleaned by dipping in a warm solution composed of 3 parts of concentrated hydrochloric acid, 1 part of concentrated nitric acid, and 4 parts of water. The same portion of this cleaning solution was used repeatedly for stripping platinum and palladium.

The necessity for very pure (oxygen-free) hydrogen was emphasized by MacInnes and Cowperthwaite [1] in their adaptation of the differential method to the use of hydrogen electrodes. The hydrogen used in the present work was passed through a tube of soda-lime and through a two-stage purifier consisting of a platinum catalyst at room temperature and a tube containing finely divided copper heated to 500° C.

2.3. Method and Apparatus

The intercomparison consisted essentially in a determination of the weights of each acid stoichiometrically equivalent to a given weight of the refer-

[3] See, for example, references [6] and [7].

ence base, sodium carbonate. The purity of the sodium carbonate did not, therefore, influence the result, but it was necessary that the portions of the carbonate used in all the determinations of a given series be identical in composition. Accordingly, all of the portions were transferred, through a powder funnel, into the weighed weighing bottles in as short a time as possible. The transfers, which required only about 30 sec for a series of six, were performed in a dry box at an atmosphere of 15- to 20-percent relative humidity. A glass scoop holding approximately 3 g of carbonate made this rapid transfer possible.

Potassium hydrogen phthalate and benzoic acid are not appreciably hygroscopic, and the samples of these substances could be adjusted readily to the desired weight, within 1 or 2 mg. Anhydrous oxalic acid, however, is converted into the dihydrate if the relative humidity exceeds about 11 percent at 25° C [8] and is, accordingly, more hygroscopic than sodium carbonate. For this reason, it was considered desirable to adjust the weight of the carbonate rather than that of the oxalic acid, after an approximate amount had been transferred as described above, to about the quantity required. This final adjustment was made on a balance contained in a dry box. The operation was completed within about 30 min after the bulk of the material was transferred. The weighing bottles were closed when a transfer of carbonate was not actually being made.

The reaction between the acid and the carbonate took place in the flask shown in figure 1 (A), provided with a spray trap plugged with platinum gauze. The caps were removed from the weighing bottles containing the samples of carbonate and acid. The larger bottles in which the acid was weighed were lowered into the reaction flask by means of the platinum device shown at B (fig. 1); the smaller carbonate bottles were placed in the flask with a pair of cork-tipped tweezers. The caps were washed with a small quantity of water, the washings being allowed to pass into the flask. Ninety milliliters of water was then added, the spray traps moistened, and the reaction flask stoppered.

In order to effect complete solution of the benzoic acid samples, the reaction flask was placed in a water bath at 70° after the sodium carbonate was entirely dissolved. In the oxalic acid titrations, it was sometimes necessary to warm the flask to dissolve precipitated sodium oxalate. The solution, now containing only a slight excess of the free acid, was rinsed carefully into the cell vessel (A, fig. 2), from which the inner chamber (g) and accessory apparatus had been removed. It was found possible to rinse the reaction flask and the bottles therein thoroughly with about 90 ml of water. The cell was of such size that the total volume of solution could not exceed 225 ml without interfering with the addition of accurately reproducible increments (usually 2 drops) from the tip of the buret.

After the solution had been transferred to the cell, the openings for electrodes, buret, and hydrogen delivery tubes were stoppered. A tube carrying a sintered-glass thimble at its lower end was inserted in the cell, and a vigorous stream of carbon-dioxide-free hydrogen was passed through the solution for 1 hr to purge it of dissolved carbon dioxide.

A considerable number of preliminary experiments demonstrated that removal of carbon dioxide was incomplete at *p*H values exceeding 7. Accordingly, *p*H-titration curves in the vicinity of the end point were constructed from measurements with a glass electrode. With the aid of these, an excess of 0.25 percent of oxalic or benzoic acid was found to be sufficient to insure the removal of the carbon dioxide in 1 hr, but an excess of 0.7 percent of potassium acid phthalate was required.

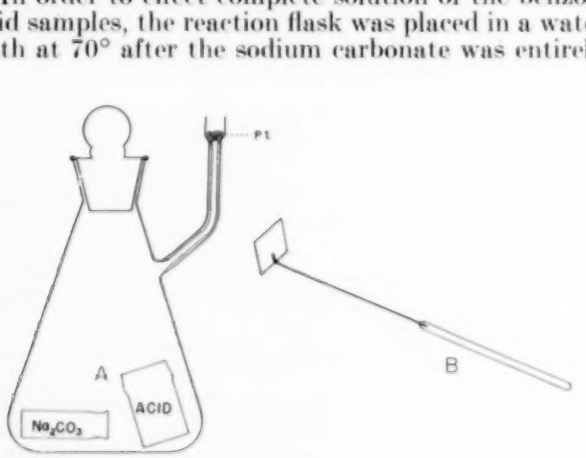

FIGURE 1. *Reaction flask (A) and platinum lowering device (B).*

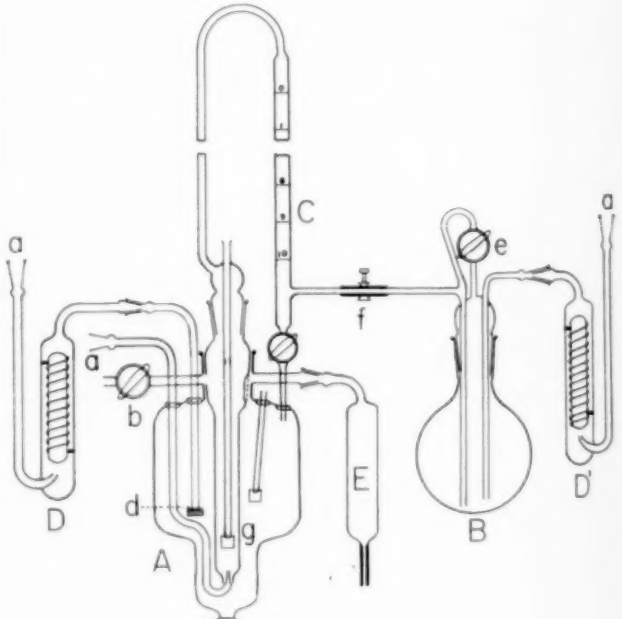

FIGURE 2. *Assembly of apparatus for the differential titration.*

A, Titration cell; B, alkali reservoir; C, buret; D, D′, hydrogen saturators; E, hydrogen exit chamber; a, hydrogen inlets; b, e, stopcocks; d, hydrogen bubbler; f, screw clamp; and g, inner chamber of cell.

In the intercomparison experiments, the excess of acid was determined by titration with a 0.02-N carbonate-free solution of sodium hydroxide, the inflection point being established by the differential method utilizing two hydrogen electrodes. The method derives its precision from the fact that the neutralization takes place to the extent of at least 99.3 percent by reaction of two materials that can be weighed with high accuracy in solid form. A precision of 0.1 percent in the location of the inflection point and in the determination of the excess of acid corresponds to a precision of 0.0007 percent in the equivalence ratio.

2.4. Determination of the Inflection Point

After the purging had been completed, the thimble and delivery tubes were rinsed with a small quantity of carbon-dioxide-free water and the apparatus assembled as shown in figure 2. Pure hydrogen was supplied at the three standard-taper joints, a. The jet of gas emerging in fine bubbles from the bubbler, d, of the Branham-Sperling type [*9*] served both to stir the solution effectively and to furnish the hydrogen electrode in the body of the cell with an adequate supply of gas. In the work of MacInnes and Cowperthwaite [*1*], a lift pump served the dual function of circulating the solution through the inner chamber (g), whose purpose was to isolate a small portion of solution from the remainder, and of supplying gas to the "retarded" electrode mounted inside this chamber. It was necessary, therefore, to interrupt the flow of gas to the inner electrode when an increment of alkali was added to the bulk of the solution. In the present work, it was believed that somewhat steadier readings were obtained if the flow of hydrogen was maintained. The tube delivering the gas to the inner electrode fitted the aperture at the lower end of the inner chamber rather snugly. The rate of bubbling was reduced during a measurement, and the stability of the potential difference between the electrodes indicated that the two solutions did not mix appreciably.

The 0.02-N carbonate-free solution of sodium hydroxide used to titrate the excess acid in the cell was kept in a paraffin-lined flask and was standardized against the Standard Sample of potassium hydrogen phthalate at the beginning and again at the end of each series. In order to remove dissolved oxygen from the alkali, a portion of the alkali solution was placed in flask B, and hydrogen bubbled through it for 1 hr before the buret (C) was filled. The short length of thick-walled rubber tubing at f was impregnated with a paraffin-petrolatum mixture [*1*]. The saturator, D, prevented deposition of salt by evaporation in the fine passages of the bubbler, d, whereas D′ guarded the alkali solution in B from changes of concentration during the purging. Both saturators were filled with distilled water.

Ten to twenty minutes was usually required for the potential difference between the two hydrogen electrodes, as measured by a potentiometer, to drop to 0.1 to 0.2 mv. The inner chamber, which had a volume of about 12 ml, was occasionally flushed by closing stopcock b. The chamber, E, through which hydrogen escaped from the body of the cell, prevented air from gaining entrance as solution rose again in g. The buret, C, was flushed by the hydrogen escaping from B before it was filled by closing stopcock e. The approximate volume of alkali required to complete the titration was calculated, and 1 ml less than this amount was added after carefully filling the tip of the buret. The chamber, g, was flushed repeatedly until the potential difference was again near zero and the titration continued, with the addition of increments of 2 drops, until the inflection point (as indicated by the peak in the potential difference) had been exceeded by at least 0.5 ml. The inner chamber was flushed four times before the addition of each 2-drop increment.

About 3 g of sodium carbonate was used in most of the determinations reported in this paper, and accordingly the amounts of the acids were approximately as follows: Benzoic acid, 7 g; oxalic acid, 2.8 g; and potassium hydrogen phthalate, 12 g. Somewhat smaller weights of material were used in series II. With these quantities of carbonate and acid, the peak potential differences at the inflection point, resulting from addition of an increment of 2 drops of 0.02-N sodium hydroxide, were about 7.5 mv in the phthalate titrations and 28 to 35 mv in the titrations of the stronger benzoic and oxalic acids. About 18 to 22 ml of the alkali solution was required to titrate the 0.7 percent excess of potassium hydrogen phthalate, whereas 7 to 9 ml was necessary to neutralize the 0.25 percent excess of the other two acids. One milliliter of 0.02-N sodium hydroxide is equivalent in neutralizing power to slightly more than 1 mg of sodium carbonate.

In order to locate the inflection point in the titration curve with the greatest possible accuracy, a suitable method of interpolating between successive increments must be sought. For this purpose, either the measured potential difference, ΔE, between the two hydrogen electrodes, or the reciprocal of ΔE, was plotted against some function of the corresponding volume of alkali. The latter was $v_t+v_i/2$, where v_t is the total volume of alkali used prior to the addition of the increment in question, and v_i is the increment volume.

Plots of the potential differences (ΔE) in the phthalate titrations against this function of the number of milliliters of dilute alkali added were nearly straight lines on either side of the inflection point, as the data for a typical titration (shown at the top of fig. 3) demonstrate. The intersection of these lines was taken to be the true inflection point, and the corresponding quantity of dilute alkali was read from the plot. This method of plotting the data for benzoic and oxalic acids gave curved lines on either side of the inflection point, but the reciprocal plot suggested by Gran [*10*] gave straight lines, as shown in the bottom half of figure 3. The volume corresponding to 0.005 percent in the purity of the acid sample is indicated on each of the plots in figure 3.

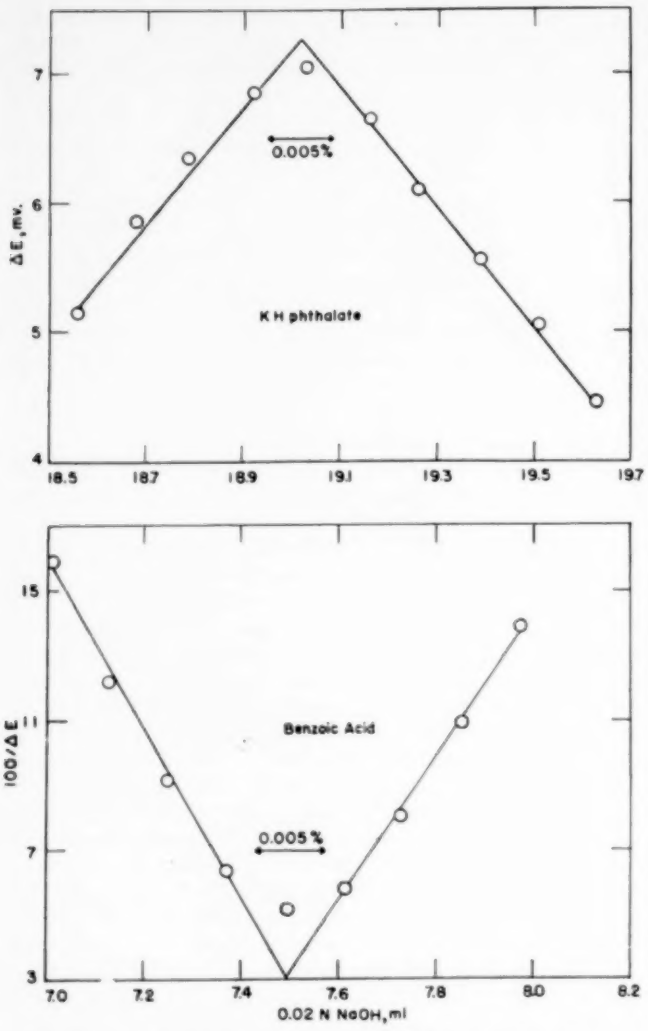

FIGURE 3. *Graphical determination of the inflection point.*

3. Results and Calculations

3.1. Design of Experiments

The determinations were made in four series, designated I, II, III, IV. The first three consisted of six individual titrations, and the fourth consisted of 10. The general pattern used in the first three series was 1–2–3–3–2–1 and, in the fourth series, 1–2–3–4–5–5–4–3–2–1, where each number represents 1 of the 8 acid preparations. The repetition of the titrations in reverse order eliminates any linear trend that might cause the result obtained to be influenced by position in the series. The averages are unaffected by a linear drift arising from either known or unknown sources.

3.2. Weighings

All of the weighings were made on a semimicrobalance that had a reciprocal sensitivity of 0.007 to 0.008 mg per scale division at a load of 10 to 20 g. The new set of weights used was calibrated just before the determinations reported here were begun. The corrections to the weights of denominations less than 1 g were known to 0.001 mg. Inasmuch as the rest points were usually reproducible to ± 1 scale division, or somewhat better than 0.01 mg, all weights were recorded to 0.001 mg.

The observed weight of each substance was corrected to the vacuum basis. For this purpose, the density of dry air at the temperature and barometric pressure obtaining at the time of the weighing was used. The density of each of the solid materials was determined at 25° C. A 25-ml volumetric flask served as a pycnometer. The liquids used were benzene (for sodium carbonate, oxalic acid, and potassium hydrogen phthalate) and ligroin (for benzoic acid). The values obtained were 2.42 for the density of sodium carbonate, 1.32 for fused benzoic acid, 1.88 for anhydrous oxalic acid, and 1.62 for potassium hydrogen phthalate.

In view of the drying treatment accorded the oxalic acid preparations 2 Ox and 3 Ox, it was necessary to weigh the weighing bottles charged with acid on a different day from that on which the weight of the empty bottles was obtained. The effect of the changed buoyancy of the air was largely nullified by the tare used in all the weighings. The weight of the tare and that of an empty weighing bottle differed in all cases by less than 1.2 g. This difference should cause an error of only 0.0003 percent in the weight of the smallest sample (2.6 g) of the acid under the conditions of temperature and barometric pressure at the time the two sets of weighings were made.

3.3. Titration Data

The results of the 27 determinations are given in tables 1 and 2. The percentages listed in column 6 of table 2 are based on the arbitrary figure of 100.0000

TABLE 1. *Corresponding weights of acids and sodium carbonate*

Acid sample	Series	Weight of acid (vacuum)	Weight of Na_2CO_3 (vacuum)	Weight of acid / Weight of Na_2CO_3
		g	g	
1 B benzoic acid	I	7.147879	3.102206	2.304128
	I	7.003172	3.038350	2.304168
	II	4.370418	1.896986	2.304227
	II	4.567110	1.982118	2.304156
	III	6.634762	2.879444	2.304182
	III	7.179268	3.115792	2.304155
	IV	7.286298	3.162192	2.304192
	IV	6.834195	2.966012	2.304170
2 B benzoic acid	IV	6.971129	3.025517	2.304112
	IV	6.448033	2.798579	2.304038
1 Ox oxalic acid	I	2.919566	3.436884	0.849481
	I	3.332296	3.922713	.849488
	II	2.530442	2.978886	.849459
	II	2.273362	2.676117	.849500
	III	3.460188	4.073228	.849495
	III	3.303727	3.889079	.849488
2 Ox oxalic acid	IV	3.036824	3.575211	.849411
	IV	2.963550	3.488951	.849410
3 Ox oxalic acid	IV	3.173541	3.735047	.849666
	IV	2.559824	3.012443	.849750
1 P potassium hydrogen phthalate	I	12.298343	3.191380	3.853601
	I	12.246136	3.177886	3.853548
2 P potassium hydrogen phthalate	II	7.883861	2.045916	3.853463
	III	11.852784	3.075933	3.853395
3 P potassium hydrogen phthalate	III	11.177509	2.900985	3.853005
	IV	11.625558	3.017257	3.853022
	IV	11.546783	2.996777	3.853067

TABLE 2. *Summary of results*

Acid sample	Series	Molarity of salt at equivalence point	*p*H change for 0.01% excess alkali	$\beta \times 10^5$	Purity (versus Na_2CO_3=100.0000%)	Purity (versus 2 B benzoic acid=100.0000%)
				Moles *p*H	%	%
1 B benzoic acid	I	0.27	0.65	3.9	100.0144	
	I	.27	.65	3.9	100.0126	
	II	.17	.41	3.5	100.0101	
	II	.18	.41	3.5	100.0131	
	III	.26	.60	3.8	100.0120	
	III	.27	.65	3.9	100.0131	
	IV	.28	.65	3.9	100.0116	
	IV	.27	.65	3.9	100.0126	
	Mean				100.0124	99.9957
	Standard deviation				0.0013	
2 B benzoic acid	IV	0.27	0.65	3.9	100.0151	
	IV	.25	.60	3.8	100.0182	
	Mean				100.0167	(100.0000)
	Standard deviation				0.0022	
1 Ox oxalic acid	I	0.16	1.0	2.5	99.9999	
	I	.18	1.2	2.5	99.9991	
	II	.14	0.90	2.5	100.0025	
	II	.12	.84	2.5	99.9976	
	III	.18	1.3	2.5	99.9982	
	III	.17	1.2	2.5	99.9990	
	Mean				99.9994	99.9827
	Standard deviation				0.0017	
2 Ox oxalic acid	IV	0.16	1.0	2.5	100.0081	
	IV	.16	1.0	2.5	100.0082	
	Mean				100.0081	99.9914
	Standard deviation				0.0001	
3 Ox oxalic acid	IV	0.17	1.1	2.5	99.9782	
	IV	.14	0.9	2.5	99.9682	
	Mean				99.9732	99.9565
	Standard deviation				0.0071	
1 P potassium hydrogen phthalate	I	0.29	0.25	10.6	100.0021	
	I	.29	.25	10.6	100.0034	
	II	.18	.22	7.1	100.0057	
	Mean				100.0037	99.9870
	Standard deviation				0.0018	
2 P potassium hydrogen phthalate	III	0.28	0.25	9.8	100.0074	
	III	.26	.24	8.9	100.0176	
	Mean				100.0125	99.9958
	Standard deviation				0.0072	
3 P potassium hydrogen phthalate	IV	0.27	0.25	9.3	100.0171	
	IV	.27	.25	9.3	100.0159	
	Mean				100.0165	99.9998
	Standard deviation				0.0008	

percent for the assay of the sodium carbonate used as a reference base. The mean of all determinations on each acid preparation and the standard deviation of each mean are also found in col mn 6. The percentages given in column 7 are based on a figure of 100.0000 percent for the purity of the 2 B benzoic acid, which is believed to be the purest of the eight preparations included in the study. The 1955 atomic weights [*11*] were used in the computations.

The approximate molarity of salt at the equivalence point is listed in column 3 of table 2. The *p*H change caused by the addition of 0.01 percent of alkali in the immediate vicinity of the inflection point (column 4), and β, the Van Slyke buffer value [*12*] near the equivalence point (column 5), indicate the sensitivity of the titrations.

The solubilities of the salts were sufficiently great that large samples of the acids could be conveniently titrated, and the precision of the results was thereby enhanced. It seemed desirable, however, to ascertain whether the results were substantially different when the titrations were performed in a more dilute

solution. Some titrations of benzoic acid 1 B and potassium hydrogen phthalate 1 P were accordingly conducted with samples of such size that the concentration of salt at the equivalence point was about 0.05 *M*. The results, expressed in terms of ideal purity for the sodium carbonate, were as follows:

1 B: Benzoic acid (%)	100. 010 100. 014
Mean (%)	100. 012
Standard deviation (%)	0. 003
1 P: Potassium hydrogen phthalate (%)	100. 000 100. 023 99. 995 100. 030 100. 006
Mean (%)	100. 011
Standard deviation (%)	0. 015

By comparison with column 6 of table 2, it will be seen that the results obtained from the dilute solutions, although of lower precision than those from the more concentrated ones, have the same average value, within the estimated uncertainty of the measurements.

3.4. Inflection Point Versus Equivalence Point

It is important to inquire whether the inflection point established electrometrically is indeed the true stoichiometric equivalence point of the neutralization reaction. There are two reasons, one of them experimental and the other theoretical, why this may not be so. The first is the error caused by the isolation of a portion of the solution, not quite brought to the equivalence point, in chamber g when the bulk of the solution is brought to exact equivalence. MacInnes and Dole [*13*] have shown that this error in volume of reagent cannot exceed $(v/V)v_1$, where v and V are respectively the volumes of the retarded solution and the bulk solution, and v_1 is the volume of the increment of added alkali solution. In these experiments, v, V, and v_1 were about 12, 225, and 0.12 ml, respectively; hence, the error is less than 0.01 ml and alters the final result by considerably less than 0.001 percent.

The other error stems from the well-known fact that as the acids become progressively weaker and hydrolysis of their salts more extensive, the inflection point occurs somewhat before the stoichiometric equivalence point is reached. This matter has been considered in detail by Eastman [*14*], Roller [*15*, *16*], Kilpi [*17*], MacInnes [*2*], and Ricci [*18*]. These derivations differ somewhat in method and detail, but all lead to substantially the same result.

Roller [*15*] gives for the difference in pH at the true equivalence point (ep) and at the inflection point (ip) the expression

$$(p\mathrm{H})_{\mathrm{ep}}-(p\mathrm{H})_{\mathrm{ip}}=0.65\sqrt{K_{\mathrm{w}}/cK_{\mathrm{a}}}, \qquad (1)$$

where K_{w} is the ion-product constant for water ($K_{\mathrm{w}}=10^{-14}$ at 25° C), c is the concentration of the salt at the equivalence point, and K_{a} is the dissociation constant of the weak acid. Equation (1), which applies to the "unsymmetrical" titration of a weak acid with a strong base, indicates that the error is larger the weaker the acid and the smaller the salt concentration at the equivalence point. In the titrations reported here, c varied between 0.12 and 0.29 and K_{a} was in each case greater than 10^{-6}. Hence, the difference of pH should be less than 0.001 unit, and the error from this source should be completely negligible.

The comparison of the inflection point with the equivalence point has recently been the subject of a separate experimental study [*19*]. The course of the titration curve adjacent to, and on both sides of, the inflection point was carefully determined from electrometric titrations in cells with hydrogen and silver–silver-chloride electrodes and without a liquid junction. In every case, the inflection point determined experimentally appeared at a pH slightly lower than the equivalence point computed from the dissociation constant of the acid and the ion-product constant for water, together with estimated values of the activity coefficients. The differences were, in most instances, somewhat greater than the uncertainties in the calculations and much larger than the estimate afforded by eq (1).

The results pertinent to the titrations reported here are presented in the following summary, where "ip" and "ep" refer to the inflection point and the equivalence point, respectively:

Acid	Molar concentration of salt at equivalence point	$(p\mathrm{H})_{\mathrm{ep}}-(p\mathrm{H})_{\mathrm{ip}}$
Benzoic	0. 2	0. 12
	. 05	. 05
Oxalic	. 2	. 02
	. 05	. 03
Phthalic	. 2	. 08
	. 05	. 08

As the concentration of salt at the equivalence point increases, the accuracy with which this point, $(p\mathrm{H})_{\mathrm{ep}}$, can be calculated decreases markedly. Further, for acids as strong as benzoic and oxalic, the inflection point, $(p\mathrm{H})_{\mathrm{ip}}$, is difficult to locate exactly. For these reasons, the tabulated differences must be assigned an uncertainty of at least ± 0.03, although there seems to be little doubt that the inflection point precedes the equivalence point by a measurable amount.

The data given in column 4 of table 2, together with the estimates of the pH interval between inflection and equivalence points, shed some light on the accuracy with which the purity of two acids can be compared. In this way, it may be judged that the apparent purity versus sodium carbonate as listed in column 6 of table 2 is probably too low by about 0.0025 percent for titrations of benzoic

acid, by about 0.0003 percent for titrations of oxalic acid, and by about 0.0032 percent for titrations of potassium hydrogen phthalate.

4. Evaluation of Results

If the above estimates are valid, the purities relative to preparation 2 B benzoic acid (table 2, column 7) should be changed by the following amounts: Oxalic acid, decreased by 0.002_2 percent; potassium hydrogen phthalate, increased by 0.000_7 percent. The corrected figures, relative to 2 B benzoic acid as ideally pure, become

	Percent
1 B benzoic acid	99.996
1 Ox oxalic acid	99.981
2 Ox oxalic acid	99.989
3 Ox oxalic acid	99.954
1 P potassium hydrogen phthalate	99.988
2 P potassium hydrogen phthalate	99.997
3 P potassium hydrogen phthalate	100.000

Preparation 3 P potassium hydrogen phthalate appears to be exactly equivalent to benzoic acid 2 B, within the precision of the observations, and therefore may be regarded as having the exact composition $KHC_8H_4O_4$. This equivalence attests the validity of optical perfection in a single crystal as a criterion of the purity of crystalline solids. This criterion is, of course, only applicable when there is assurance of the absence of significant amounts of impurities in solid solution.

Acknowledgements are due the following for services rendered in the highly specialized preparations and for evaluations of purity: To D. Enagonio for the preparation and determination of the purity of benzoic acid 1 B; G. T. Furukawa for the calorimetric purity-evaluation of 1 B; A. T. Horton for preparing benzoic acid 2B; W. E. Kuper for growing the single crystals of potassium hydrogen phthalate; C. P. Saylor for the selection of the portions of single-crystalline phthalate represented by preparations 2 P and 3 P; and W. W. Walton for preparing the three lots of anhydrous oxalic acid. The authors are likewise indebted to N. C. Craig for assistance in preliminary studies and to T. J. Murphy for performing the titrations of dilute phthalate solutions reported in section 3.3.

5. References

[1] D. A. MacInnes and I. A. Cowperthwaite, J. Am. Chem. Soc. **53,** 555 (1931).
[2] D. A. MacInnes, The principles of electrochemistry, pp. 306–312 (Reinhold Publishing Corp., New York, N. Y., 1939).
[3] F. W. Schwab and E. Wichers, J. Research NBS **32,** 253 (1944) RP1588.
[4] F. W. Schwab and E. Wichers, J. Research NBS **34,** 333 (1945) RP1647.
[5] R. B. Scott, C. H. Meyers, R. D. Rands, Jr., F. G. Brickwedde, and N. Bekkedahl, J. Research NBS **35,** 39 (1945) RP1661.
[6] C. Z. Draves and H. V. Tartar, J. Am. Chem. Soc. **47,** 1226 (1925).
[7] W. J. Hamer and S. F. Acree, J. Research NBS **33,** 87 (1944) RP1598.
[8] International critical tables, Vol. VII, p. 245.
[9] J. R. Branham and E. O. Sperling, J. Research NBS **22,** 701 (1939) RP1214.
[10] G. Gran, Acta Chem. Scand. **4,** 559 (1950); Analyst **77,** 661 (1952).
[11] E. Wichers, J. Am. Chem. Soc. **78,** 3235 (1956).
[12] D. D. Van Slyke, J. Biol. Chem. **52,** 525 (1922).
[13] D. A. MacInnes and M. Dole, J. Am. Chem. Soc. **51,** 1119 (1929).
[14] E. D. Eastman, J. Am. Chem. Soc. **47,** 332 (1925); **50,** 418 (1928); **56,** 2646 (1934).
[15] P. S. Roller, J. Am. Chem. Soc. **50,** 1 (1928).
[16] P. S. Roller, J. Am. Chem. Soc. **54,** 3485 (1932); **57,** 98 (1935).
[17] S. Kilpi, Z. physik. Chem. **173,** 223, 427, 435 (1935); **175,** 239 (1935).
[18] J. E. Ricci, Hydrogen ion concentration, p. 164 (Princeton University Press, Princeton, N. J., 1952).
[19] R. G. Bates and R. G. Canham, unpublished measurements.

Washington, December 3, 1956.

Journal of Research of the National Bureau of Standards Vol. 59, No. 1, July 1957 Research Paper 2770

Mixed-Path Ground-Wave Propagation: 2. Larger Distances

James R. Wait and James Householder

The theoretical results given in part 1 (NBS Research Paper 2687) for ground wave propagation over a mixed path on a flat earth are generalized to a spherical earth. The problem is formulated in terms of the mutual impedance between two vertical dipoles which are located on either side of the boundary of separation. Extensive numerical results are given in graphical form for a mixed land-sea path at frequencies of 10, 20, 50, 100, and 200 kilocycles per second.

1. Introduction

In a previous paper [1] [1] (designated hereafter as part 1), calculations were presented for the propagation of vertically polarized ground waves across a boundary separating two contrasting homogeneous media. The earth was assumed to be flat so that the results were restricted to short distances. It is the purpose of this sequel to extend the analysis and computations to larger distances, where the curvature of the earth must be considered.

The mutual impedance, Z', between two vertical electric dipoles located at A and B, depicted in figure 1, is considered. The earth medium to the left of the boundary line has a

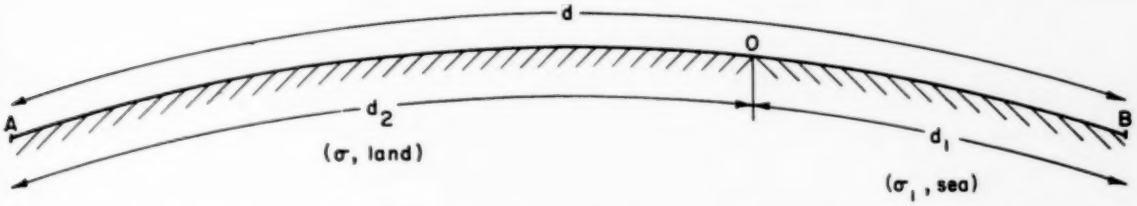

FIGURE 1. *Model for propagation between* A *and* B *straddling a land-sea boundary on a smooth spherical earth.*

conductivity, σ, and dielectric constant, ϵ, and the corresponding constants for the medium to the right of the boundary line are σ_1 and ϵ_1. Using the same approach as in part I, it follows that

$$Z'=Z+\frac{1}{I^2}\iint_S \left[\vec{}_{\mathrm{A}}\times\vec{H}'_{\mathrm{B}}-\vec{E}'_{\mathrm{B}}\times\vec{H}_{\mathrm{A}}\right] ds, \tag{1}$$

where Z is the mutual impedance between the dipoles over a homogeneous curved surface of conductivity σ and dielectric constant ϵ. E_{A}, E'_{B}, H_{A}, H'_{B} are the electric and magnetic fields tangential to the surface S which is the portion of the curved surface to the right of the boundary line. The unprimed quantities refer to the case where the dipoles are in the presence of a corresponding homogeneous surface of constants σ and ϵ throughout. The primed quantities refer to the case where A and B are on the modified surface. The subscripts A or B on E_{A}, E'_{B}, etc., specify that the source of the respective field is a dipole carrying a current, I, at A or B, respectively.

[1] Figures in brackets indicate the literature references at the end of this paper.

Invoking the principle of stationary phase, the surface integral in eq (1) can be reduced to a line integral between the coast line at O and the dipole B. The reasoning here is almost identical to that used in part 1. AOB, rather than being a straight line on a flat earth, is now the path of stationary phase between A and B. In the case of a spherical earth, AOB is on a great circle.[2] In the present problem, the concept of surface impedance is introduced as it was in part 1, the tangential electric and magnetic fields are assumed to be related by a complex constant of proportionality. For the medium to the left of the boundary, this constant is η and the corresponding constant for the medium to the right of the boundary is η_1, where, in ohms,

$$\eta=120\pi\frac{i\beta}{\alpha}\left(1+\frac{\beta^2}{\alpha^2}\right)^{\frac{1}{2}} \tag{2a}$$

and

$$\eta_1=120\,\pi\frac{i\beta}{\alpha_1}\left(1+\frac{\beta^2}{\alpha_1^2}\right)^{\frac{1}{2}} \tag{2b}$$

with $\beta=2\pi/\text{wavelength}$, $\alpha=(i\sigma\mu\omega-\epsilon\mu\omega^2)^{\frac{1}{2}}$, $\alpha_1=(i\sigma_1\mu\omega-\epsilon_1\mu\omega)^{\frac{1}{2}}$ and $\mu=4\pi\times10^{-7}$ h/m.

The mutual impedance, Z, between the short antennas A and B for the homogeneous ground of electrical constants σ and ϵ is given by

$$Z=\frac{h_a h_b i\mu\omega}{2\pi d}\,e^{-i\beta d}W(d,\eta,a)\left[1+\frac{1}{i\beta d}-\frac{1}{\beta^2 d^2}\right], \tag{3}$$

where d is the great circle distance AOB, h_a and h_b are the effective heights of the dipole antennas at A and B, and $W(d,\eta,a)$ is a slowly varying function that approaches unity for a flat, perfectly conducting earth. The function W is obtainable from the Van der Pol-Bremmer theory [2] for the field of a dipole over a homogeneous sphere. It is given, in convenient form, by

$$W(d,\eta,a)=\left(\frac{2\pi d}{a}\right)^{1/2}e^{-i\pi/4}(\beta a)^{1/6}\sum_{s=0}^{\infty}\frac{\exp[-i\tau_s(\beta\alpha)^{1/3}d/a]}{(2\tau_s-1/\delta^2)} \tag{4a}$$

with $\delta=-i(\beta a)^{-1/3}(120\pi/\eta)$ and (4b)

$$\tau_s=\nu_s-\frac{1}{2\nu_s\delta}-\frac{1}{8\nu_s^3\delta^2}-\frac{1+\frac{3}{4\nu_s^3}}{12\nu_s^2\delta^3}\cdots, \tag{4c}$$

and

$\nu_0=0.808e^{-i\pi/3}$
$\nu_1=2.577e^{-i\pi/3}$
$\nu_2=3.824e^{-i\pi/3}$
$\nu_s\cong1/2[3\pi(s+1/4)]^{\frac{2}{3}}e^{-i\pi/3}$ for $s>2$.

An expansion for the coefficients τ_s in a power series in δ is also available [2]. In the preceding formula, a is the effective radius of curvature of the surface in the principal plane containing AOB.

The mutual impedance for the inhomogeneous path is now written in the form

$$Z'=\frac{h_a h_b i\mu\omega}{2\pi d}\,e^{-i\beta d}W'(d,\eta,\eta_1,a)\left[1+\frac{1}{i\beta d}-\frac{1}{\beta^2 d^2}\right], \tag{5}$$

where W' is some function of d, η, η_1, and a and can be expected to be slowly varying compared to $e^{-i\beta d}$ and must necessarily approach unity as d tends to zero or if η and η_1 tend to zero and a approaches infinity.

---

[2] The coastal refraction effect is neglected here because for most cases it is very small, as shown in part 1.

The essential modification here to the flat-earth theory in part 1 is to replace the functions $F(d,\eta)$ and $F'(d,\eta,\eta_1)$ by $W(d,\eta,a)$ and $W'(d,\eta,\eta_1,a)$. It then follows that

$$W'(d,\eta,\eta_1,a)\simeq W(d,\eta,a)-\left(\frac{i\beta d}{2\pi}\right)^{1/2}\left(\frac{\eta_1-\eta}{120\pi}\right)\int_0^{d_1}\frac{W(d-\alpha,\eta,a)W(\alpha,\eta_1,a)}{[\alpha(d-\alpha)]^{1/2}}\,d\alpha, \tag{6}$$

which is the spherical-earth counterpart of eq (13) of part 1. In the above, α, the integration variable, ranges from B to O (i. e., $d_1=\mathrm{OB}$). This result is an approximation that is not valid near the boundary line because it utilizes a stationary phase principle, as in part 1. Furthermore, the wave reflected from the boundary is neglected. Actually, this effect is very small at distances greater than a wavelength from the boundary line.

The prime task now is the evaluation of the integral in eq (6). Inserting the Van der Pol-Bremmer formula for the W's, the integrations can be carried out to yield

$$W'(d,\eta,\eta_1,a)=W(d,\eta,a)+(2\pi i\beta d)^{1/2}\left(\frac{\eta_1-\eta}{120\pi}\right)\sum_{s=0}^{\infty}\sum_{q=0}^{\infty}\frac{\exp[-i\tau_s(\beta a)^{1/3}d/a]\left[\exp\left[i(\tau_s-\tau_q^1)\frac{d_1}{a}(ka)^{1/3}\right]-1\right]}{(2\tau_s-1/\delta^2)(2\tau_q^1-1/\delta_1^2)(\tau_s-\tau_q^1)}, \tag{7}$$

where the coefficients τ_s are given the eq (4c) et seq. and τ_q^1 are identical in form to τ_s, except that σ_1 and ϵ_1 replace σ and ϵ. This double summation is very cumbersome and converges poorly. An alternative formula may be derived by employing the following series formula [3, 4] for the W's:

$$W(d-\alpha,\eta,a)=\sum_{n=0}^{\infty}A_n\left(\frac{d-\alpha}{T}\right)^{n/2}, \tag{8}$$

where $1/T=-(i\beta/2)(\eta/120\pi)^2$. The coefficients up to order 9 are given by

$$\begin{aligned}
&A_0=1,\ A_1=-i\sqrt{\pi},\ A_2=-2,\ A_3=i\sqrt{\pi}(1-\delta^3/2)\\
&A_4=\frac{4}{3}(1-\delta^3),\ A_5=-\frac{i\sqrt{\pi}}{2}(1-3\delta^3/2),\ A_6=-\frac{8}{15}\left(1-2\delta^3+\frac{7}{8}\delta^6\right),\\
&A_7=\frac{i\sqrt{\pi}}{6}\left(1-\frac{5}{2}\delta^3+2\delta^6\right),\ A_8=\frac{16}{105}\left(1-3\delta^3+\frac{27}{8}\delta^6\right),\\
&A_9=\frac{-i\sqrt{\pi}}{24}\left(1-\frac{7}{2}\delta^3+5\delta^6-\frac{21}{8}\delta^9\right),
\end{aligned} \tag{9}$$

where $\delta=-i(\beta a)^{1/3}(120\pi/\eta)$. The corresponding expression for $W(\alpha,\eta_1,a)$, for example, is identical to the above with $d-\alpha$, T, and δ being replaced by α, T_1 and δ_1, respectively, where $1/T_1=-(i\beta/2)(\eta_1/120\pi)^2$ and $\delta_1=-i(\beta a)^{-\frac{1}{3}}(120\pi/\eta_1)$. Therefore,

$$W(\alpha,\ \eta_1\ a)=\sum_{m=0}^{\infty}A_m^1\left(\frac{\alpha}{T_1}\right)^{m/2}, \tag{10}$$

where the A_m^1 coefficients are functions of δ_1. After carrying out the integration indicated in eq (6), the formula for W' takes the form

$$W'(d,\eta,\eta_1,a)=W(d,\eta,a)-\left(\frac{i\beta d}{2\pi}\right)^{1/2}\left(\frac{\eta_1-\eta}{120\pi}\right)\sum_{n=0}^{\infty}\sum_{m=0}^{\infty}A_nA_m^1I_{m,\,n}, \tag{11}$$

where

$$I_{m,\,n}=\int_0^{d_1}\alpha^{\frac{m-1}{2}}(d-\alpha)^{\frac{n-1}{2}}\,d\alpha. \tag{12}$$

The integral $I_{m,n}$ can be reduced by the formulas

$$I_{m,n}=\frac{2}{m+n}(d_1)^{\frac{m+1}{2}}(d-d_1)^{\frac{n-1}{2}}+\frac{(n-1)d}{m+n}I_{m,n-2},$$

$$I_{m,n}=\frac{1}{m+n}\left[(m-1)dI_{m-2,n}-2(d-d_1)^{\frac{n+1}{2}}(d_1)^{\frac{m-1}{2}}\right],$$

$$I_{m,1}=\left(\frac{2}{m+1}\right)(d_1)^{\frac{m+1}{2}}, \tag{13}$$

$$I_{1,n}=\left(\frac{2}{n+1}\right)\left(d^{\frac{n-1}{2}}-(d-d_1)^{\frac{n-1}{2}}\right),$$

and

$$I_{0,0}=2\tan^{-1}\left(\frac{d_1}{d-d_1}\right)^{\frac{1}{2}}.$$

The preceding expression for W' is useful when distance d is small compared to T and T_1.

In view of the fact that extensive numerical data for the W functions are available [5, 6], it would seem to be preferable to evaluate the integral by a numerical method. Certainly this appears simpler than attempting to sum the doubly-infinite series formulas discussed above. To convert the integral to a form suitable for numerical integration, it is desirable to change the variable of integration to remove the singularity at $\alpha=0$. Then, letting $\alpha=x^2$, it follows that

$$W'=W+2\left(\frac{\rho_0}{\pi}\right)^{\frac{1}{2}}\left[\frac{1-k^{\frac{1}{2}}}{k^{\frac{1}{2}}}\right]e^{-i\frac{\pi}{2}}\int_0^{d^{\frac{1}{2}}}\frac{W(d-x^2,\eta,a)W(x^2,\eta_1,a)dx}{\sqrt{d-x^2}}, \tag{14}$$

where

$$k=\frac{\sigma_1+i\omega\epsilon_1}{\sigma+i\omega\epsilon}\text{ and }\rho_0=-\frac{i\beta d}{2}\left(\frac{\eta}{120\pi}\right)^2.$$

At low radiofrequencies, displacement currents in the ground are small, and consequently k and ρ_0 are real and positive.

For purposes of computation, the following values of the parameters are employed:

$\sigma=10^{-2}$ mho/m corresponding to land,
$\sigma_1=4$ mhos/m corresponding to sea, and
$a=4/3$ times the earth's radius.

In figure 2 the amplitude of W' is shown plotted as a function of distance d for frequencies of 10, 20, 50, 100, and 200 kc. Two values of d_1/d are indicated on the curves, namely, 0 corresponding to an all land path, and 0.8, corresponding to an 80 percent sea path. For the lower frequencies, the curves are almost indistinguishable, and the shape of W' is determined primarily by diffraction by the earth's curvature. The phase lag ϕ' (i. e., $\phi'=-\arg W'$) is shown plotted in figures 3 to 7 as a function of d for the same frequencies. The values of d_1/d, which indicate the ratio of the length of the sea path to the length of the total path, are 0, 0.2, 0.4, 0.6, 0.8, and 1.0.

The preceding analysis has been discussed in relation to the mutual impedance between two dipole antennas at A or B. It is probably desirable to express the results in terms of the vertical electric field, E, at B (or A) for a standard source at A (or B). For example,

$$E=E_0W'=E_0|W'|e^{-i\phi'}, \tag{15}$$

where

$$E_0=\frac{160.5}{d}\left[1-\frac{1}{(\beta d)^2}-\frac{i}{\beta d}\right]e^{-i\beta d}=|E_0|e^{-i\phi_0}e^{-i\beta d}. \tag{16}$$

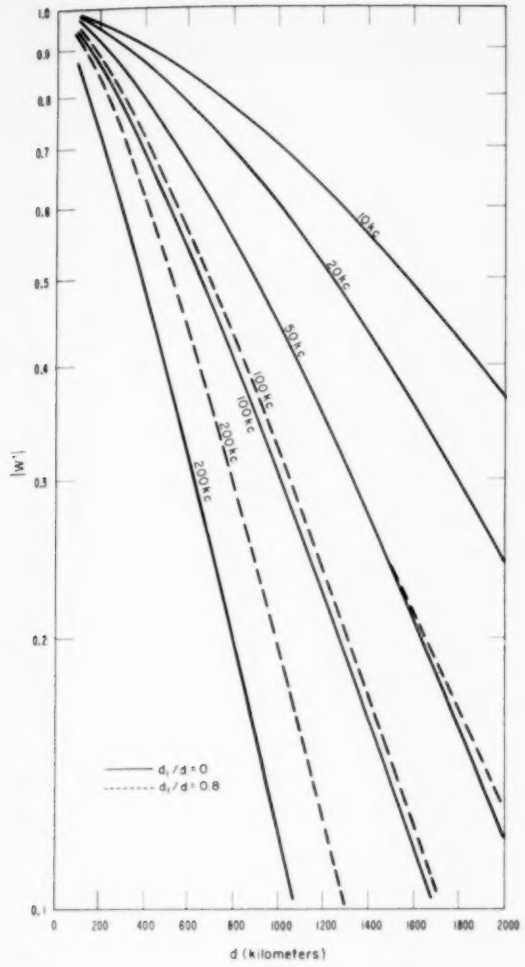

FIGURE 2. *Amplitude factor for mixed-path propagation.*

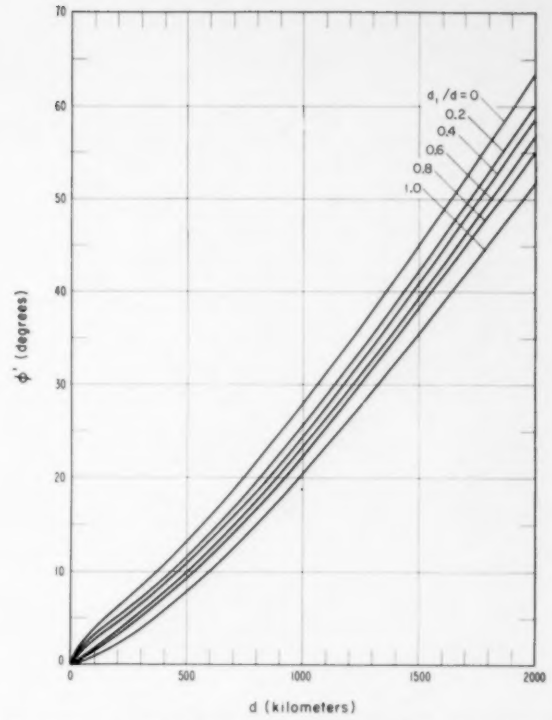

FIGURE 3. *Phase factor for mixed-path propagation.* f=10 kc.

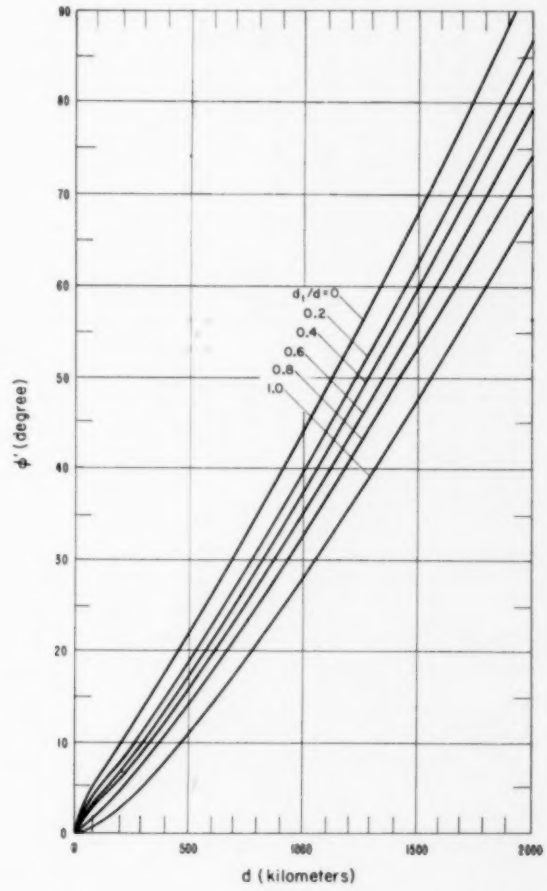

FIGURE 4. *Phase factor for mixed-path propagation.* f=20 kc.

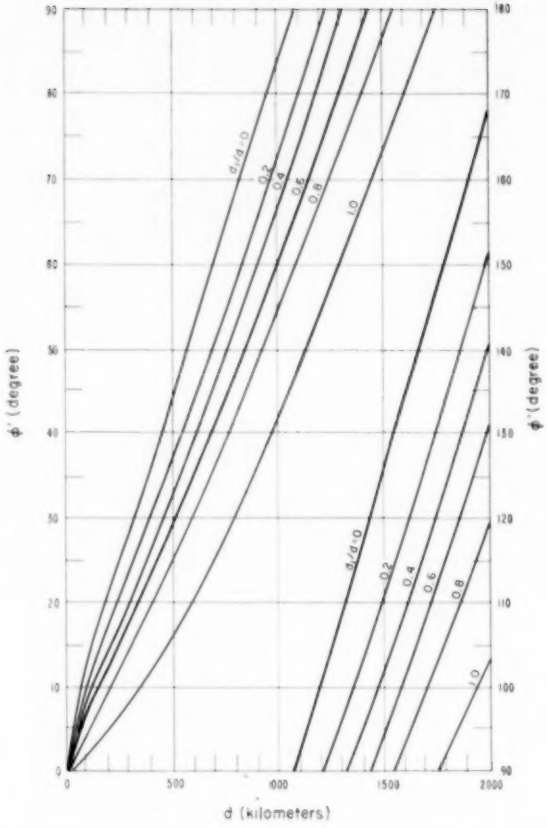

FIGURE 5. *Phase factor for mixed-path propagation.*
f=50 kc.

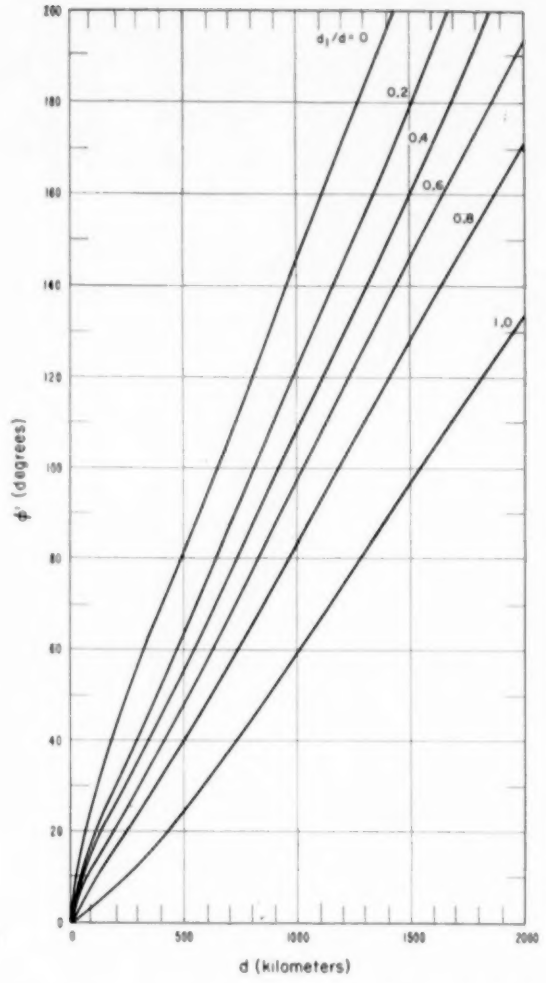

FIGURE 6. *Phase factor for mixed-path propagation.*
f=100 kc.

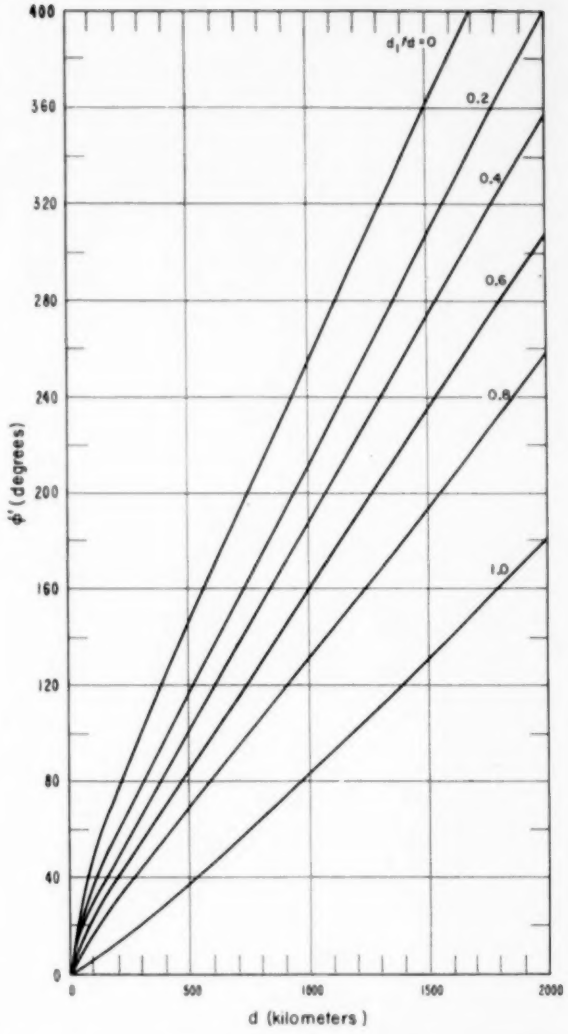

FIGURE 7. *Phase factor for mixed-path propagation.*
f=200 kc.

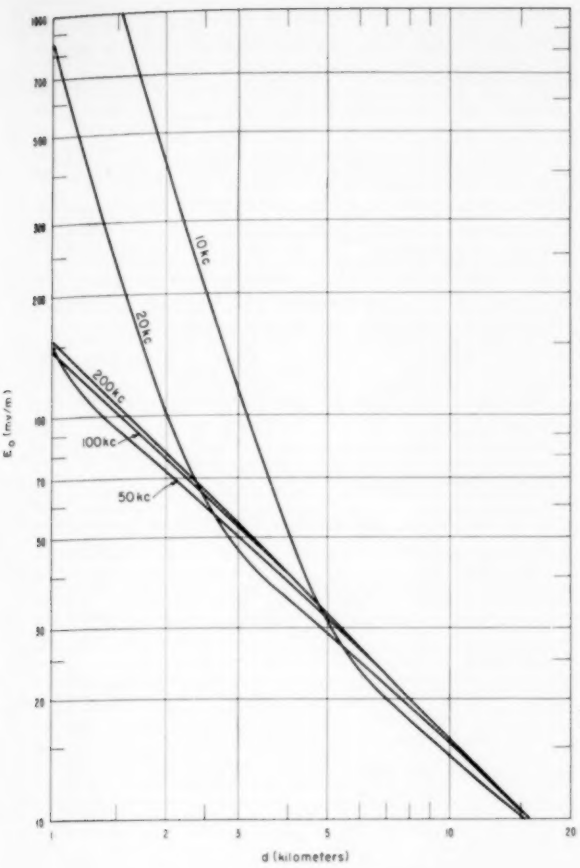

FIGURE 8. *Amplitude for near field.*

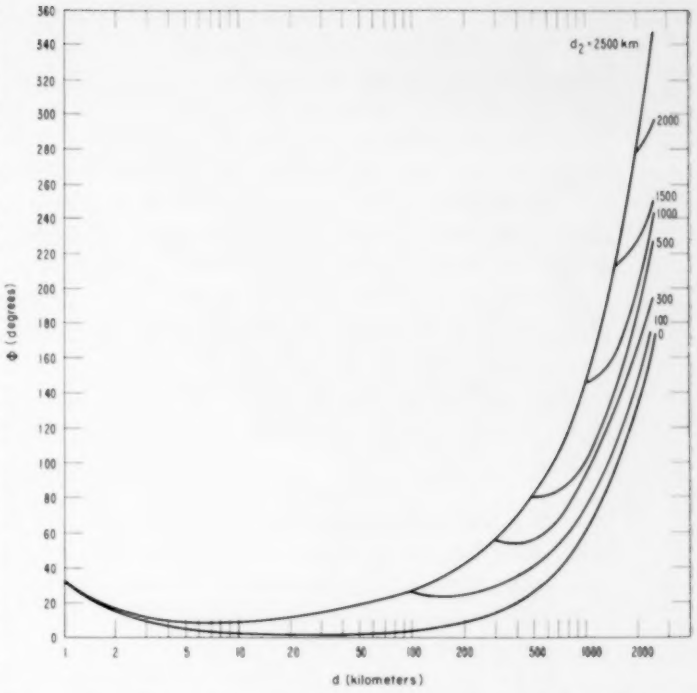

FIGURE 10. *Phase of the ground wave for propagation from land to sea.*
(Transmitter is distance d_2 from the coast) f=100 kc.

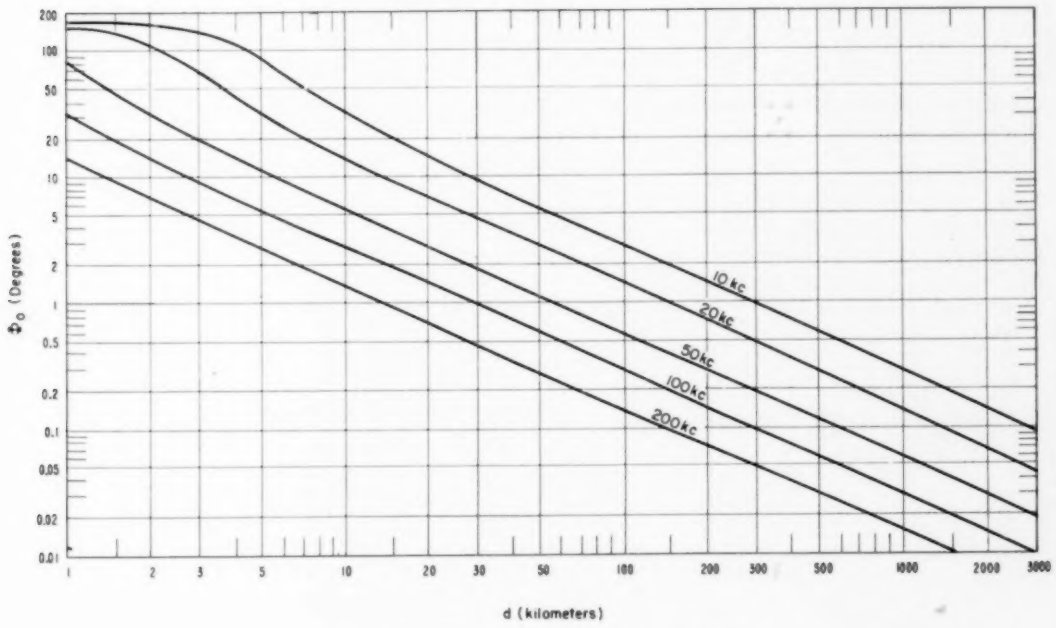

FIGURE 9. *Phase correction for near field.*

The "near field", E_0, is chosen such that the radiation component is 0.10 v/m at $d=1$ mile $=1{,}605$ m. The amplitude, E_0, and the phase, Φ_0, are shown plotted in figures 8 and 9, respectively, for frequencies of 10, 20, 50, 100, and 200 kc. It should be noted that $|E_0| \simeq 160.5/d$ and $\Phi_0 \simeq 1/\beta d$ when $\beta d >> 1$. Actually, E_0 is the total field of the source on a flat, perfectly conducting earth. To a good first approximation the total field E over a mixed path on a spherical earth is obtained by multiplying the near field E_0 by the attenuation function, W', as indicated above [1].

To provide an illustration of the applicability of the numerical results, the total phase correction $\Phi(=\Phi_0+\phi')$ at 100 kc, is shown in figure 10 for the case of a transmitter on land, a distance d_2 from the coast. The plotted curves show how Φ varies with $d(=d_1+d_2)$ for various values of d_2. As the receiver moves away from the transmitter, the rate of increase of the phase is characteristic of propagation over land. As the coastline is crossed at $d=d_2$, the phase lag is reduced somewhat and eventually continues to increase at a much slower rate as the receiver moves out to sea. This abrupt reduction of the rate of increase of phase lag is known as a "recovery effect" and has been verified experimentally [7].

2. Concluding Remarks

The results presented here should be useful in predictions of ground-wave propagation at low radiofrequencies over a two-part mixed land-sea path. It should be emphasized that the sky waves have not been considered. At ranges greater than 200 km or so, the ionospherically reflected waves must be separately accounted for. In any case, the ground wave is omnipresent even out to 2,000 km and is a substantial contribution to the field.

It is of interest to note that a formula almost identical to eq (13) of part 1 has been reported by Godzinski [8] in Poland at the recent International Radio Consultive Committee meeting in Warsaw. His results, however, are not valid for short distances or very low frequencies, where the induction and static fields are significant. He has also developed a formula essentially equivalent to eq (6) of the present paper, when $(d/a)^3 << 1$. Furutsu [9] has also recently investigated the problem of ground-wave propagation over an inhomogeneously conducting spherical earth. He has indicated that the basic integral equation can be solved by an iterative procedure. The first term of his rather elaborate analysis agrees with eq (7) of the present paper. Neither Godzinski or Furutsu present any explicit numerical result for the mixed-path attenuation function.

The results in this paper, as well as in part 1, are not valid for points close to the boundary because a first-order stationary-phase evaluation of the integrals has been employed. Furthermore, the wave reflected from the boundary has been neglected. A somewhat different analytical approach has been used [10] to study the field very close to the boundary, which indicates the stationary-phase approximation is valid if A and B are at least two wavelengths from the boundary or coastline.

3. References

[1] J. R. Wait, Mixed path ground wave propagation: 1. Short distances, J. Research NBS **57,** 1 (1956) RP2687. (Numerous references to related investigations were given here.)

[2] H. Bremmer, Terrestrial radio waves (Elsevier Publishing Co., Amsterdam, 1949).

[3] H. Bremmer, C. C. I. R. Document 162 E (London, Mar. 1953).

[4] J. R. Wait, Radiation from a vertical antenna over a curved stratified ground, J. Research NBS **56,** 237 (1956) RP2671.

[5] J. R. Wait and H. H. Howe, Amplitude and phase curves for ground wave propagation in the band 200 c/s to 500 kc, NBS Circular 574 (1956).

[6] J. R. Johler, W. J. Keller, and L. C. Walters, Phase of the low radiofrequency ground wave, NBS Circular 573 (1956).

[7] B. G. Pressey, G. E. Ashwell, and C. S. Fowler, Change of phase of a low frequency ground wave propagated across a coast line, Proc. Inst. Elect. Engrs. [B] **103,** 527 (1956).

[8] Z. Godzinski (Institute of Technology, Wroclaw, Poland) (unpublished communication).

[9] K. Furutsu, Propagation of electro-magnetic waves over the spherical earth across boundaries separating different media, J. Radio Research Laboratories (Tokyo) **2,** 345 (Oct. 1955).

[10] J. R. Wait, The amplitude and phase of the low-frequency ground wave near a coastline, J. Research NBS (in press).

BOULDER, COLO., December 13, 1956.

Journal of Research of the National Bureau of Standards Vol. 59, No. 1, July 1957 Research Paper 2771

A Spectroscopic Study of Oils Used in Oil-Extended Rubber[1]

Frederic J. Linnig and James E. Stewart

Knowledge of the composition of oils used in oil-extended rubber is useful in specifying oil types and in understanding the properties of the oil-rubber master batches. In this work, elucidation of structure has been attempted by a comparison of infrared spectra between 2 and 15 microns of two series of oil fractions obtained by basically different methods. Fractions of a number of different oils or oil distillates were studied. The spectra were compared with reference to the method of separation and in some cases to the physical and chemical properties of the fractions. There are marked similarities between certain of the fractions separated by the two methods. However, the study indicates a variability of structural types from one oil to another. This is especially true for the more polar fractions. It is suggested that this varability, especially with respect to polar groups and other structures leading to active hydrogens, could account for the observed variability in the aging properties of master batches containing different oils or oil fractions.

Spectra were also obtained of a few typical fractions in the ultraviolet range between 210 and 340 millimicrons and in the far infrared between 15 and 40 microns.

1. Introduction

It has become common practice during the last few years to combine petroleum distillates in emulsion form with GR–S synthetic rubber latex to yield, on coagulation, what is termed an "oil-rubber master batch" or an "oil-extended GR–S".

The GR–S used is a copolymer of butadiene and styrene that had been polymerized to a high-molecular weight. Thus, the rubber itself is much stiffer than usual. As a result, the final homogeneous mixture of oil and rubber has properties quite similar to the lower molecular weight GR–S without the added oil. The added oil extends the available supply of rubber, and because of its very low cost, reduces the price of the final products. The oils used are predominantly the resinous portions of high-boiling petroleum distillates from which the paraffinic material, employed as lubricating oil, has been largely extracted. They are, or course, highly complex mixtures of many compounds widely different in type, consisting of more than 20 carbon atoms.

It is well recognized that the physical properties and the compounding and aging characteristics of the oil-extended polymers depend, to some extent, on the type of oil used [9, 14, 25, 26, 27, 28, 29, 34, 35, 36, 37, 38, 39, 40, 42].[2] In order to facilitate the specification of oil types, a number of methods of analysis have been developed, one based on acid extraction and physical properties [25, 27] and several on chromatographic techniques [9, 13, 18]. In one chromatographic method, ring types and carbon types are identified from physical properties [18]. The method devised by Rostler and Sternberg [25, 27] depends on the separation of the oil into sxi fractions extracted from the pentane soluble portion of the sample by anhydrous hydrogen chloride and by sulfuric-acid solutions of different strengths. This procedure has been generally used in classifying oil types. It has, however, been shown that some properties, such as aging of master batches containing certain of these fractions, depends on the oil from which the fraction came [36].

A method developed at the National Bureau of Standards by Termini and Glasgow [13] depends on the chromatographic separation of the oil into five fractions, using silica gel as the adsorbent and eluting the material successively with two portions of pentane, followed by benzene, carbon tetrachloride, and ethanol.

Knowledge of the composition of the oil fractions themselves and the variations in the composition of fractions obtained from different oils should be helpful in further characterizing these materials and in explaining observed variations in the properties of rubber containing them. The present work constitutes a part of the program undertaken at the National Bureau of Standards to elucidate the chemical composition of extender oils. In this study, infrared and, to a lesser extent, ultraviolet spectroscopy have been used to accomplish the following: (1) To compare the over-all spectroscopic features of the fractions obtained by the method of Termini and Glasgow with the fractions of a single oil obtained by the method of Rostler and Sternberg; (2) to indicate molecular types in the fractions; (3) to show how these molecular types may vary from one oil to another; and (4) to explore the correlation between reported performance tests and structural groups present in the different oil fractions. To this end, infrared spectra were obtained on a number of fractions furnished by Rostler. They represent a number of the fractions obtained by acid extraction of three different distillates of the same crude oil. Spectra were also obtained on fractions of six different oils from various parts of the country, separated chromatographically by Termini and Glasgow [13], and furnished by them.

[1] This work was presented, in part, at the Pittsburgh Conference on Analytical Chemistry and Applied Spectroscopy, Pittsburgh, Pa., March 1955.

[2] Figures in brackets indicate the literature references at the end of this paper.

The chemical and physical properties of the particular fractions separated by the acid-extraction method and used in this study are presented and discussed in a paper by Rostler and White [29]. For convenience, these fractions are described in this paper in terms of the familiar analytical method [25,27] rather than the modified procedure actually used in preparing them [29]. Values for the refractive index of the fractions separated chromatographically were furnished by Termini and Glasgow [13]. These two sets of data are presented in tables 1 and 2, respectively. The analysis of the six different oils by the two methods is given in table 3. The data for the chromatographic procedure were furnished by Termini and Glasgow [13] and those for the acid extraction procedure by Rostler [24].

TABLE 1. *Physical properties and composition of oil fractions separated by acid-extraction method*

Data of Rostler and White [29]

Oil Fraction [1]	Designation of R and W [29]	Density, d_4^{20}	Refractive index, n_D^{25}	Molecular weight	Elementary composition					Carbon-hydrogen weight ratio
					C	H	N	S	Total	
DISTILLATE 1										
First acidaffins (a)	985–A–(1)	1.002	1.5780	226	wt. % 88.95	wt. % 9.14	wt. % 0.04	wt. % 1.08	wt. % 99.21	9.732
Second acidaffins (a)	985–A–II (1)	0.988	1.5612	233	89.73	9.88	.02	0.66	100.29	9.082
First acidaffins (b)	985–A–(2)	1.054	1.6036	250	89.49	8.75	.06	1.01	99.31	10.257
Second acidaffins (b)	985–A–II (2)	1.010	1.5706	239	89.59	9.25	.02	1.01	99.87	9.685
Nitrogen bases, group I	N–960–I	1.025	1.5698	260	84.68	9.75	4.36	0.70	99.49	8.685
Nitrogen bases, group II	N–960–II	1.018	1.5578	267	83.81	10.08	3.81	.94	98.64	8.314
DISTILLATE 3										
Paraffins (a)	P–940	0.910	1.4921	373	86.50	13.46	.....	.....	99.96	6.426
Paraffins (b)	P–955	.891	1.4833	408	86.28	13.43	.....	.....	99.71	6.424
First acidaffins	973–A	1.055	1.6172	298	89.53	8.82	0.17	1.35	99.87	10.151
Second acidaffins	982–A–II	1.017	1.5854	303	88.84	9.50	.05	1.02	99.41	9.352
Nitrogen bases, group I	N–947–I	1.061	1.6087	271	86.12	8.89	3.83	0.47	99.31	9.687
Nitrogen bases, group II	N–947–II	1.027	1.5608	366	83.98	10.42	3.18	.53	98.11	8.060
DISTILLATE 4										
First acidaffins	980–A	1.053	1.6152	335	89.09	8.84	0.02	1.14	99.09	10.078
Second acidaffins	986–A–II	1.017	1.5879	348	88.68	9.60	.03	1.05	99.36	9.238
Nitrogen bases, group I	N–956–I	1.079	1.614	332	87.34	8.61	2.91	0.68	99.54	10.144
Nitrogen bases, group II	N–956–II	1.007	1.565	390	84.70	10.38	2.54	.69	98.31	8.160

[1] The terminology is that of Rostler and Sternberg [25,27] and is intended, especially in the case of the acidaffins and nitrogen bases, to indicate that these fractions are concentrates of the designated component (see group analysis of Rostler and White [29] table II).

TABLE 2. *Index of refraction of oil fractions separated chromatographically*

(Data of Glasgow and Termini [13])

Oil fraction	I Circosol 2×H	II Sundex 53	III SPX 97	IV Philrich 5	V Dutrex 20	VI Califlux TT
First pentane	1.4882	1.4805	1.4800	1.4845	1.4915	1.4923
Second pentane	1.5017	1.4993	1.4995	1.5015	1.5020	1.5018
Benzene	1.5635	1.4796	1.5865	1.5780	1.6065	1.5885
Carbon tetrachloride	1.5552	1.5630	.....	.....	1.6070	.....
Ethanol	.....	.....	.....	.....	.....	.....

TABLE 3. *Analysis of six oils*

Oil samples	Chromatographic separation [13], eluants					Sulfuric-acid extraction [24]			
	First portion of pentane	Second portion of pentane	Benzene	Carbon tetrachloride	Ethanol	Paraffins	Second acidaffins	First acidaffins	Nitrogen bases
	wt. %	wt. %	wt. %	wt. %	wt. %	wt. %	wt. %	wt. %	wt. %
I Circosol 2×H	53.4	2.0	41.3	0.7	2.6	50.1	41.5	6.2	2.2
II Sundex 53	25.13	1.68	67.98	.94	5.98	23.8	54.9	14.8	6.5
III SPX97	25.97	4.84	64.25	.79	5.00	24.5	53.3	14.5	7.7
IV Philrich 5	11.04	6.15	75.67	.25	6.33	9.6	61.2	16.8	12.4
V Dutrex 20	5.98	1.24	80.58	.78	10.57	6.1	46.5	23.5	23.9
VI Califlux TT	10.66	0.81	75.18	1.08	12.12	10.5	47.2	20.9	21.4

2. Experimental Procedure

The infrared spectra were obtained with a Perkin-Elmer 21 double-beam spectrophotometer equipped with a sodium chloride prism for the range between 2 and 15 μ and with a cesium bromide prism for the range between 15 and 40 μ. A cell holder was used, which was heated to 50° or 60° C for the more viscous materials, such as the nitrogen-base fractions. It was shown that the spectrum of the heated materials was the same as that of the same material cooled in the cell to room temperature. The cells were assembled in the holder with a two-piece lead spacer open at the top and bottom. The sample was drawn downward between the windows by a suction tube applied to the bottom of the assembly. In this way it was possible to hold the percentage transmittance for successive loadings constant to within 0.5 percent. Solid samples were incorporated in KBr disks [31, 33], 9.5 mm in diameter and about ½ mm thick.

The ultraviolet spectra were obtained with a Cary 12 double-beam spectrophotometer, using as solvent methylcyclohexane, which had been purified by fractionating it through a column of silica gel. Only those cuts having the spectrum characteristic of the pure material were used. Twenty-millimeter cells were used throughout.

3. General Discussion

It would not be expected, of course, that a spectroscopic study would completely elucidate the extremely complex composition of the oils themselves. However, the fractionations separated the molecules present into groups having similar characteristics. Consequently, the number and types of compounds in the fractions are not only greatly reduced, but the nature of the separation itself serves, to some extent, as a guide to indicate the type of compounds that may be present, thus supplementing the interpretation of the spectra.

Even following chemical fractionation, it would not be expected that spectroscopic studies would elucidate individual molecular species in these fractions, which are themselves mixtures of many compounds of either similar polarity or similar affinity for sulfuric acid. However, spectroscopic studies, especially infrared spectroscopy, can elucidate certain structural configurations and functional groups. If the optical absorption, due to a given structure, is virtually independent of the rest of the molecule, as are most structures absorbing in the region between 2 and 7.5 μ, and many molecules in the mixture contain such a structure, then the absorptions will reinforce each other, and a well-defined absorption band will be found. An example of such an absorption band is that due to the aliphatic C—H stretching vibration at 3.4 μ. However, if an absorption can occur anywhere in a wide wavelength region, depending on the structures adjacent to the group, as is often the case in the region beyond 7.5 μ, then the resulting absorption by the mixture will, at best, be seen as a broad, poorly defined "swelling" in the general background. In many cases, the meaning of the absorption will be understood only by comparing several curves made from mixtures containing varying quantities of structures of this type, along with other more readily identified structures related to them in some fashion. It is here that a knowledge of the probable chemical nature of the fraction in question and correlation of the absorption phenomena with known physical and chemical properties becomes important. An example of this type of absorption is the skeletal stretching vibration of aliphatic chains in the region between 8 and 11 μ.

Because it facilitates understanding and interpretation of the spectra, we will consider the fractions in the order in which they are eluted successively from the chromatographic column, and relate, where possible, similar fractions obtained by acid extraction. In most cases, only one curve will be presented as representative of those obtained for the particular fraction under discussion. Variation of the other similar fractions from the one presented will be discussed in the text.

In the following discussion, reference has often been made to the recent book by Bellamy [2], which contains assignment charts and a detailed discussion of the relation between structural groups and absorption bands, with appropriate references to the original literature. Similar use has been made of the book by Randall, Fowler, Fuson, and Dangl [23] and of the article by Colthup [7], which also contain assignment charts and appropriate discussion.

4. Infrared Spectra—2- to 15-Micron Region

Figures 1, 3, 4, 5, 6, and 7 give the spectra in the region from 2 to 15 μ for samples obtained by acid extraction and chromatographic separation. The spectra displaced to the lower part of figures 1, 4, and 5, were obtained from samples of the first pentane-benzene-, and carbon tetrachloride-eluted portions, respectively, of the six oils separated chromatographically. The curves in the upper portion of these figures are for typical fractions of the four distillates separated by acid extraction. Figures 3 and 6 show examples of spectra of the second pentane- and ethanol-eluted portions, respectively.

5. Paraffins and First Pentane-Eluted Fractions

The spectrum in the upper portion of figure 1 was obtained on the portion of an oil insoluble in 30-percent fuming sulfuric acid (distillate 3, paraffin (a)). It is qualitatively similar to that obtained on the first pentane-eluted portion of oil V in the lower part of the same figure.

These two spectra show the usual absorption pattern of a typical mineral oil [19]. There is no evidence of O—H, N—H, C=C, etc., except that the spectrum of one of the oil fractions (oil IV) has a weak band at 6.22 μ, suggesting aromatic or conjugated unsaturation and one at 12.2 μ, which could be caused by out-of-plane bending of a carbon-

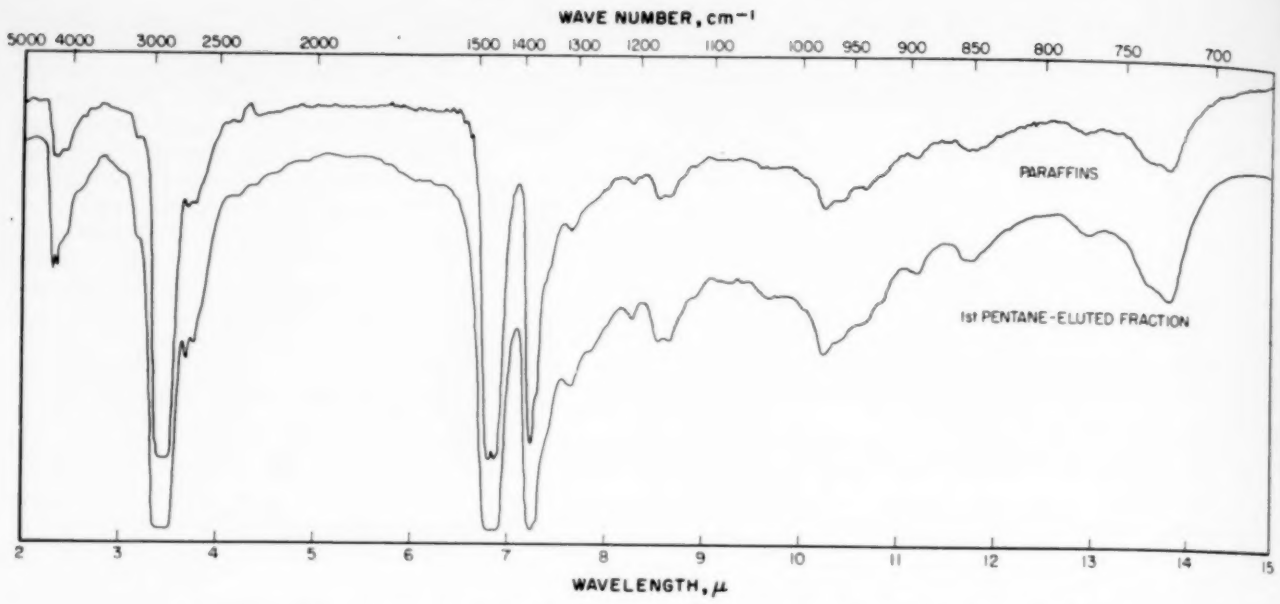

FIGURE 1. *Infrared spectra of paraffins (a) distillate 3, and first pentane-eluted fraction of oil V.*

hydrogen bond on an aromatic ring. The absence of these groups is consistent with the chemistry of the methods of separation [13, 25, 27].

There is a strong absorption-band characteristic of C—H stretching at 3.4 to 3.5 μ, one in the region of 6.8 to 6.9 μ related to CH_2 deformation and asymmetric CH_3 deformation, and one at 7.2 to 7.3 related to symmetric CH_3 deformations. The strong band at 13.8 μ is characteristic of CH_2 rocking vibrations. This band is not observed at this wavelength in aliphatic chains containing less than four successive CH_2 groups, and it shifts to shorter wavelengths with a decrease in chain length. From the work of Hastings, Watson, Williams, and Anderson [15], it seems reasonable, in the absence of aromatic absorption at 6.2 μ to assign the weak absorption at 13 μ to CH_2 groups in a chain 1 or 2 methylene units in length, the shoulder at 13.6 μ to chains containing 3 methylene units, and the peak at 13.80 to 13.85 μ to chains containing 4 or more methylene units. Even this latter absorption shifts slightly to longer wavelengths as its intensity increases.

A study of the American Petroleum Institute (API) series [1] of infrared curves of branched isomers of decane shows that increased branching produces a number of bands in the 8- to 12-μ region. In many cases these new bands seem to cluster about the 8- to 9- and 10- to 11-μ regions. The presence of saturated rings seems to produce a similar spectrum, but Bellamy [2] cites articles in which evidence is given to show that the absorption in the 8- to 9-μ region tends to be due to branching and that in the 10- to 11-μ region to ring formation, in the absence of unsaturation and certain polar groups that also absorb in this region.

Figure 2 shows spectra in the 7.5- to 15-μ range for the first pentane-eluted portion of six oils from different parts of the country. There are three fairly good isosbestic points (wavelengths at which absorption is independent of the concentration of components) for these mixtures at 7.8, 12.4, and 14.8 μ, which divide the spectra into two parts. It will be noted that there is a negative correlation between the transmittance at 8.5 and 10.2 μ and that due to the methylene rocking vibration at 13.8 μ. This is indicated by the inverted order of the arabic numbers. A decrease in CH_2 groups implies, for this type of material, an increase in either branching or cyclization, and in the light of Bellamy's evidence, it is reasonable to assume that the absorption centered at 8.5 μ is due to branching and the one at 10.2 μ to ring formation. It is interesting to observe that there is a correlation between the absorbances of the bands at 8.5 and 10.2 μ and the refractive index of the respective fractions. It has been shown, from a study of many compounds [30], that increased branching, except in the 2 position, or cyclization, tends to raise the index of refraction. However, in this case, variations in molecular weight among the fractions could cause a similar effect. The changes in transmittance for the three wavelengths and the corresponding values for refractive index are given in table 4. The first high value for refractive index was obtained on the fraction that showed signs of aromatic absorption at 6.22 μ.

Thus, these materials can be said to contain varying quantities of saturated rings and chains of different lengths, some of which are branched. It is consistent with chemical knowledge that materials of this type should be eluted from silica gel by a hydrocarbon such as pentane, and that they should be least reactive with 30-percent fuming sulfuric acid.

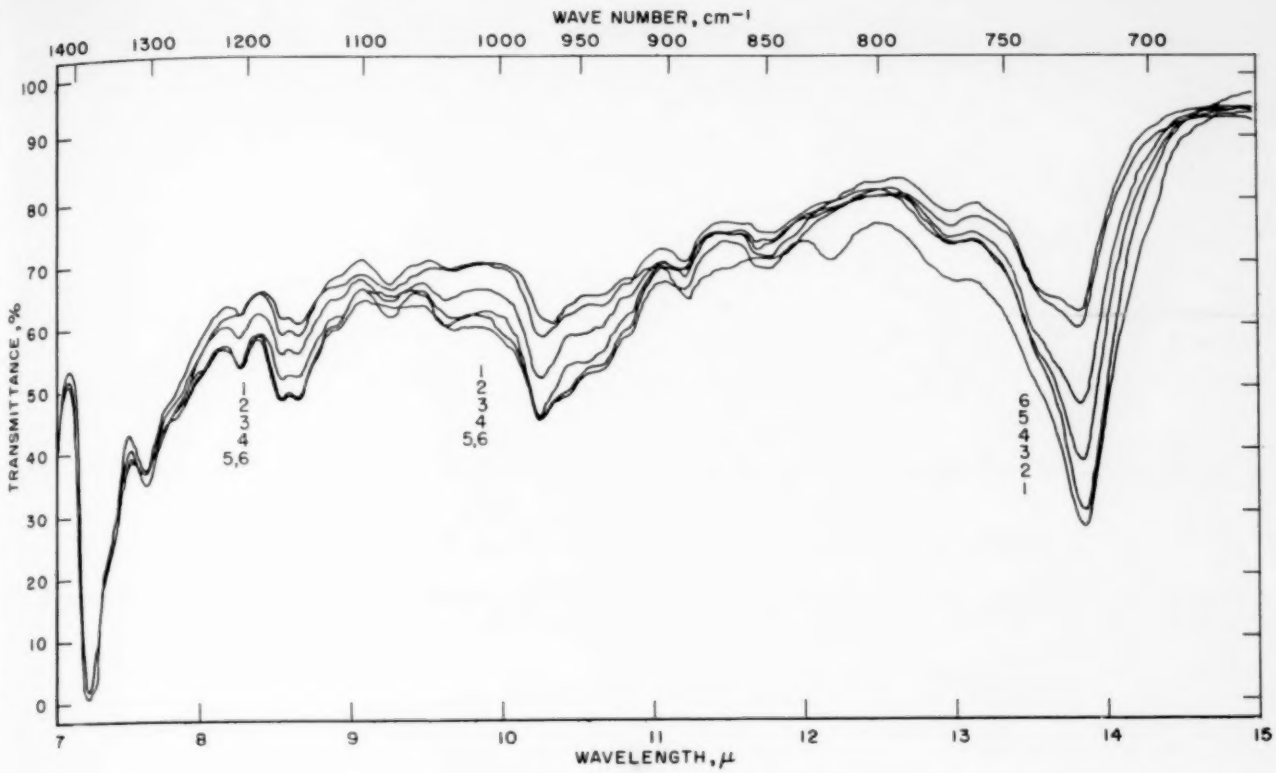

FIGURE 2. *Infrared spectra of first pentane-eluted fractions from six different oils (7 to 15 μ range).*

See table 4 for identification of the oils.

TABLE 4. *Index of refraction versus percentage transmittance*

First pentane-eluted fractions

Number of oil [a]	Transmittance (micron)			n_D^{25}
	13.8	10.2	8.5	
	$\frac{C_T}{C_C}$	$\frac{C_T}{C_C}$	$\frac{C_T}{C_C}$	
IV (1)	27.9	60.3	61.2	1.4845
III (2)	30.3	58.3	58.7	1.4800
II (3)	38.3	51.7	55.6	1.4805
I (4)	47.2	45.2	51.6	1.4882
V (5)	59.6	44.9	48.1	1.4915
VI (6)	61.9	44.9	48.1	1.4925

[a] The numbers in parentheses are the designations given in figure 2.

6. Second Pentane-Eluted Fractions

The spectrum in figure 3 was obtained on the material eluted from oil II by the second half of the pentane put through the column. This spectrum has a number of bands not present in the spectrum of the first portion eluted with pentane; these bands, in turn, are different from those in the spectrum of the benzene-eluted portion in the lower part of figure 4.

First, there is a strong band at 6.2 μ, with some indication of doubling (shoulder at about 6.26) and another shoulder at 6.7 μ, all of which are probably due to aromatic ring C=C stretching vibrations, although the band at 6.2 μ might also indicate nonaromatic conjugated double bonds. As shown by Young, DuVall, and Wright [43], the pattern of bands between 5 and 6 μ is characteristic of aromatic compounds. The pattern of bands beyond 11 μ (about 11.37, 11.7, 12.2, 12.84, 13.3 to 13.5, 13.8, and 14.3 μ) cannot, of course, in themselves, give positive identification of structural groups. However, it is consistent with Colthup's chart [7], and with Bellamy [2], to correlate these absorptions with mono-, di-, tri-, tetra-, and penta-substituted aromatic compounds and with α- and β-substituted napthalenes.

The above absorptions are due to C–H perpendicular bending modes, typical of these types of substitution. Again, the band at 13.8 μ is probably very largely due to the methylene rocking absorption from the substituted side chains. Plots of intensities of the other bands beyond 11 μ for different oils show a rough correlation with the intensity of the band at 6.2 μ. This is in agreement with the assignment of these bands to absorption from aromatic molecules. No more than a rough correlation is to be expected, because variations among the several types of aromatic compounds from oil to oil would be anticipated. This type of variation is emphasized by the fact that one of the fractions was markedly different from the others with respect to the relative intensities of the bands beyond 11 μ.

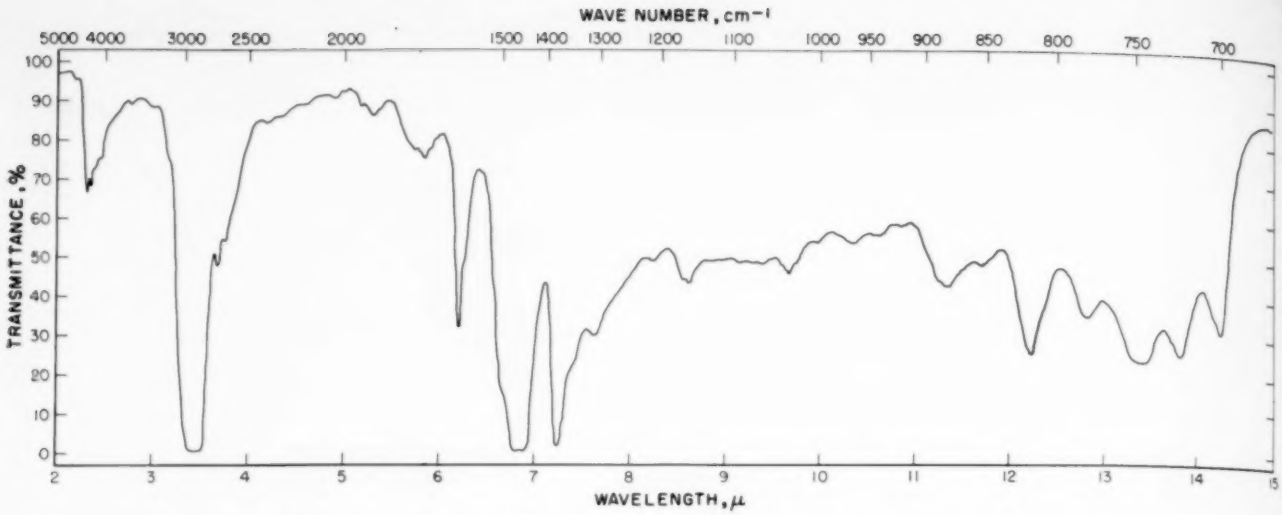

FIGURE 3. *Infrared spectrum of second pentane-eluted fraction of oil II.*

The intensity of the band at 8.54 μ, attributed to branching, may be somewhat reduced in comparison to that in the first pentane-eluted portions. The intensities of this band in this fraction of the different oils are inversely related to the intensities of the band near 13.8 μ. The position of the band near 13.8 μ shifts again to longer wavelengths with increasing intensity just as in the case of the first pentane-eluted portions. The band at 10.2 μ attributed to alicyclic compounds appears to be greatly reduced, if not eliminated, when compared to the first pentane-eluted portion. However, aromatic compounds also produce weak to medium bands in the region from 8.5 to 10 μ. Indeed, the absorption at 9.6 μ is probably due to the aromatic compounds discussed previously. It is possible, therefore, that aromatic absorptions below 10 μ and above 11 μ may increase the general background, making the reduction in the absorption at 10.2 μ more apparent than real.

Some of the absorption at 5.84 μ might be due to compounds containing carbonyl groups. The absorption characteristics in this region seem to vary from oil to oil, with some fractions having an absorption at 5.74 μ, suggesting the presence of two types of carbonyls. There is only very slight evidence of OH or NH in one of the oils.

The spectrum of one of the oils (oil VI) was different from that given in figure 3, in that it showed strong aromatic absorptions near 11.4 and 12.2, and no band at 9.6 μ.

Thus, these materials are probably hydrocarbons containing mono-, di-, and tri-substituted aromatic rings, with perhaps some naphthenic rings. The aliphatic side chains may be branched and could connect one ring to another. However, unpublished work of Termini and Glasgow [13], based on absorption studies, has shown that these compounds probably contain no more than a single aromatic nucleus. It is reasonable to assume that materials of this type would adhere more strongly to the silica gel than do simple aliphatic, branched, and cyclic hydrocarbons.

7. First and Second Acidaffins and Benzene-Eluted Fractions

The two spectra in the upper portion of figure 4 were obtained respectively from two portions of an oil (distillate 3); one portion does not react with 85-percent sulfuric acid, but is removed by 98-percent sulfuric acid (1st acidaffins); and the other portion does not react with 98-percent sulfuric acid, but is removed with 30-percent fuming sulfuric acid (2d acidaffins). These spectra are remarkably similar to that of the benzene-eluted portion of oil V in the lower part of figure 4.

It will be noted that over the whole spectrum the first acidaffins are more optically dense than the second acidaffins. This is generally true for all the acidaffin portions of the three distillates examined. The reasons for an increase in over-all optical density are not too well understood. An inspection of table 1, however, shows that the indices of refraction, densities, and carbon-to-hydrogen ratios are greater for the first acidaffins, whereas the molecular weights of the second acaidffins are greater, with one exception. It is reasonable to assume that the more chemically active materials in the first acidaffins would be more subject to carbonization than the second acidaffins. Such effects would tend to raise the density, carbon-to-hydrogen ratio, and optical density of the first acidaffins. Furthermore, the optical density over the whole spectrum is less for the benzene-eluted fraction, which is not subject to this treatment, than for any of the acidaffins. It should be noted that the transmittance ordinate has been omitted from figure 4 because the benzene-eluted fraction has been displaced below the other two curves.

The spectra of the three types of fractions show, in addition to the aromatic bands between 5 and 6 μ and those at 6.2 and 6.7 μ present in figure 3, shoulders at 3.3 μ, which are expected from the C—H

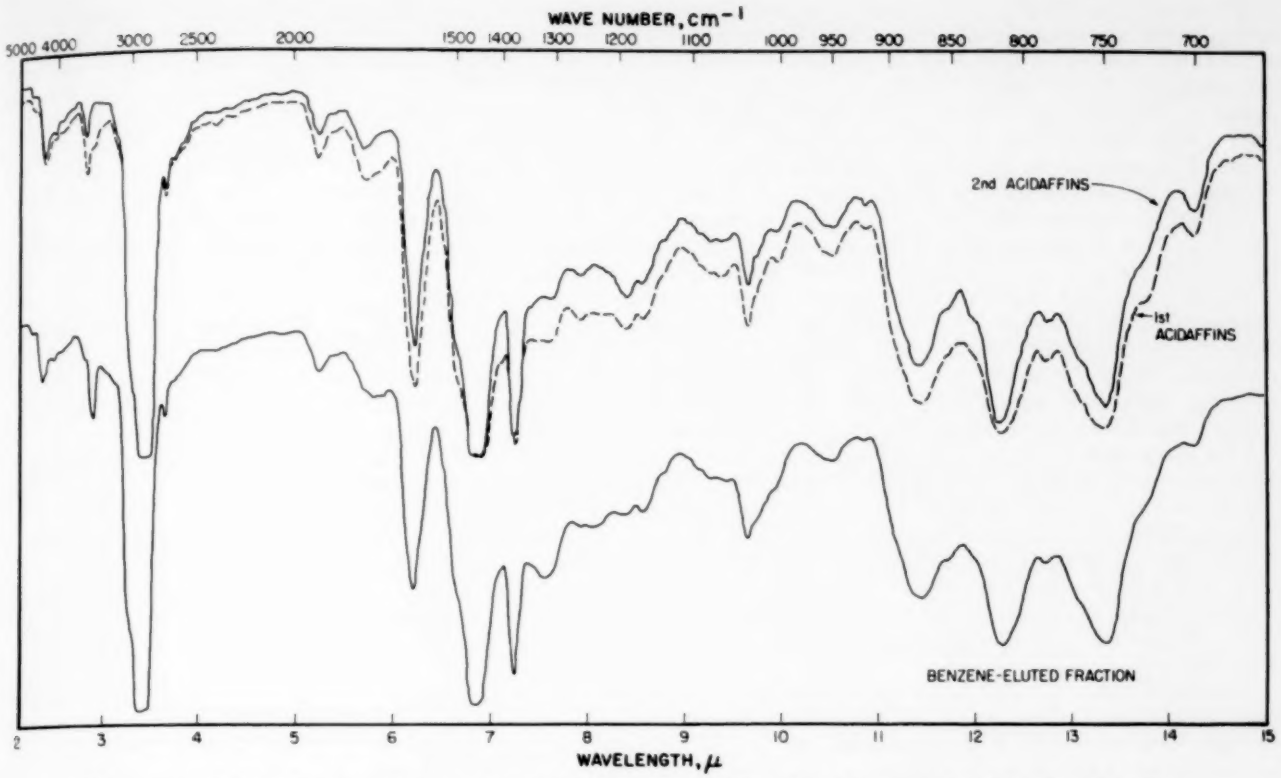

FIGURE 4. *Infrared spectra of first and second acidaffins of distillate 3 and benzene-eluted fraction of oil V.*

vibrations of aromatic molecules. Furthermore, the aromatic absorptions at 11.4, 12.2, and 13.4 μ are greatly increased, with the other absorptions observed in figure 3 at 11.7, 12.8, 13.1, and 14.3 μ fading into the background. This could result from the following effects: (1) A change in the distribution of the substituted aromatics, and (2) the presence of polynuclear aromatic compounds.

Benzanthracene and dibenzanthracene, as well as their derivatives, can be shown from the curves of Cannon and Sutherland [5] to have absorption bands of this type. The spectrum of diphenyl benzidene [17], with the N—H bands deleted and aliphatic C—H bands added, strongly resembles that of the spectra in figure 4. Finally, other polynuclear aromatic compounds have bands occurring at one or another of these positions [5,8], so that the envelope produced by a mixture of them would be expected to have the contour found here. This pattern of bands near 11.4 12.2, and 13.4 μ has been observed in the spectra of other natural products. Friedel and Pelipetz [11] and Friedel and Queiser [12] reported them in the spectra of coal fractions. Cannon [4] has reported them in the spectra of powdered coal, and Stewart [32] has observed them in fractions of petroleum asphalts. Furthermore, in their mass-spectrometer studies of high-molecular-weight hydrocarbons, O'Neal and his coworkers [20] have found polynuclear aromatics in lubricating-oil extracts, which generally contain substantial amounts of resins.

A strong correlation is once more found between the variation in the intensities of the bands at 11.4, 12.2, and 13.4 μ among the chromatographic fractions and the intensity of the aromatic band at 6.2 μ.

It is well known that an increase in aromaticity tends to increase the index of refraction. It is, therefore, interesting to note that a plot of n_D versus I/I_0 for the 6.2-μ band of these fractions yields a fairly straight line of negative slope. As before, this effect could also be due to variations in molecular weight. The increase in the band at 9.65 μ over that noted in figure 3 is consistent with either a change in the distribution of substituted aromatics or the presence of smaller fused-ring systems. An examination of Cannon and Sutherland's curves [5] shows that the intensities of the bands near 9.6 μ are relatively lower for the larger fused systems. Either possibility is consistent with the increased index of refraction.

Furthermore, the above effects are also consistent with the observed reduction in the intensity of the band at 13.8 μ due to the methylene rocking mode that depends on the presence of at least four consecutive CH_2 groups. The bands near 8.5 μ attributed to chain branching are still present and especially noticeable in the acidaffin fraction. However, the band at 10.2 μ assigned to saturated rings appears to have disappeared at least in the form present in figure 1. The band of 10.5 μ, not present in previous fractions, could result from the fused aromatic rings. The out-of-plane motion of the hydrogens in the *trans* double-bond configuration also causes absorptions in this region.

There is a possibility that some carbonyl groups are present in these fractions, contributing to the absorption near 5.75 and 5.84 μ. Again, conjugated nonaromatic C=C bonds might contribute to the absorption at 6.2 μ. Weak, but sharp, bands at 2.88 μ might arise from OH or NH groups. There is a general increase in absorption in the region near 8μ, where Friedel and Pelipetz [11] observed aromatic ether bands in their coal fractions. This absorption has the effect of obscuring the 8.5—μ chain-branching band, particularly in the benzene-eluted portion.

Thus, the first and second acidaffins and the benzene-eluted portion of the oils appear to be largely hydrocarbons with more marked aromatic character than those in the second pentane-eluted portion, but still containing some side chains of more than four carbon atoms in length. These side chains may also be branched. These fractions may be mixtures of substituted aromatic rings joined with methylene groups as well as polynuclear aromatic hydrocarbons. In the chromatographic fractions, the degree of aromaticity and the concentration of OH and NH groups vary from one oil to another. There is also some variation of these polar groups from one distillate to another of the acidaffin fractions.

In considering the foregoing discussion of the first and second acidaffins, and the following discussion of the two nitrogen-base fractions, it should be remembered that these fractions are actually mixtures and are, therefore, only concentrates of the designated component (see the group analysis of these samples in table II of Rostler and White [29]).

8. Nitrogen Bases, Groups I and II and Carbon Tetrachloride-Eluted Fractions

The two spectra in the upper portion of figure 5 were obtained on the nitrogen bases, groups I and II from distillate 3, as indicated. Nitrogen bases, group I, are removed from a petroleum ether solution of the oil with dry HCl gas. Nitrogen bases, group II, are removed from the remaining solution with 85-percent sulfuric acid. Groups I and II may be removed together with 85-percent sulfuric acid. These spectra are remarkably similar to the spectrum in the lower portion of figure 5, which was obtained on the material of oil IV eluted from the column with carbon tetrachloride.

It will be noted that the optical density of the nitrogen bases, group I, is greater in the region between 11 and 13.5 μ, whereas it is less in the region between 7.5 and 11 μ. Furthermore, the carbon-to-hydrogen ratio is larger for the nitrogen bases, group I, than for the nitrogen bases, group II. These facts may be interpreted to indicate that the compounds in the nitrogen bases, group I, are more highly aromatic than those in group II. It will be noted that the spectra of these fractions show some loss of detail as compared with those in figure 4, as well as other evidences of a difference in aromatic character.

Both nitrogen-base fractions have fairly strong absorptions near 3.1 μ, probably due to N—H stretching, and bands in the region between 5.9 and 6.0 μ, probably due to amide carbonyls, although unsaturated aldehydes and ketones can also absorb in this region. However, there is no evidence of the bands characteristic of aldehydes in the 3.4- to 3.7-μ region. The carbonyl absorption is much stronger in the nitrogen bases, group II, suggesting that nitrogen in this group is predominantly amide in nature, whereas that in the nitrogen bases, group I, is largely present in the form of amines. This appears to be consistent with the elemental analysis of the three sets of fractions given in table 1. In each case the amount by which the sum of the elements fails to equal 100 percent is greater for the nitrogen bases, group II, suggesting a higher oxygen content. It can be noted that the absorptions of both N—H and C=O stretching vibrations occur at slightly longer wavelengths in the nitrogen bases, group I; this possibly indicates that hydrogen bonding is more pronounced in this fraction. It might be expected that susceptibility to hydrogen bonding would be related to reactivity toward dry HCl. Absorptions due to N—H deformation in unsubstituted amides and primary amines contribute to the band at 6.25 μ. Weak bands at 6.5 μ found in some of the spectra of both nitrogen bases and in a number of the spectra of the carbon tetrachloride-eluted fractions are probably due to the N—H deformation of monosubstituted amides and secondary amines, but could also result from nitro compounds. A weak band appears at 5.2 μ for the nitrogen bases and 5.3 μ for the carbon tetrachloride-eluted fractions. This is in the region where amine hydrochlorides absorb. There is still evidence of straight chains of four or more methylene groups, none of cyclization, and little of branching. However, the general absorption near 8.0 μ attributed to aromatic ethers in the spectra in figure 4 has increased in all fractions in figure 5. The spectrum of the carbon tetrachloride-eluted portion appears most similar to that of the nitrogen bases, group II, with regard to the position of the bands for the polar groups. It should be noted that in all the spectra the absorption near 3.0 μ could result in part from OH stretchings.

The aromatic absorptions between 11 and 15 μ in the carbon tetrachloride-eluted portions differed widely from one oil to another. There were also differences in the polar absorptions near 3.0 and 6.0 μ. In fact, even the type of spectrum given in figure 5 was obtained for only 4 of the 6 oils studied (oils I, III, IV, and VI), the spectra of the other 2 oils being different. Oil II had sharp bands at 7.9 and 8.9 μ, a widely different aromatic character with absorption bands at 11.8, 12.6, 13.7, and 14.3 μ, quite different polar absorptions near 3.0 and 6.0 μ, and a much reduced CH stretching absorption. Oil V had a rather high over-all absorption, with broad slight absorptions at 3.0, 3.4, 5.9, 6.2, 6.9, and 7.2 μ and slight swellings at 11.7, 12.4, and 13.5 μ. Even the nitrogen bases, groups I and II, from the different distillates of the same crude oil showed a variability in polar and aromatic constituents

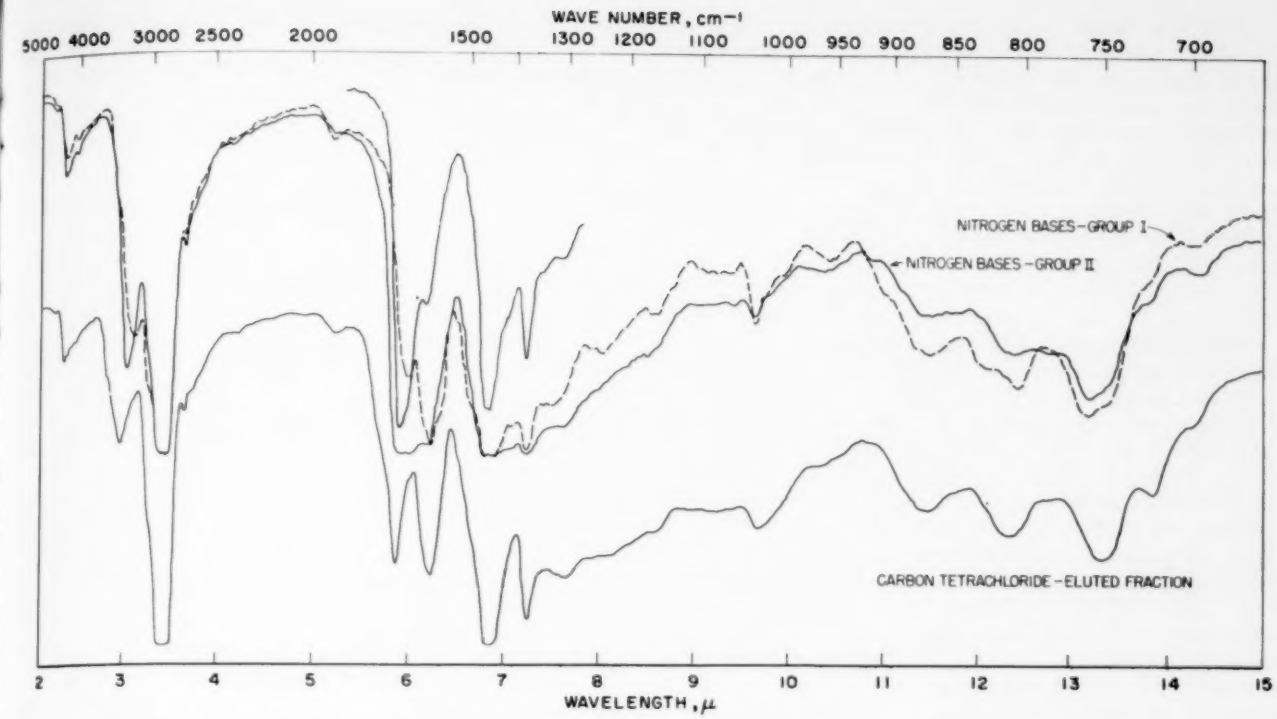
WAVE NUMBER, cm⁻¹
5000 4000 3000 2500 2000 1500 1300 1200 1100 1000 950 900 850 800 750 700
NITROGEN BASES – GROUP I
NITROGEN BASES – GROUP II
CARBON TETRACHLORIDE – ELUTED FRACTION
2 3 4 5 6 7 8 9 10 11 12 13 14 15
WAVELENGTH, μ

FIGURE 5. *Infrared spectra of nitrogen bases, groups I and II, of distillate 3 and carbon tetrachloride-eluted fraction of oil IV.*

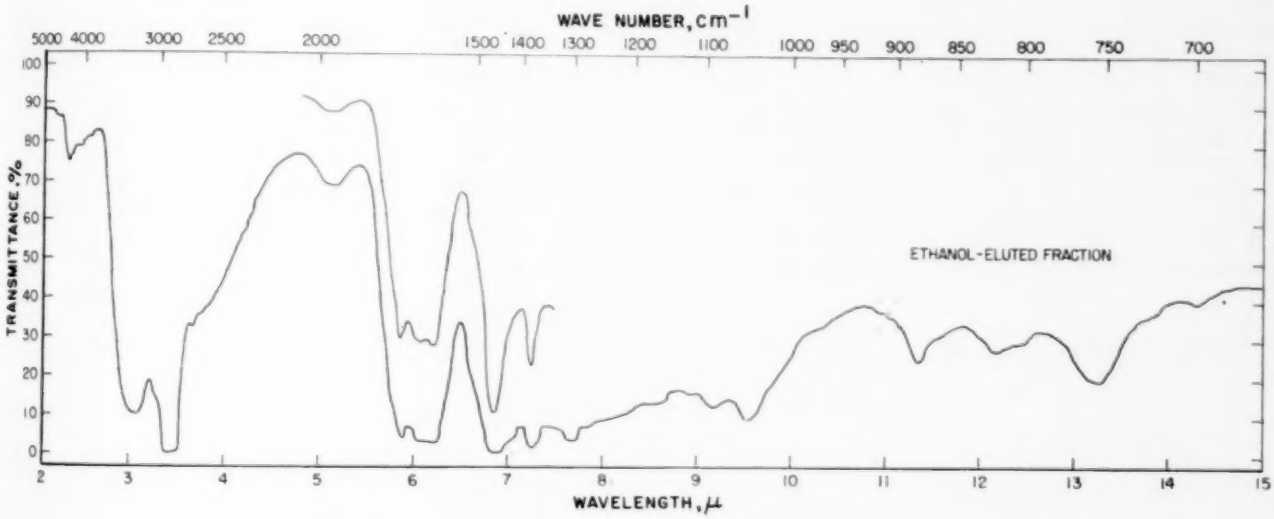

FIGURE 6. *Infrared spectra of ethanol-eluted fraction of oil III.*

from distillate to distillate. In the spectrum of one of the nitrogen bases, a strong band appeared at 8.6 μ (nitrogen bases, group II of distillate IV). The observed variability, in all cases, is much greater than that found in any of the fractions discussed previously. It is consistent with the chemistry of the separation to find a variety of amines in the nitrogen bases, group I, and a large variety of polar compounds containing N—H, O—H, and carbonyl groups in the nitrogen bases, group II.

9. Ethanol-Eluted Fractions

The spectrum in figure 6 obtained on the portion of oil III eluted with ethanol is similar to those in figure 5, except for the marked broadening of the absorption region on the long wavelength side of the C—H stretching band at 3.4 μ. This is apparently due to the breadth of the band at 3.0 μ, which appears to extend "through" the C—H band to beyond 4 μ. This conformation is characteristic of hydrogen

bonding, as found, for example, in carboxylic acids. The band near 3.0 μ varies considerably in wavelength and intensity from one oil to another. The aromatic character (bands beyond 11 μ) is again different from that found in the acidaffins, and there is variation from one oil to another. There are very strong bands in the range 5.64 to 6.08 μ. These are resolved in the spectrum of a thin film, as shown in the upper curve of figure 6. The patterns of bands near 6.0 μ for the six oils seem to fall into three categories. The two oils in category 1 (oils I and II) have common bands at 5.63 (weak), 5.8 (shoulder), 5.85 (strong), and 6.08 μ (weak). Oil II has an additional weak band at 6.01 μ. Only these two oils have a strong peak at less than 3.0 μ. The three oils in category 2 (oils IV, V, and VI) have bands at 5.66 (shoulder), 5.82 (strong), and 6.02 to 6.04 μ (strong). The single oil in category 3 (oil III) has bands at 5.87 and 6.08 μ. These bands probably represent a variety of carbonyl structures. There is evidence of saturated hydrocarbons from the strong bands at 3.4, 6.8, and 7.25 μ, but there is little evidence of branching, cyclization, or chains containing more than four CH_2 groups. The general absorption near 8.0 μ seems to have increased still further, and the band near 5.2 μ has increased markedly in intensity.

These fractions contain compounds with aromatic nuclei, condensed or otherwise, and in addition to carboxylic acids, combinations of OH, NH, and C=O in any form, including alcohols, phenols, amines, amides, aldehydes, and ketones. They also contain unconjugated C=C (6.08-μ band), conjugated C=C, and aliphatic CH_2 and CH_3. The most marked characteristic of these fractions is the variation in composition, even of polar groups, from one oil to another, a variation that is probably greater than in the case of the carbon tetrachloride-eluted fraction. This variation may be expected because it is the most strongly polar group alone and not the remainder of the molecule, including other polar groups, which places a compound in this fraction. The variation in aromatic character of both the carbon tetrachloride- and ethanol-eluted fractions is to be expected because they are separated from the column on the basis of a polarity greater than their aromatic character alone.

10. Asphaltenes

The asphaltenes, figure 7, show their aromatic character by the absorptions at 6.2, 11.4, 12.2, and 13.4 μ. These bands are especially noticeable in the spectrum obtained with the KBr pellet containing the greater concentration of asphaltenes (lower curve). The presence of CH_2 and CH_3 groups is evident from the absorptions at 3.4, 6.8 to 6.9, and 7.25 μ. The asphaltenes used here were obtained by *n*-nentane precipitation from a crude oil that had been airblown (designation (A—O) of Rostler and White [29]). They exhibit a fairly strong absorption band at 5.9 μ due to the presence of carbonyl groups. This band was not present in the spectrum of asphaltenes obtained from crude oil that had not been airblown or in the spectrum of Gilsonite. The airblown sample was shown to contain more oxygen than either of the other samples [29]. The band at 2.9 μ is due to the presence of water in the potassium bromide of the pellet. The low transmittance at shorter wavelengths is the result of scatter by the asphaltene particles. It is well known that asphaltenes may result from condensation or oxidation of aromatic portions of the oil. Thus, they may consist of polyamides (from the polar compounds) or condensed aromatic rings or both.

One of the oils was also separated by Kleinschmidt into four fractions by means of his chromatographic procedure for petroleum asphalts employing fuller's earth as an adsorbent and a different series of eluents from those used here [16]. The infrared spectra of these fractions resembled those of the fractions studied here.

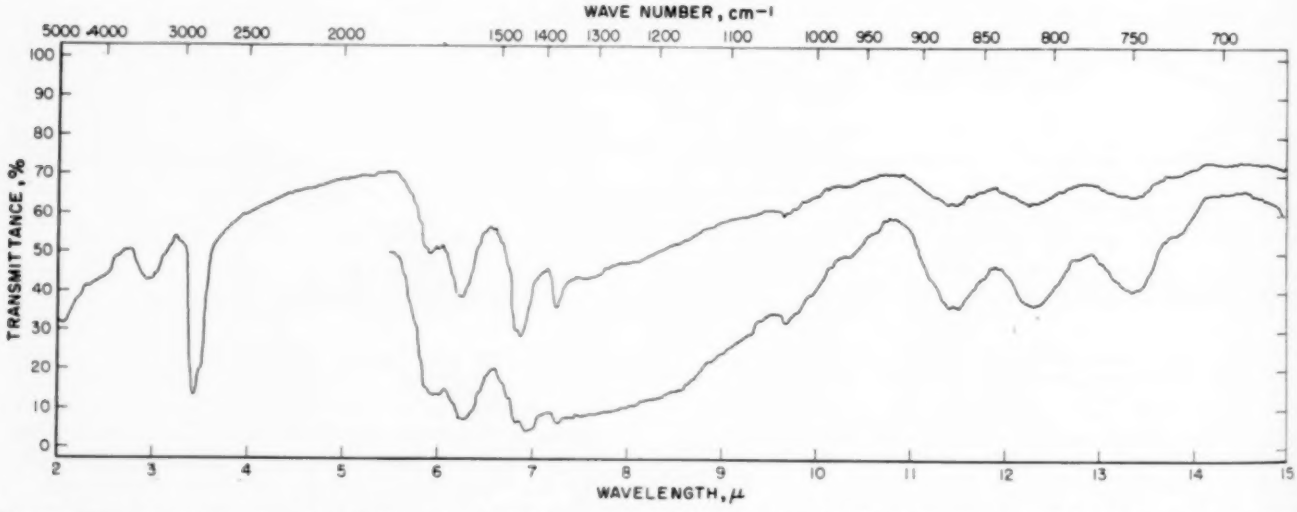

FIGURE 7. *Infrared spectra of asphaltenes from air-blown crude oil (designation (A–O) of Rostler and White [29],) using the KBr pellet technique.*

11. Far Infrared and Ultraviolet Spectra-Exploratory Studies

Some exploratory work was done in the region between 15 and 40 μ, using typical benzene-, carbon-tetrachloride- and ethanol-eluted portions of oil IV. The curves in figure 8 indicate the type of spectra obtained in this region. The spectrum of the paraffins or the first pentane-eluted portion was not obtained; a typical mineral oil with no aromatic bands in the rock-salt region, shows no bands in this region. The absorption bands at 21 and 23.3 μ in the benzene- and carbon-tetrachloride-eluted portions occur in a region where aromatic compounds absorb [7]. The spectrum of the ethanol-eluted portion retains the band at about 23 μ, but the 21-μ band is missing. No other well-defined bands are found in these spectra, except for the weak bands at longer wavelengths, which are due to uncompensated atmospheric water vapor.

Ultraviolet spectra (fig. 9) were obtained on fractions of oil II eluted from silica gel with pentane, benzene, and methanol, using an earlier chromatographic procedure. These fractions had infrared spectra similar to those of the corresponding fractions presented earlier, with the exception that the methanol-eluted fraction had more pronounced aromatic bands at 11.4, 12.2, and 13.4 μ, and less pronounced bands arising from polar groups than did the ethanol-eluted fraction. Spectra of a number of fractions obtained by acid extraction are included in figure 10.

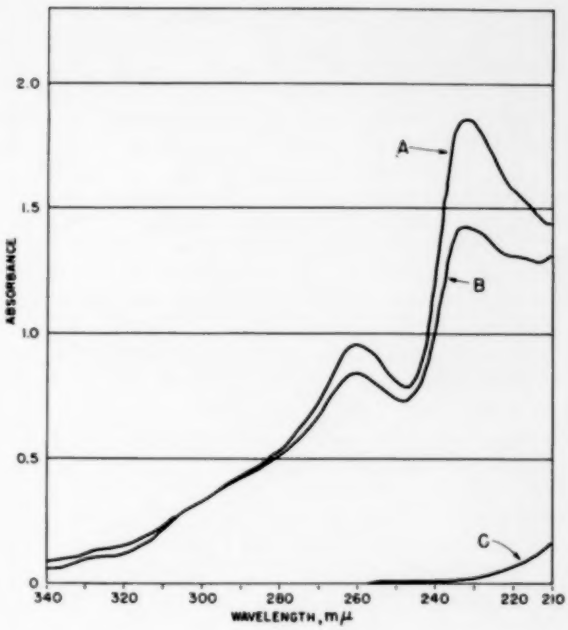

FIGURE 9. *Ultraviolet spectra of fractions obtained by chromatographic separation of oil II.*

A, Benzene-eluted fraction (concentration 10.60 mg/liter); B, methanol-eluted fraction (concentration 10.30 mg/liter); and C, pentane-eluted fraction (concentration 136.8 mg/liter).

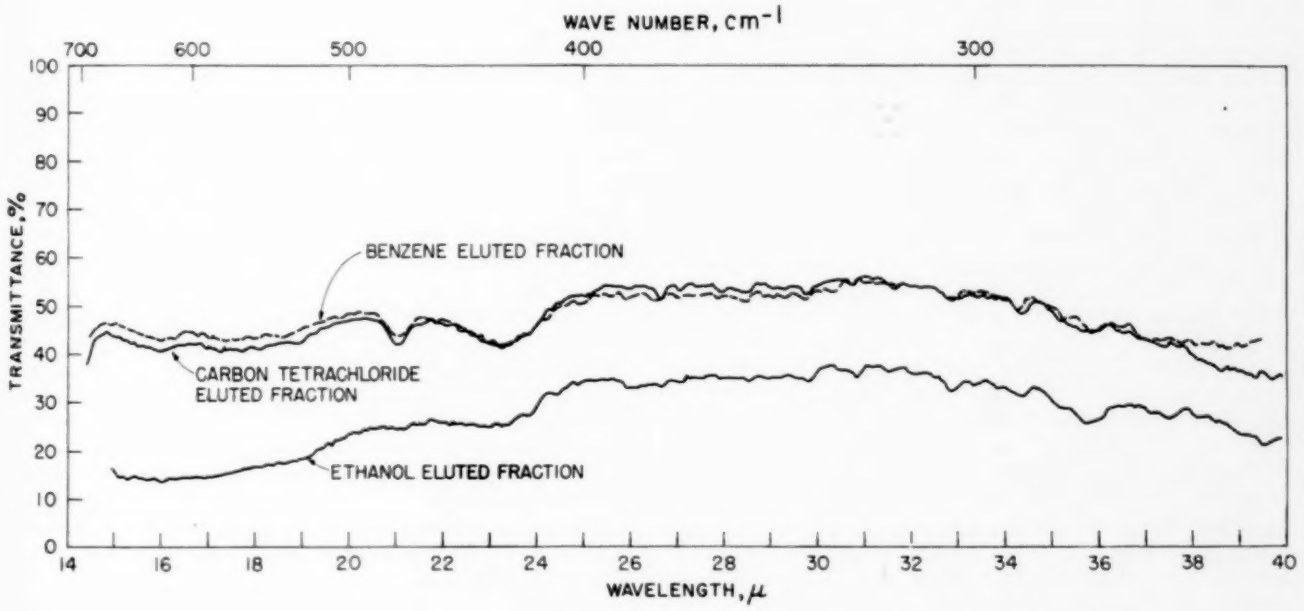

FIGURE 8. *Far infrared spectra (15 to 40 μ range) of typical benzene-, carbon tetrachloride-, and ethanol-eluted fractions of oil IV.*

There is a possibility that some carbonyl groups are present in these fractions, contributing to the absorption near 5.75 and 5.84 μ. Again, conjugated nonaromatic C=C bonds might contribute to the absorption at 6.2 μ. Weak, but sharp, bands at 2.88 μ might arise from OH or NH groups. There is a general increase in absorption in the region near 8μ, where Friedel and Pelipetz [11] observed aromatic ether bands in their coal fractions. This absorption has the effect of obscuring the 8.5—μ chain-branching band, particularly in the benzene-eluted portion.

Thus, the first and second acidaffins and the benzene-eluted portion of the oils appear to be largely hydrocarbons with more marked aromatic character than those in the second pentane-eluted portion, but still containing some side chains of more than four carbon atoms in length. These side chains may also be branched. These fractions may be mixtures of substituted aromatic rings joined with methylene groups as well as polynuclear aromatic hydrocarbons. In the chromatographic fractions, the degree of aromaticity and the concentration of OH and NH groups vary from one oil to another. There is also some variation of these polar groups from one distillate to another of the acidaffin fractions.

In considering the foregoing discussion of the first and second acidaffins, and the following discussion of the two nitrogen-base fractions, it should be remembered that these fractions are actually mixtures and are, therefore, only concentrates of the designated component (see the group analysis of these samples in table II of Rostler and White [29]).

8. Nitrogen Bases, Groups I and II and Carbon Tetrachloride-Eluted Fractions

The two spectra in the upper portion of figure 5 were obtained on the nitrogen bases, groups I and II from distillate 3, as indicated. Nitrogen bases, group I, are removed from a petroleum ether solution of the oil with dry HCl gas. Nitrogen bases, group II, are removed from the remaining solution with 85-percent sulfuric acid. Groups I and II may be removed together with 85-percent sulfuric acid. These spectra are remarkably similar to the spectrum in the lower portion of figure 5, which was obtained on the material of oil IV eluted from the column with carbon tetrachloride.

It will be noted that the optical density of the nitrogen bases, group I, is greater in the region between 11 and 13.5 μ, whereas it is less in the region between 7.5 and 11 μ. Furthermore, the carbon-to-hydrogen ratio is larger for the nitrogen bases, group I, than for the nitrogen bases, group II. These facts may be interpreted to indicate that the compounds in the nitrogen bases, group I, are more highly aromatic than those in group II. It will be noted that the spectra of these fractions show some loss of detail as compared with those in figure 4, as well as other evidences of a difference in aromatic character.

Both nitrogen-base fractions have fairly strong absorptions near 3.1 μ, probably due to N—H stretching, and bands in the region between 5.9 and 6.0 μ, probably due to amide carbonyls, although unsaturated aldehydes and ketones can also absorb in this region. However, there is no evidence of the bands characteristic of aldehydes in the 3.4- to 3.7-μ region. The carbonyl absorption is much stronger in the nitrogen bases, group II, suggesting that nitrogen in this group is predominantly amide in nature, whereas that in the nitrogen bases, group I, is largely present in the form of amines. This appears to be consistent with the elemental analysis of the three sets of fractions given in table 1. In each case the amount by which the sum of the elements fails to equal 100 percent is greater for the nitrogen bases, group II, suggesting a higher oxygen content. It can be noted that the absorptions of both N—H and C=O stretching vibrations occur at slightly longer wavelengths in the nitrogen bases, group I; this possibly indicates that hydrogen bonding is more pronounced in this fraction. It might be expected that susceptibility to hydrogen bonding would be related to reactivity toward dry HCl. Absorptions due to N—H deformation in unsubstituted amides and primary amines contribute to the band at 6.25 μ. Weak bands at 6.5 μ found in some of the spectra of both nitrogen bases and in a number of the spectra of the carbon tetrachloride-eluted fractions are probably due to the N—H deformation of monosubstituted amides and secondary amines, but could also result from nitro compounds. A weak band appears at 5.2 μ for the nitrogen bases and 5.3 μ for the carbon tetrachloride-eluted fractions. This is in the region where amine hydrochlorides absorb. There is still evidence of straight chains of four or more methylene groups, none of cyclization, and little of branching. However, the general absorption near 8.0 μ attributed to aromatic ethers in the spectra in figure 4 has increased in all fractions in figure 5. The spectrum of the carbon tetrachloride-eluted portion appears most similar to that of the nitrogen bases, group II, with regard to the position of the bands for the polar groups. It should be noted that in all the spectra the absorption near 3.0 μ could result in part from OH stretchings.

The aromatic absorptions between 11 and 15 μ in the carbon tetrachloride-eluted portions differed widely from one oil to another. There were also differences in the polar absorptions near 3.0 and 6.0 μ. In fact, even the type of spectrum given in figure 5 was obtained for only 4 of the 6 oils studied (oils I, III, IV, and VI), the spectra of the other 2 oils being different. Oil II had sharp bands at 7.9 and 8.9 μ, a widely different aromatic character with absorption bands at 11.8, 12.6, 13.7, and 14.3 μ, quite different polar absorptions near 3.0 and 6.0 μ, and a much reduced CH stretching absorption. Oil V had a rather high over-all absorption, with broad slight absorptions at 3.0, 3.4, 5.9, 6.2, 6.9, and 7.2 μ and slight swellings at 11.7, 12.4, and 13.5 μ. Even the nitrogen bases, groups I and II, from the different distillates of the same crude oil showed a variability in polar and aromatic constituents

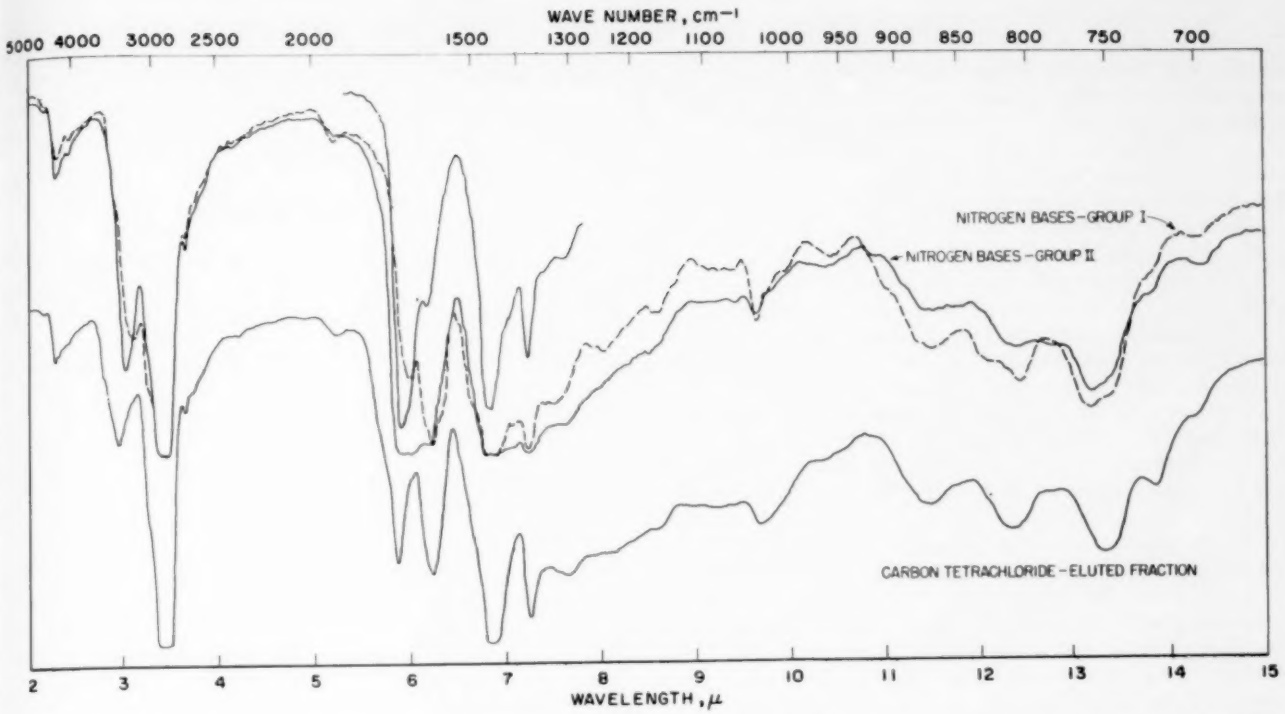
WAVE NUMBER, cm⁻¹
5000 4000 3000 2500 2000 1500 1300 1200 1100 1000 950 900 850 800 750 700
NITROGEN BASES-GROUP I
NITROGEN BASES-GROUP II
CARBON TETRACHLORIDE-ELUTED FRACTION
2 3 4 5 6 7 8 9 10 11 12 13 14 15
WAVELENGTH, μ

FIGURE 5. *Infrared spectra of nitrogen bases, groups I and II, of distillate 3 and carbon tetrachloride-eluted fraction of oil IV.*

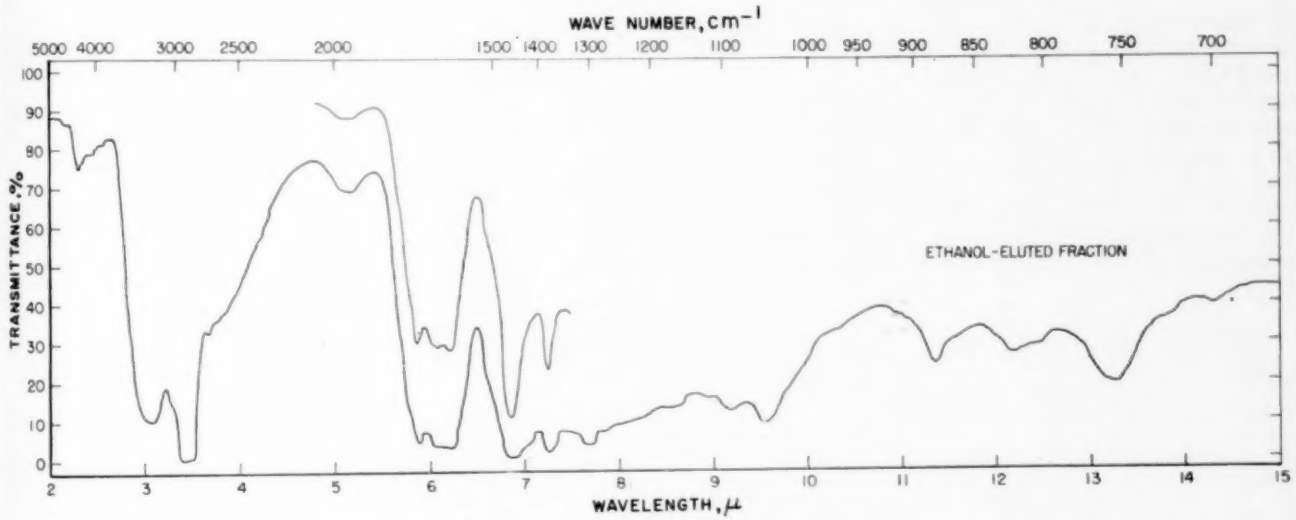

FIGURE 6. *Infrared spectra of ethanol-eluted fraction of oil III.*

from distillate to distillate. In the spectrum of one of the nitrogen bases, a strong band appeared at 8.6 μ (nitrogen bases, group II of distillate IV). The observed variability, in all cases, is much greater than that found in any of the fractions discussed previously. It is consistent with the chemistry of the separation to find a variety of amines in the nitrogen bases, group I, and a large variety of polar compounds containing N—H, O—H, and carbonyl groups in the nitrogen bases, group II.

9. Ethanol-Eluted Fractions

The spectrum in figure 6 obtained on the portion of oil III eluted with ethanol is similar to those in figure 5, except for the marked broadening of the absorption region on the long wavelength side of the C—H stretching band at 3.4 μ. This is apparently due to the breadth of the band at 3.0 μ, which appears to extend "through" the C—H band to beyond 4 μ. This conformation is characteristic of hydrogen

bonding, as found, for example, in carboxylic acids. The band near 3.0 μ varies considerably in wavelength and intensity from one oil to another. The aromatic character (bands beyond 11 μ) is again different from that found in the acidaffins, and there is variation from one oil to another. There are very strong bands in the range 5.64 to 6.08 μ. These are resolved in the spectrum of a thin film, as shown in the upper curve of figure 6. The patterns of bands near 6.0 μ for the six oils seem to fall into three categories. The two oils in category 1 (oils I and II) have common bands at 5.63 (weak), 5.8 (shoulder), 5.85 (strong), and 6.08 μ (weak). Oil II has an additional weak band at 6.01 μ. Only these two oils have a strong peak at less than 3.0 μ. The three oils in category 2 (oils IV, V, and VI) have bands at 5.66 (shoulder), 5.82 (strong), and 6.02 to 6.04 μ (strong). The single oil in category 3 (oil III) has bands at 5.87 and 6.08 μ. These bands probably represent a variety of carbonyl structures. There is evidence of saturated hydrocarbons from the strong bands at 3.4, 6.8, and 7.25 μ, but there is little evidence of branching, cyclization, or chains containing more than four CH_2 groups. The general absorption near 8.0 μ seems to have increased still further, and the band near 5.2 μ has increased markedly in intensity.

These fractions contain compounds with aromatic nuclei, condensed or otherwise, and in addition to carboxylic acids, combinations of OH, NH, and C=O in any form, including alcohols, phenols, amines, amides, aldehydes, and ketones. They also contain unconjugated C=C (6.08-μ band), conjugated C=C, and aliphatic CH_2 and CH_3. The most marked characteristic of these fractions is the variation in composition, even of polar groups, from one oil to another, a variation that is probably greater than in the case of the carbon tetrachloride-eluted fraction. This variation may be expected because it is the most strongly polar group alone and not the remainder of the molecule, including other polar groups, which places a compound in this fraction. The variation in aromatic character of both the carbon tetrachloride- and ethanol-eluted fractions is to be expected because they are separated from the column on the basis of a polarity greater than their aromatic character alone.

10. Asphaltenes

The asphaltenes, figure 7, show their aromatic character by the absorptions at 6.2, 11.4, 12.2, and 13.4 μ. These bands are especially noticeable in the spectrum obtained with the KBr pellet containing the greater concentration of asphaltenes (lower curve). The presence of CH_2 and CH_3 groups is evident from the absorptions at 3.4, 6.8 to 6.9, and 7.25 μ. The asphaltenes used here were obtained by *n*-nentane precipitation from a crude oil that had been airblown (designation (A—O) of Rostler and White [29]). They exhibit a fairly strong absorption band at 5.9 μ due to the presence of carbonyl groups. This band was not present in the spectrum of asphaltenes obtained from crude oil that had not been airblown or in the spectrum of Gilsonite. The airblown sample was shown to contain more oxygen than either of the other samples [29]. The band at 2.9 μ is due to the presence of water in the potassium bromide of the pellet. The low transmittance at shorter wavelengths is the result of scatter by the asphaltene particles. It is well known that asphaltenes may result from condensation or oxidation of aromatic portions of the oil. Thus, they may consist of polyamides (from the polar compounds) or condensed aromatic rings or both.

One of the oils was also separated by Kleinschmidt into four fractions by means of his chromatographic procedure for petroleum asphalts employing fuller's earth as an adsorbent and a different series of eluents from those used here [16]. The infrared spectra of these fractions resembled those of the fractions studied here.

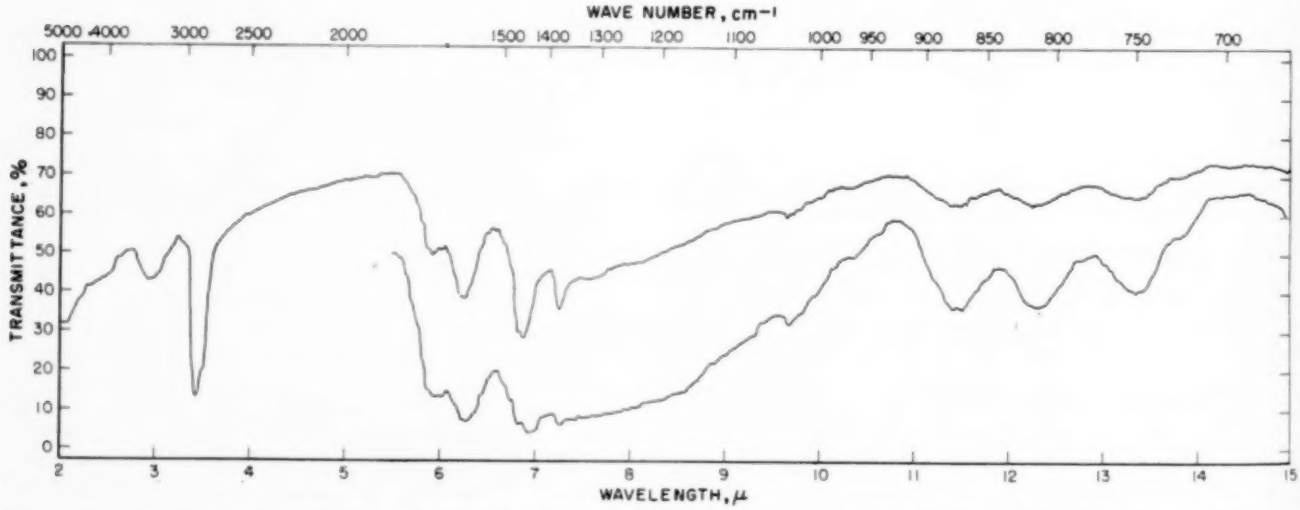

FIGURE 7. *Infrared spectra of asphaltenes from air-blown crude oil (designation (A–O) of Rostler and White [29],) using the KBr pellet technique.*

11. Far Infrared and Ultraviolet Spectra-Exploratory Studies

Some exploratory work was done in the region between 15 and 40 μ, using typical benzene-, carbon-tetrachloride- and ethanol-eluted portions of oil IV. The curves in figure 8 indicate the type of spectra obtained in this region. The spectrum of the paraffins or the first pentane-eluted portion was not obtained; a typical mineral oil with no aromatic bands in the rock-salt region, shows no bands in this region. The absorption bands at 21 and 23.3 μ in the benzene- and carbon-tetrachloride-eluted portions occur in a region where aromatic compounds absorb [7]. The spectrum of the ethanol-eluted portion retains the band at about 23 μ, but the 21-μ band is missing. No other well-defined bands are found in these spectra, except for the weak bands at longer wavelengths, which are due to uncompensated atmospheric water vapor.

Ultraviolet spectra (fig. 9) were obtained on fractions of oil II eluted from silica gel with pentane, benzene, and methanol, using an earlier chromatographic procedure. These fractions had infrared spectra similar to those of the corresponding fractions presented earlier, with the exception that the methanol-eluted fraction had more pronounced aromatic bands at 11.4, 12.2, and 13.4 μ, and less pronounced bands arising from polar groups than did the ethanol-eluted fraction. Spectra of a number of fractions obtained by acid extraction are included in figure 10.

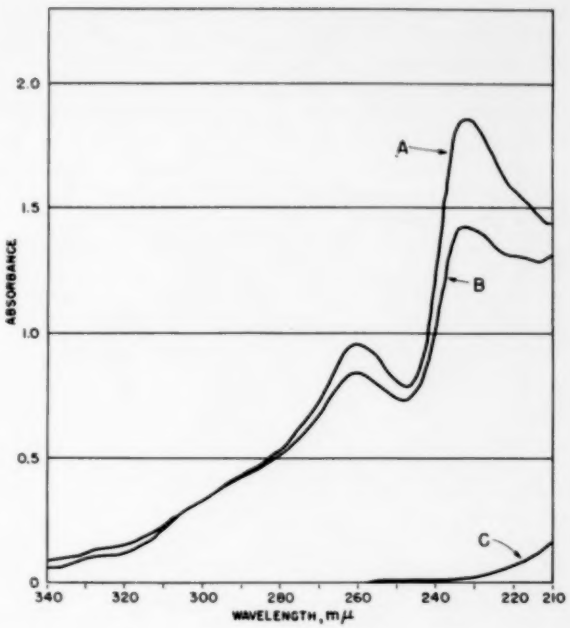

FIGURE 9. *Ultraviolet spectra of fractions obtained by chromatographic separation of oil II.*

A, Benzene-eluted fraction (concentration 10.60 mg/liter); B, methanol-eluted fraction (concentration 10.30 mg/liter); and C, pentane-eluted fraction (concentration 136.8 mg/liter).

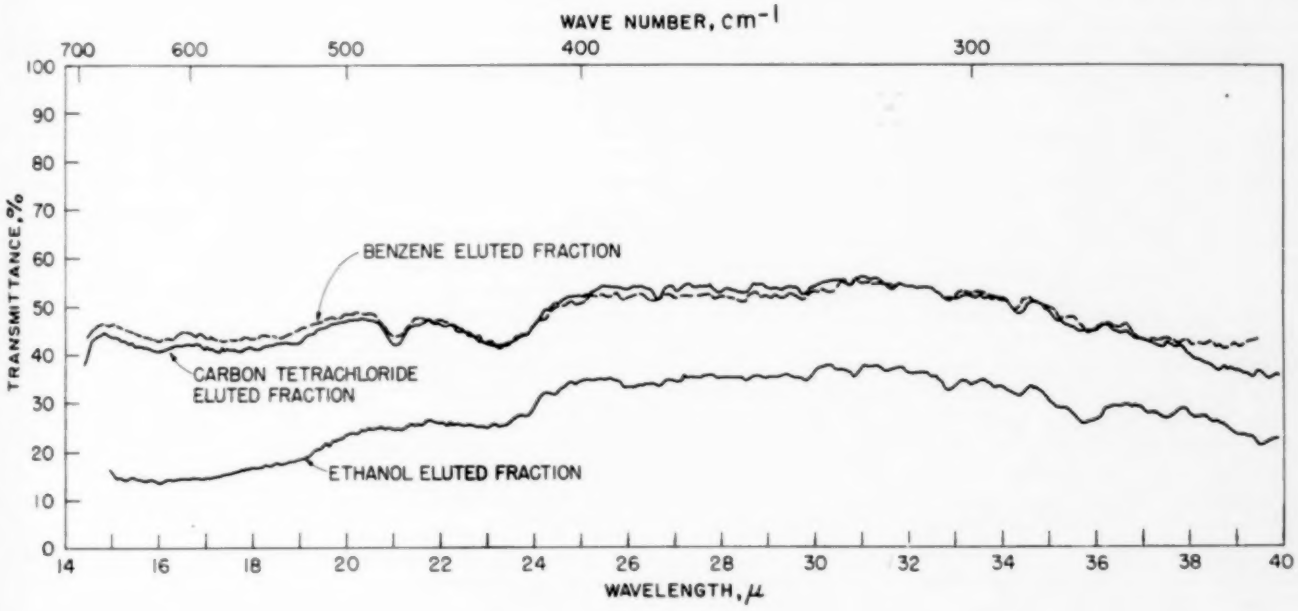

FIGURE 8. *Far infrared spectra (15 to 40 μ range) of typical benzene-, carbon tetrachloride-, and ethanol-eluted fractions of oil IV.*

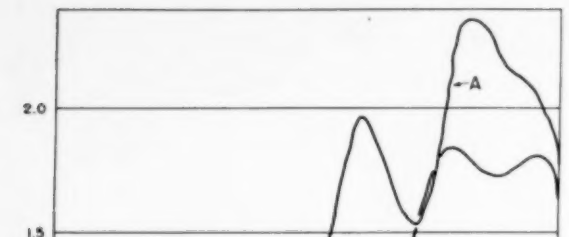

FIGURE 10. *Ultraviolet spectra of fractions obtained by acid extraction.*

A, First acidaffins, distillate 3 (concentration 12.44 mg/liter); B, nitrogen bases, group I, distillate 3 (concentration 12.24 mg/liter); C, second acidaffins, distillate 3 (concentration 6.10 mg/liter); D, nitrogen bases, group II, distillate 3 (concentration 11.44 mg/liter); E, paraffins (a), distillate 3 (concentration 129.6 mg/liter); and F, asphaltenes from crude oil, not air blown, designation AC of Rostler and White [29] (not entirely soluble).

It will be noted that there is a similarity in the mineral-oil fractions separated by the two methods. The acidaffins are similar to the benzene-eluted fraction and also, in this part of the spectrum, to the nitrogen bases and the polar compounds eluted with methanol. A study of the spectra compiled by Friedel and Orchin [10] indicates that the shape of the curves for the acidaffins, nitrogen bases, and benzene- and methanol-eluted portions could result from mixtures of various aromatic and aromatic polar compounds, in agreement with the results of the infrared studies. However, the data of Braude [3] show that conjugated dienes and trienes absorb at 217 and 265 μ, respectively. Thus, the possible presence of compounds containing conjugated double bonds along with the aromatic compounds cannot be ruled out. Assuming these absorptions to be largely due to aromatic compounds, the fact that they are more intense in the nitrogen bases, group I, than in the nitrogen bases, group II, is consistent with the conclusion derived from the infrared spectra that the nitrogen bases, group I, are more aromatic. Prem and Duke [21,22], from more extended studies have developed a method of identifying oils in oil-extended rubber. Charlet and his coworkers [6] by means of ultraviolet and infrared studies, have identified specific compound types (aromatic) in fine cuts of gas oil and cycle stock from catalytic cracking.

12. Quantitative Comparison of Fractions

In table 5, a quantitative comparison is made of the chromatographic and acid-extraction procedures. The data given here are derived from table 3. It will be noted that for all six oils, the first pentane-eluted portion is nearly the same in quantity as the paraffin portions. It is also apparent that the combined acidaffins vary from being slightly more than the combined benzene and second pentane-eluted portions in the "paraffinic" oils to considerably less in the highly "aromatic" oils. In oils I, II, and III the two nitrogen-base fractions are roughly equal in quantity to the combined polar fractions, but in the remaining oils the combined nitrogen-base fractions are about twice as large as the combined polar fractions.

TABLE 5. *Quantitative comparison of procedures*

	Oil samples	First pentane	Paraffins	Second pentane and benzene	First and second acidaffins	Carbon tetrachloride and ethanol	Nitrogen bases, groups I and II
		%	%	%	%	%	%
I	Circosol 2×H	53.4	50.1	43.3	47.7	3.3	2.2
II	Sundex 53	25.1	23.8	69.7	69.7	6.9	6.5
III	SPX 97	26.0	24.5	69.1	67.8	5.8	7.7
IV	Philrich 5	11.0	9.6	81.8	78.0	6.6	12.4
V	Dutrex 20	6.0	6.1	81.8	70.0	11.4	23.9
VI	Califlux TT	10.7	10.5	76.0	68.1	13.2	21.4

The nitrogen-base fractions examined spectroscopically were obtained from an oil high in nitrogen bases and acidaffins. Apparently, a part of the material left behind by the 85-percent H_2SO_4 in the more "paraffinic-type" oils is probably removed by this reagent from the more "aromatic-type" oils. This additional material would tend to mask the characteristics of the polar compounds noted (i. e., acidic groups, etc.) explaining the greater similarity between the acidaffins and the nitrogen-bases studied, than between the benzene-eluted material and the polar compounds. Chemically, most of the polar groups would be expected to be found in the material extracted with 85-percent sulfuric acid. Dunkel, Ford, and McAteer [9] have observed a similar correlation between the quantities of material separated by the acid-extraction method and those separated by their chromatographic procedure. They also observed the same discrepancies between polar compounds and nitrogen bases for oils containing large quantities of nitrogen bases. It may thus be assumed that some of the variations from oil to oil present in the polar fractions are also present in the nitrogen-base fractions but masked in the more highly "aromatic-type" oils. This could be verified, if desired, by an examination of the nitrogen-base fractions from a number of different "paraffinic-type" oils. Furthermore, the observed variation in the correlation between the two methods of analysis with change in oil type suggests a variability from oil to oil and of the compounds in both the acidaffin and the nitrogen-base fractions.

The concentrations of the compounds found in the fractions eluted with the second portion of pentane and with carbon tetrachloride are too small (table 3) to affect the spectra of the fractions into which they are separated by the sulfuric-acid extraction procedure.

13. Summary and Conclusions

There is a similarity between the paraffin fractions obtained from the oils by the acid-extraction procedure and by the chromatographic method. They contain straight chain, branched, and cyclic hydrocarbons. The benzene-eluted portion and the first and second acidaffins are also similar to each other. They contain substituted aromatic compounds possibly joined together by side chains or polynuclear aromatic compounds with side chains, as well as some hydroxyl or amine groups. The nitrogen bases, group I, appear to be composed largely of amines, whereas the nitrogen bases, group II, seems to consist mainly of amides, as well as carbonyls, hydroxyl groups, and ethers. The carbon tetrachloride-eluted portion appears to contain some amines, hydroxyl compounds, amides, and ethers, whereas, in addition to these, the ethanol-eluted portion also contains organic acids. Quantitative comparisons of the two methods indicates the likelihood that compounds whose presence is quite apparent in the ethanol-eluted fraction (mainly acids) are also present in the nitrogen-base fractions, especially the nitrogen bases, group II.

Furthermore, this study indicates a variability of the components in each fraction from one oil to another. From the standpoint of the performance of oil-rubber master batches, this variability appears to be more important in the aromatic and polar materials than in the paraffinic fractions [36, 38]. The polar compounds, such as carbonyls, ethers, amines, and hydroxyl groups, have been found to vary from one oil to another. It is known that compounds such as these can affect the rate of degradation of polymers and may, therefore, account in part for variations in the rate of oven aging reported in laboratory studies [36] for both acidaffins and nitrogen bases obtained from different oils.

It has been suggested by Taft et al. [40] and Rostler and White [29] that active hydrogens on tertiary carbon atoms in the oil fractions might have similar effects. This hypothesis is also consistent with the results of this study because increasing complexity of branching and ring structure could naturally lead to a greater number of tertiary carbon atoms differing in activity from oil to oil. It is to be anticipated that this effect would be emphasized in the more complex fractions, such as the acidaffins and nitrogen bases, and especially in the polar materials, where a more marked variation in aromatic ring structure was noted from oil to oil. This effect in these fractions is further enhanced by variations in unsaturated polar groups, such as ketones, acids, amides, etc., which activate the hydrogens on the carbon atom alpha to the unsaturated group.

It has been reported that the rates of oven aging and Banbury breakdown vary for different fractions of the same oil, as well as for different oils [36, 38]. The cause of this behavior is now apparent. For example, paraffins, in spite of their branched character, have been found to retard heat deterioration of master batches [38]. Apparently, the GR–S polymer chain with its unsaturation and conjugation in the phenyl ring contains hydrogens that are more labile than those in the paraffinic portion of the oil. The paraffins thus tend to dilute and protect the more susceptible polymer chains from oxygen attack. Even in the case of polystyrene, Wall, Harvey, and Tryon [41] have shown that oxidative attack occurs on the carbon atom alpha to the phenyl ring.

On the other hand, the more reactive fractions, such as the acidaffins or nitrogen bases, show sufficient evidence of combined polar, aromatic, and saturated structures, so that active centers could be produced upon oxidation. Such centers are apparently more active than those produced on the polymer itself and act as promoters or initiators of free-radical oxidation of the polymer molecule, leading to the observed marked reduction in molecular weight [36, 38].

Variations in these polar, aromatic, and saturated structures from oil to oil probably account for observed variations in oven aging and Banbury breakdown for the different oils.

Amines were among the earliest organic accelerators, and their presence in the nitrogen bases, group I, readily explains the effect these fractions have on the rate of cure [38]. The reported increased demand for sulfur in going from paraffins to acidaffins to nitrogen bases [38] is consistent with the increased reactivity of the compounds in these fractions.

Evidence for other groupings of possible interest in these connections, such as S—S, C—S, C=S, S—H, and aromatic rings containing nitrogen, have not been obtained in this study; bands due to some of them may have been concealed by the strong hydrocarbon absorption.

The authors express their indebtedness to F. S. Rostler of the Golden Bear Oil Co., and to A. R. Glasgow, Jr., D. J. Termini, and L. R. Kleinschmidt of the National Bureau of Standards for supplying the samples and analytical data used in this study, and for continuing constructive discussion of the work. Stimulating and valuable discussions were also held with W. K. Taft of the Government Laboratories, University of Akron. The ultraviolet spectra used in this work were obtained by J. A. Gould of the Bureau.

This work was performed as part of a research project sponsored by the Federal Facilities Corporation, Office of Synthetic Rubber, in connection with the Government Synthetic Rubber program.

14. References

[1] American Petroleum Institute Research Project 44, Catalogue of Infrared Spectral Data.
[2] L. J. Bellamy, The infrared spectra of complex molecules (Methuen and Co., London, 1954).
[3] E. A. Braude, The chemistry society annual reports **42,** 105 (1946).
[4] C. G. Cannon, Nature **171,** 308 (1953).
[5] C. G. Cannon and G. B. B. M. Sutherland, Spectrochim. Acta. **4,** 373 (1951).
[6] E. M. Charlet, K. P. Lanneau, and F. B. Johnson, Anal. Chem. **26,** 861 (1954).
[7] N. B. Colthup, J. Opt. Soc. Am. **40,** 397 (1950).
[8] H. Dannenberg, U. Schiedt, and W. Steidel, Z. Naturforsch. **8b,** 269 (1953).
[9] W. L. Dunkel, F. P. Ford, and J. H. McAteer, Ind. Eng. Chem. **46,** 578 (1954).
[10] R. A. Friedel and M. Orchin, Ultraviolet spectra of aromatic compounds (John Wiley & Sons, Inc., New York, N. Y., 1951).
[11] R. A. Friedel and M. G. Pelipetz, J. Opt. Soc. Am. **43,** 1051 (1953).
[12] R. A. Friedel and J. A. Queiser, Anal. Chem. **28,** 22 (1956).
[13] D. J. Termini and A. R. Glasgow (unpublished).
[14] H. D. Harrington, K. V. Weinstock, N. R. Legge, and E. B. Storey, India Rubber World **124,** 435 (1951).
[15] S. H. Hastings, A. T. Watson, R. B. Williams, and J. A. Anderson, Jr., Anal. Chem. **24,**, 612 (1952).
[16] L. R. Kleinschmidt, J. Research NBS **54,** 163 (1955) RP2577.
[17] L. E. Kuentzel, Spectrum #604 contributed to the National Research Council, NBS, infrared spectral data program.
[18] S. S. Kurtz, Jr., and C. C. Martin, India Rubber World **126,** 495 (1952).
[19] F. A. Miller and C. H. Wilkins, Anal. Chem. **24,** 1253 (1952).
[20] M. J. O'Neal, A. Hood, R. J. Clere, M. L. Andre, and C. K. Hines, Proc. Fourth World Petroleum Congress Rome, Section V/C Preprint 3 (1955).
[21] D. Prem and J. Duke, Rubber World **133,** 659 (1956).
[22] D. Prem and J. Duke, Rubber World **133,** 383 (1955).
[23] H. M. Randall, R. G. Fowler, N. Fuson, and J. R. Dangl, Infrared determination of organic structures (D. Van Nostrand Co., Inc., New York, N. Y., 1949).
[24] F. S. Rostler (private communication).
[25] F. S. Rostler, Rubber Age **71,** 223 (1952).
[26] F. S. Rostler, Rubber Age **69,** 559 (1951).
[27] F. S. Rostler and H. W. Sternberg, Ind. Eng. Chem. **41,** 598 (1949).
[28] F. S. Rostler and R. M. White, Ind. Eng. Chem. **47,** 1069 (1955).
[29] F. S. Rostler and R. M. White, Ind. Eng. Chem. **46,** 610 (1954).
[30] F. S. Rostler and R. M. White, Rubber Age **70,** 735 (1952).
[31] U. Schiedt and H. Reinwein, Z. Naturforsch. **7b,** 270 (1952).
[32] J. E. Stewart, J. Research NBS **58,** 265 (1957) RP 2759.
[33] M. M. Stimson and M. J. O'Donnell, J. Am. Chem. Soc. **74,** 1805 (1952).
[34] H. G. Swart, E. S. Pfau, and K. V. Weinstock, India Rubber World **124,** 309 (1951).
[35] W. K. Taft, J. Duke, R. W. Laundrie, A. D. Synder, D. C. Prem, and H. Mooney, Ind. Eng. Chem. **46,** 396 (1954).
[36] W. K. Taft, J. Duke, A. D. Synder, M. Feldon, and R. W. Laundrie, Ind. Eng. Chem. **45,** 1043 (1953).
[37] W. K. Taft, J. Duke, A. D. Snyder, and R. W. Laundrie, Rubber Age **75,** 61 (1954).
[38] W. K. Taft, M. Feldon, J. Duke, R. W. Laundrie, and D. C. Prem, Ind. Eng. Chem. **47,** 1077 (1955).
[39] W. K. Taft, R. W. Laundrie, T. B. Harrison, and J. Duke, Rubber Age **75,** 223 (1954).
[40] W. K. Taft, A. D. Snyder, and J. Duke, Rubber Age **75,** 838 (1954).
[41] L. A. Wall, M. R. Harvey, and M. Tryon, J. Phys. Chem. **60,** 1306 (1956).
[42] K. V. Weinstock, E. B. Storey, and J. S. Sweeley, Ind. Eng. Chem. **45,** 1035 (1953).
[43] C. W. Young, R. B. DuVall, and N. Wright, Anal. Chem. **23,** 709 (1951).

WASHINGTON, August 3, 1956.

Journal of Research of the National Bureau of Standards Vol. 59, No. 1, July 1957 Research Paper 2772

Infrared Spectra of Sugar Acetates in Solution[1]

Horace S. Isbell, Francis A. Smith, E. Carroll Creitz, Harriet L. Frush, Joseph D. Moyer, and James E. Stewart

Infrared absorption spectra are reported for a group of structurally and configurationally related carbohydrate derivatives. The conformation of the pyranose ring and other structural features of the compounds are discussed in relation to the spectra. Most of the absorption that is characteristic of the cyclic carbohydrate structure occurs in the region of 8.4 to 15 μ. Although the spectra are complex and difficult to interpret, they show features from which a number of provisional conclusions have been drawn.

It was found that fully acetylated monosaccharides with an axial glycosidic acetate group give a moderately strong absorption band at 8.63 ± 0.04 μ, and at most a weak band at 8.87 ± 0.06 μ; whereas compounds having an equatorial glycosidic acetate group absorb weakly at 8.63 μ, and give a moderately strong band at 8.87 μ. The spectra for the acetates having the *gulo-*, *ido-*, or *talo*-configurations appear to indicate the presence of the C′2, or less common chair conformation, or a mixture of conformations.

Acetylated methyl glycosides with the methoxyl group in the axial position give characteristic absorption at 8.33 ± 0.02 μ and at 8.80 ± 0.05 μ; none of the compounds with the methoxyl group in the equatorial position shows absorption in these regions. Absorption at 8.80 μ is enhanced further by the presence of axial acetyl groups on the ring. On the basis of this generalization, an acetylated methyl glycoside with the *β-gulo* structure gives evidence for the presence of the C′2 conformation.

Overlapping bands in the region of 8.0 to 8.2 μ arise from acetyl groups of diverse character, with the result that spectra in this region show characteristic features for some compounds. Thus the pyranose acetates of the pentoses and of rhamnose give a sharp, well-defined band at 8.0 μ, but the acetates of the hexoses and higher sugars give a poorly defined band that seems to include an overlapping component with a maximum at higher wavelength. This characteristic may serve to distinguish acetates that do, or do not, have a primary acetyl group.

1. Scope and Purpose of the Project

This project was undertaken with the object of providing infrared spectrograms of an extensive group of carbohydrates and carbohydrate derivatives, for the purpose of discovering correlations that might be of value in structural analysis. It was particularly desired to obtain information concerning the conformation of the pyranose ring. For this reason, the study has included some rare configurations that might exist in unusual conformations.

Spectrograms of crystalline materials suspended in mineral oil, or in a pellet of an alkali metal halide, differ from spectrograms of the same material dissolved in a solvent, or cast in an amorphous film. The differences arise from the presence or absence of intercrystalline forces, hydrogen bridging, intermolecular combinations, intramolecular steric effects, and other factors. By a study of the infrared absorption of materials both in the crystalline state and in solution, changes in ring conformation, hydrogen bridging, and other properties can be detected [1].[2] Infrared absorption spectra are reported in this paper for compounds dissolved in suitable solvents, whereas absorption spectra for the same compounds and many others in pellets of an alkali metal halide will be reported separately.[3] Comparison of these ultimately will be used to detect possible changes in conformation with change in state.

The use of infrared absorption spectra for structural studies depends on absorption bands that can be correlated either directly or indirectly with definite structures. The presence or absence of the characteristic absorption, in an unknown substance, is then taken as evidence for the presence or absence of the structure in question. The position and intensity of the absorption bands produced by each atomic linkage vary somewhat with structure. Hence the spectra of many compounds of known structure must be mapped before the method can be used to study unknown structures. The reliability of the structural assignments increases with the accumulation of spectra for substances of known structure that confirm the assignment [7, 8].

2. Ring Conformation

Interpretation of the infrared spectra of the carbohydrates requires consideration not only of structure and configuration but also of ring conformation, or shape. The presence of large groups in axial positions, bridged groups, fused rings, eclipsed atoms, and other types of steric hindrance make some conformations less stable than others. Ordinarily, large groups tend to take equatorial positions and thus greatly influence ring conformation [9]. In most cases, the pyranose ring assumes 1 of 2 chair conformations in which carbons 1, 2, 4, and 5 lie in one plane, and carbon 3 and the ring oxygen lie outside of the plane in the *trans* position [10].

[1] This paper is based on work supported by the Chemistry Branch of the Office of Naval Research, done under contract No. NR055208.

[2] Figures in brackets indicate the literature references at the end of this paper. The references for table 2 are given at the end of the table.

[3] While the work was in progress, several papers appeared that presented infrared absorption spectra of some of the carbohydrate derivatives reported here [2 to 6]. However, none of the compounds was studied under the conditions of the present project.

423777—57——4

The two conformations differ in that carbon 3 and the ring oxygen are *trans* to each other in the opposite sense. This difference causes the axial groups of one conformation to be the equatorial groups of the other, and vice versa. In order to facilitate comparison of the spectra of carbohydrate derivatives, a system of classification has been devised in which these conformations are designated C′1 and C′2 [11]. The normal, or C′1, conformation has the reference group [4] at carbon 5 in the equatorial position, and the C′2 conformation has this group in the axial position.[5] The positions of the reference groups in the two conformations are listed in table 1. In contrast to the classification of Reeves [10], this system has the advantage of classifying in the same group, *in both* D *and* L *series*, that conformation having the same equatorial and axial arrangement of groups. The relationship to the Reeves classification is:

Isbell nomenclature	*Reeves nomenclature*	
D- or L-hexose	D-hexose	L-hexose
C′1	C1	1C
C′2	1C	C1

TABLE 1. *Positions of reference groups in pyranose structures* [a]

Code	C′1 conformation		Code	C′2 conformation	
	Configuration	Position of reference groups		Configuration	Position of reference groups
.11	*α-gluco*	a e e e e	.53	*β-ido*	a e e e a
.12	*β-gluco*	e e e e e	.54	*α-ido*	e e e e a
.21	*α-manno*	a a e e e	.63	*β-gulo*	a a e e a
.22	*β-manno*	e a e e e	.64	*α-gulo*	e a e e a
.31	*α-galacto*	a e e a e	.73	*β-altro*	a e e a a
.32	*β-galacto*	e e e a e	.74	*α-altro*	e e e a a
.41	*α-talo*	a a e a e	.83	*β-allo*	a a e a a
.42	*β-talo*	e a e a e	.84	*α-allo*	e a e a a
.51	*α-ido*	a a a a e	.13	*β-gluco*	a a a a a
.52	*β-ido*	e a a a e	.14	*α-gluco*	e a a a a
.61	*α-gulo*	a e a a e	.23	*β-manno*	a e a a a
.62	*β-gulo*	e e a a e	.24	*α-manno*	e e a a a
.71	*α-altro*	a a a e e	.33	*β-galacto*	a a a e a
.72	*β-altro*	e a a e e	.34	*α-galacto*	e a a e a
.81	*α-allo*	a e a e e	.43	*β-talo*	a e a e a
.82	*β-allo*	e e a e e	.44	*α-talo*	e e a e a

[a] Axial and equatorial positions for reference groups of the ring are shown consecutively, with increasing carbon number from left to right. Hydrogen atoms occupy the remaining positions.

Table 1 shows that the positions of the reference groups and hydrogen atoms with respect to the ring depend on both configuration and ring conformation. For example, α-gulose C′1 (aeaae) differs at all carbons from α-gulose C′2 (eaeea), whereas α-gulose C′1 and β-mannose C′2 (aeaaa) have like axial and equatorial arrangements at all carbons except carbon 5. Furthermore, in the C′1 conformation, the glycosidic group of an alpha hexose or higher sugar is axial, but in the C′2 conformation it is equatorial. Therefore, with regard to the axial and equatorial positions of the glycosidic group only, this relationship makes the alpha C′1 comparable to the beta C′2 derivatives,[6] and the beta C′1 comparable to the alpha C′2 derivatives. It follows that the axial and equatorial positions of the glycosidic carbon are not definitive of alpha and beta configuration except in a given conformation. These examples show that in rationalizing the reactions and properties of carbohydrate derivatives, configuration and conformation must be considered to be mutually dependent. Because all of the axial groups of one chair conformation are the equatorial groups of the other, then for a substance having a known configuration and a chair conformation, the axial or equatorial position of any specific atom or group attached to the ring will define the conformation of a pyranose structure.

Classification of the pyranose derivatives only in the C′1 and C′2 groups involves oversimplification. Some of the compounds may exist in mixtures even including boat forms. To interpret the infrared spectra, definite conformations must be assumed. As a working hypothesis, the C′1 conformation is considered as a first choice, the C′2 conformation as a second. Finally, the possibility of various boat conformations must be considered. With provisional assignments, attempts can be made to rationalize the experimental results with the postulated conformations. The method is one of trial and error, but should ultimately lead to the recognition of absorption bands characteristic of the structure of the compounds.

To facilitate comparison, code numbers have been assigned to compounds listed in table 2 by means of the scheme previously published [11]; the codes are suitable for classifying and separating the data by punched-card techniques. Generic classification is obtained by means of only one or two of the digits in the code number, and a more specific classification by use of a sequence of digits following a decimal point. For example, all aldohexose derivatives are characterized by 2 to the right of the decimal point, and all substances having the α-glucopyranosyl structure and the C′1 conformation by the sequence .211. For reference purposes, the code numbers are based on a postulated C′1 ring conformation. The usefulness of the system for study of infrared spectra arises from the ease with which carbohydrate derivatives can be sorted and correlated according to structure, configuration, and ring conformation. A complete analysis of the spectrograms would be beyond the scope of the present report, but certain aspects of the work will be considered briefly in sections 4 and 5.

[4] A reference group is defined as any group, other than hydrogen, that is attached to the ring structure. Inasmuch as the pentoses and ketohexoses do not have a reference group at carbon 5, this rule is not applicable. However, on the basis of similarities in properties, the pentoses and ketohexoses are classified with the aldohexoses, in both the C1 and C2 conformations, as follows: xylose and sorbose with glucose, lyxose and tagatose with mannose, arabinose and fructose with galactose, and ribose and psicose with talose.

[5] The symbols C1 and 1C have been used extensively to represent the two chair conformations of the pyranose ring. Reeves defines the symbols on the basis of formulas given in his publication [10]. The arrangement of the ring-forming atoms in the two conformations are related as object and mirror image, and consequently the conformation designated C1 in the D-pyranose series is 1C in the L-pyranose series. To facilitate comparison of structurally related substances in the D- and L-series, Isbell used the C1 term in a slightly different sense. Inasmuch as use of the same symbol with different meaning may lead to confusion, hereafter the conformations defined by Isbell [11] will be designated C′1 and C′2.

[6] The alpha C′1 and the beta C′2 derivatives of a given pyranose have the glycosidic group in the axial position on the opposite sides of the plane of carbons 1, 2, 4, and 5.

TABLE 2. *Compounds measured and index to spectrograms*

Code	Compound	Constants reported			Constants found			Spectrogram
		mp	Specific rotation [a] $[\alpha]_D^{20}$	Reference	mp	Specific rotation [a] $[\alpha]_D^{20}$	Solubility in CCl_4	
	FULLY ACETYLATED MONOSACCHARIDES							
		°C			°C		g/100 ml	
12.11121	Tetra-*O*-acetyl-α-D-xylopyranose	59	+89.3	1	59 to 60	+89.8	v. s.	1
12.11221	Tetra-*O*-acetyl-β-D-xylopyranose	128	−25.1	1	126 to 127	−25.3	1.8	2
12.12121	Tetra-*O*-acetyl-α-D-lyxopyranose	93 to 94	+25	2	94 to 95	+24.4	3.4	3
12.13221	Tetra-*O*-acetyl-α-L-arabinopyranose	97	+42.5	3	96 to 97	+43.1	4.2	4
12.21121	Penta-*O*-acetyl-α-D-glucopyranose	114	+101.2	4	113 to 114	+101.3	2.5	5
12.21221	Penta-*O*-acetyl-β-D-glucopyranose	132	+3.9	5	132 to 133	+3.9	1.9	6
12.22121	Penta-*O*-acetyl-α-D-mannopyranose	64	+55.0	6	73 to 74	+55.0	21.6	7
12.22221	Penta-*O*-acetyl-β-D-mannopyranose	117 to 118	−25.2	7	116 to 117	−25.1	4.7	8
12.23121	Penta-*O*-acetyl-α-D-galactopyranose	96	+106.7	8	96 to 97	+106.8	5.4	9
12.23221	Penta-*O*-acetyl-β-D-galactopyranose	142	+25	8	144 to 145	+23.3	0.8	10
12.23621	Penta-*O*-acetyl-β-D-galactofuranose	98	−41.6	9	98 to 99	−42.6	1.9	11
12.26121	Penta-*O*-acetyl-α-D-guiopyranose	105 to 106	+86.2	10	105 to 106	+86.3	2.9	12
12.71121	Penta-*O*-acetyl-α-L-sorbopyranose	97	−56.5	11	95	−57.3	2.2	13
12.33221	Hexa-*O*-acetyl-D-*glycero*-β-D-*gala*-heptopyranose	107	+34.1	12	106 to 107	+33.8	3.8	14
12.35221	Hexa-*O*-acetyl-D-*glycero*-β-D-*ido*-heptopyranose	136	−9.1	10	135 to 136	−8.9	3.5	15
12.36121	Hexa-*O*-acetyl-D-*glycero*-α-D-*gulo*-heptopyranose	164	+87.0	13	171 to 172	+94.9	0.4	16
12.36221	Hexa-*O*-acetyl-D-*glycero*-β-D-*gulo*-heptopyranose	135	+4.8	13	134 to 135	+4.4	6.3	17
12.42121	Hexa-*O*-acetyl-D-*glycero*-α-L-*manno*-heptopyranose	----------	---------	14	132 to 133	−25.8	2.9	18
	FULLY ACETYLATED METHYL GLYCOSIDES							
12.11111	Methyl tri-*O*-acetyl-α-D-xylopyranoside	86	+119.6	15	85 to 86	+119.5	23.3	19
12.11211	Methyl tri-*O*-acetyl-β-D-xylopyranoside	115	−60.8	16	115 to 116	−61.0	3.0	20
12.12111	Methyl tri-*O*-acetyl-α-D-lyxopyranoside	96	+30.1	17	96	+30.4	20.1	21
12.13111	Methyl tri-*O*-acetyl-β-L-arabinopyranoside	85	+182.0	3	85 to 86	+182.1	34.7	22
12.21111	Methyl tetra-*O*-acetyl-α-D-glucopyranoside	100 to 101	+130.5	5	102 to 103	+129.6	32.7	23
12.21211	Methyl tetra-*O*-acetyl-β-D-glucopyranoside	104 to 105	−18.2	5	104 to 105	−18.2	2.7	24
12.22111	Methyl tetra-*O*-acetyl-α-D-mannopyranoside	65	+49.1	18	64 to 65	+48.8	53.8	25
12.22111(6)80	Methyl tri-*O*-acetyl-α-L-rhamnopyranoside	86 to 87	−53.7	19	88 to 89	−60.1	4.5	26
12.22211	Methyl tetra-*O*-acetyl-β-D-mannopyranoside	161	−50.4	20	160 to 161	−49.4	0.3	27
12.22211(6)80	Methyl tri-*O*-acetyl-β-L-rhamnopyranoside	151 to 152	+45.7	19	152 to 153	+45.5	------	28
12.23111	Methyl tetra-*O*-acetyl-α-D-galactopyranoside	87	+133.0	21	86 to 87	+132.6	20.7	29
12.23211	Methyl tetra-*O*-acetyl-β-D-galactopyranoside	93 to 94	−14.0	21, 22	95 to 96	−13.9	6.2	30
12.36211	Methyl penta-*O*-acetyl-D-*glycero*-β-D-*gulo*-heptopyranoside.	150	−16.0	23	153 to 154	−20.8	2.2	31
	ACETYLATED METHYL ORTHOACETATES							
12.22263	1,2[3,4,6-Tri-*O*-acetyl-D-mannopyranose] methyl orthoacetate.	105	−26.6	24	105 to 106	−26.8	------	32
12.22263(6)80	1,2[3,4-Di-*O*-acetyl-L-rhamnopyranose] methyl orthoacetate.	83	+35	25	86 to 87	+33.9	------	33
	ACETYLATED SUGARS WITH FREE GLYCOSIDIC HYDROXYL							
12.2120	2,3,4,6-Tetra-*O*-acetyl-β-D-glucopyranose	138	−3.0	26	137 to 139	−1.9	0.05	34
12.2210	2,3,4,6-Tetra-*O*-acetyl-α-D-mannopyranose	93	+26.3	27	95 to 96	+24.1	.2	35
12.7110	1,3,4,5-Tetra-*O*-acetyl-α-L-sorbopyranose	101	−21.3	11	101 to 102	−19.8	.7	36
12.8110	1,3,4,5,7-Penta-*O*-acetyl-α-D-glucoheptulopyranose	114 to 115	+45.9	10	114 to 115	+46.0	.3	37
	ACETYLATED OXO-DERIVATIVES							
12.1360	Tetra-*O*-acetyl-*aldehydo*-L-arabinose	113 to 115	−65.4	28	113 to 115	---------	------	38
12.2360	Penta-*O*-acetyl-*aldehydo*-D-galactose	120 to 121	−25	29	118 to 120	---------	------	39
12.23618	Penta-*O*-acetyl-*aldehydo*-D-galactose aldehydrol	124 to 126	+19.5	29	126 to 127	---------	------	40
12.23617	Penta-*O*-acetyl-*aldehydo*-D-galactose ethyl hemiacetal.	133 to 134	−0.5	29	134 to 135	---------	------	41
12.7160	Penta-*O*-acetyl-*keto*-L-sorbose	99	+2.9	30	99 to 100	+2.2	0.3	42
12.13645	Tetra-*O*-acetyl-*aldehydo*-L-arabinose ethyl mercaptal.	79 to 80	−29.9	28	78 to 79	−27.9	------	43
12.23645	Penta-*O*-acetyl-*aldehydo*-D-galactose ethyl mercaptal.	78	+9.7	29	80 to 81	+11.2	------	44
	ACETYLATED POLYOLS							
12.22521	Hexa-*O*-acetyl-D mannitol	123 to 124	+25.0	31	123 to 124	+25.0	2.1	45
12.25521	Hexa-*O*-acetyl-D-iditol	121 to 122	+25.3	31	121 to 122	+25.7	0.6	46
12.99821	Hexa-*O*-acetyl-inositol	216	Inactive	32	216 to 217	Inactive	.14	47

TABLE 2. *Compounds measured and index to spectrograms*—Continued

Code	Compound	Constants reported			Constants found			Spectrogram
		mp	Specific rotation [a] $[\alpha]_D^{20}$	Reference	mp	Specific rotation [a] $[\alpha]_D^{20}$	Solubility in CCl_4	
	FULLY ACETYLATED DISACCHARIDES							
22.211°(1–4).21221	Octa-*O*-acetyl-β-maltose [Octa-*O*-acetyl-α-D-glucopyranosyl-(1→4)-β-D-glucopyranose].	159 to 160	+62.6	33	161 to 162	+62.5	2.9	48
22.211°(1–1).211°	Octa-*O*-acetyl-trehalose [Octa-*O*-acetyl-α-D-glucopyranosyl-(1→1)-α-D-glucopyranoside].	96 to 98	+162.3	1	99 to 101	+162.1	.....	49
22.212°(1–4).21121	Octa-*C*-acetyl-α-cellobiose [Octa-*O*-acetyl-β-D-glucopyranosyl-(1→4)-α-D-glucopyranose].	229	+41	33	227 to 228	+41.7	0.03	50
22.212°(1–6).21221	Octa-*O*-acetyl-β-gentiobiose [Octa-*O*-acetyl-α-D-glucopyranosyl-(1→6)-β-D-glucopyranose].	192 to 193	−5.3	34	194 to 195	−6.0	.06	51
22.231°(1–6).21221	Octa-*O*-acetyl-β-melibiose [Octa-*O*-acetyl-α-D-galactopyranosyl-(1→6)-β-D-glucopyranose].	177	+102.5	35	179 to 180	+102.6	.14	52
22.232°(1–4).21121	Octa-*O*-acetyl-α-lactose [Octa-*O*-acetyl-β-D-galactopyranosyl-(1→4)-α-D-glucopyranose].	152	+53.6	36	155 to 156	+53.4	2.9	53
22.232°(1–4).21221	Octa-*O*-acetyl-β-lactose [Octa-*O*-acetyl-β-D-galactopyranosyl-(1→4)-β-D-glucopyranose].	90	−4.7	36	91 to 93	−4.8	1.4	54
22.232°(1–4).73521	Octa-*O*-acetyl-lactulose [Octa-*O*-acetyl-β-D-galactopyranosyl-(1→4)-β-D-fructofuranose]. [b]	138	−6.6	10	138 to 139	−6.5	0.2	55
22.211°(1–2).735°	Octa-*O*-acetyl-sucrose [Octa-*O*-acetyl-α-D-glucopyranosyl-(1→2)-β-D-fructofuranoside].	89	+59.7	37	89 to 90	+60.3	3.9	56

[a] In a few cases the temperature reported in the literature differed from that employed at the Bureau. The original literature should be consulted.
[b] Structure uncertain.

REFERENCES

1. C. S. Hudson and J. M. Johnson, J. Am. Chem. Soc. **37,** 2748 (1915).
2. P. A. Levene and M. L. Wolfrom, J. Biol. Chem. **78,** 525 (1928).
3. C. S. Hudson and J. K. Dale, J. Am. Chem. Soc. **40,** 992 (1918).
4. A. Georg, Helv. Chim. Acta. **12,** 261 (1929).
5. C. S. Hudson and J. K. Dale, J. Am. Chem. Soc. **37,** 1264 (1915).
6. C. S. Hudson and J. K. Dale, J. Am. Chem. Soc. **37,** 1280 (1915).
7. D. H. Brauns, J. Research NBS **7,** 573 (1931) RP358.
8. C. S. Hudson and H. O. Parker, J. Am. Chem. Soc. **37,** 1589 (1915).
9. C. S. Hudson, J. Am. Chem. Soc. **37,** 1591 (1915).
10. H. L. Frush and H. S. Isbell, J. Research NBS **35,** 111 (1945) RP1663.
11. H. H. Schlubach and G. Graefe, Liebigs Ann. Chem. **532,** 211 (1937).
12. E. Montgomery and C. S. Hudson, J. Am. Chem. Soc. **56,** 2463 (1934).
13. C. S. Hudson and E. Yanovsky, J. Am. Chem. Soc. **38,** 1575 (1916).
14. H. S. Isbell and H. L. Frush, unpublished.
15. C. S. Hudson and J. K. Dale, J. Am. Chem. Soc. **40,** 997 (1918).
16. J. K. Dale, J. Am. Chem. Soc. **37,** 2745 (1915).
17. F. P. Phelps and C. S. Hudson, J. Am. Chem. Soc. **50,** 2049 (1928).
18. J. K. Dale, J. Am. Chem. Soc. **46,** 1046 (1924).
19. E. Fischer, M. Bergmann, and A. Rabe, Ber. deut. chem. Ges. **53,** 2362 (1920).
20. T. L. Harris, E. L. Hirst, and C. E. Wood, J. Chem. Soc **1932,** 2108.
21. J. K. Dale and C. S. Hudson, J. Am. Chem. Soc. **52,** 2534 (1930).
22. W. Koenigs and E. Knorr, Ber. deut. chem. Ges. **34,** 957 (1901).
23. W. N. Haworth, E. L. Hirst, and M. Stacey, J. Chem. Soc. **1931,** 2864.
24. J. K.Dale, J. Am. Chem. Soc. **46,** 1046 (1924).
25. W. N. Haworth, E. L. Hirst, and E. J. Miller, J. Chem. Soc **1929,** 2469.
26. S. B. Hendricks, O. R. Wulf, and U. Liddel, J. Am. Chem. Soc. **58,** 1997 (1936).
27. P. A. Levene and R. S. Tipson, J. Biol. Chem. **90,** 89 (1931).
28. M. L. Wolfrom and M. R. Newlin, J. Am. Chem. Soc. **52,** 3619 (1930).
29. M. L. Wolfrom, J. Am. Chem. Soc. **52,** 2464 (1930).
30. G. Arragon, Compt. rend. **196,** 1733 (1933); H. Schlubach and J. Vorwerk, Ber. deut. chem. Ges. **66,** 1251 (1933).
31. R. M. Hann and C. S. Hudson, J. Am. Chem. Soc. **64,** 925 (1942).
32. E. G. Griffin and J. M. Nelson, J. Am. Chem. Soc. **37,** 1552 (1915).
33. C. S. Hudson and J. M. Johnson, J. Am. Chem. Soc. **37,** 1276 (1915).
34. C. S. Hudson and J. M. Johnson, J. Am. Chem. Soc. **39,** 1272 (1917).
35. C. S. Hudson and J. M. Johnson, J. Am. Chem. Soc. **37,** 2752 (1915).
36. C. S. Hudson and J. M. Johnson, J. Am. Chem. Soc. **37,** 1270 (1915).
37. R. P. Linstead, A. Rutenberg, W. G. Dauben, and W. L. Evans, J. Am. Chem. Soc. **62,** 3260 (1940).

3. Experimental Procedures

3.1. Preparation and Purification of the Compounds

The compounds listed in table 2 were prepared by the methods given in the references cited. Each substance was recrystallized from a suitable solvent until further crystallization caused no change in either melting point or optical rotation. In most cases the melting point and optical rotation agree with values found in the literature. Some discrepancies can be seen, but because the purifications were conducted with great care, it is believed that the values reported here are correct.

3.2. Solubility of Compounds in Carbon Tetrachloride

The approximate solubilities of the materials in carbon tetrachloride were determined in order to facilitate preparation of solutions, and not as a criterion of purity. The values were obtained in the following manner: A sufficient quantity of the compound was added to 10 ml of carbon tetrachloride to provide a saturated solution at 20° C. After 24 hours, during which the mixture was occasionally shaken, 5 ml of the solution was drawn through a cotton filter into a pipet and transferred to a tared dish; the solvent was evaporated and the weight of the residue determined.

3.3. Solvents Used for Spectrograms

The choice of solvents used in these measurements was determined by their suitability for use in cells with rock salt windows, by their transparency in the range of wavelengths studied, and by their effectiveness in dissolving the samples.

The following solvents were used in this work:

Carbon tetrachloride—This solvent was purified by

efficient fractional distillation; purity was checked by refractive index.

Carbon disulfide—A commercial analytical reagent was used; purity was checked by determination of boiling point and residue.

Chloroform—This solvent was purified in small quantities at frequent intervals (every 2 to 3 days). U. S. P. chloroform was washed several times with concentrated sulfuric acid, with water, with a solution of sodium bicarbonate, and finally with water. It was then dried with anhydrous calcium sulfate, filtered, and stored in the dark over silica gel.

Dioxane—Peroxides present in commercial dioxane were removed by treatment of the solvent with solid potassium iodide. The dioxane was decanted from the iodide, and the free iodine and most of the water were removed by shaking the material with an excess of solid potassium hydroxide. The dioxane was decanted, and treated with sodium to remove traces of water and iodine. After 24 hours the product was distilled, and then stored in the dark.

3.4. Measurement of Spectrograms

The spectrograms[7] of the substances listed in table 2 were made with a model 12B Perkin-Elmer spectrometer with the auxiliary equipment and working conditions described by Creitz and Smith [12]. The observed transmission in percentage, corrected for solvent, was plotted with respect to wavelength and wave number. The resulting spectrograms are presented in the figures at the end of this paper, in which the solid lines represent absorption in carbon tetrachloride solutions, and the broken lines, absorption in chloroform, dioxane, or carbon disulfide solutions, as shown by the key. When solubility of the compounds permitted, measurements were made in carbon tetrachloride; in the region in which carbon tetrachloride is opaque, either carbon disulfide or dioxane was used. For some compounds of low solubility, it was necessary to use chloroform solutions. In a few cases, measurements are given at more than one concentration and in cells of different length.

3.5. Estimation of the Molar Absorbancy Indices

Molar absorbancy indices were calculated by means of the Beer-Lambert law in the form

$$-\log_{10}T_s=-\log_{10}(T_{\text{soln.}}/T_{\text{solv.}})=a_M bc,$$

where T_s is the transmittancy of the sample, $T_{\text{soln.}}$ and $T_{\text{solv.}}$ are the transmittances of the cell containing solution and solvent, respectively, b is the cell length in centimeters, c is the concentration in moles per liter, and a_M is the molar absorbancy index [13]. The integrated molar absorbancy index equals $\int a_M(\nu)d\nu$, where ν is a measure of the frequency expressed in wave numbers (reciprocal centimeters) and the limits of integration are selected to cover the area enclosed by the bands. When $-\log_{10}T_s$ is plotted against wave number, the area beneath a given absorption band is proportional to the integrated molar absorbancy index. In a few cases, integrated molar absorbancy indices were compared by cutting out and weighing the area of paper enclosed. The results were reduced to a comparable basis by dividing the weight of the clipping by the product of the molar concentration of the substance and the cell length. In the study of absorbancy due to the acetyl carbonyl group, the molar absorbancy index was divided by the number of these groups (n) per molecule. The resulting value (a_M/n) is termed the "group absorbancy index" (see table 5).

4. Assignment of Ring Conformation From Infrared Absorption

One of the main objects of the present investigation was to obtain information concerning the conformation of the pyranose ring. Although the structure and configuration of most carbohydrates are known, there is comparatively little information concerning ring conformation. Assignments of ring conformation based on the formation of copper complexes [10, 14] and other products may be open to question because of changes under the influence of the reagent; assignments based on reaction rates [15] require the interpretation of mechanisms that may not always be correct. Ultimately, the study of infrared absorption spectra may provide a more satisfactory means for the assignment of ring conformation. Some progress in this direction has already been made. Thus, Jones, Ramsay, Herling, and Dobriner [16] have found that the carbonyl stretching vibration of α-bromo-ketosteroids is displaced in a characteristic manner according to whether the bromine atom has an axial or equatorial position in the cyclohexanone ring; Cole, Jones, and Dobriner [17, 18] have shown that an axial or equatorial position of an acetate group on the A ring of steroids is characterized by different band patterns, as well as by a shift of the stretching vibration of the acetyl carbonyl. Also, Barker, Bourne, Stacey, and Whiffen [4] have made the suggestion that certain absorption bands for pyranose derivatives may be characteristic of the axial or equatorial position of the hydrogen of carbon 1 (see also [5]).

The results of the present study show clearly that infrared absorption provides the basis for a promising method of studying the ring conformation of carbohydrates. A few of the bands that seem characteristic of certain structures or conformations will be discussed here; others will be considered in future publications.

Table 3 lists certain bands for the fully acetylated monosaccharides that seem to vary with the axial or equatorial positions of the glycosidic acetate groups. Interpretation of the absorption spectra in terms of structure requires knowledge of the ring conformation of at least some of the members of the group. Rates of oxidation with bromine [15], indicate that

[7] The spectrograms were given in an NBS unpublished report to the Office of Naval Research dated December 31, 1951. The report was distributed to numerous research workers, and the data for some of the compounds have been included in a review article [3].

TABLE 3. *Absorption bands at 8.64 and 8.87 μ for fully acetylated monosaccharides*

Compound	Configuration	Probable conformation	Position of reference groups	Hypothetical a-pyranose band [a] 8.63±0.04 μ	Hypothetical e-pyranose band [a] 8.87±0.06 μ	Molar absorbancy indices			Spectrum
						a_M at 8.64 μ	a_M at 8.87 μ	Difference	
Tetra-*O*-acetyl-α-D-xylopyranose	*α-gluco*	C′1	a e e e -	8.61 s	8.83 w	300	173	+127	1
Penta-*O*-acetyl-α-D-glucopyranose	*α-gluco*	C′1	a e e e e	8.63 s	8.85 w	382	160	+222	5
Tetra-*O*-acetyl-α-D-lyxopyranose	*α-manno*	C′1	a a e e -	8.67 s	8.84 w	390	77	+313	3
Penta-*O*-acetyl-α-D-mannopyranose	*α-manno*	C′1	a a e e e	8.65 s	8.92 (tr)	593	98	+495	7
Hexa-*O*-acetyl-D-*glycero*-α-L-*manno*-heptopyranose	*α-manno*	C′1	a a e e e	8.65 m	8.92 (tr)	444	223	+221	18
Penta-*O*-acetyl-α-D-galactopyranose	*α-gala*	C′1	a e e a e	8.61 m 8.65 m	8.84 (tr)	366	158	+208	9
Tetra-*O*-acetyl-β-D-xylopyranose	*β-gluco*	C′1	e e e e -	8.62 (tr)	8.89 m	71	223	−152	2
Penta-*O*-acetyl-β-D-glucopyranose	*β-gluco*	C′1	e e e e e	(c)	8.92 m	(118)	233	(−115)	6
Penta-*O*-acetyl-β-D-mannopyranose	*β-manno*	C′1	e a e e e	8.67 (tr)	8.89 m	107	161	−54	8
Tetra-*O*-acetyl-α-L-arabinopyranose	*β-gala*	C′1	e e e a -	(c)	8.86 m	(90)	232	(−142)	4
Penta-*O*-acetyl-β-D-galactopyranose	*β-gala*	C′1	e e e a e	(c)	8.86 m	(92)	233	(−141)	10
Hexa-*O*-acetyl-D-*glycero*-β-D-*gala*-heptopyranose	*β-gala*	C′1	e e e a e	8.62 w	8.83 m	139	282	−143	14
Penta-*O*-acetyl-α-D-gulopyranose	*α-gulo*	C′2 [b]	e a e e a	(c)	8.83 m 8.90 m	(95)	342 312	(−247) (−217)	12
Hexa-*O*-acetyl-D-*glycero*-α-D-*gulo*-heptopyranose	*α-gulo*	C′2 [b]	e a e e a	8.59 m	8.86 m 8.93 m	206	294 309	−88 −103	16
Hexa-*O*-acetyl-D-*glycero*-β-D-*gulo*-heptopyranose	*β-gulo*	C′2 [b]	a a e e a	8.60 m	8.91 (tr)	199	172	+27	17
Hexa-*O*-acetyl-D-*glycero*-β-D-*ido*-heptopyranose	*β-ido*	C′2 [b]	a e e e a	8.65 w	8.83 (tr)	222	207	+15	15
Penta-*O*-acetyl-α-D-talopyranose	*α-talo*	C′2 [b]	e e a e a	.....	8.90 s	(d)	(d)	neg.	(d)

[a] s, m, and w indicate strong, moderately strong, and weak bands, respectively; (tr) indicates the weakest observable absorption.

[b] Although the spectra indicate the presence of the C′2 conformation, the data are not conclusive, and both conformations may be present.

[c] No absorption band was evident. For purposes of comparison only, a_M at 8.63 μ was calculated and deducted from that at 8.87 μ to give the difference cited in parentheses.

[d] The spectrogram, previously published [19], was made by the potassium chloride pellet technique. Hence values for a_M comparable to those reported here cannot be assigned. In accordance with the C′2 conformation indicated, the absorption in the region of 8.63 μ was less than that in the region of 8.87 μ.

the free pyranose sugars having the *gluco-*, *manno-*, and *galacto*-configurations ordinarily exist in the C′1 conformation. If the C′1 conformation is postulated for all of the fully acetylated monosaccharides having these three configurations, it is found that the modifications having an axial glycosidic acetate group give a moderately strong absorption band near 8.63 μ and at most a weak band near 8.87 μ; whereas, the modifications having an equatorial glycosidic acetate group absorb weakly near 8.63 μ but give a moderately strong band near 8.87 μ. Thus, strong absorption near 8.63 μ appears to be characteristic of a structure having an axial glycosidic acetyl group; similarly, strong absorption near 8.87 μ appears to be characteristic of a structure having an equatorial glycosidic group. The differences between the molar absorbancy indices in the two regions for all of the acetates having the *gluco-*, *manno-*, and *galacto*-configurations (table 3) are in agreement with this generalization. At present, little is known concerning conformation in the *gulo-*, *ido-*, and *talo*-configurations. If the above generalization is applied to these three configurations, it indicates the presence of the a-pyranose C′2 conformation in hexa-*O*-acetyl-D-*glycero*-β-D-*ido*-heptose (fig. 15) and hexa-*O*-acetyl-D-*glycero*-β-D-*gulo*-heptose (fig. 17), and the e-pyranose C′2 conformation in penta-*O*-acetyl-α-D-gulose (fig. 12), hexa-*O*-acetyl-D-*glycero*-α-D-*gulo*-heptose (fig. 16) and penta-*O*-acetyl-α-D-talose.[8]

However, the spectra for these compounds show that the situation is not entirely clear, and it seems possible that both conformations may be present. Consideration of stereomeric factors seems to indicate that some of the compounds in this group should exist in the C′1 form. Both the β-*gulo*- and the β-*talo*-structures have three equatorial reference groups when in the C′1 conformation, and two when in the C′2 conformation. The reverse distribution is present in the alpha forms (see table 1). In view of the tendency of large groups to take equatorial, rather than axial positions, the C′1 conformation would seem to be the more probable for the β-*gulo*- and β-*talo*- structures, and the C′2 conformation for the corresponding alpha modifications. One of the two modifications of the talose configuration is not available for comparison, but the distinction suggested is not apparent from the absorption bands for the alpha and beta modifications of hexa-*O*-acetyl-D-*glycero*-D-*gulo*-heptose (figs. 16, 17).

Table 4 gives a summary of absorption bands for the acetylated methyl glycosides in the regions of 8.33 and 8.80 μ. These regions seem particularly promising for study of the conformation of the ring in the acteylated methyl pyranosides. All of the acetylated methyl pyranosides in the *gluco-*, *manno-*, and *galacto*-configuration that have been assigned the a-pyranose C′1 conformation show absorption bands at 8.30 to 8.35 μ (1,205 to 1,198 cm^{-1}) with the possible exception of methyl tri-*O*-acetyl-α-D-lyxoside (fig. 21), the spectrogram of which shows a slight inflection. None of the corresponding compounds having the e-pyranose C′1 conformation gives a band in this region. Table 4 shows that the a-pyranose acetylglycosides absorb more strongly than the e-pyranose acetylglycosides in the region of 8.80 μ. Methyl penta-*O*-acetyl-D-*glycero*-β-D-*gulo*-heptoside (fig. 31), the conformation of which is unknown, shows no distinctive band near 8.33 μ, but a fairly strong one at 8.83 μ. Classification of the compound is therefore uncertain, but it seems possible that it has both the C′1 and C′2 ring conformations.

The absorption in the region of 8.80 μ appears to depend not only on the axial and equatorial positions

[8] The numbers of the spectra are given in parentheses. Because of lack of material, the spectrum of penta-*O*-acetyl-α-D-talose, previously measured by the potassium chloride pellet technique [19], was not measured in solution.

TABLE 4. *Absorption bands at 8.33 and 8.80 μ for acetylated methyl glycosides*

	Configuration	Probable conformation	a and e groups	Absorption bands at—		Molar absorbancy index at 8.80 μ	Spectrum
				8.33±0.02 μ [a]	8.80±0.05 μ [a]		
				μ	μ	a_M	
Methyl tri-*O*-acetyl-α-D-xylopyranoside	*α-gluco*	C'1	aeee-	8.33 w	8.85 w	186	19
Methyl tetra-*O*-acetyl-α-D-glucopyranoside	*α-gluco*	C'1	aeeee	8.33 w	8.80 m	137	23
Methyl tri-*O*-acetyl-α-D-lyxopyranoside	*α-manno*	C'1	aaee-	8.32 (tr)	8.76 s	510	21
Methyl tetra-*O*-acetyl-α-D-mannopyranoside	*α-manno*	C'1	aaeee	8.31 w	8.78 s	475	25
Methyl tri-*O*-acetyl-α-L-rhamnopyranoside	*α-manno*	C'1	aaeee	8.33 w	8.78 s	378	26
Methyl tri-*O*-acetyl-β-L-arabinopyranoside	*α-gala*	C'1	aeea-	8.33 w	8.78 s	387	22
Methyl tetra-*O*-acetyl-α-D-galactopyranoside	*α-gala*	C'1	aeeae	8.35 w	8.80 m	286	29
Methyl tri-*O*-acetyl-β-D-xylopyranoside	*β-gluco*	C'1	eeee-	---	---	---	20
Methyl tetra-*O*-acetyl-β-D-glucopyranoside	*β-gluco*	C'1	eeeee	---	---	---	24
Methyl tetra-*O*-acetyl-β-D-mannopyranoside	*β-manno*	C'1	eaeee	---	---	---	27
Methyl tri-*O*-acetyl-β-L-rhamnopyranoside	*β-manno*	C'1	eaeee	---	---	---	28
Methyl tetra-*O*-acetyl-β-D-galactopyranoside	*β-gala*	C'1	eeeae	---	(b)	---	30
Methyl penta-*O*-acetyl-D-*glycero*-β-D-*gulo*-heptopyranoside	*β-gulo*	C'1 / C'2	eeaae / aaeea	---	8.83 m	214	31

[a] s, m, and w indicate strong, moderately strong, and weak bands, respectively; (tr) indicates the weakest observable absorption. [b] A weak band at 8.73 μ appear to be outside the region to be considered.

at the glycosidic carbon but also on those positions at other carbons of the ring. Table 4 shows that those glycosides having the a-pyranose structure with no axial acetyl group have an average molar absorbancy index of 162, and those with one axial acetyl group have an average index of 407. It thus appears that absorbancy at 8.80 μ is enhanced by the presence of axial acetate groups.

The examples given clearly show the usefulness of infrared spectra for the study of the structure of carbohydrate derivatives. Most of the bands characteristic of the cyclic carbohydrate structure occur in the region of 8.4 to 15 μ. The spectra are complex and difficult to interpret because there are many variables, and in some cases the bands are weak and poorly resolved. Part of the difficulty arises from lack of solubility of the compounds, and opacity of the solvents, especially in the range of 10 to 15 μ. More satisfactory spectra were obtained in this range with solid substances in potassium chloride pellets. However, comparison of spectra for configurationally related substances in the solid state will be deferred to a later paper, and the remainder of the discussion restricted to a less comprehensive treatment of the absorption found in the range 2.5 to 8.3 μ.

5. Miscellaneous Absorption Bands

5.1. The O–H Stretching Vibrations (2.5 to 3.2 μ, or 4,000 to 3,125 cm^{-1})

The infrared absorption in the region of 2.5 to 3.2 μ arises from O–H stretching vibrations. The absorption corresponding to vibration of free hydroxyl groups lies in the region of about 2.75 μ. The absorption band for the free hydroxyl is sharp, and is given by most hydroxyl-containing substances in dilute solution in nonpolar solvents, or in the form of vapor. It is also given by substances in which steric hindrance prevents association [20]. The hydroxyl group normally associates with groups of atoms having polar attraction. The resulting hydrogen bridges vary from weak to strong according to the character of the bridged atoms and the stereomeric conditions. Two types of bridges are generally recognized: Intermolecular bridges linking two or more molecules, and intramolecular bridges. Intermolecular (polymeric) bridges give rise to broad absorption bands between 2.9 and 3.1 μ. Intramolecular bridges are similar to the intermolecular bridges but differ in that they are not broken by dilution with a nonpolar solvent. Bands due to intramolecular bridges vary considerably, but are generally broad.

Spectrograms 34, 35, 36, 37, 40, and 41 are of compounds containing hydroxyl groups. The shape and intensity of the O–H absorption bands in the range 2.7 to 3.2 μ provide information as to the state of the hydroxyl groups in the molecules. At this time, a detailed analysis of the spectra for most substances in this region is not feasible but a brief structural analysis will be presented for penta-*O*-acetyl-*aldehydo*-D-galactose aldehydrol (fig. 40) and penta-*O*-acetyl-*aldehydo*-D-galactose hemiacetal (fig. 41). The absorption bands under consideration show two maxima, caused by the presence of free and of hydrogen-bridged hydroxyls. With the aldehydrol, the maximum absorption for the free hydroxyl (2.78 μ) is greater than that for the bridged hydroxyl (2.87 μ), but with the hemiacetal, the reverse is true. Thus, a larger proportion of the hydroxyl groups seems to be free in the aldehydrol than in the hemiacetal. A plausible explanation is that some of the hydroxyl groups in both compounds are bridged to the oxygen of the neighboring acetyl groups. The structure for the aldehydrol and hemiacetyl with a bridged hydroxyl would be as follows:

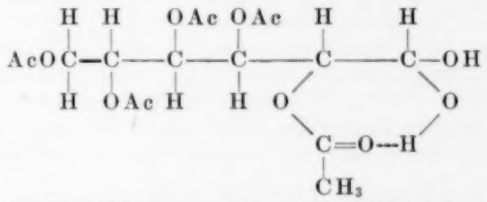

Penta-*O*-acetyl-*aldehydo*-D-galactose aldehydrol (40)

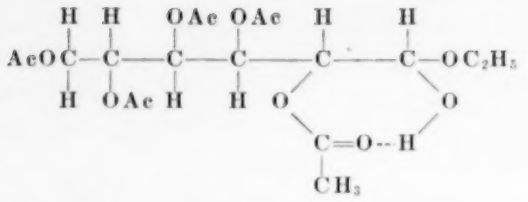

Penta-*O*-acetyl-*aldehydo*-D-galactose ethyl hemiacetal (41)

Comparisons of the maxima at 2.78 and 2.87 μ for curves 1, 2, and 3 of figure 41 show that there is little variation in the proportions of the free and bridged hydroxyls with dilution, in agreement with the proposed intramolecular linkage. The product from the aldehydrol would have one bridged and one free hydroxyl; that from the hemiacetal would have only the bridged hydroxyl. Thus, with an equal amount of hydrogen bridging, the aldehydrol would be expected to show a higher proportion of free hydroxyl groups, in agreement with the bands found in the spectra of the two compounds. In this connection, it is recognized that the intensities of bands arising from the same functional group in different environments are not necessarily invariant, but the differences found appear to be too large to be ascribed to minor variations in absorbancies.

A comparison of the total absorption for the hydroxyl groups can be used to confirm the existence of two hydroxyls in the aldehydrol and one in the hemiacetal. When measured by the method described on page 45, the integrated molar absorbancy indices for the aldehydrol and the hemiacetal in the region between 3,300 and 3,800 cm^{-1} (3.03 and 2.63 μ) had a ratio of 1.88. It is known that hydrogen-bridged hydroxyls absorb more strongly than free hydroxyls [20, 21]. Hence absorbancy for the bridged and free hydroxyls should not be weighted equally, and the ratio of integrated absorbancy indices must be somewhat larger than 1.88, in substantial agreement with the existence of twice as many hydroxyls in the aldehydrol as in the hemiacetal.

5.2. The C—H Stretching Vibrations (3.2 to 3.5 μ, or 3,125 to 2,857 cm^{-1})

The sugar acetates in carbon tetrachloride [9] were found to give absorption in the region of 3.3 to 3.5 μ. The absorption seems to be composed of at least five overlapping bands. The intensity of the bands, or of the components of a broad band, varies for different materials, and gives rise to characteristic shapes for the spectrograms in this region. Presumably the absorption arises from C—H bands of diverse type, such as those of the acetyl CH_3 groups, the terminal CH_2OR groups, and the pyranose ring. It would be desirable, if possible, to obtain independent evidence for the orientation of the ring hydrogens, and detailed study of absorption in this region with a high-dispersion prism or grating might possibly shed light on this important question.

[9] Because of its absorption in this region, chloroform is not satisfactory for use as a solvent.

5.3. The Spectral Range 3.5 to 5.5 μ, or 2,857 to 1,818 cm^{-1}

The few weak bands observed in this region, like the bands often encountered at wavelengths shorter than those of the O—H region, are overtones and combination bands. It might be of interest to observe this region at higher concentrations, and attempt to assign the bands in terms of fundamental frequencies.

5.4. The C=O Stretching Vibration (5.5 to 6.0 μ, or 1,818 to 1,667 cm^{-1})

All of the compounds, as expected, show strong absorption bands in the regions characteristic of the carbonyl group. To explore the effect of solvent and structure on the position and intensity of the C=O stretching band at 5.6 to 5.8 μ the maximum absorbancy index, a_M, was determined for each spectrum. The results, summarized in table 5, show that the group absorbancy indices, a_M/n, of the substances are considerably lower in chloroform than in carbon tetrachloride solution. The difference may be caused by bridging between the hydrogen of the chloroform, and the oxygen of the acetyl carbonyl groups, resulting in a broadening of the carbonyl absorption band, and hence a lowering of the absorption maximum. Furthermore, the absorption peak for the carbonyl band seems to be at a slightly longer wavelength in chloroform than in carbon tetrachloride solution. However, it is unnecessary to postulate hydrogen bridging in order to explain the reduced absorption in chloroform solution. Electrostatic dispersion forces in condensed phases are apparently sufficient to produce this effect [22].

TABLE 5. *Group absorbancy indices for the carbonyl stretching band at 5.65 to 5.8 μ*

$a_M/n=(-\log_{10}T_c)/nc\overline{b}$

Type	Carbon tetrachloride			Chloroform		
	Number of spectra	Average a_M/n	Standard deviation	Number of spectra	Average a_M/n	Standard [a] deviation
Fully acetylated sugars	21	380	±24	6	330	±16
Acetylated methyl glycosides	11	444	±36	2	367	±9
Acetylated sugars with a free hydroxyl group [b]	....	....	....	6	337	±19
Acetylated open-chain derivatives	3	398	±26	4	348	±7
All types [c]	35	402	±42	18	341	±19

[a] $\sigma=\sqrt{\frac{\Sigma(x-\bar{x})^2}{N}}$

[b] Penta-*O*-acetyl-*aldehydo*-D-galactose aldehydrol (40) and penta-*O*-acetyl-*aldehydo*-D-galactose ethyl hemiacetal (41) are included with the type characterized by a free hydroxyl group rather than with the open-chain derivatives.

[c] 1,2 [3,4,6-Tri-*O*-acetyl-D-mannopyranose] methyl orthoacetate (32), 1,2 [3,4-di-*O*-acetyl-L-rhamnopyranose] methyl orthoacetate (33), and hexa-*O*-acetyl inositol (47) are special types and are not included in the treatment represented by this table.

The compounds of the present study vary with respect to the number and character of the *O*-acetyl groups. Table 5 shows that there are small but significant differences for the average group absorbancy indices obtained for the fully acetylated sugars, acetylated methyl glycosides, acetylated sugars with free glycosidic hydroxyls, and acetylated open-chain derivatives. These differences could arise from intramolecular forces between the groups attached to the glycosidic carbon, and the neighboring acetyl groups. However, because the carbonyl absorptions of the various acetate groups do not necessarily coincide, it is to be expected that the band will be broader and the maximum group absorbancy index somewhat lower for those compounds with the greatest number of acetate groups.

The acetyl derivatives of the aldehyde and ketone forms of the sugars have generally been considered to be true aldehydes and ketones. However, penta-*O*-acetyl-*aldehydo*-D-galactose forms a hydrate and an alcoholate for which Wolfrom has proposed an aldehydrol and a hemiacetal structure respectively [23]. The results of the present study, already discussed, are in agreement with these structures.[10] If the carbonyl groups of the anhydrous *aldehydo* sugar acetates are free, these compounds should show a strong *aldehydo* carbonyl band in a range of somewhat longer wavelength than that occupied by the acetate carbonyl band. However, no strong absorption in this range was found for anhydrous tetra-*O*-acetyl-*aldehydo*-L-arabinose (fig. 38), penta-*O*-acetyl-*aldehydo*-D-galactose (fig. 39), and penta-*O*-acetyl-*keto*-L-sorbose (fig. 42). Faint absorption bands at 5.95 and 6.05 μ were found in the spectrum of penta-*O*-acetyl-*keto*-L-sorbose, but these are too weak to support a free carbonyl structure, and the latter band is at too long a wavelength. A polymeric structure analogous to that of paraldehyde seemed possible, but a molecular-weight determination for penta-*O*-acetyl-*aldehydo*-D-galactose showed that this substance is truly a monomer.[11] The data, then, appear to indicate that several monomeric *aldehydo* sugar acetates fail to show absorption in a range considered to be characteristic of the *aldehydo* carbonyl group. There remains the possibility that an *aldehydo* carbonyl might absorb at so nearly the same place as the acetate carbonyl that absorption due to the former would be obscured.

5.5. The Spectral Range 6.0 to 6.7 μ, or 1,667 to 1,493 cm^{-1}

Absorption in the range of 6.0 to 6.7 μ was found to be too weak for accurate determination, with the concentrations used in most of the measurements. Some of the spectra show almost complete absence of absorption; others show weak bands, principally between 6.0 and 6.25 μ. It is interesting that penta-*O*-acetyl-*aldehydo*-D-galactose aldehydrol (fig. 40) shows a weak but definite absorption at 6.25 μ that is not observed for the anhydrous form, penta-*O*-acetyl-*aldehydo*-D-galactose (fig. 39), or for penta-*O*-acetyl-*aldehydo*-D-galactose hemiacetal (fig. 41).

5.6. The CH_3 Vibrations (6.7 to 7.5 μ, or 1,493 to 1,333 cm^{-1})

All of the spectrograms show absorption bands at approximately 7.0 and 7.3 μ, presumably caused by deformation of the CH_3 groups. The 7.0-μ band is broad and rather weak, whereas the 7.3-μ band is sharp and strong. In most cases the 7.3-μ band is symmetrical, but in the methyl orthoacetates and a few other compounds it appears as a doublet, or with irregularities at 7.2 and 7.3 μ. The absorption at 7.3 μ may be attributed to the deformation vibration of the CH_3 group of the normal acetate; the absorption at 7.2 μ may arise in the methyl orthoacetates from the deformation vibration of the CH_3 group of the orthoacetate ring structure. Tetra-*O*-acetyl-β-D-glucose (fig. 34) and penta-*O*-acetyl-α-D-glucoheptulose (fig. 37) show marked absorption at 7.25 μ in addition to the normal absorption at 7.3 μ. Slight irregularities are found in the same region in the spectrograms of a few of the remaining compounds.

The acetylated methyl glycosides show a weak band at 6.9 μ that overlaps the band due to the CH_3 symmetrical deformation vibration. This absorption seems to be in accord with the wavelength previously ascribed to the vibration of the CH_3 group of methanol (6.87 μ) and dimethyl ether (6.83 μ) [1, p. 24], although it may be analogous to the 6.89-μ band of tetrahydropyran [26].

5.7. The Acetate Bands at 8.0 and 8.2 μ (1,250 and 1,220 cm^{-1})

All of the spectra included in the present study show a strong absorption band at 8.2 μ and a weak to moderately strong band at 8.0 μ. Presumably these bands arise from the stretching vibrations of the C—O bonds in the acetyl groups, and are analogous to bands shown in the same regions by other acetates. In most cases the 8.2-μ band is broad, with several shoulders or inflections indicative of three or more components. The complex character of the bands may arise from axial or equatorial effects such as those described for the *cis* and *trans* 3-acetosteroids [17, 18]. It seems significant that the 8.0-μ band is particularly sharp for the acetates of the pentoses and of rhamnose, compounds that lack an acetyl-substituted primary alcoholic group. In the absence of this group, and if its absorption falls between 8.0 and 8.2 μ, the absorption at 8.0 μ would appear sharper. Because furanose derivatives of the pentoses, unlike the pyranose derivatives, have a primary alcoholic group, the presence or absence of a sharp band at 8.0 μ may serve to distinguish the two types of rings in the acetates of the pentoses. In accord with this possible distinction is the fact that

[10] Absorption spectra studies by Rowen, Forziati, and Reeves [24] show that the aldehyde groups in periodate-oxidized cellulose are also hydrated, and the material contains few, if any, free aldehyde groups.

[11] The semicarbazones of *aldehydo*-D-galactose pentaacetate and of *aldehydo*-L-arabinose tetraacetate are reported to have normal molecular weight [23, 25]. However, the structure of these products does not establish the structure of the parent acetates. In this investigation, *aldehydo*-D-galactose pentaacetate was found to be a monomer by means of a cryoscopic determination of molecular weight in benzene.

penta-*O*-acetyl-α-L-sorbopyranose (fig. 13), having a pyranose ring similar to that of L-xylose but an acetylated primary alcoholic group at carbon 1, fails, like the acetates of the aldohexopyranoses, to give a sharp band at 8.0 μ.

6. References

[1] L. J. Bellamy, The infra-red spectra of complex molecules (Methuen & Co., Ltd., London; John Wiley & Sons, Inc., New York, N. Y., 1954).
[2] L. P. Kuhn, Anal. Chem. **22,** 276 (1950).
[3] R. L. Whistler and L. R. House, Anal. Chem. **25,** 1463 (1953).
[4] S. A. Barker, E. J. Bourne, M. Stacey, and D. H. Whiffen, J. Chem. Soc. **1954,** 171.
[5] S. A. Barker, E. J. Bourne, R. Stephens, and D. H. Whiffen, J. Chem. Soc. **1954,** 3468.
[6] S. A. Barker, E. J. Bourne, M. Stacey, and D. H. Whiffen, Chem. and Ind. **1953,** 196.
[7] R. B. Barnes, R. C. Gore, U. Liddel, and V. Z. Williams, Infrared spectroscopy: Industrial applications and bibliography (Reinhold Publishing Corp., New York, N. Y., 1944).
[8] H. M. Randall, R. G. Fowler, N. Fuson, and J. R. Dangl, Infrared determination of organic structures (D. Van Nostrand, Inc., New York, N. Y., 1949).
[9] O. Hassel and B. Ottar, Acta. Chem. Scand. **1,** 929 (1947).
[10] R. E. Reeves, Advances in Carbohydrate Chem. **6,** 107 (1951).
[11] H. S. Isbell, J. Research NBS **57,** 171 (1956) RP2707.
[12] E. C. Creitz and F. A. Smith, J. Research NBS **43,** 365 (1949) RP2031.
[13] K. S. Gibson, Spectrophotometry, NBS Circ. 484 (1949).
[14] R. E. Reeves, J. Am. Chem. Soc. **71,** 212, 215, 1737, 2116 (1949); **72,** 1499 (1950).
[15] H. S. Isbell and W. W. Pigman, J. Org. Chem. **1,** 505 (1937).
[16] R. N. Jones, D. A. Ramsay, F. Herling, and K. Dobriner, J. Am. Chem. Soc. **74,** 2828 (1952).
[17] A. R. H. Cole, R. N. Jones, and K. Dobriner, J. Am. Chem. Soc. **74,** 5571 (1952).
[18] R. N. Jones, P. Humphries, F. Herling, and K. Dobriner, J. Am. Chem. Soc. **73,** 3215 (1951).
[19 H. S. Isbell, J. E. Stewart, H. L. Frush, J. D. Moyer, and F. A. Smith, J. Research NBS **57,** 179 (1956) RP2708.
[20] F. A. Smith and E. C. Creitz, J. Research NBS **46,** 145 (1951) RP2187.
[21] H. Tsubomura, J. Chem. Phys. **24,** 927 (1956).
[22] E. Ferguson, J. Chem. Phys. In press.
[23] M. L. Wolfrom, J. Am. Chem. Soc. **52,** 2464 (1930).
[24] J. W. Rowen, F. H. Forziati, and R. E. Reeves, J. Am. Chem. Soc. **73,** 4454 (1951).
[25] M. L. Wolfrom and M. R. Newlin, J. Am. Chem. Soc. **52,** 3619 (1930).
[26] S. C. Burket and R. M. Badger, J. Am. Chem. Soc. **72,** 4397 (1950).

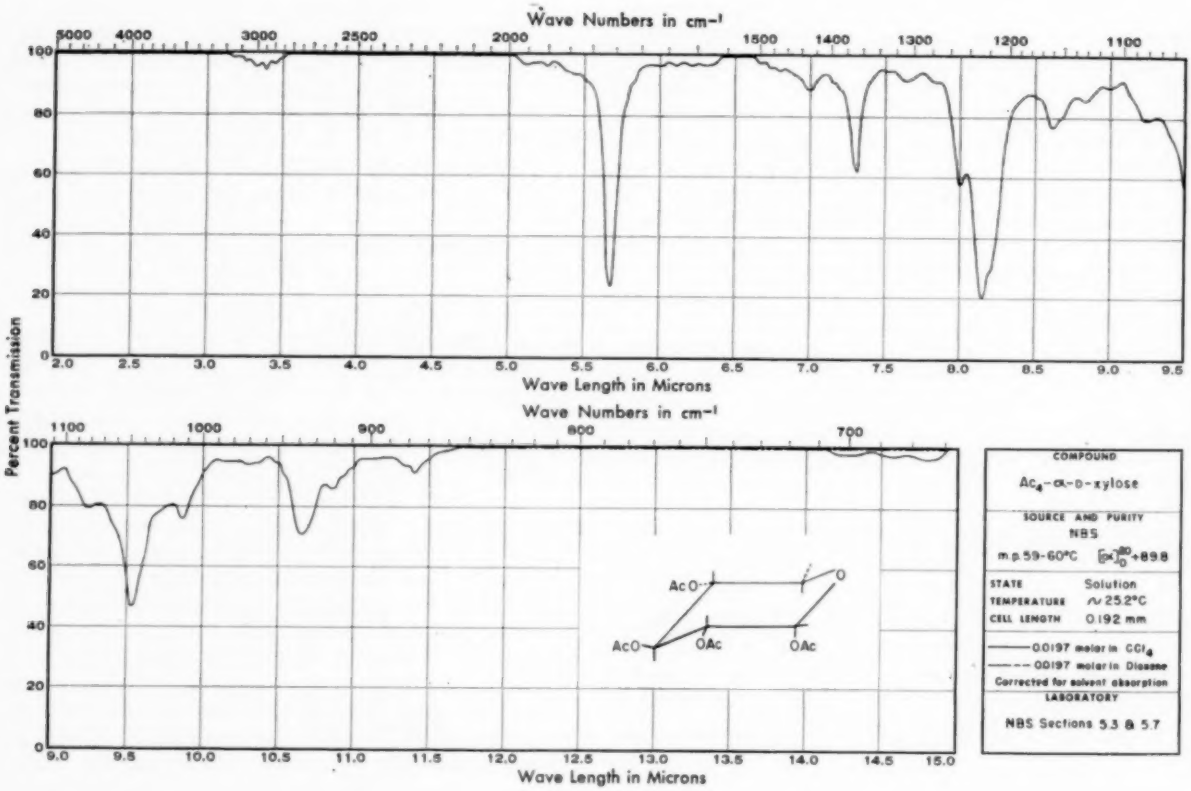
Wave Numbers in cm⁻¹
5000 4000 3000 2500 2000 1500 1400 1300 1200 1100
Percent Transmission
100 80 60 40 20 0
2.0 2.5 3.0 3.5 4.0 4.5 5.0 5.5 6.0 6.5 7.0 7.5 8.0 8.5 9.0 9.5
Wave Length in Microns
Wave Numbers in cm⁻¹
1100 1000 900 800 700
100 80 60 40 20 0
9.0 9.5 10.0 10.5 11.0 11.5 12.0 12.5 13.0 13.5 14.0 14.5 15.0
Wave Length in Microns
AcO
AcO
OAc
OAc
O
COMPOUND
Ac4-α-D-xylose
SOURCE AND PURITY
NBS
m.p. 59-60°C [α]D20 +89.8
STATE Solution
TEMPERATURE ~25.2°C
CELL LENGTH 0.192 mm
0.0197 molar in CCl4
0.0197 molar in Dioxane
Corrected for solvent absorption
LABORATORY
NBS Sections 5.3 & 5.7

FIGURE 1.

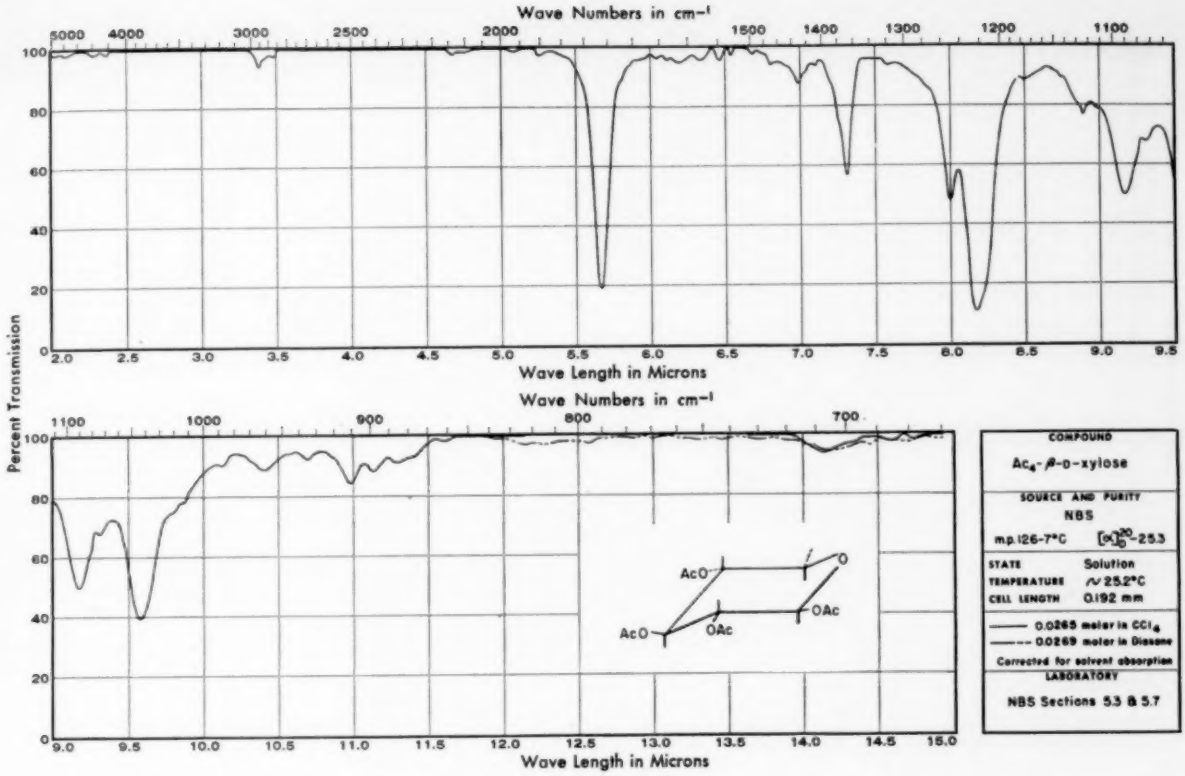

FIGURE 2.

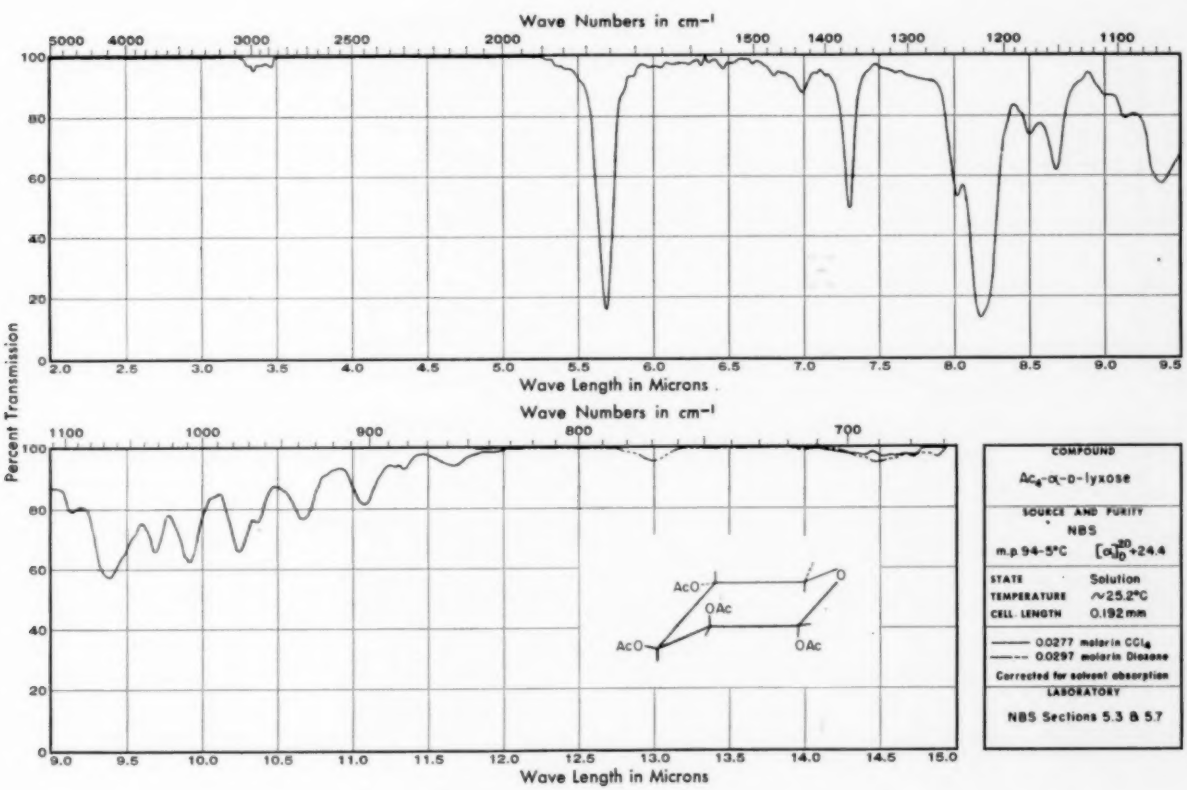

FIGURE 3.

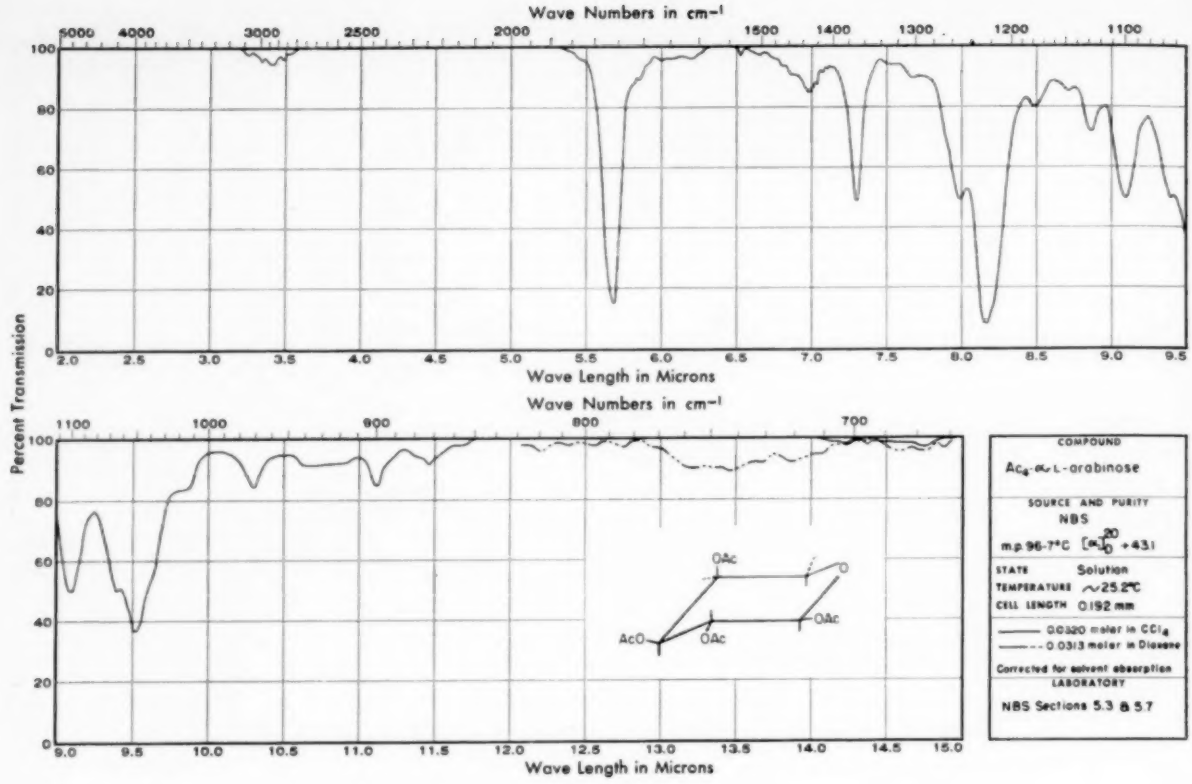

FIGURE 4.

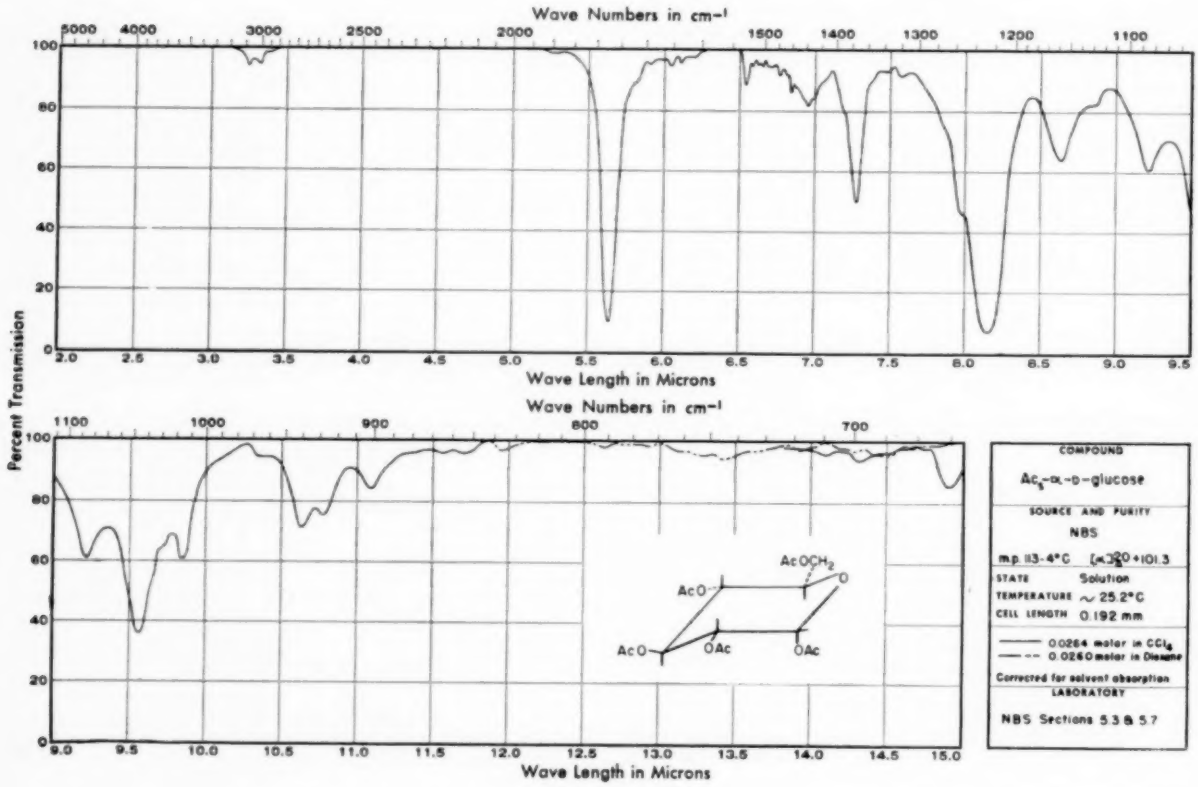

FIGURE 5.

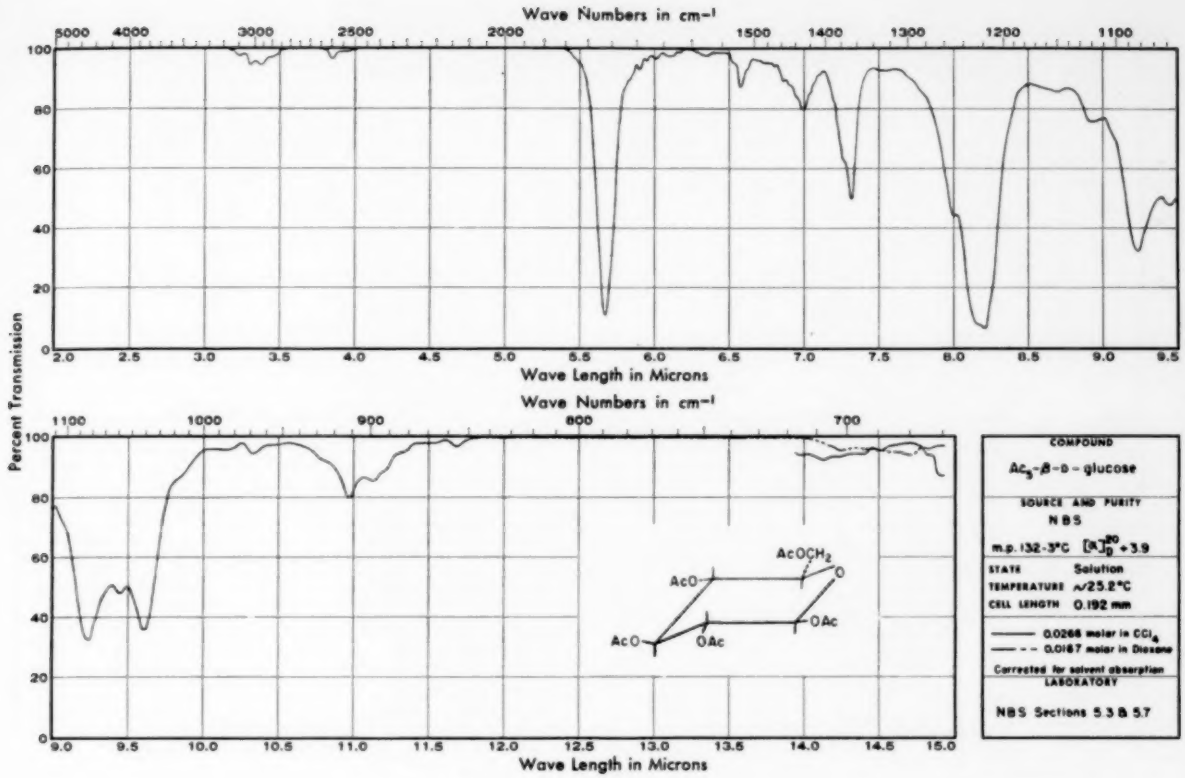

FIGURE 6.

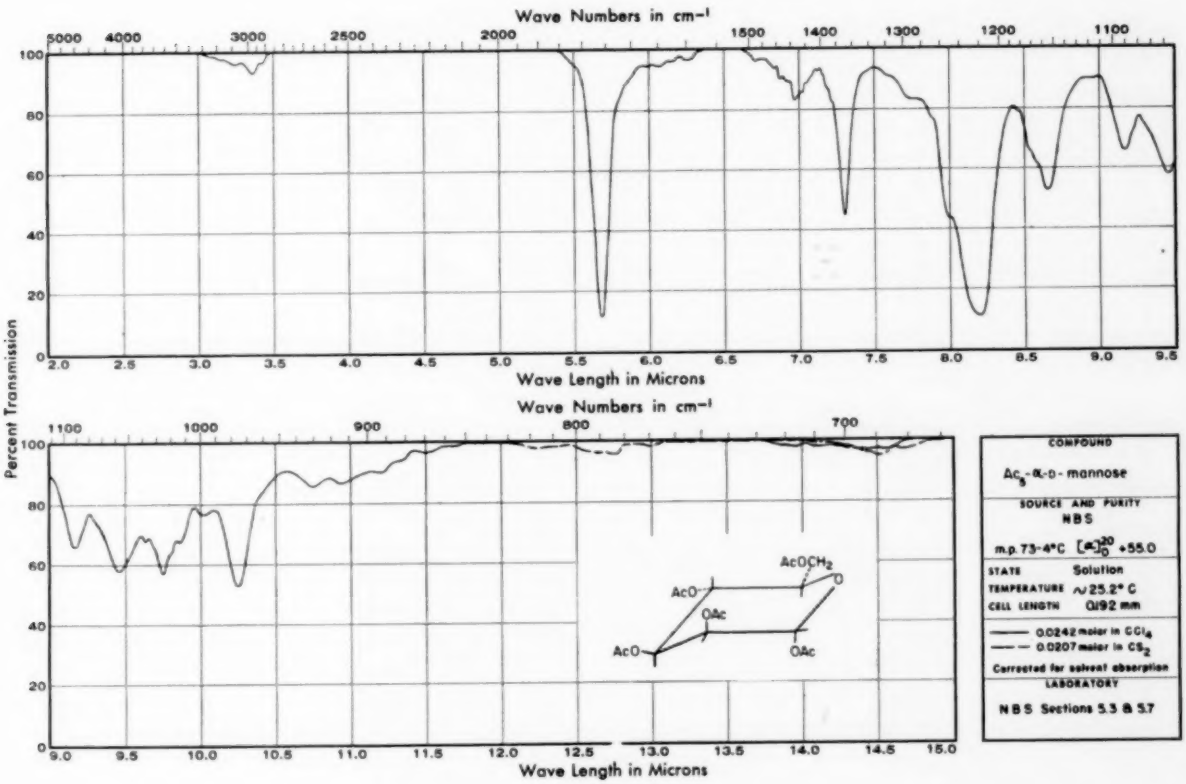

FIGURE 7.

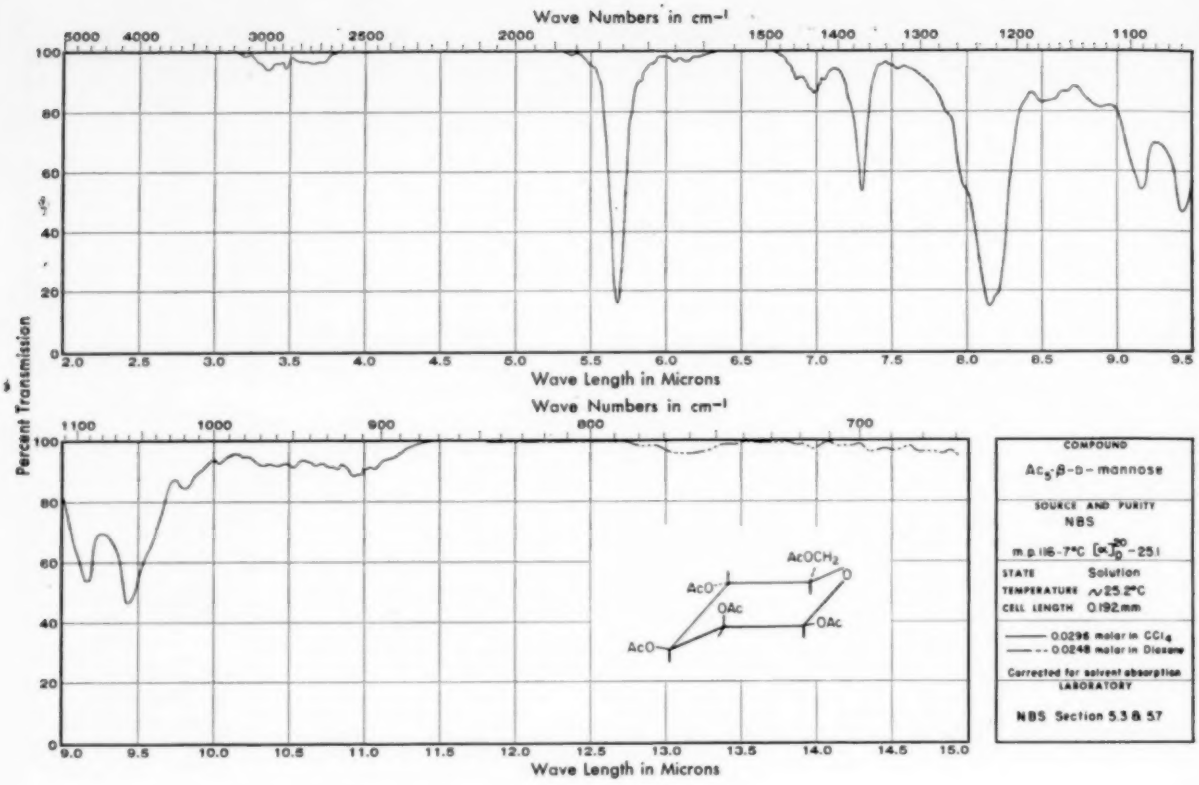

FIGURE 8.

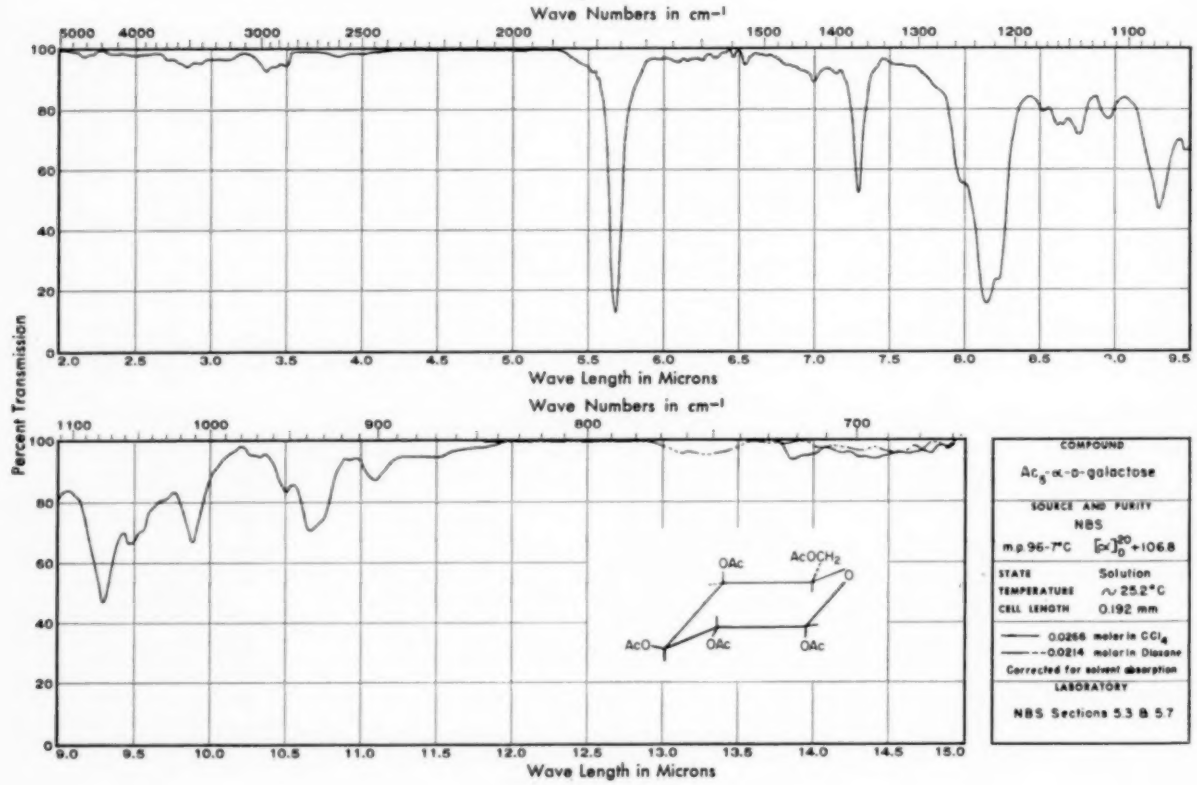

FIGURE 9.

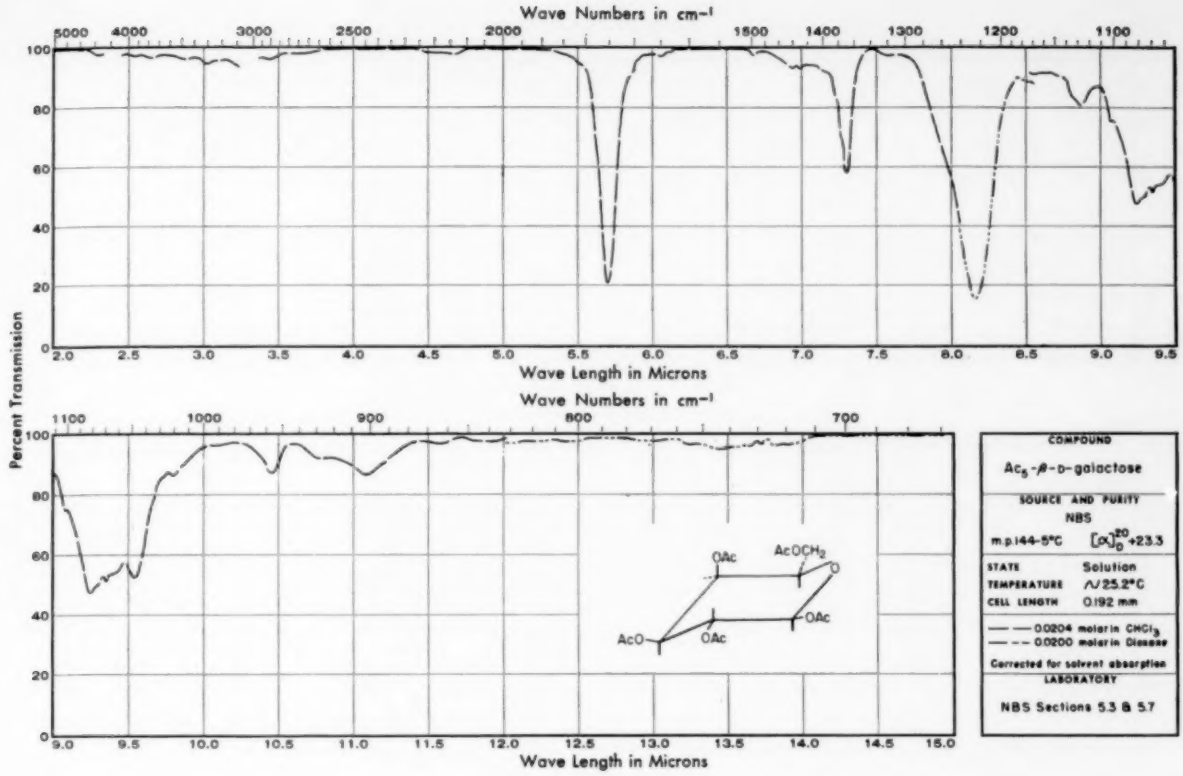

FIGURE 10.

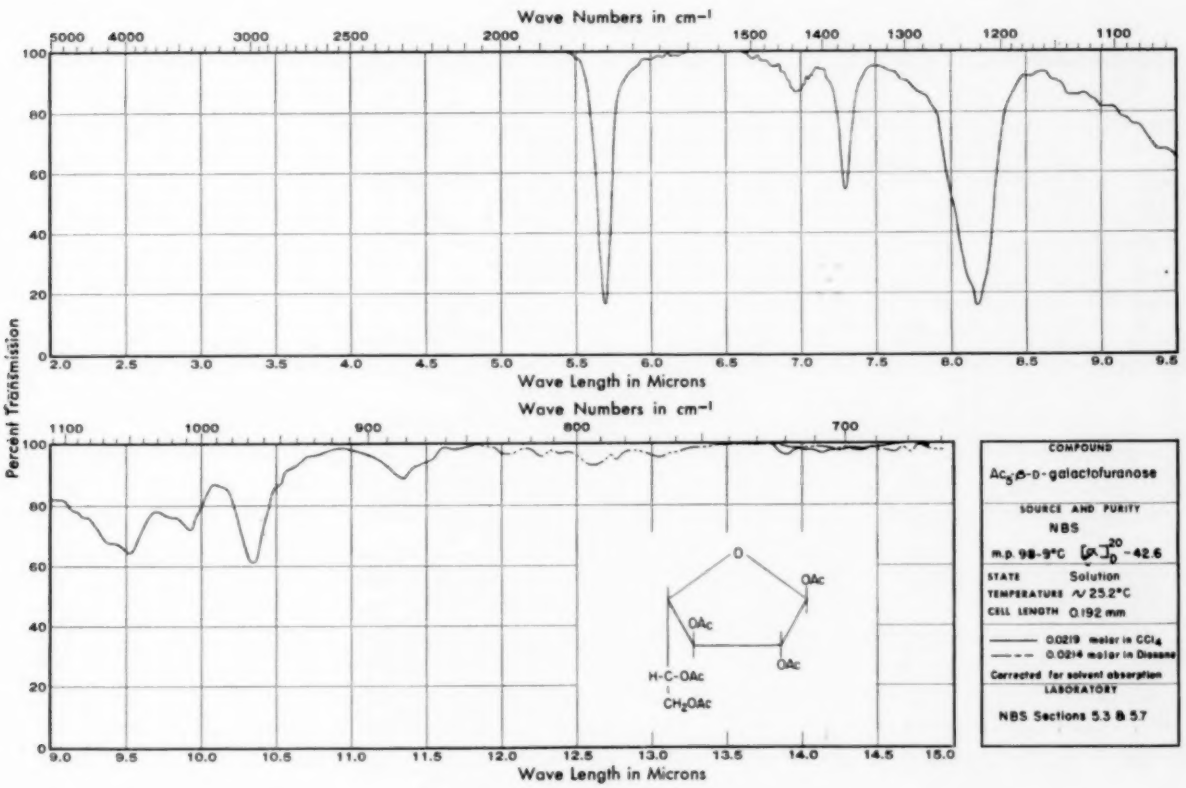

FIGURE 11.

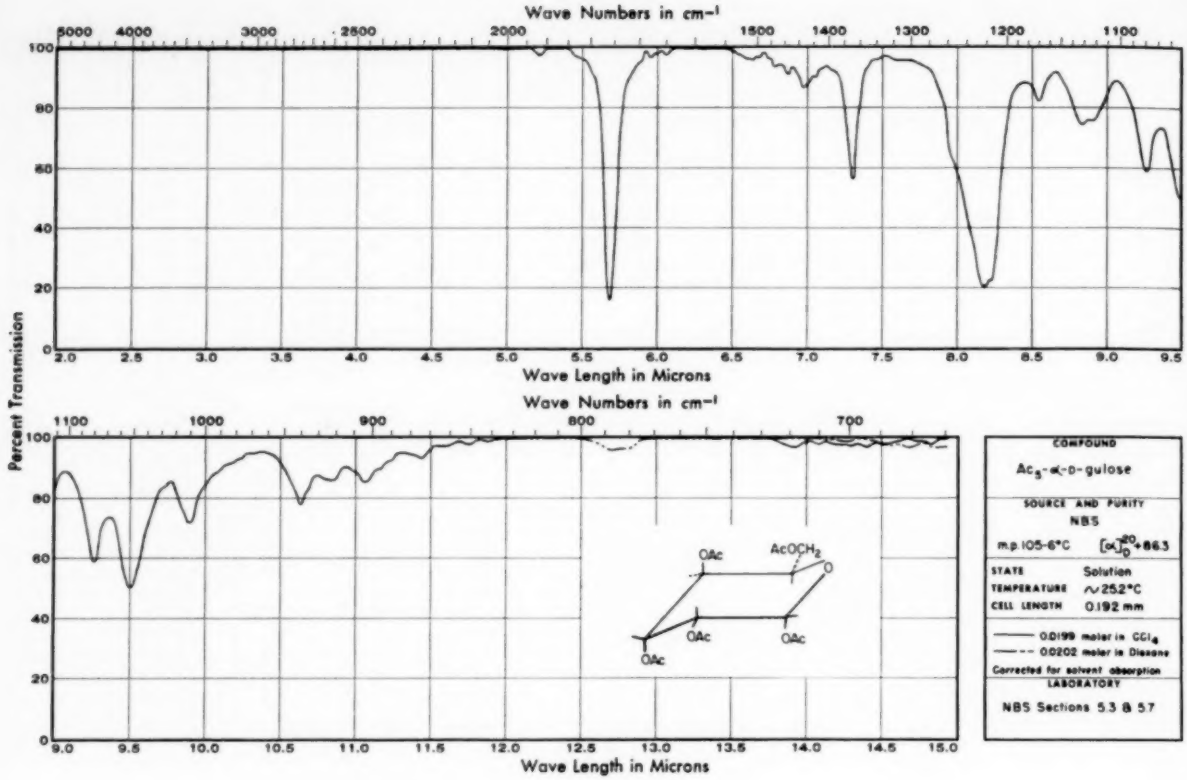

FIGURE 12.

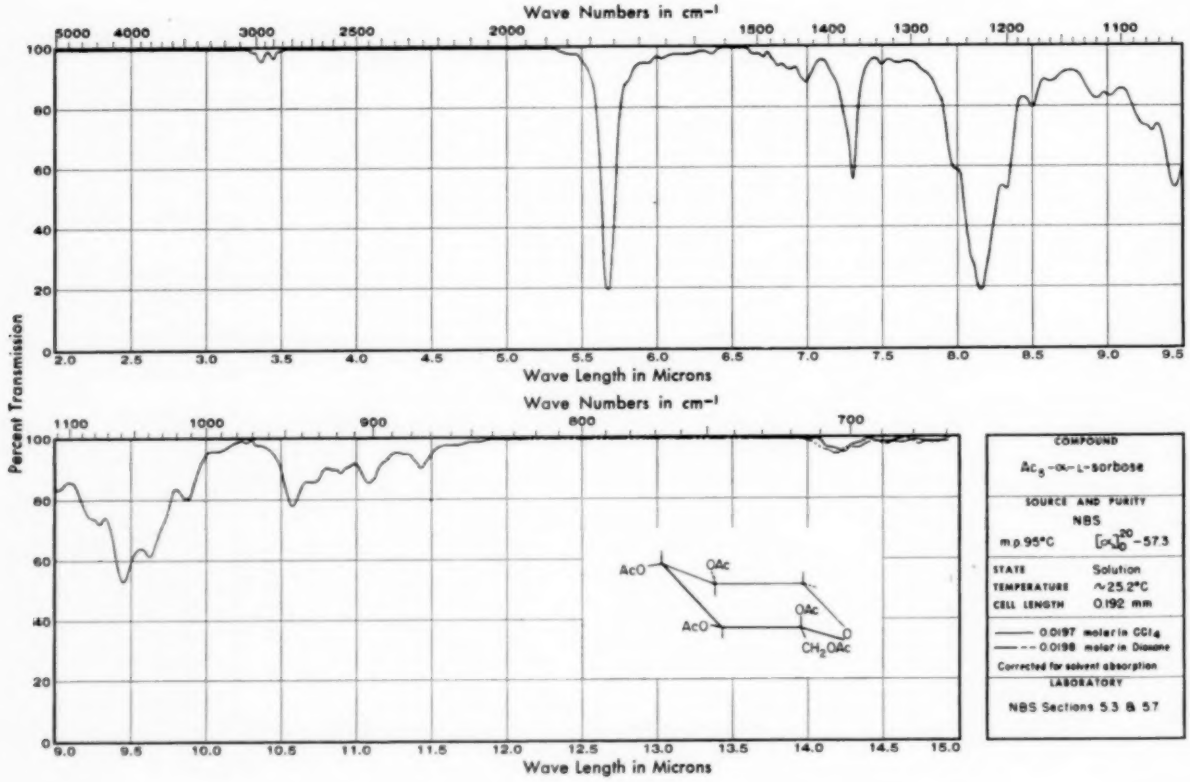

FIGURE 13.

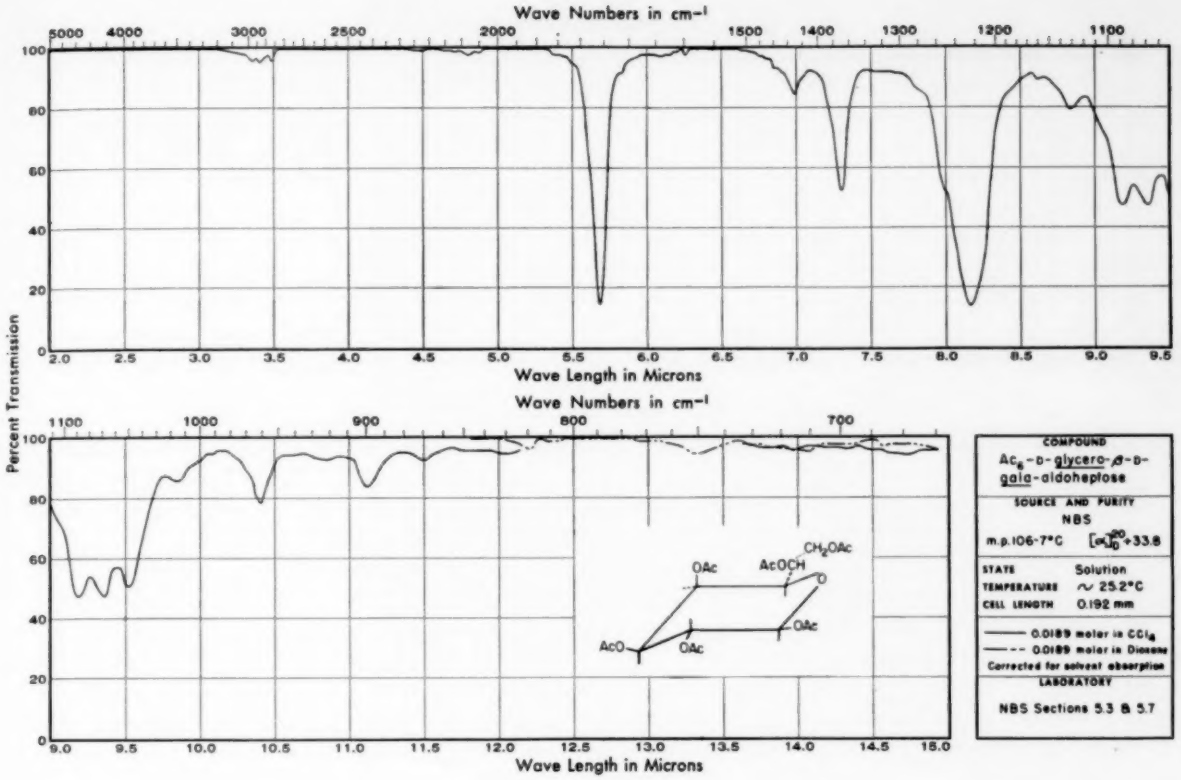

FIGURE 14.

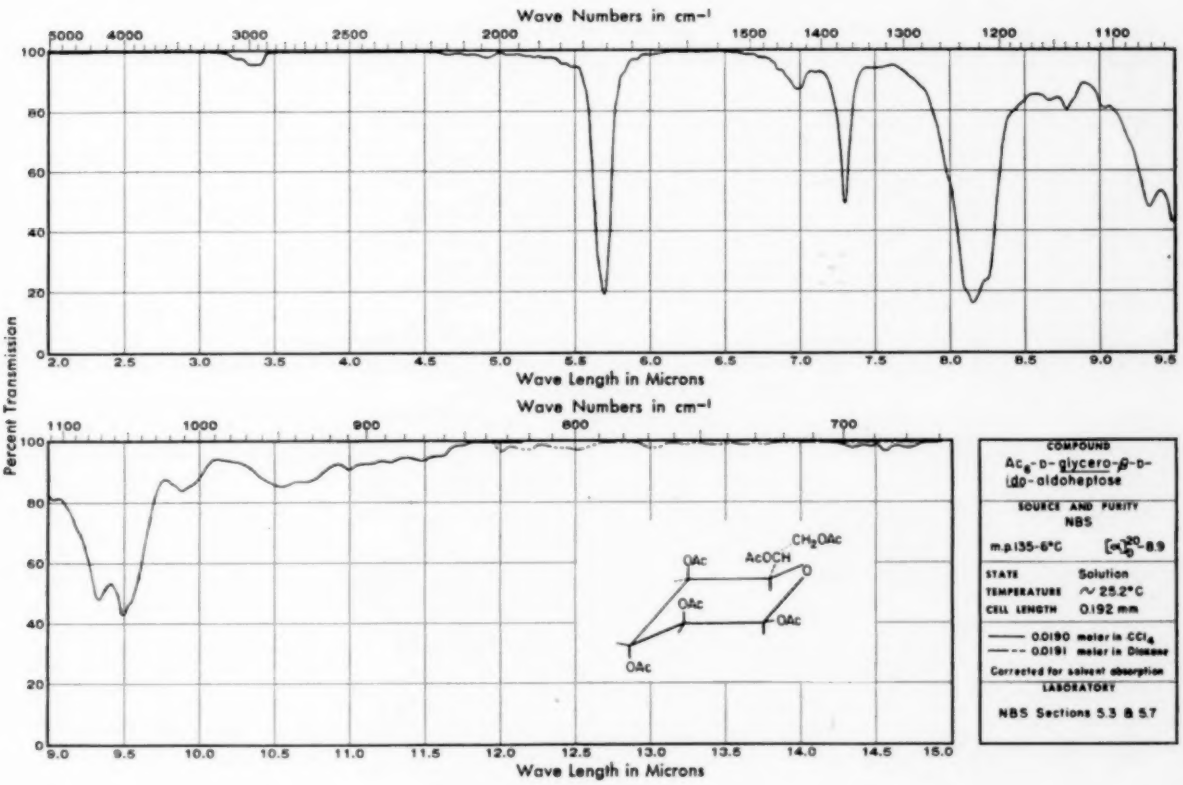

FIGURE 15.

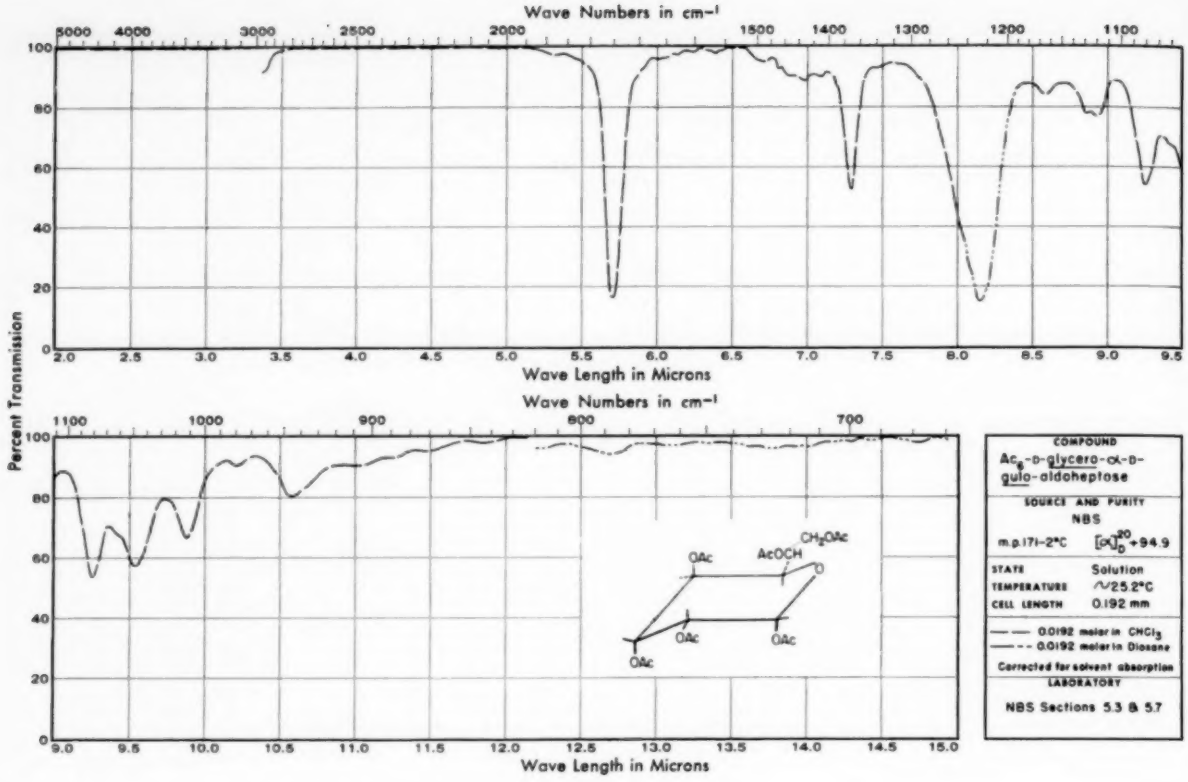

FIGURE 16.

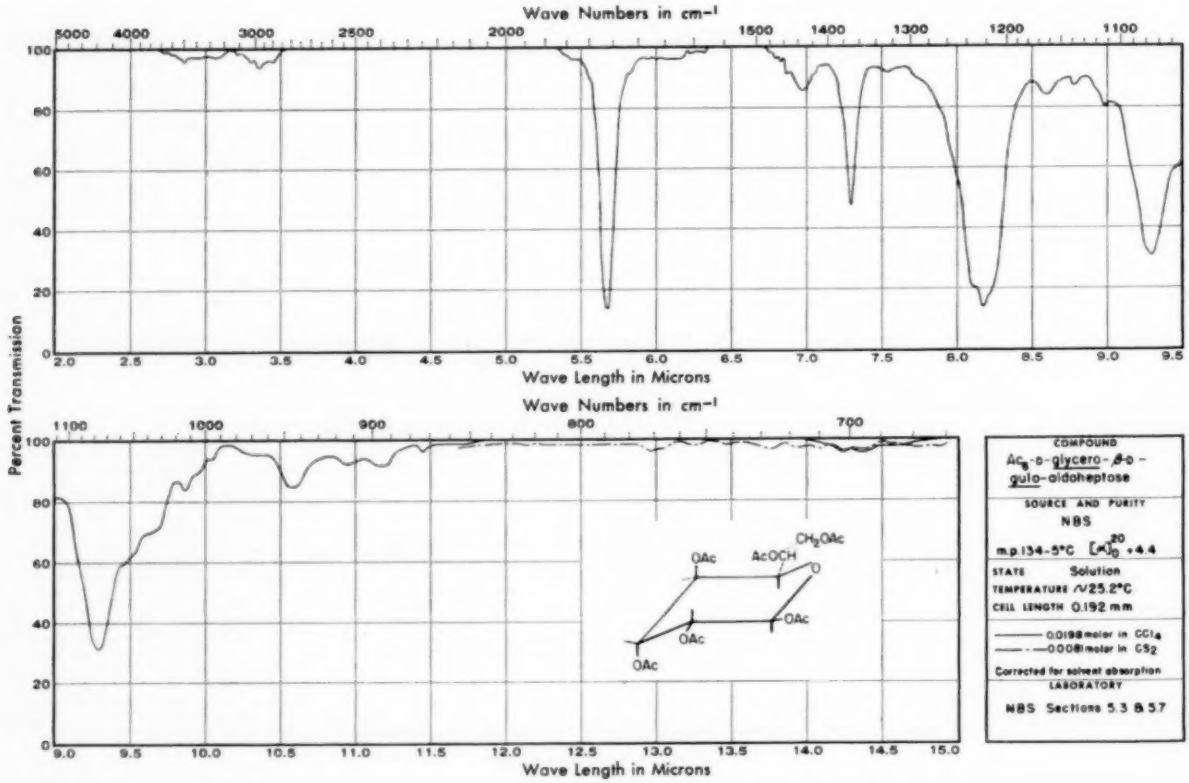

FIGURE 17.

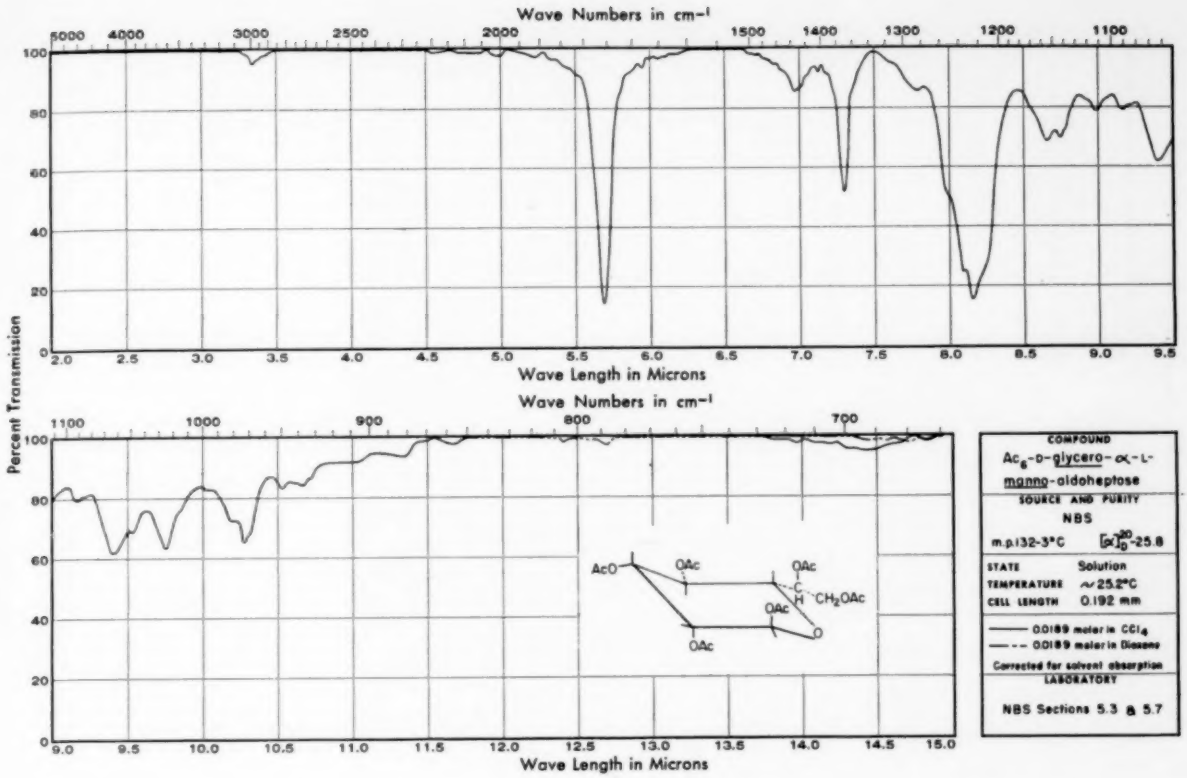

FIGURE 18.

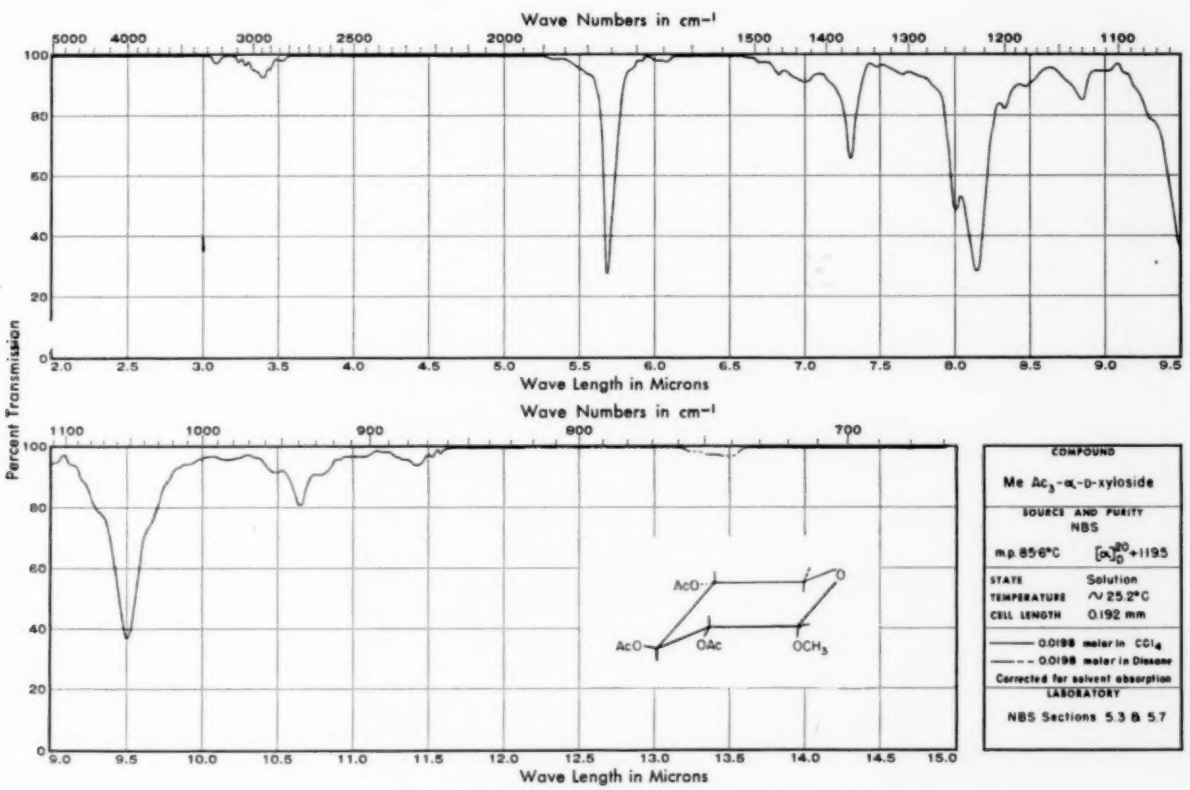

FIGURE 19.

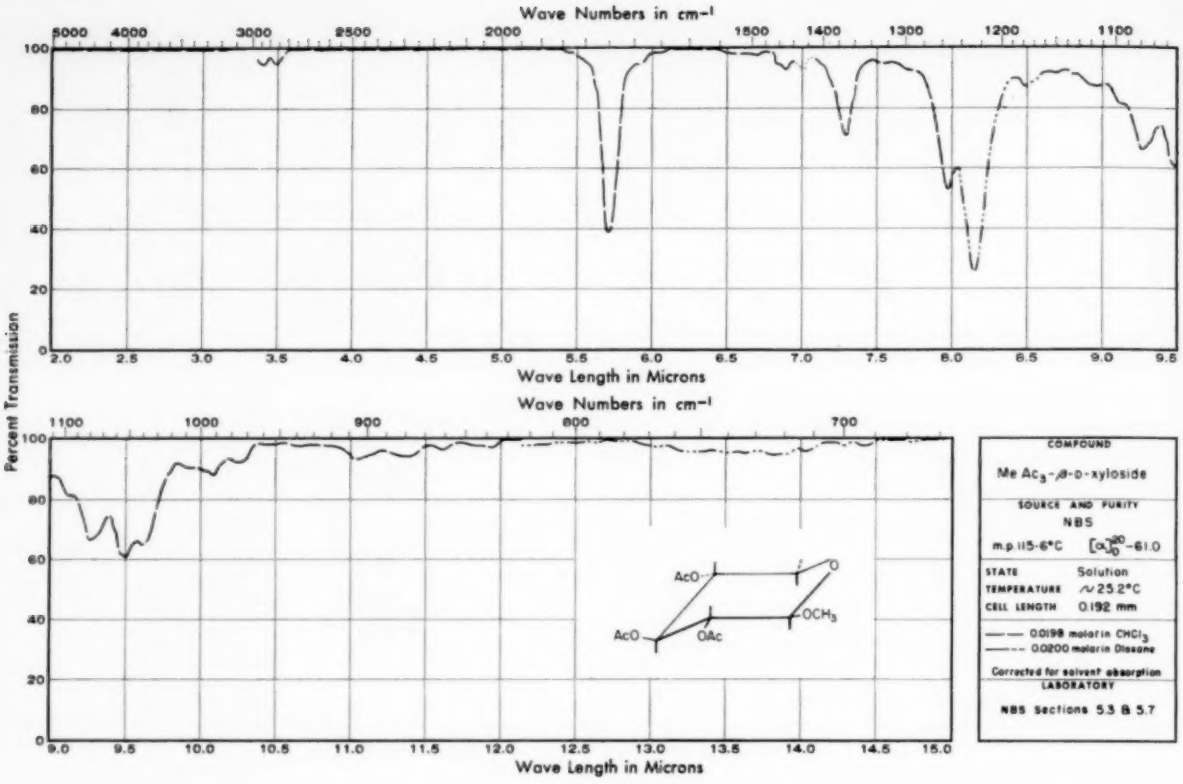

FIGURE 20.

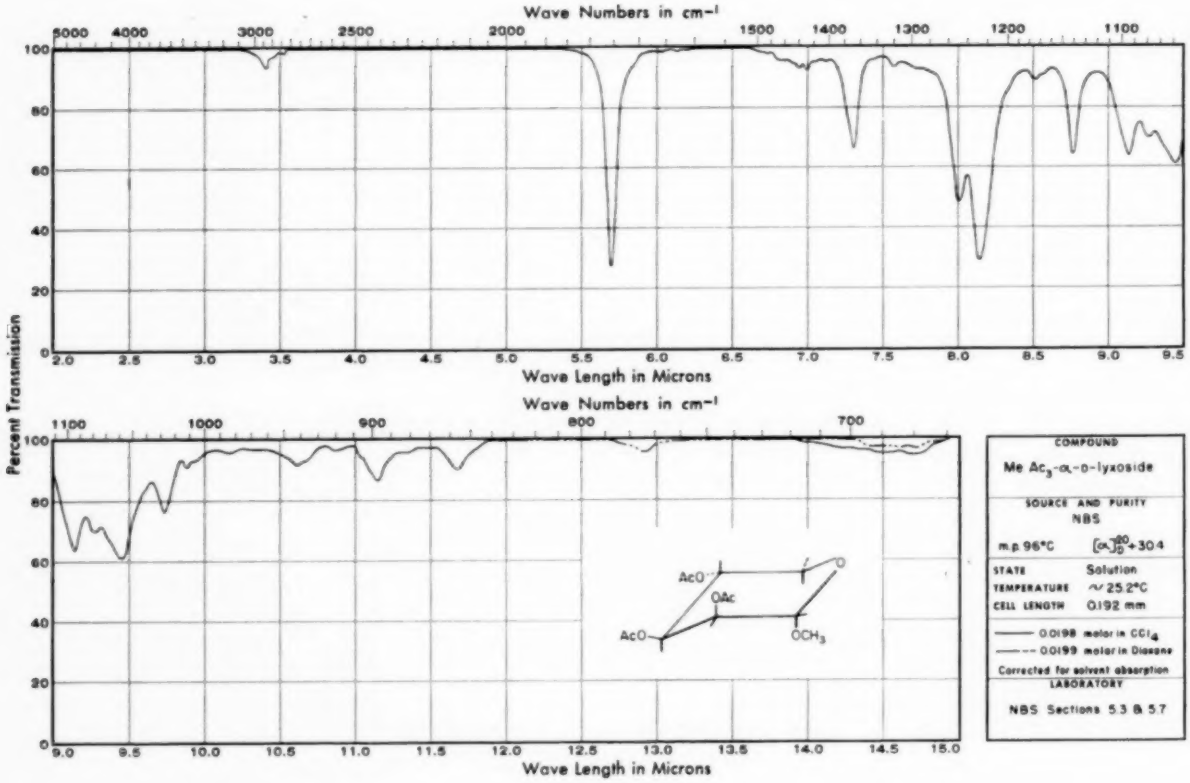

FIGURE 21.

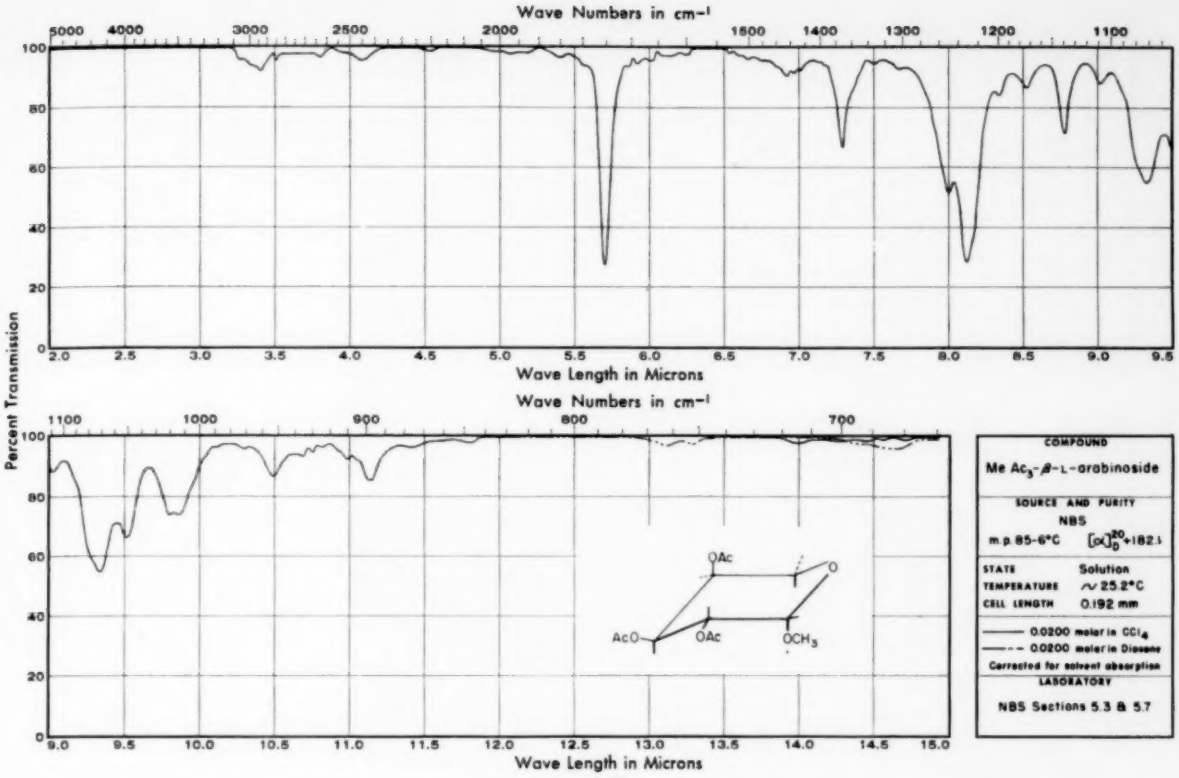

FIGURE 22.

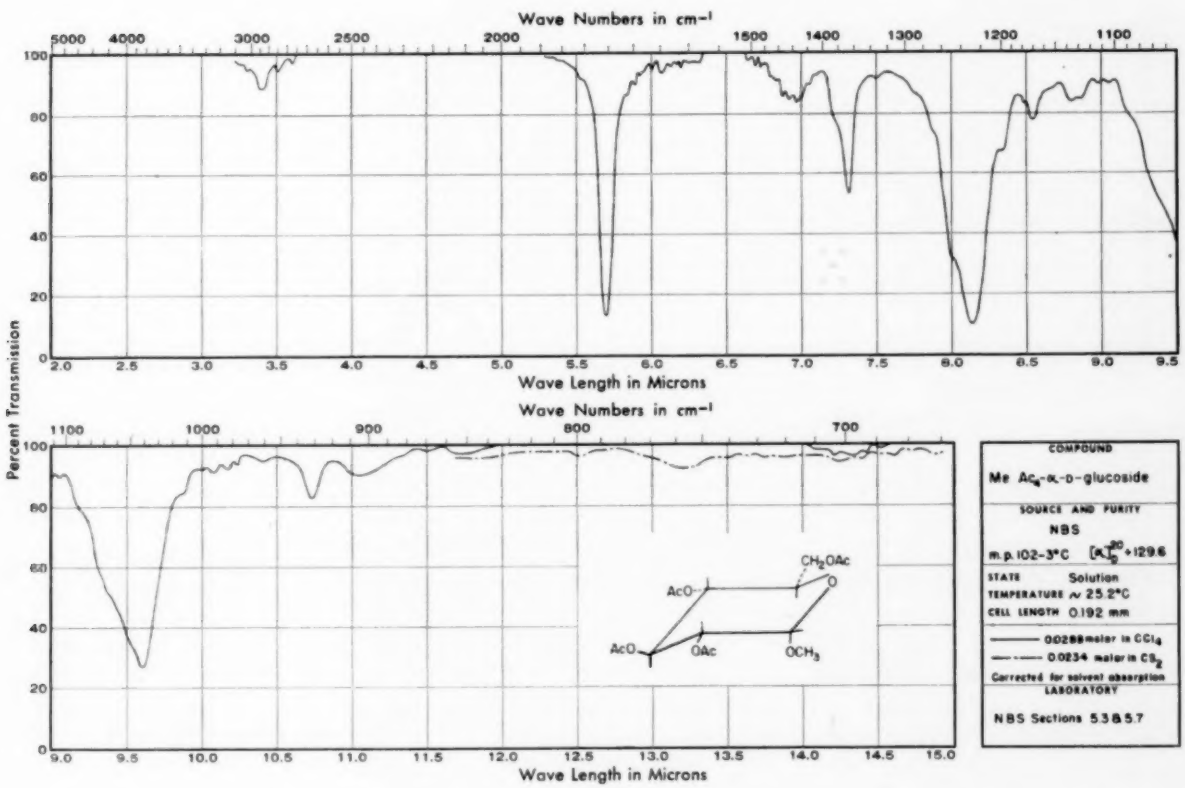

FIGURE 23.

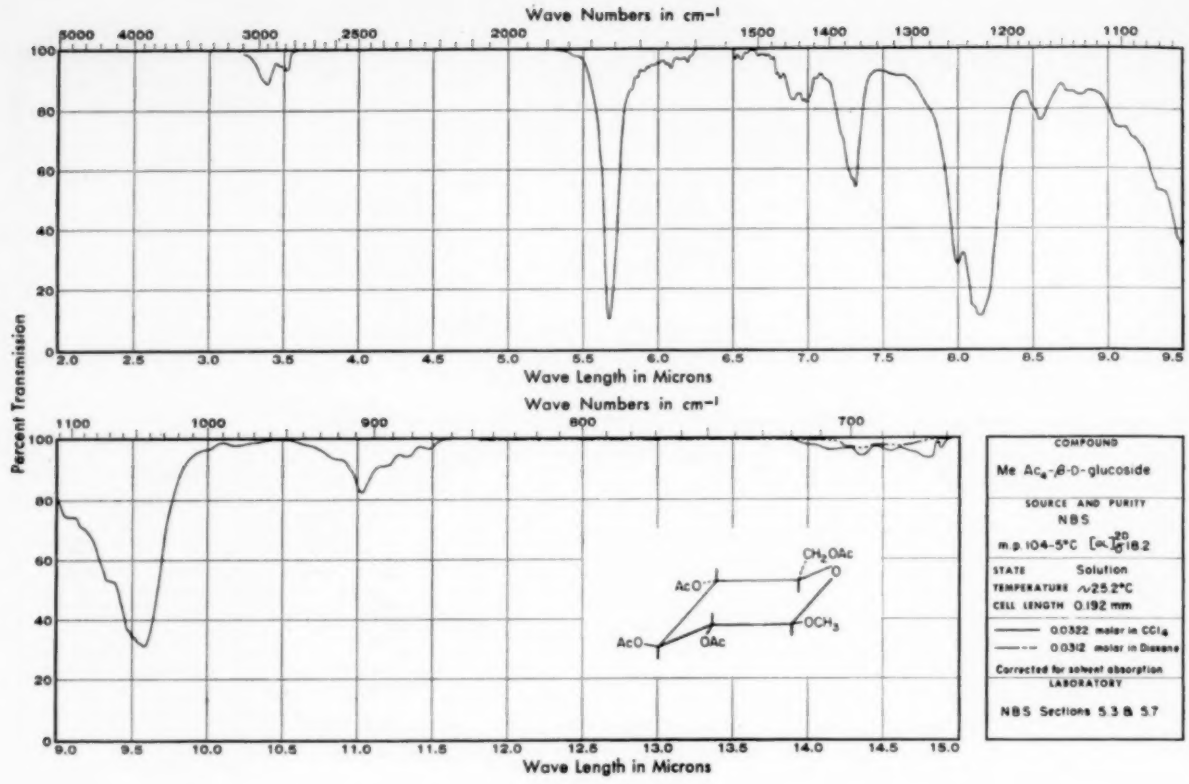

FIGURE 24.

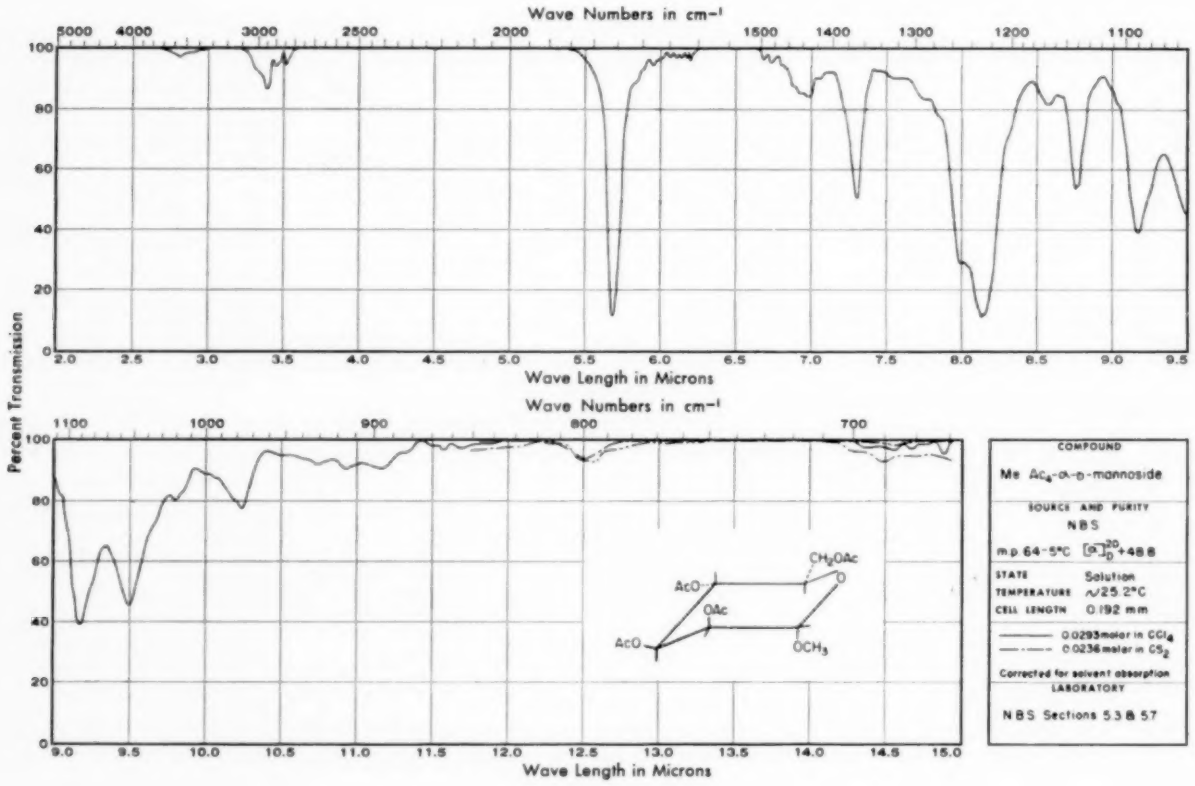

FIGURE 25.

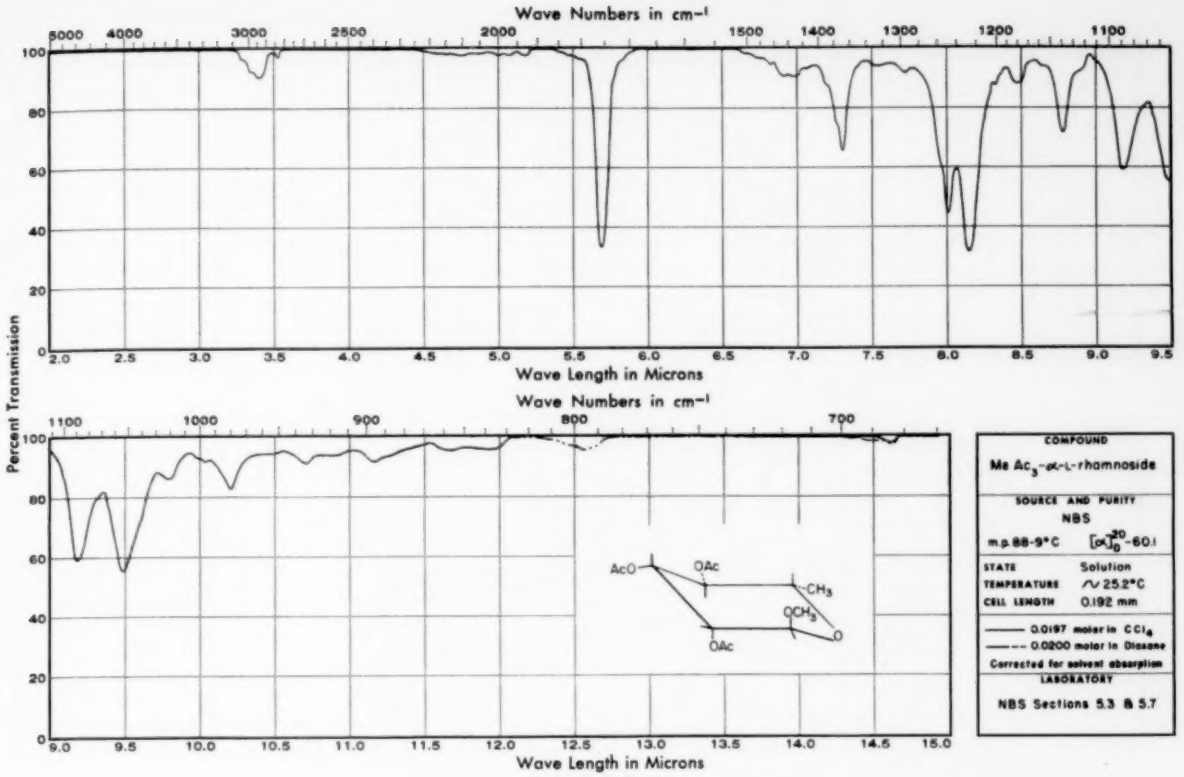

FIGURE 26.

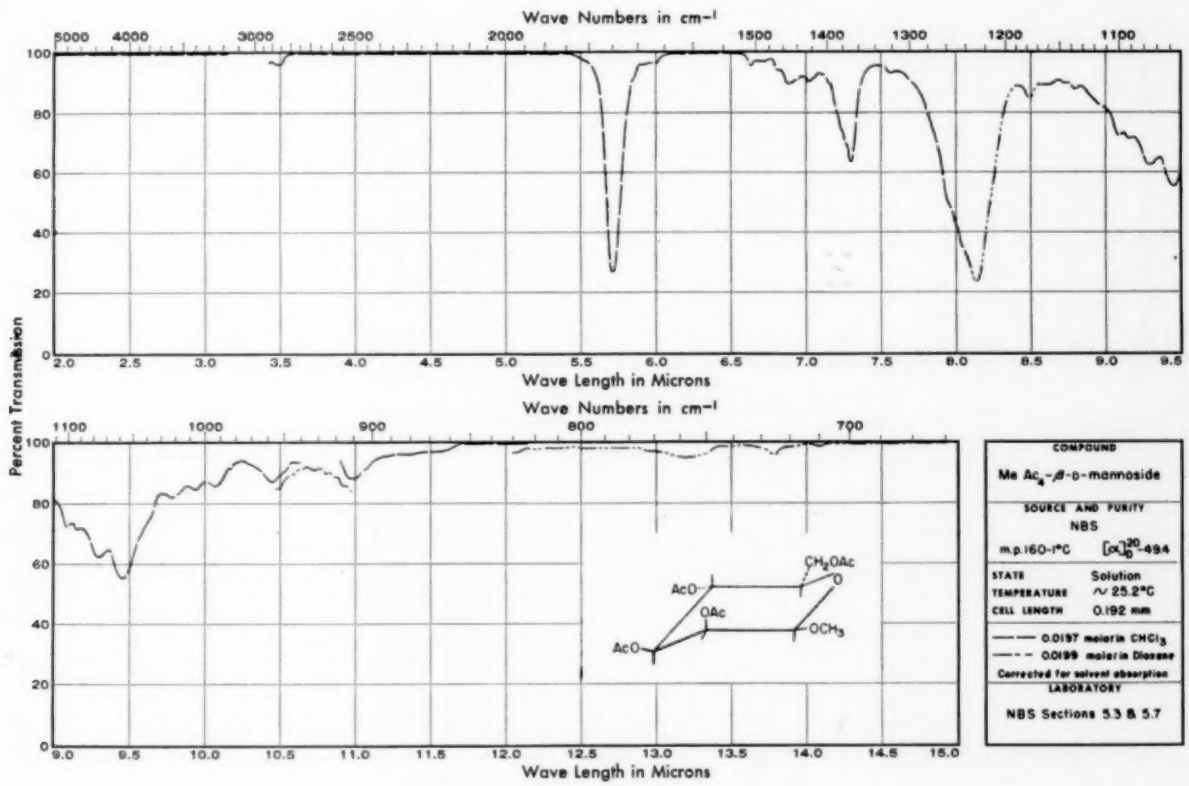

FIGURE 27.

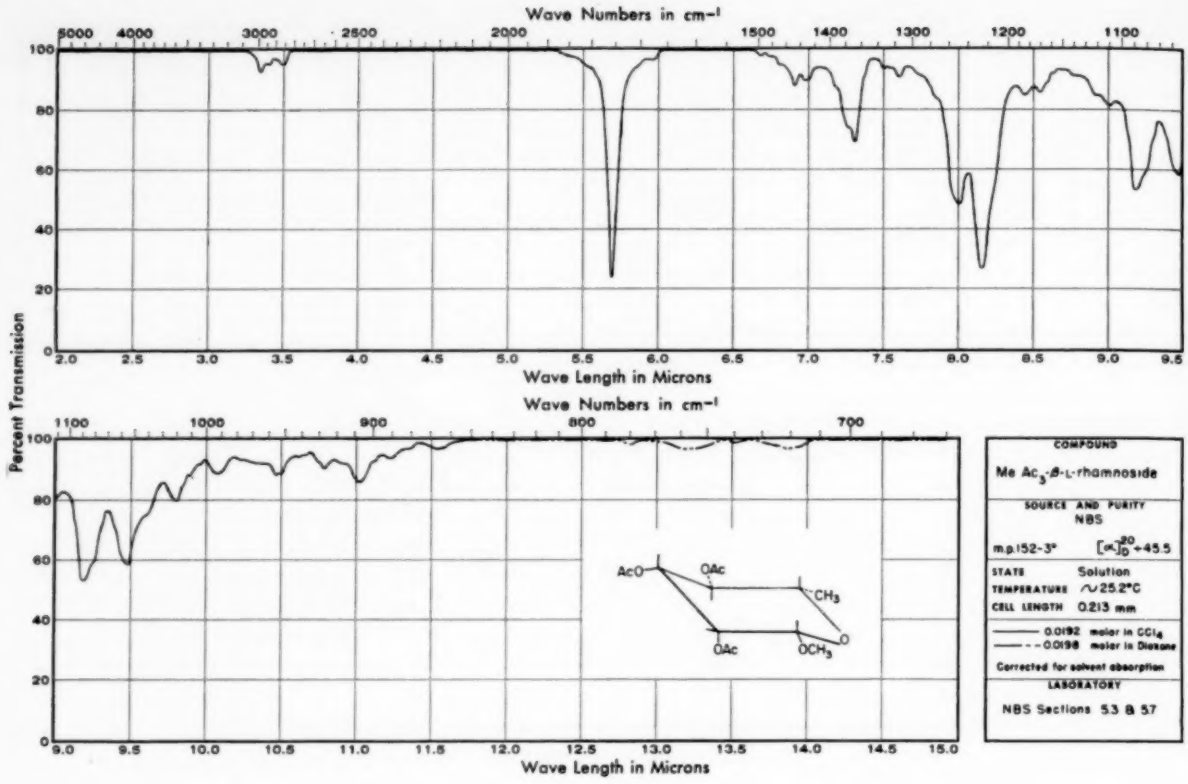

FIGURE 28.

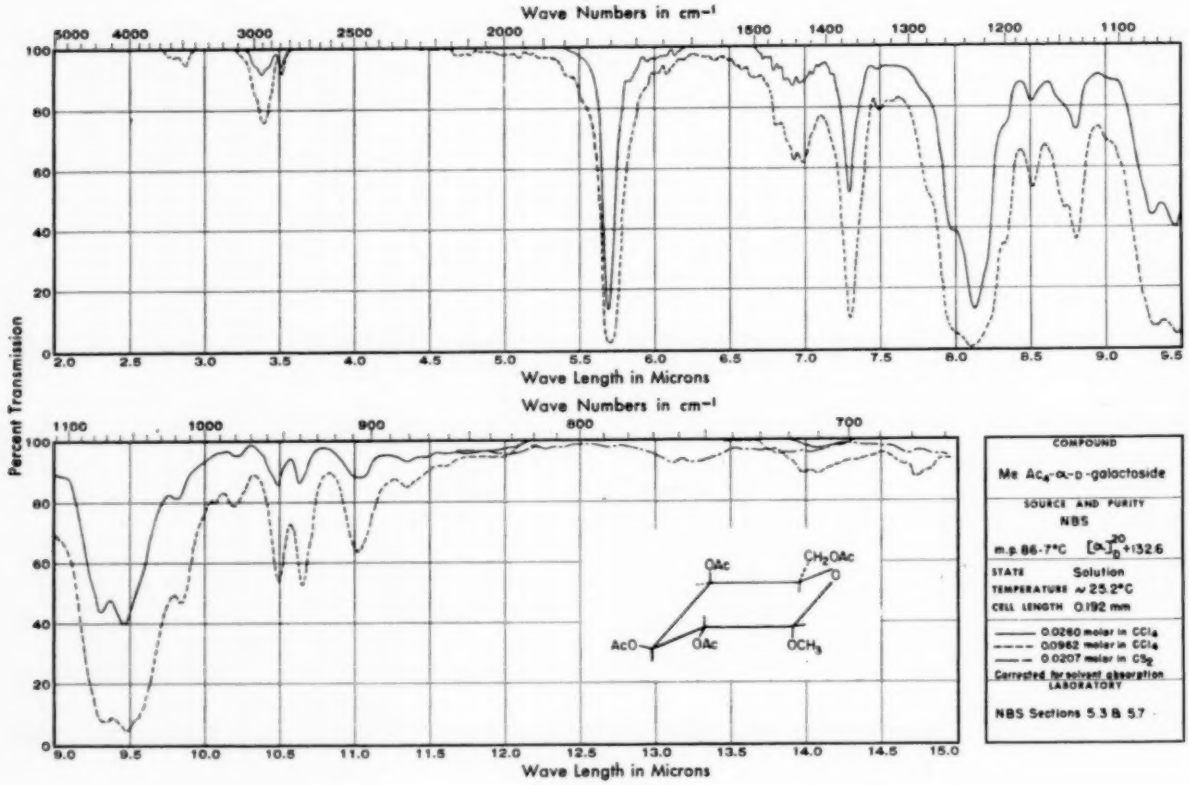

FIGURE 29.

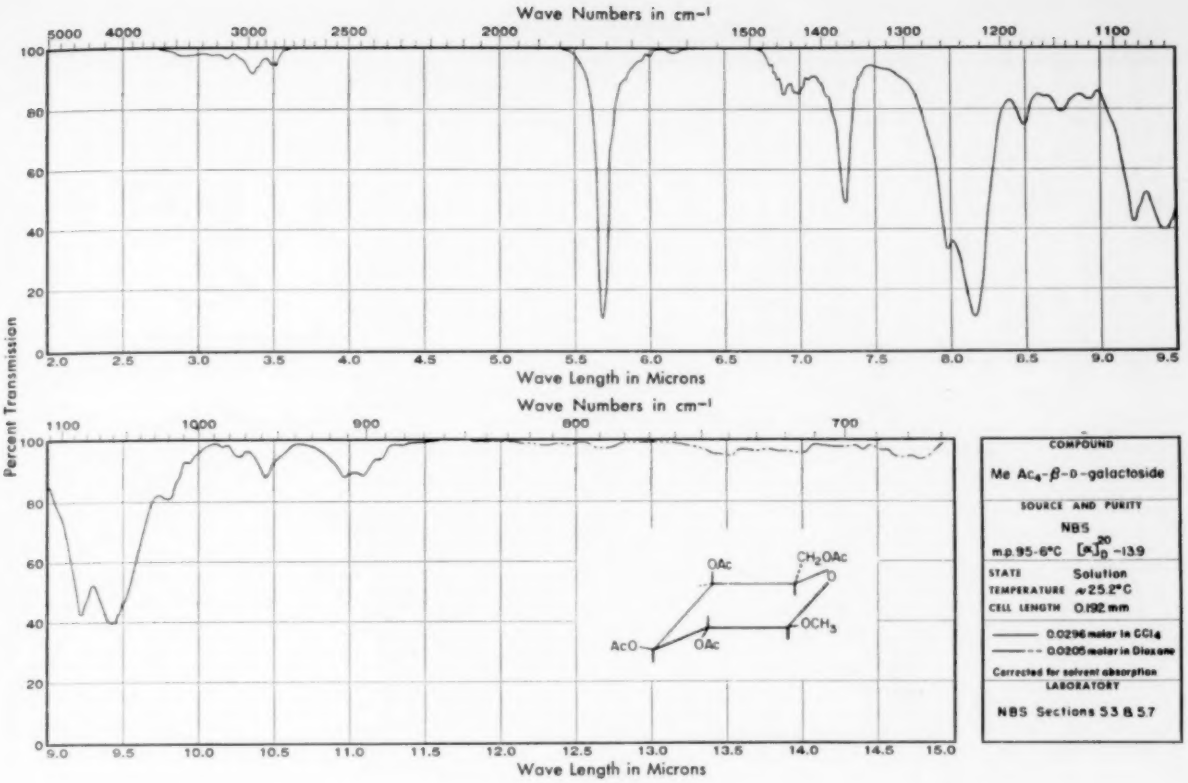

FIGURE 30.

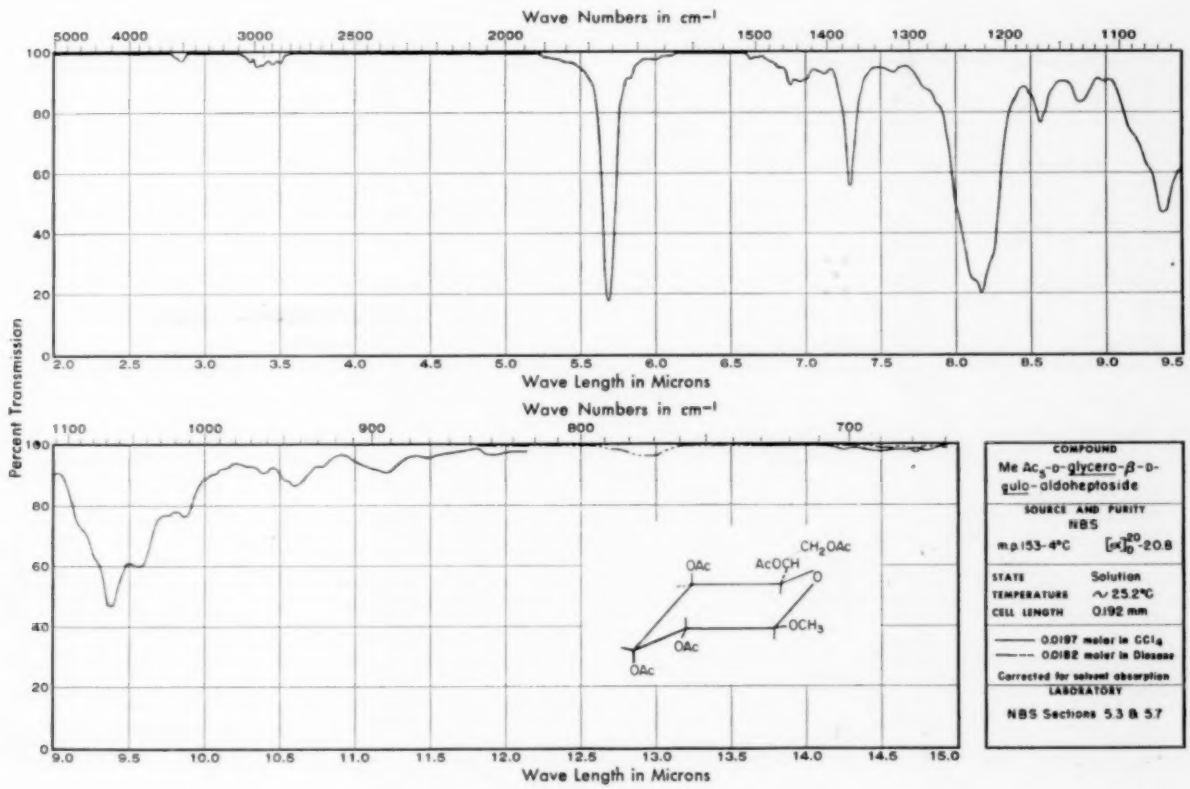

FIGURE 31.

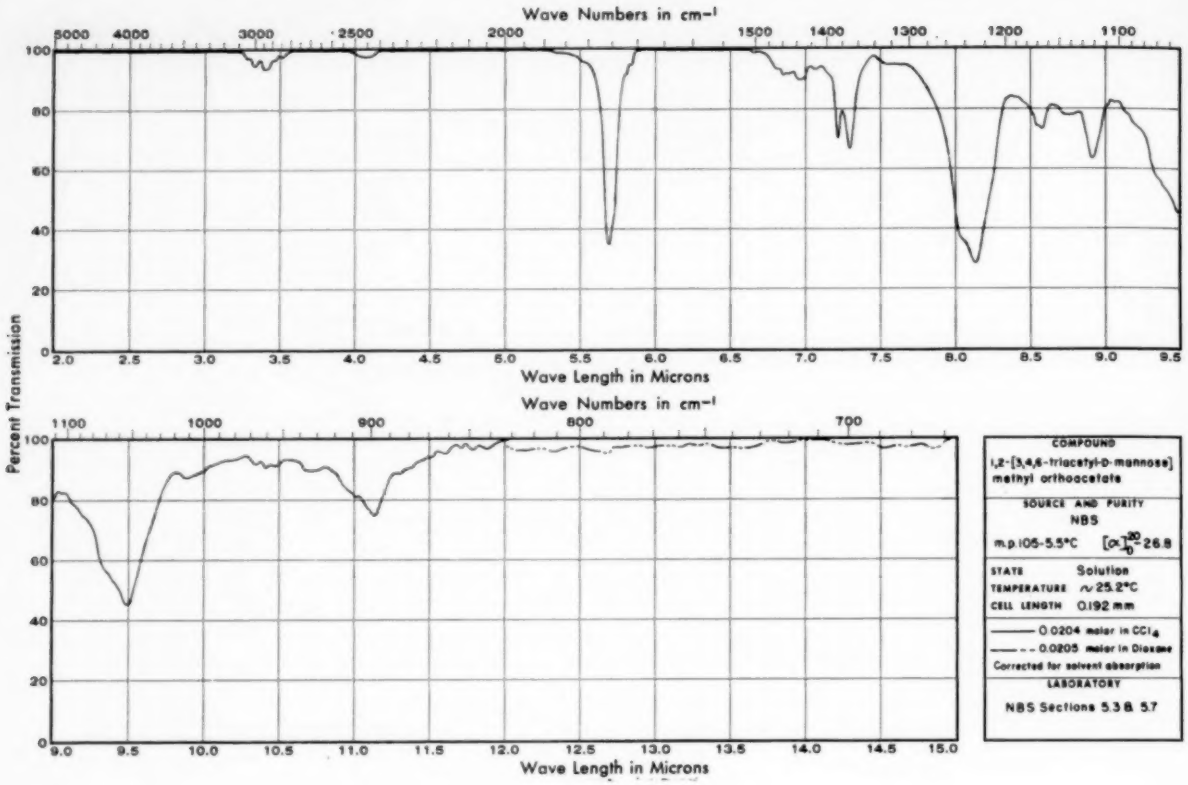

FIGURE 32

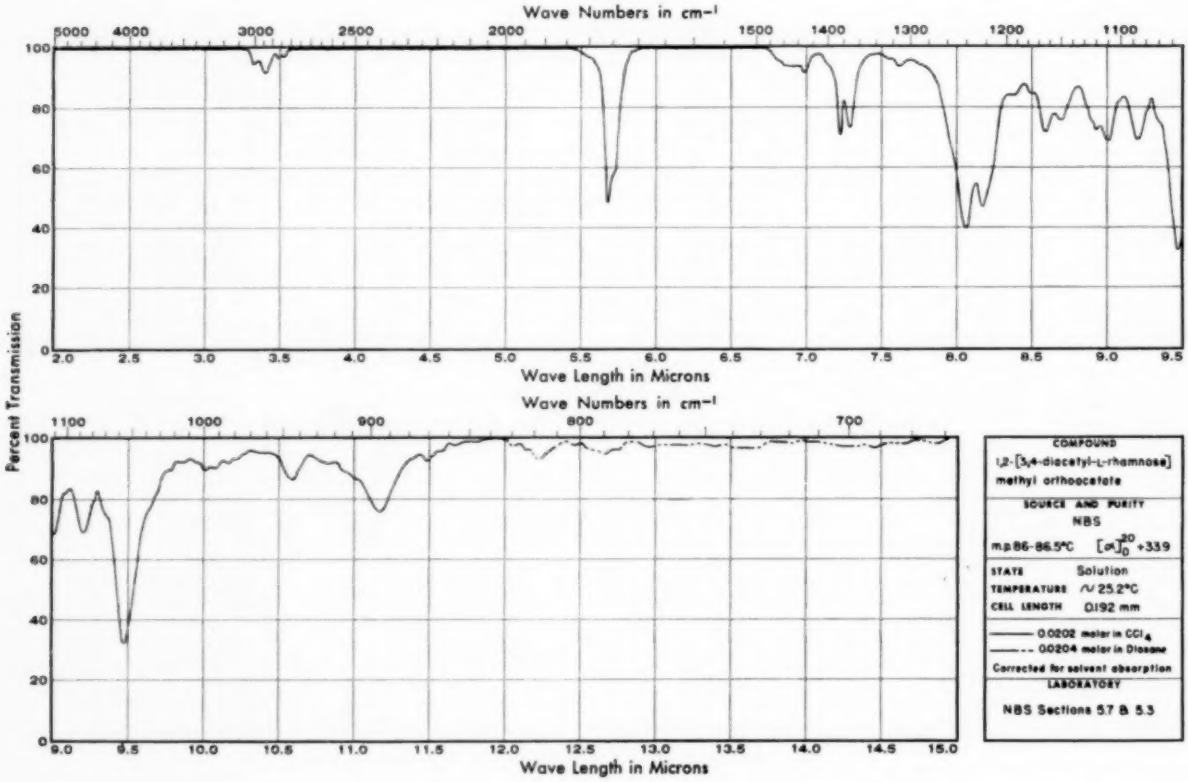

FIGURE 33.

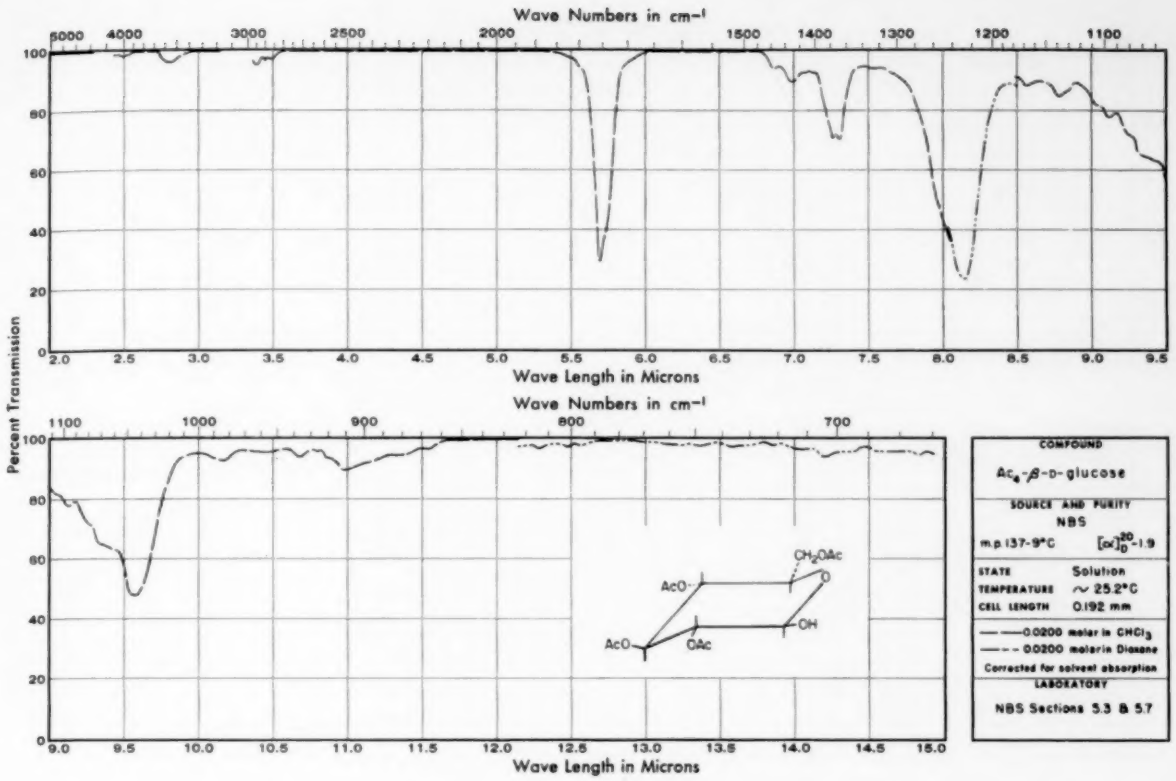

FIGURE 34.

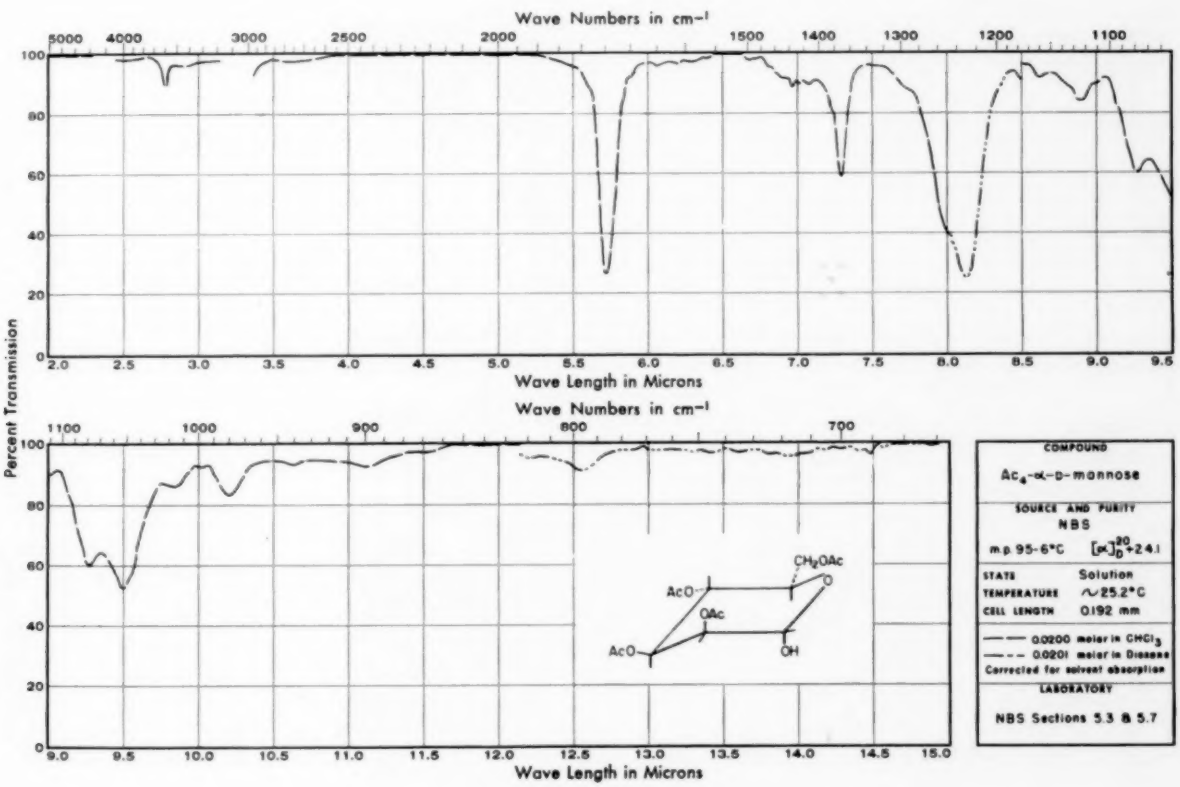

FIGURE 35.

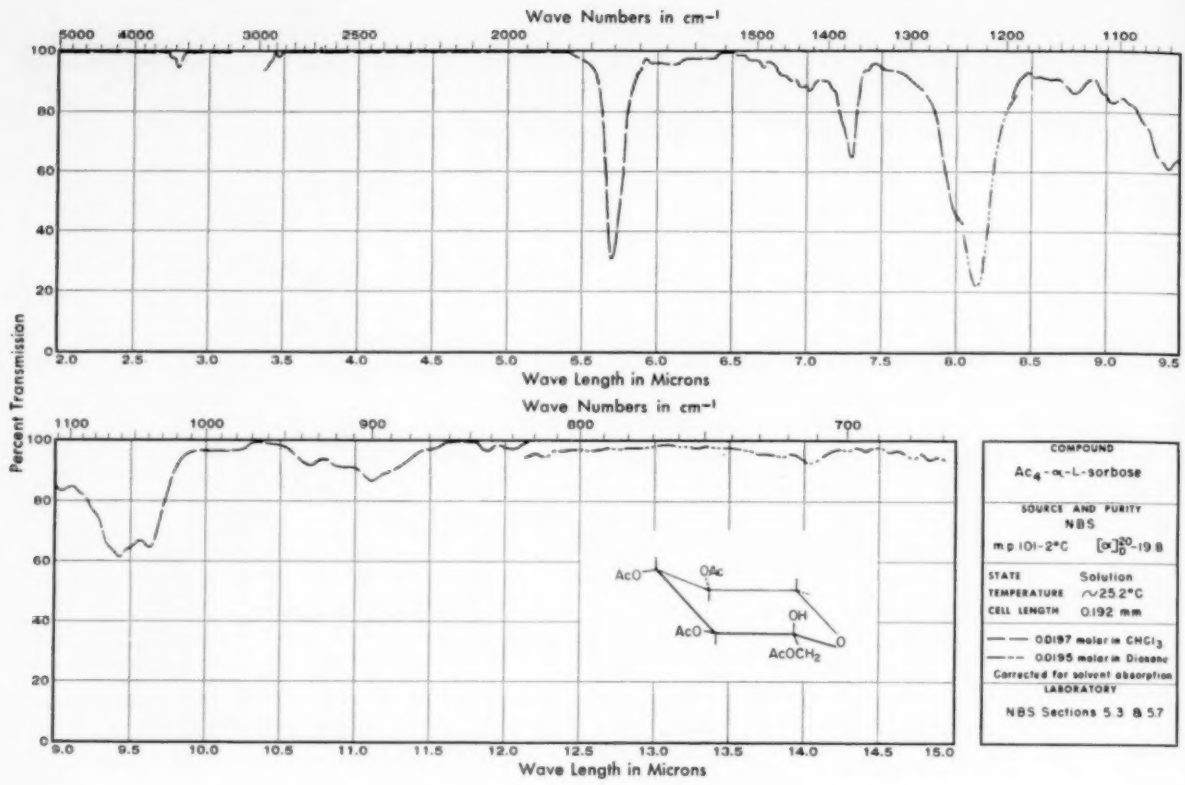

FIGURE 36.

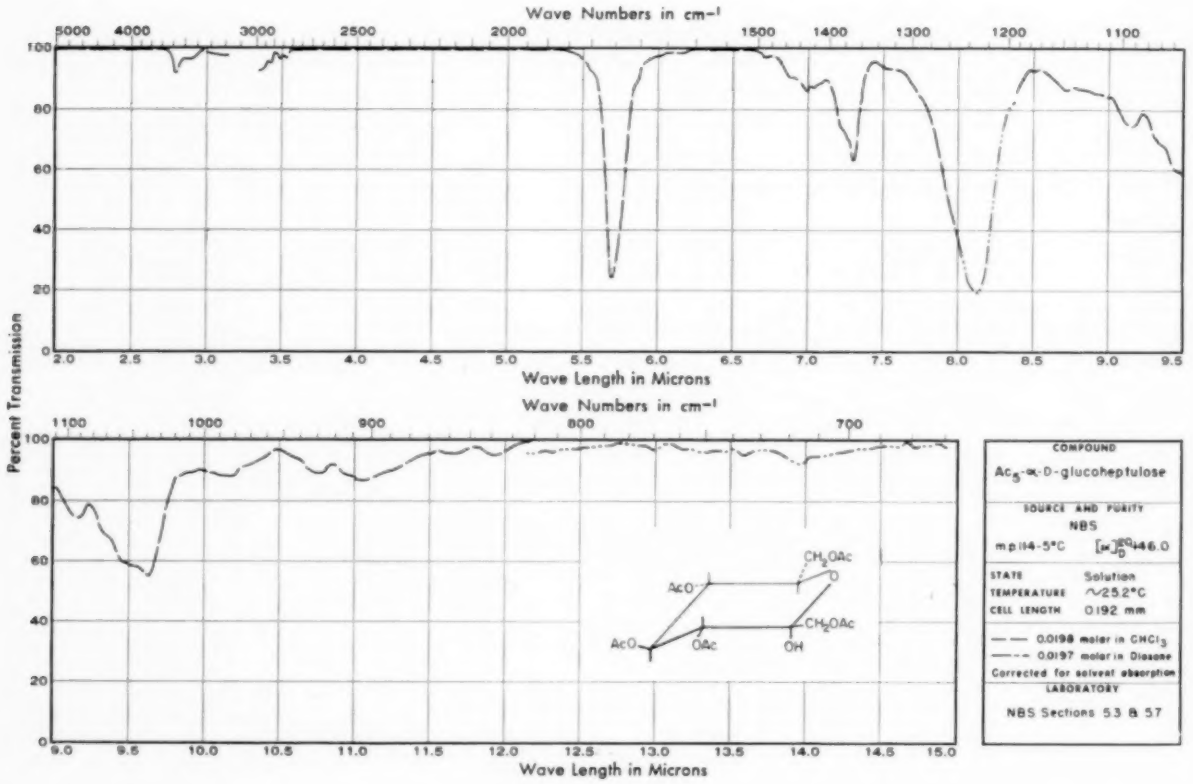

FIGURE 37.

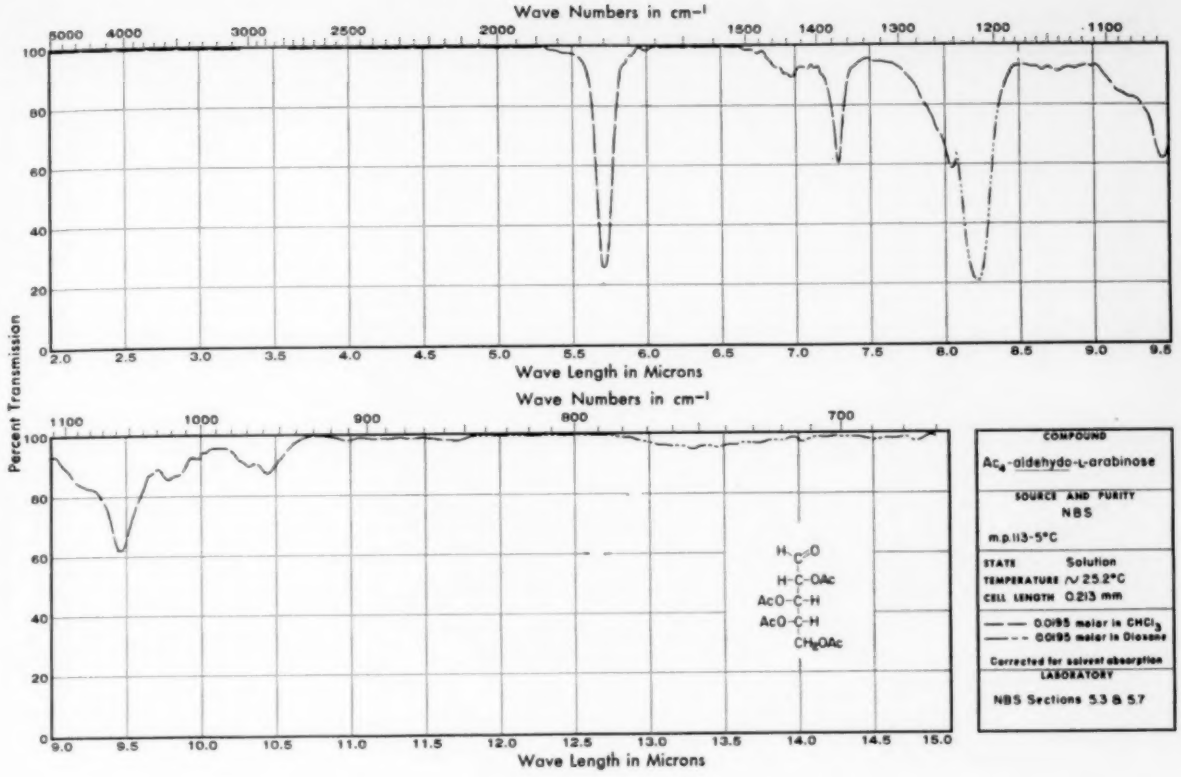

FIGURE 38.

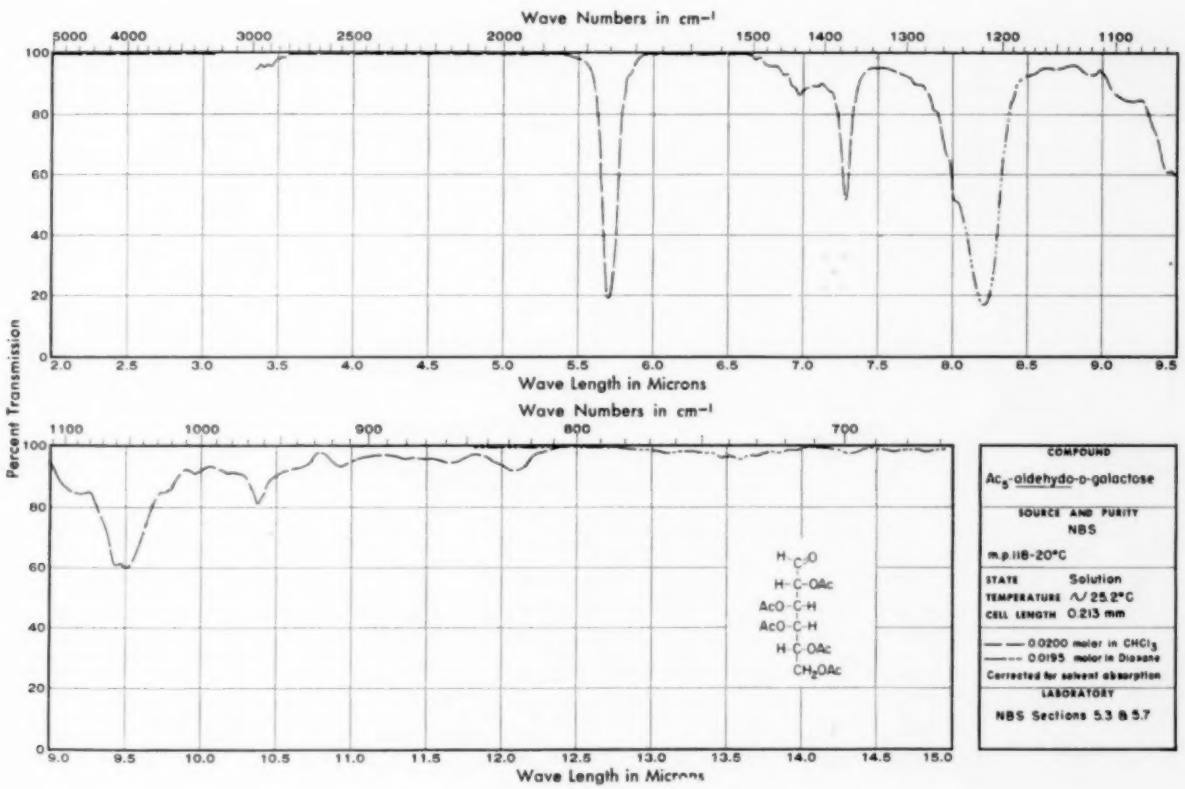

FIGURE 39.

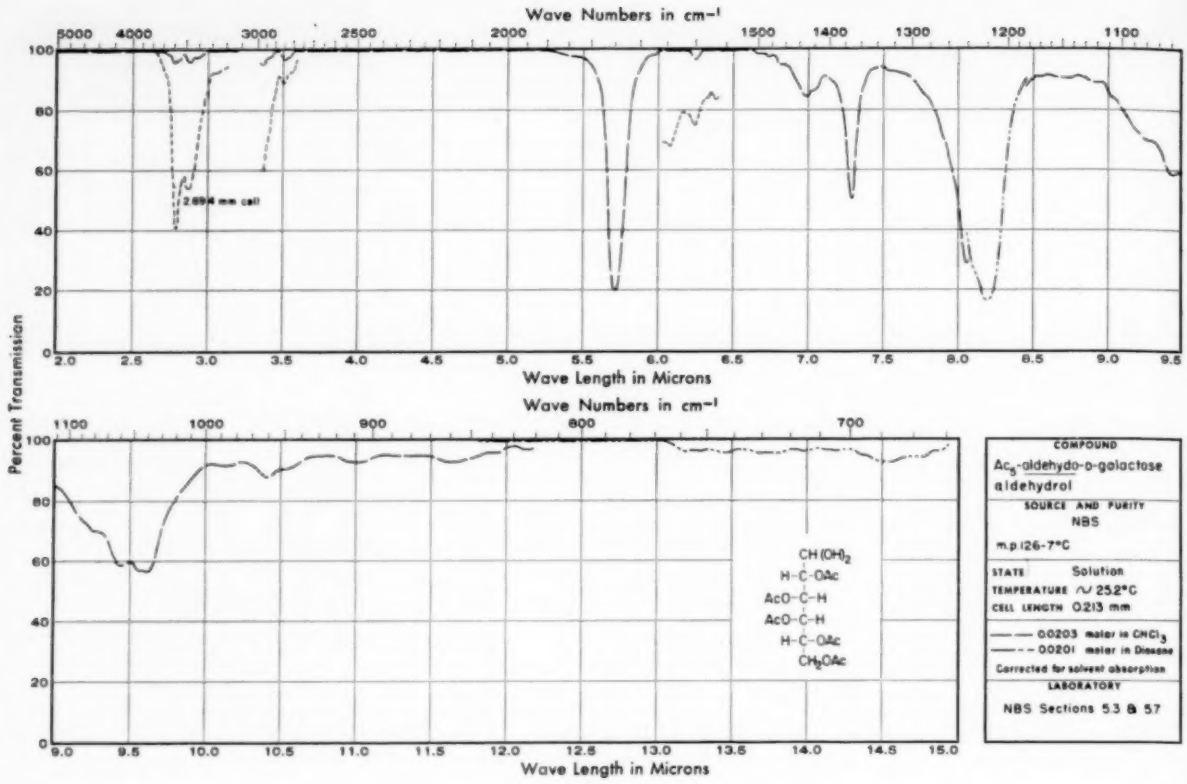

FIGURE 40.

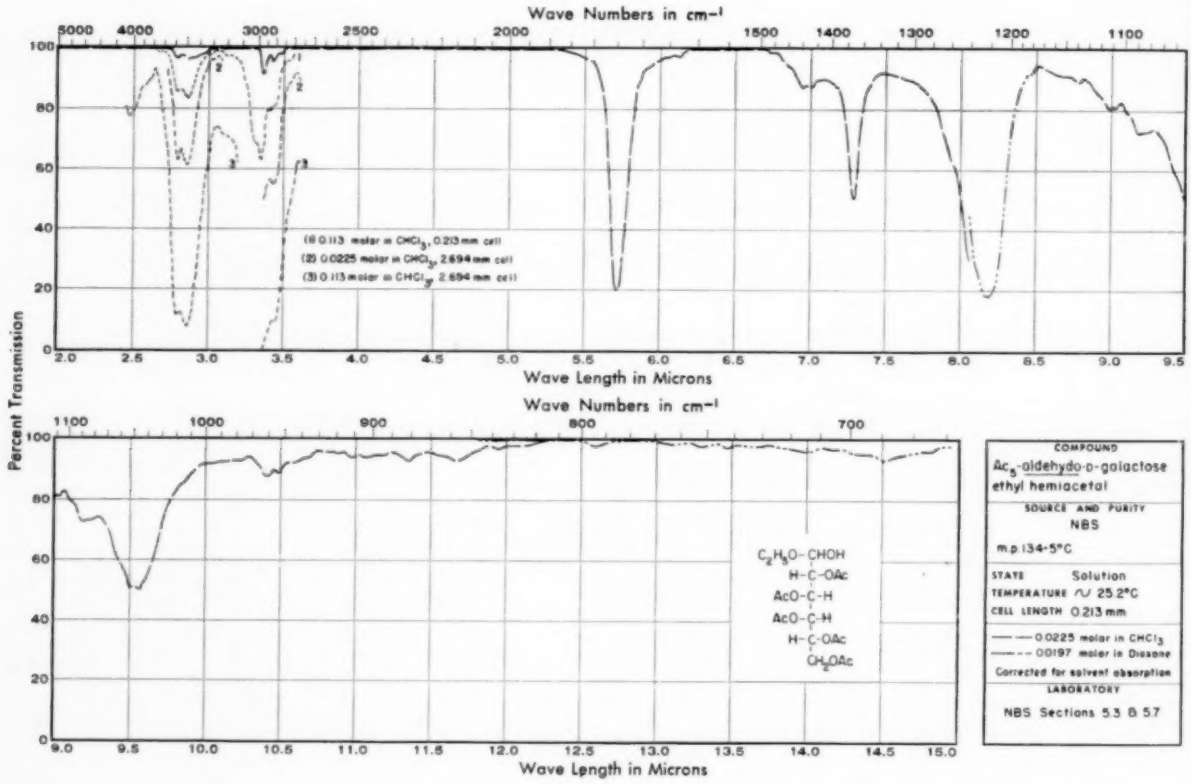

FIGURE 41.

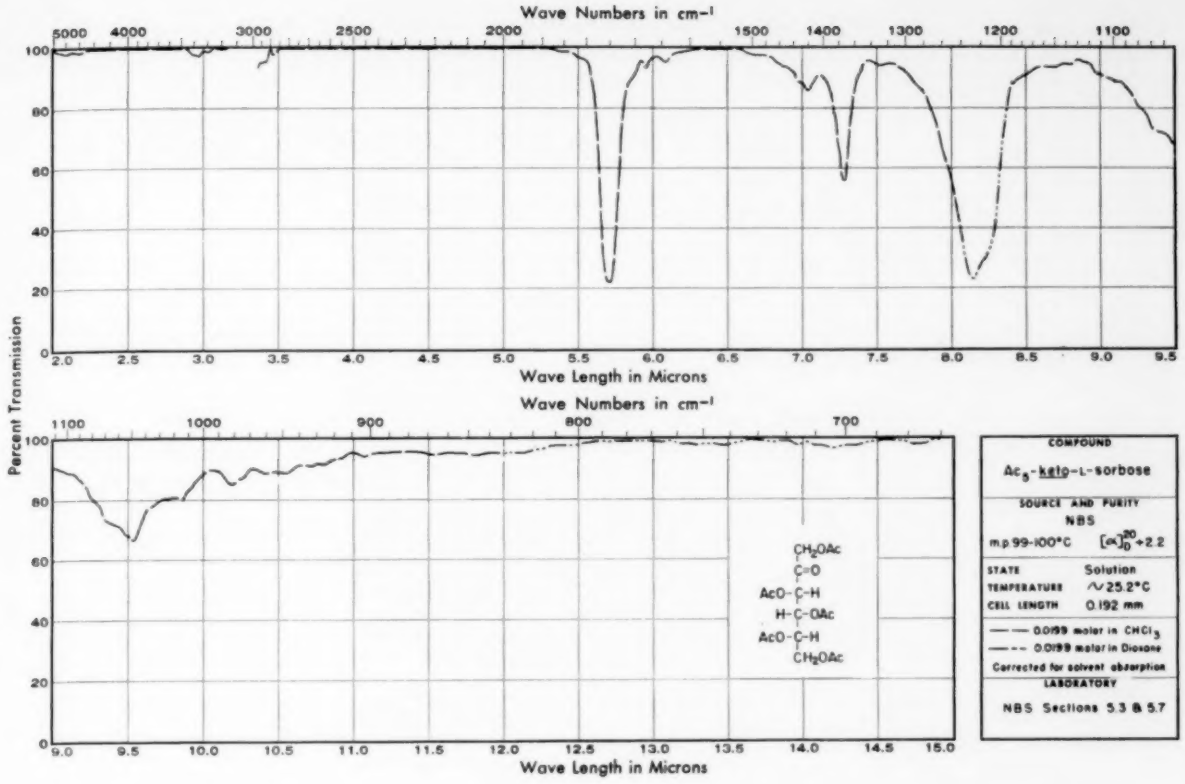

FIGURE 42.

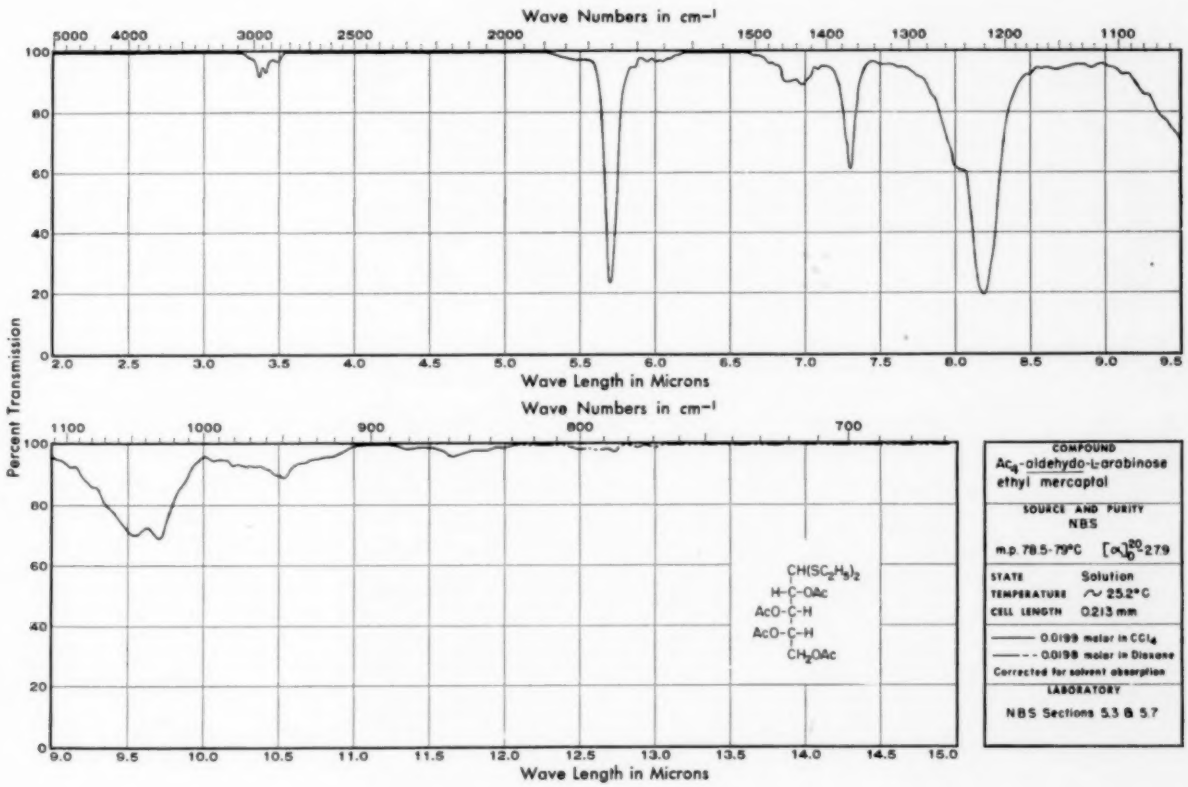

FIGURE 43.

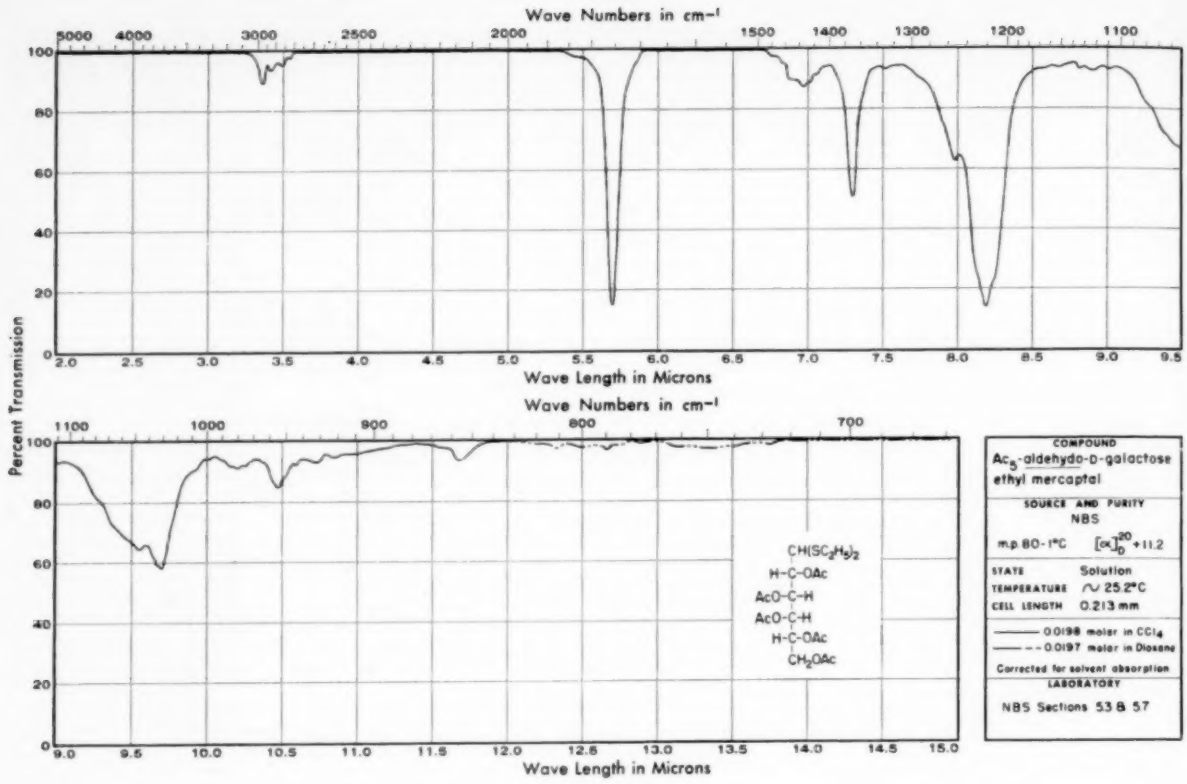

FIGURE 44.

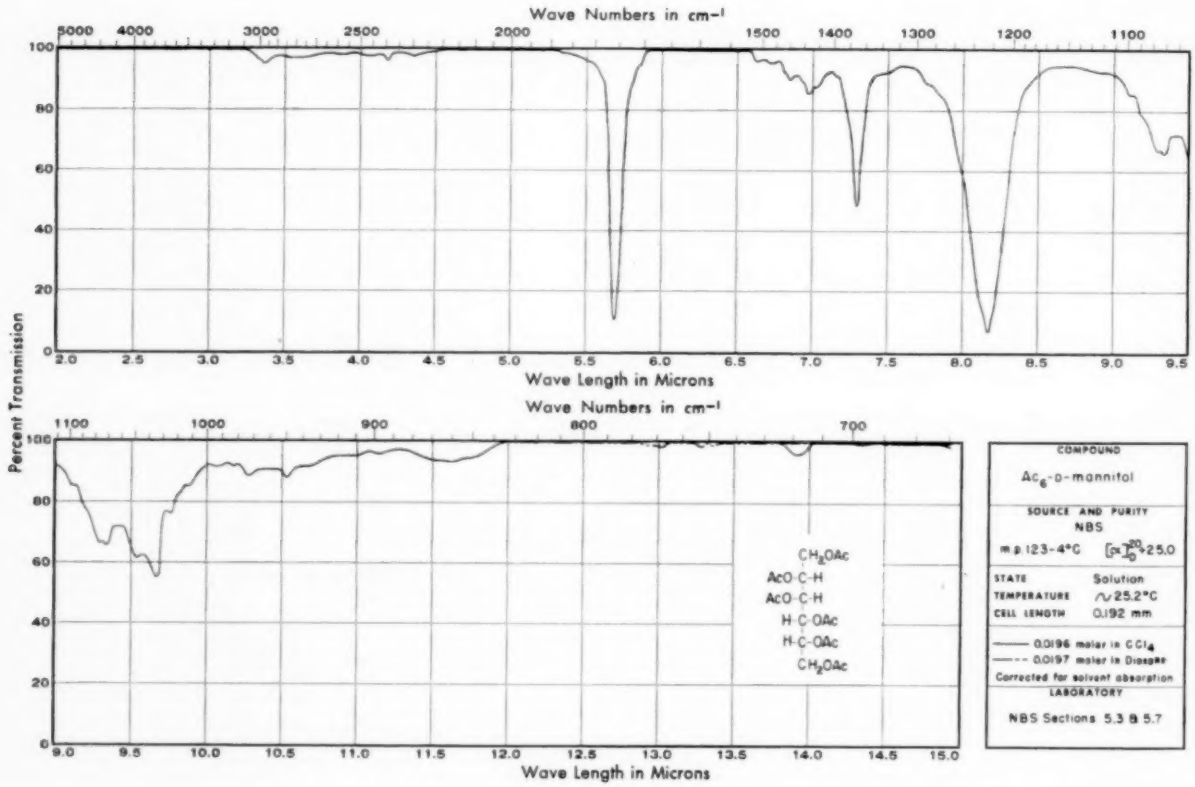

FIGURE 45.

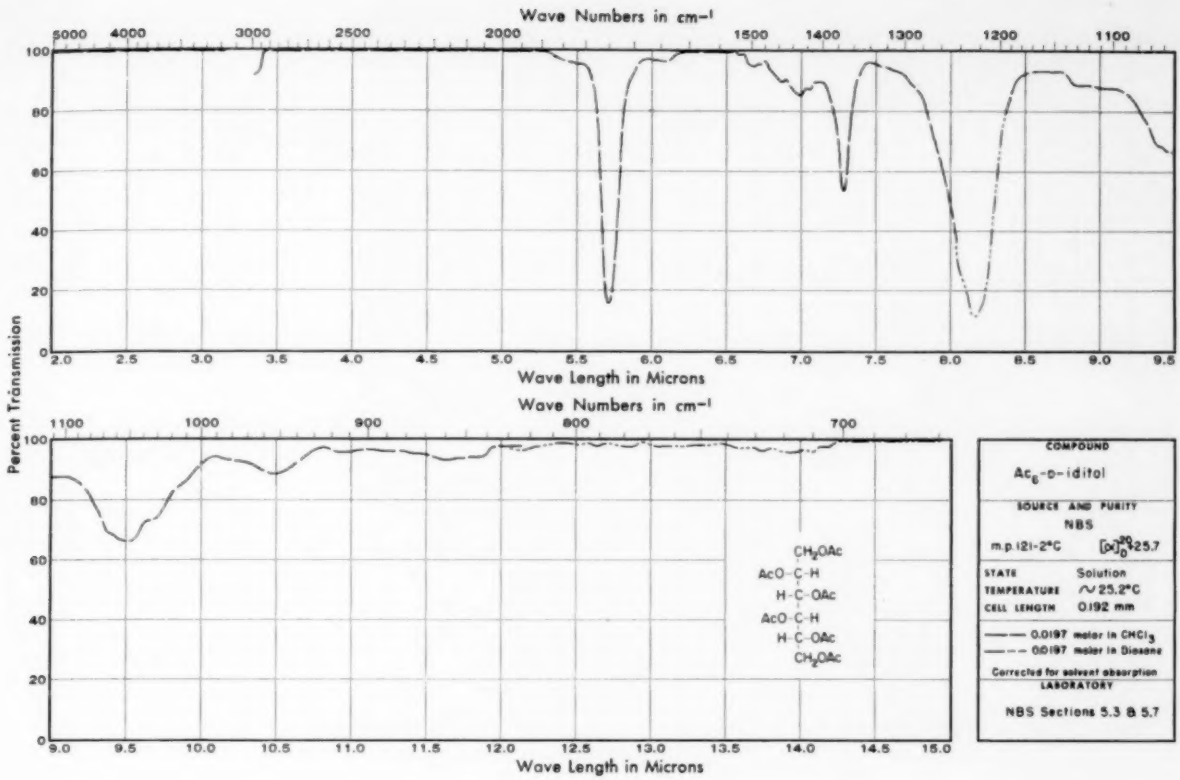

FIGURE 46.

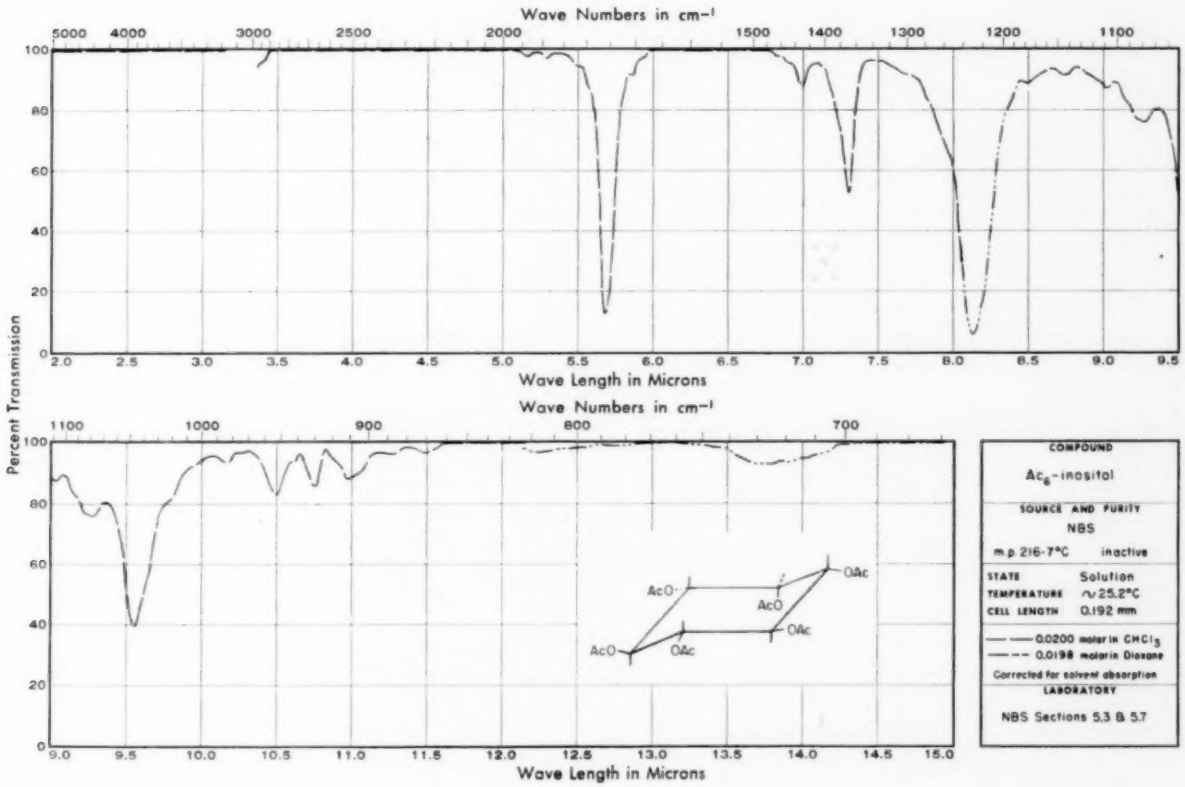

FIGURE 47.

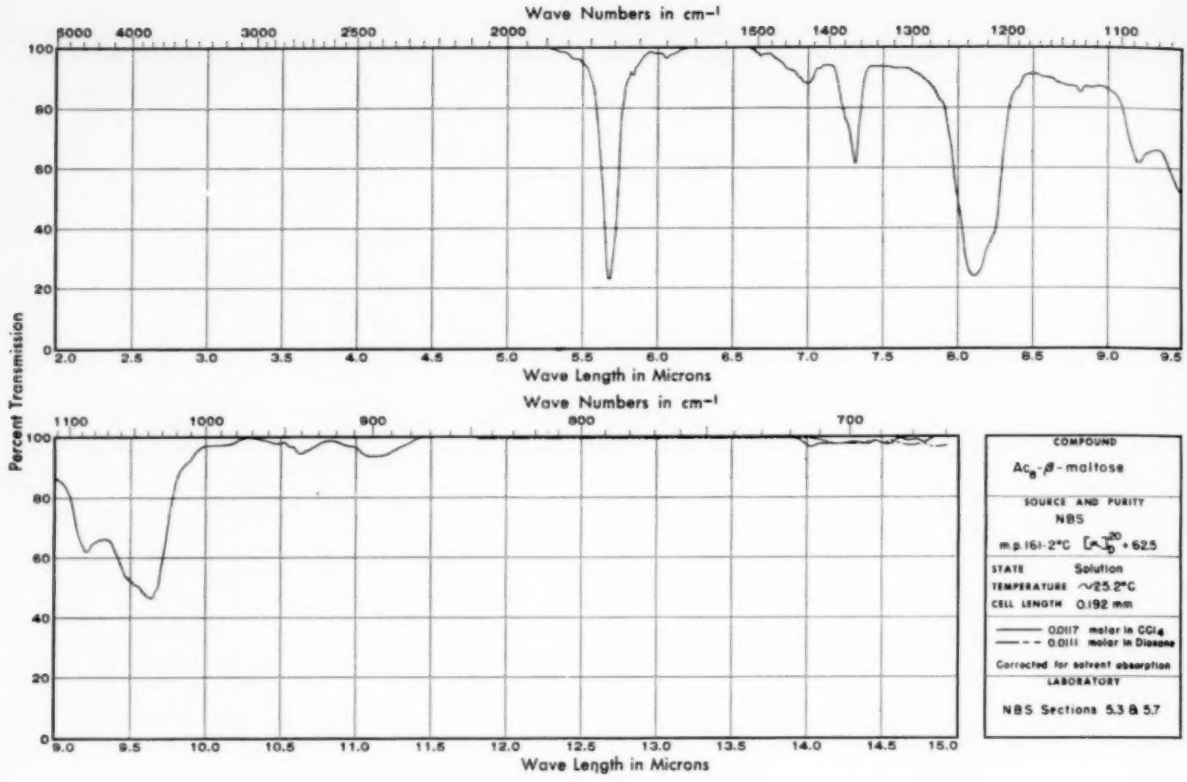

FIGURE 48.

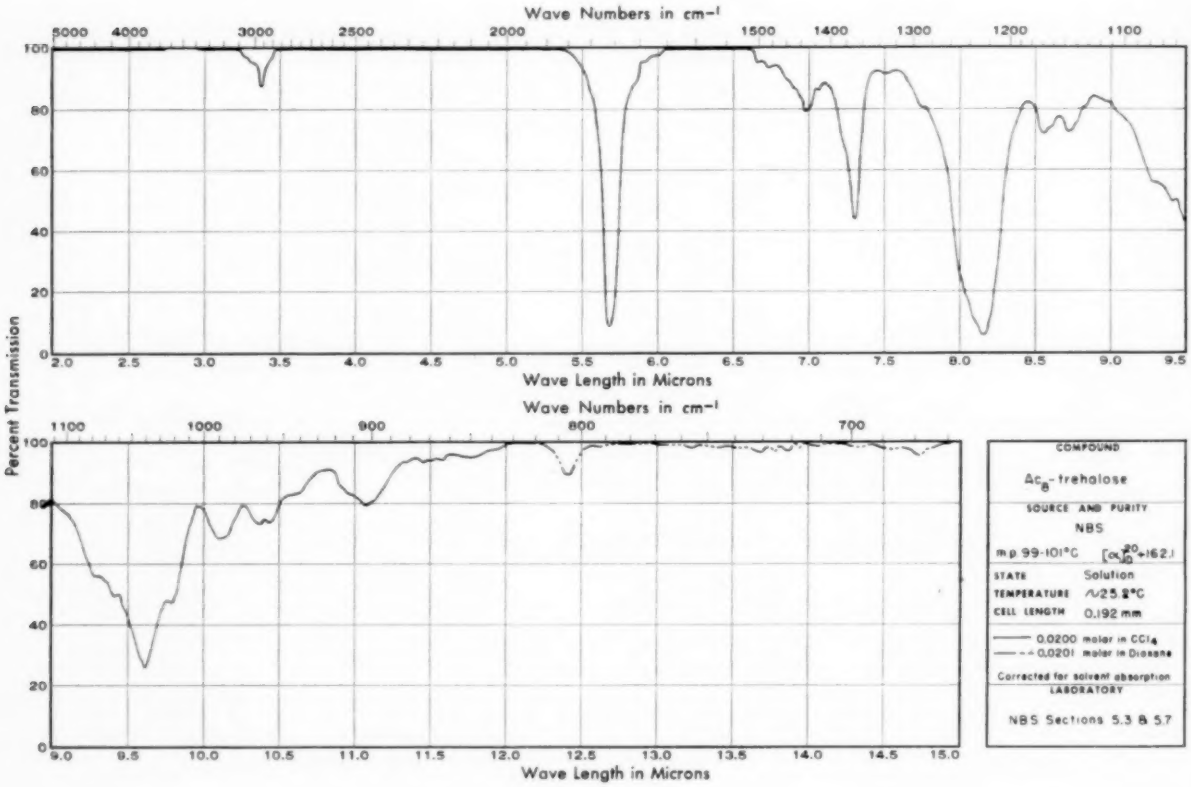

FIGURE 49.

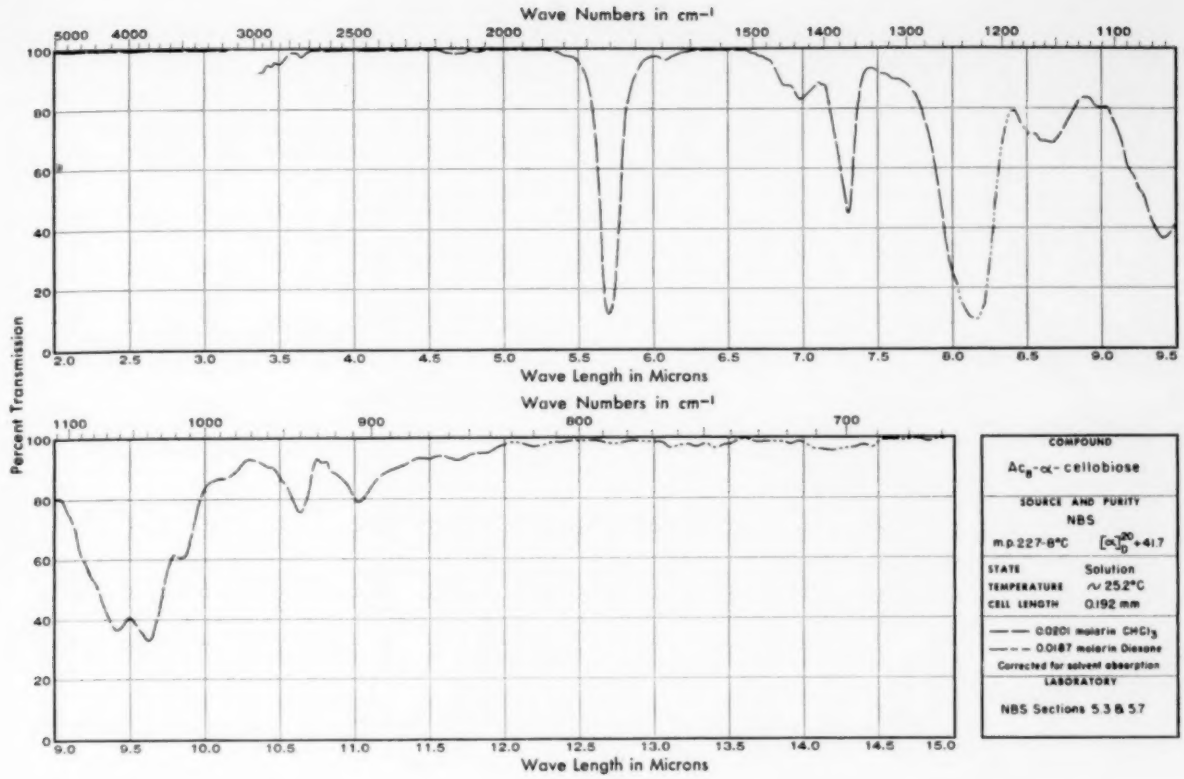

FIGURE 50.

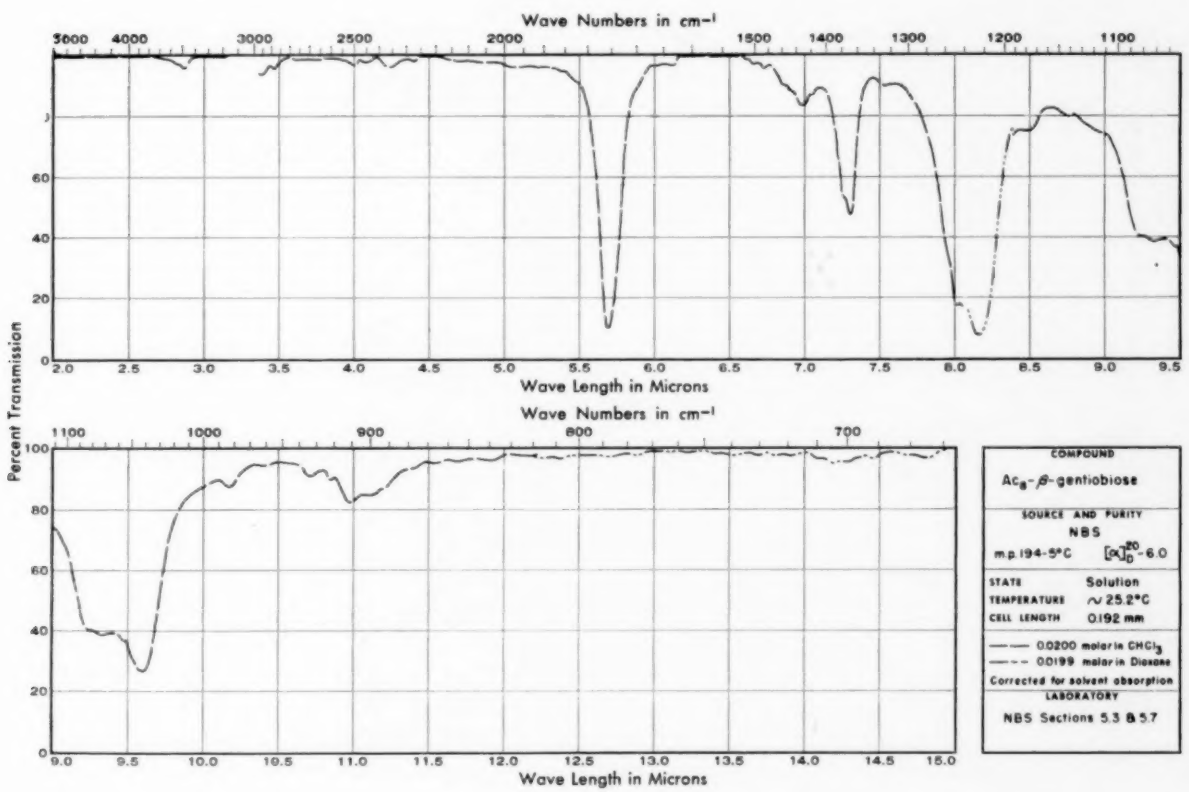

FIGURE 51.

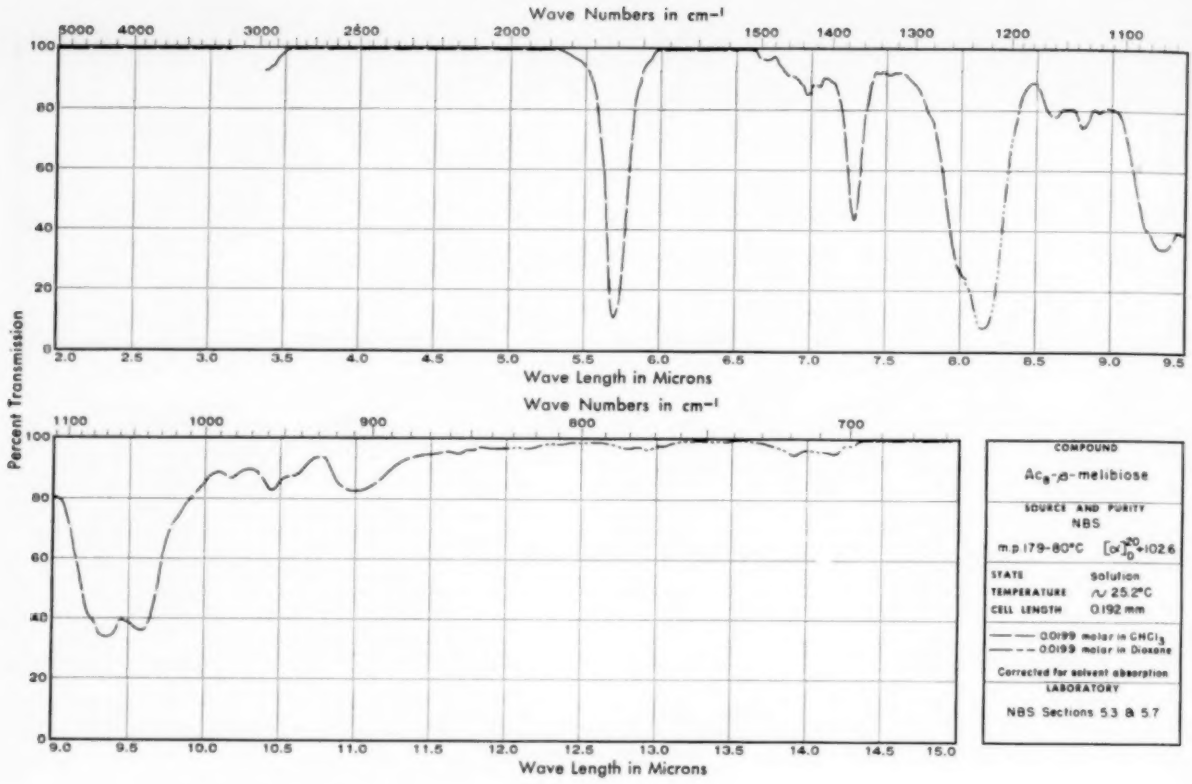

FIGURE 52.

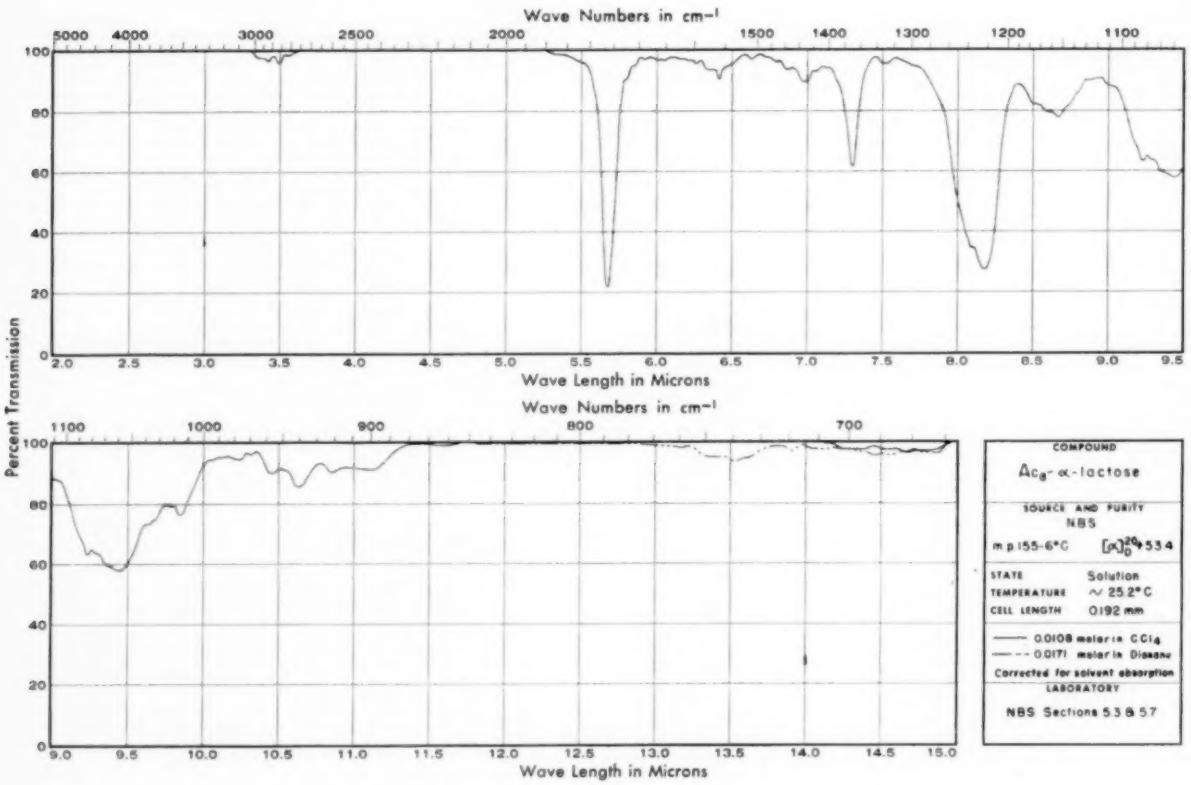

FIGURE 53.

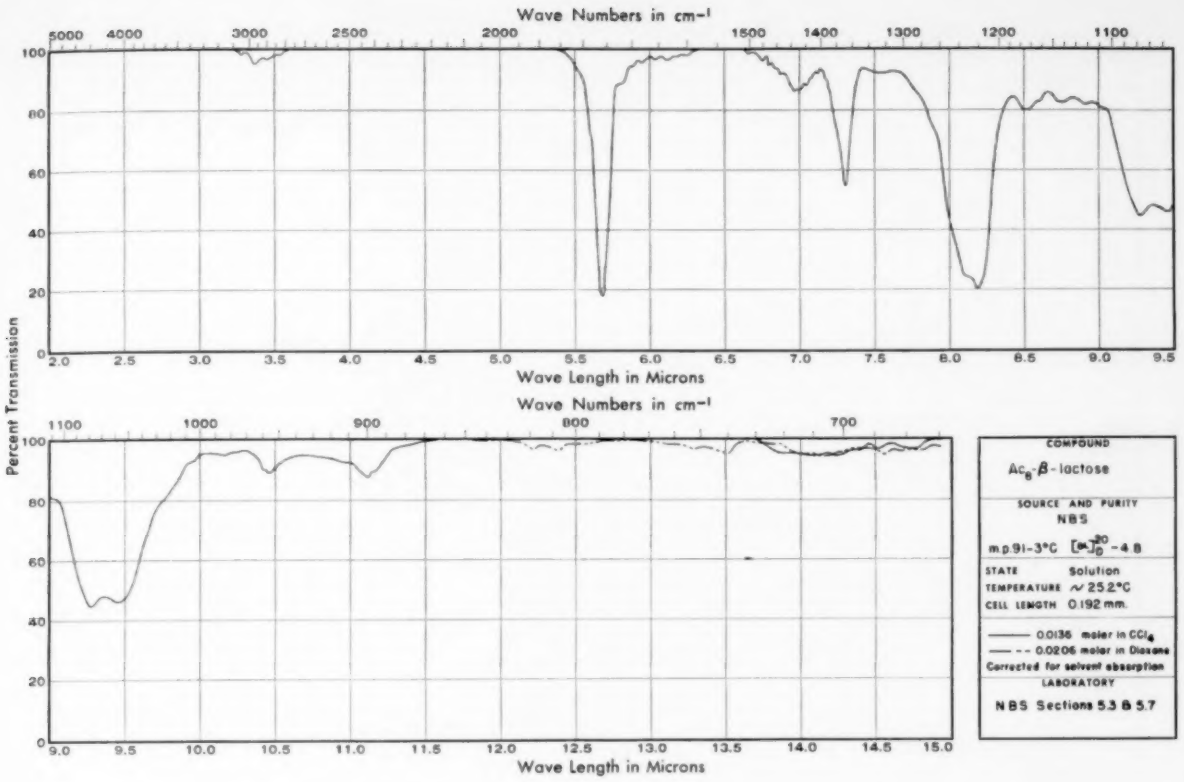

FIGURE 54.

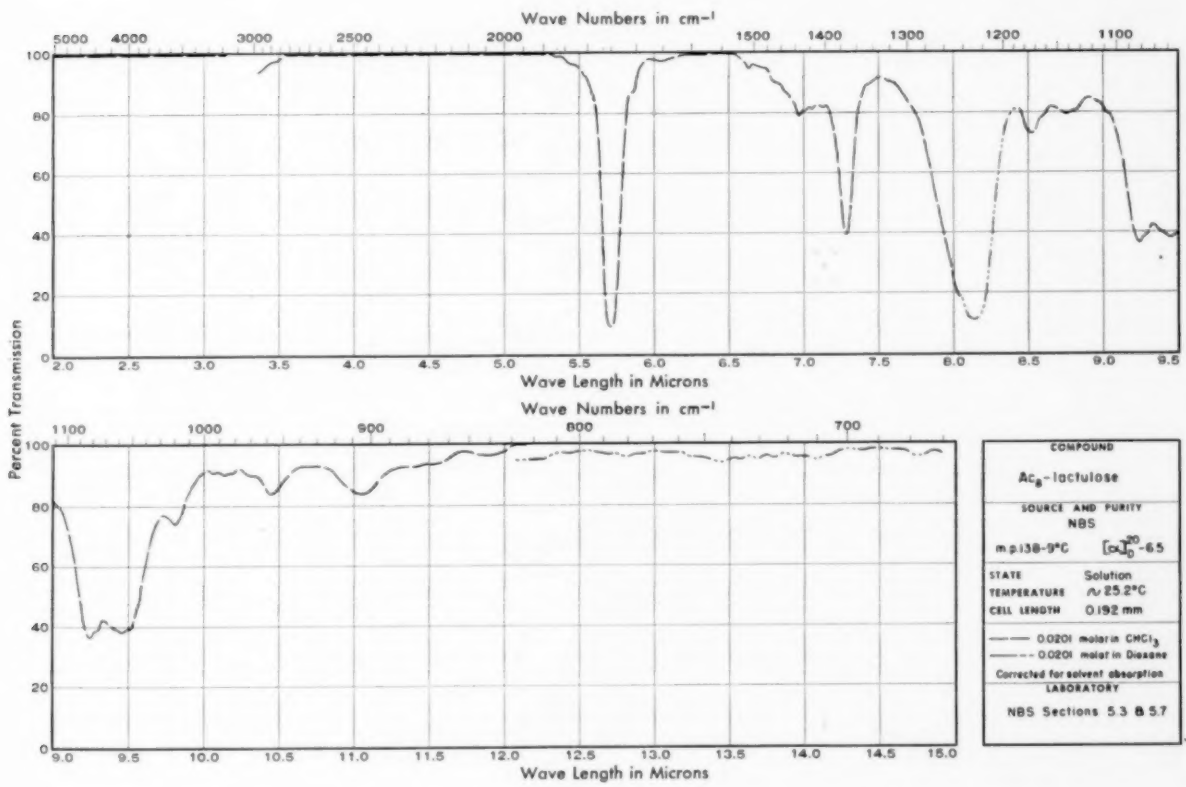

FIGURE 55.

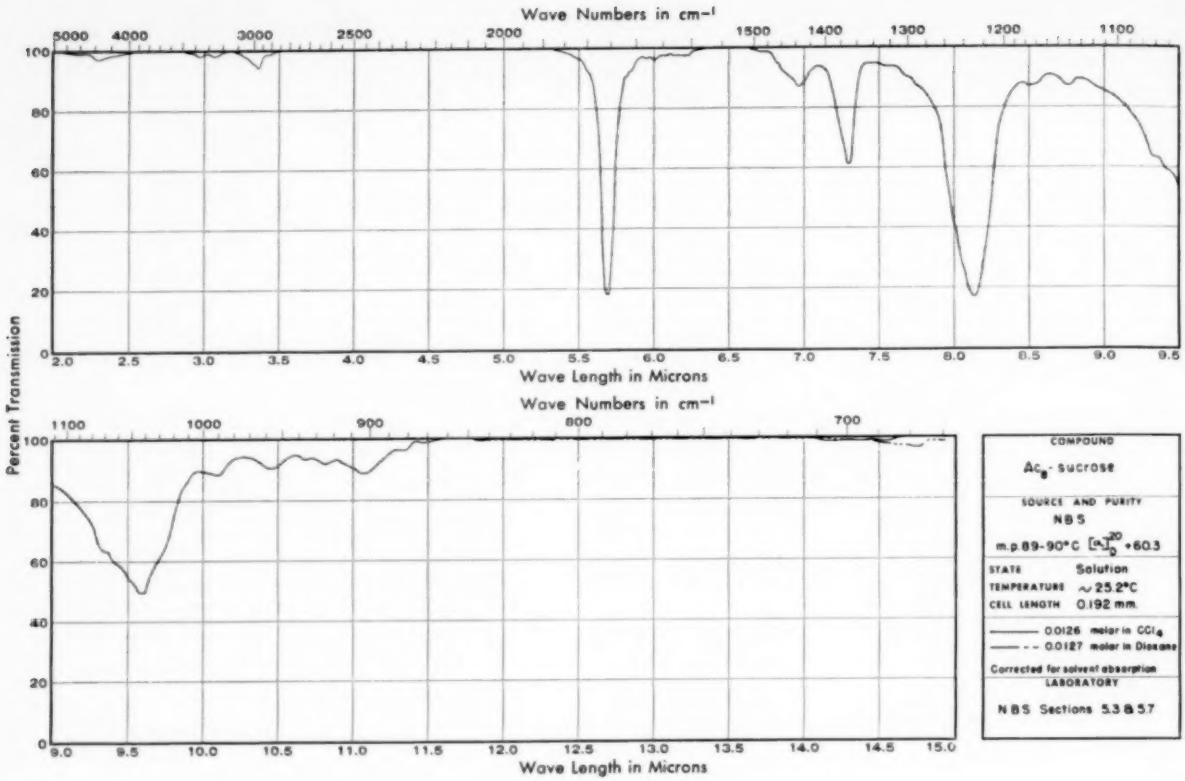

FIGURE 56.

WASHINGTON, December 19, 1956.

U. S. GOVERNMENT PRINTING OFFICE: 1957

THE NATIONAL BUREAU OF STANDARDS

The scope of activities of the National Bureau of Standards at its headquarters in Washington, D. C., and its major field laboratory in Boulder, Colorado, is suggested in the following listing of the divisions and sections engaged in technical work. In general, each section carries out specialized research, development, and engineering in the field indicated by its title. A brief description of the activities, and of the resultant publications, appears on the inside of the front cover.

WASHINGTON, D. C.

Electricity and Electronics. Resistance and Reactance. Electron Devices. Electrical Instruments. Magnetic Measurements. Dielectrics. Engineering Electronics. Electronic Instrumentation. Electrochemistry.

Optics and Metrology. Photometry and Colorimetry. Optical Instruments. Photographic Technology. Length. Engineering Metrology.

Heat and Power. Temperature Physics. Thermodynamics. Cryogenic Physics. Rheology. Engine Fuels. Free Radical Research.

Atomic and Radiation Physics. Spectroscopy. Radiometry. Mass Spectrometry. Solid State Physics. Electron Physics. Atomic Physics. Neutron Physics. Nuclear Physics. Radioactivity. X-rays. Betatron. Nucleonic Instrumentation. Radiological Equipment. AEC Radiation Instruments.

Chemistry. Organic Coatings. Surface Chemistry. Organic Chemistry. Analytical Chemistry. Inorganic Chemistry. Electrodeposition. Gas Chemistry. Physical Chemistry. Thermochemistry. Spectrochemistry. Pure Substances.

Mechanics. Sound. Mechanical Instruments. Fluid Mechanics. Engineering Mechanics. Mass and Scale. Capacity, Density, and Fluid Meters. Combustion Controls.

Organic and Fibrous Materials. Rubber. Textiles. Paper. Leather. Testing and Specifications. Polymer Structure. Plastics. Dental Research.

Metallurgy. Thermal Metallurgy. Chemical Metallurgy. Mechanical Metallurgy. Corrosion. Metal Physics.

Mineral Products. Engineering Ceramics. Glass. Refractories. Enameled Metals. Concreting Materials. Constitution and Microstructure.

Building Technology. Structural Engineering. Fire Protection. Air Conditioning, Heating, and Refrigeration. Floor, Roof, and Wall Coverings. Codes and Specifications. Heat Transfer.

Applied Mathematics. Numerical Analysis. Computation. Statistical Engineering. Mathematical Physics.

Data Processing Systems. SEAC Engineering Group. Components and Techniques. Digital Circuitry. Digital Systems. Analog Systems. Application Engineering.

• Office of Basic Instrumentation

• Office of Weights and Measures

BOULDER, COLORADO

Cryogenic Engineering. Cryogenic Equipment. Cryogenic Processes. Properties of Materials. Gas Liquefaction.

Radio Propagation Physics. Upper Atmosphere Research. Ionospheric Research. Regular Propagation Services. Sun-Earth Relationships.

Radio Propagation Engineering. Data Reduction Instrumentation. Modulation Systems. Navigation Systems. Radio Noise. Tropospheric Measurements. Tropospheric Analysis. Radio Systems Application Engineering.

Radio Standards. High Frequency Electrical Standards. Radio Broadcast Service. High Frequency Impedance Standards. Calibration Center. Microwave Physics. Microwave Circuit Standards.

Recent Publications of the National Bureau of Standards

Journal of Research of the National Bureau of Standards, Volume 58, No. 5, May 1957 (RP2755 to RP2761 incl.). 60 cents. Annual subscription $4.00.

Technical News Bulletin, Volume 41, No. 5, May 1957. 10 cents. Annual subscription $1.00.

Basic Radio Propagation Predictions for August 1957. Three months in advance. CRPL–D 153. Issued May 1957. 10 cents. Annual subscription $1.00.

Circulars

C552, 2d Edition. Standard samples—A catalog of reference materials issued by the National Bureau of Standards. 25 cents.

Handbooks

H62. Report of the International Commission on Radiological Units and Measurements (ICRU) 1956. 40 cents.

Miscellaneous Publications

M219. Report of the 41st National Conference on Weights and Measures 1956. 70 cents.

Available from the Superintendent of Documents, U. S. Government Printing Office, Washington 25, D. C. (foreign postage, one-fourth additional).

UNITED STATES
GOVERNMENT PRINTING OFFICE
DIVISION OF PUBLIC DOCUMENTS
WASHINGTON 25, D. C.

OFFICIAL BUSINESS

PENALTY FOR PRIVATE USE TO AVOID
PAYMENT OF POSTAGE, $300
(GPO)

Journal of Research of the National Bureau of Standards Vol. 59, No. 1 July 19

Contents

	Page
Thermal length changes of some refractory castables. S. J. Schneider and L. E. Mong. RP2768	1
Precise intercomparison of acids by differential potentiometric titration with hydrogen electrodes. Roger G. Bates and Edward Wickers. RP2769	9
Mixed-path ground-wave propagation: 2. Larger distances. James R. Wait and James Householder. RP2770	19
Spectroscopic study of oils used in oil-extended rubber. Frederic J. Linning and James E. Stewart. RP2771	27
Infrared spectra of sugar acetates in solution. Horace S. Isbell, Francis A. Smith, E. Carroll Creitz, Harriet L. Frush, Joseph D. Moyer, and James E. Stewart. RP2772	41

For sale by the Superintendent of Documents, U. S. Government Printing Office, Washington 25, D. C. Price 60 cents (single copy)
Subscription price: $4.00 a year; $1.25 additional for foreign mailing.

UNITED STATES GOVERNMENT PRINTING OFFICE, WASHINGTON : 1957